WHAT IS KNOWN AND WHAT REMAINS TO BE DISCOVERED ABOUT BACTERIAL OUTER MEMBRANE VESICLES, VOLUME II

EDITED BY: Araceli Contreras-Rodriguez, Rafael A. Garduno and Alejandro J. Yañez

PUBLISHED IN: Frontiers in Microbiology and Frontiers in Immunology

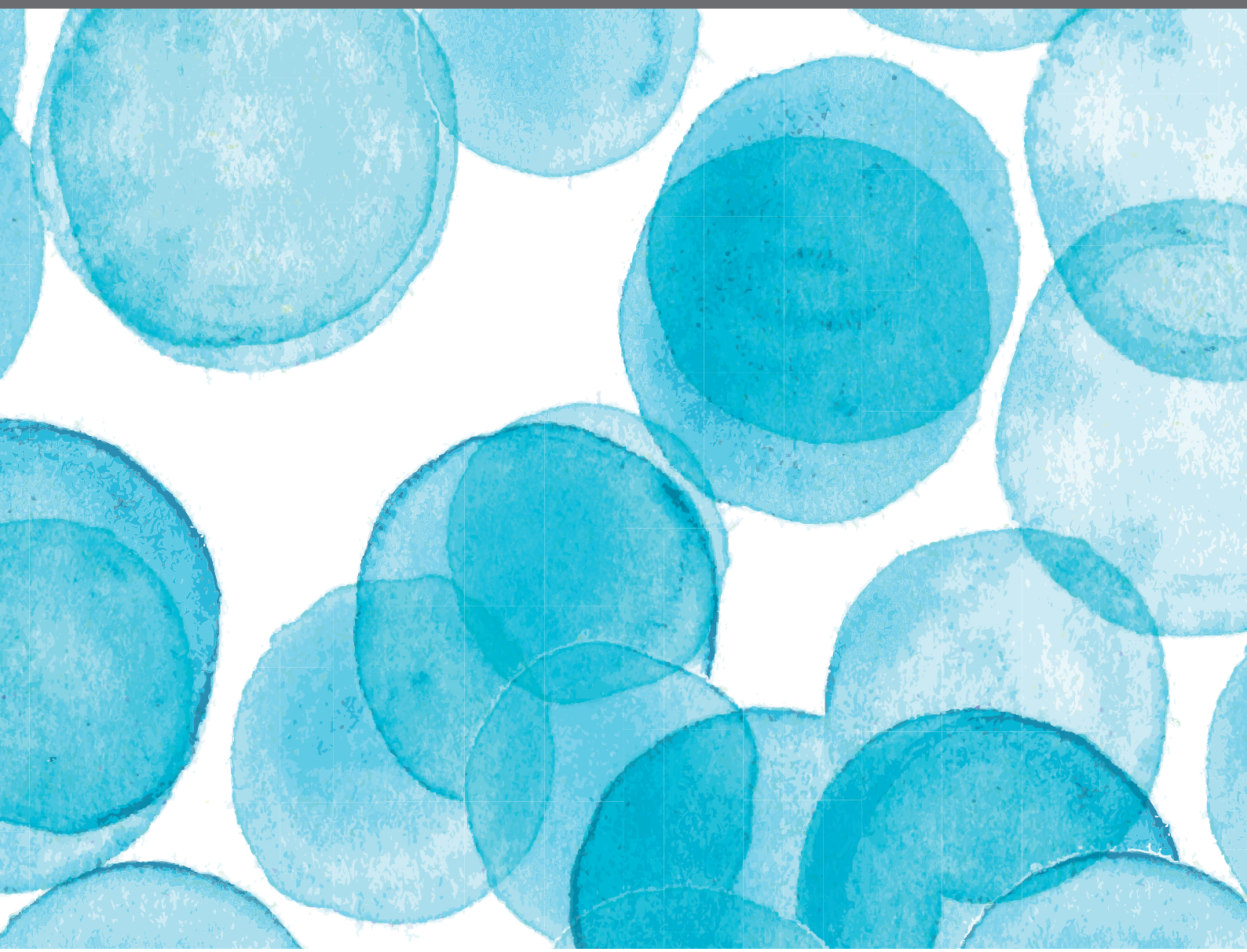

frontiers Research Topics

frontiers

ISSN 1664-8714
ISBN 978-2-83250-525-0
DOI 10.3389/978-2-83250-525-0

About Frontiers

Frontiers is more than just an open-access publisher of scholarly articles: it is a pioneering approach to the world of academia, radically improving the way scholarly research is managed. The grand vision of Frontiers is a world where all people have an equal opportunity to seek, share and generate knowledge. Frontiers provides immediate and permanent online open access to all its publications, but this alone is not enough to realize our grand goals.

Frontiers Journal Series

The Frontiers Journal Series is a multi-tier and interdisciplinary set of open-access, online journals, promising a paradigm shift from the current review, selection and dissemination processes in academic publishing. All Frontiers journals are driven by researchers for researchers; therefore, they constitute a service to the scholarly community. At the same time, the Frontiers Journal Series operates on a revolutionary invention, the tiered publishing system, initially addressing specific communities of scholars, and gradually climbing up to broader public understanding, thus serving the interests of the lay society, too.

Dedication to Quality

Each Frontiers article is a landmark of the highest quality, thanks to genuinely collaborative interactions between authors and review editors, who include some of the world's best academicians. Research must be certified by peers before entering a stream of knowledge that may eventually reach the public - and shape society; therefore, Frontiers only applies the most rigorous and unbiased reviews.
Frontiers revolutionizes research publishing by freely delivering the most outstanding research, evaluated with no bias from both the academic and social point of view. By applying the most advanced information technologies, Frontiers is catapulting scholarly publishing into a new generation.

What are Frontiers Research Topics?

Frontiers Research Topics are very popular trademarks of the Frontiers Journals Series: they are collections of at least ten articles, all centered on a particular subject. With their unique mix of varied contributions from Original Research to Review Articles, Frontiers Research Topics unify the most influential researchers, the latest key findings and historical advances in a hot research area! Find out more on how to host your own Frontiers Research Topic or contribute to one as an author by contacting the Frontiers Editorial Office: frontiersin.org/about/contact

WHAT IS KNOWN AND WHAT REMAINS TO BE DISCOVERED ABOUT BACTERIAL OUTER MEMBRANE VESICLES, VOLUME II

Topic Editors:
Araceli Contreras-Rodriguez, Instituto Politécnico Nacional (IPN), Mexico
Rafael A. Garduno, Retired Fredericton, Canada
Alejandro J. Yañez, Austral University of Chile, Chile

Citation: Contreras-Rodriguez, A., Garduno, R. A., Yañez, A. J., eds. (2022). What is Known and What Remains to Be Discovered About Bacterial Outer Membrane Vesicles, Volume II. Lausanne: Frontiers Media SA.
doi: 10.3389/978-2-83250-525-0

Table of Contents

frontiers | Frontiers in Microbiology

TYPE Editorial
PUBLISHED 03 October 2022
DOI 10.3389/fmicb.2022.929696

OPEN ACCESS

EDITED BY
Biswarup Mukhopadhyay,
Virginia Tech, United States

REVIEWED BY
Ulrike Kappler,
The University of Queensland, Australia

*CORRESPONDENCE
Araceli Contreras-Rodríguez
aracelicontreras21@gmail.com;
acontrerasr@ipn.mx

SPECIALTY SECTION
This article was submitted to Microbial Physiology and Metabolism, a section of the journal Frontiers in Microbiology

RECEIVED 27 April 2022
ACCEPTED 25 August 2022
PUBLISHED 03 October 2022

CITATION
Yañez A, Garduño RA and Contreras-Rodríguez A (2022) Editorial: What is known and what remains to be discovered about bacterial outer membrane vesicles, volume II. *Front. Microbiol.* 13:929696. doi: 10.3389/fmicb.2022.929696

Editorial: What is known and what remains to be discovered about bacterial outer membrane vesicles, volume II

Alejandro Yañez[1,2], Rafael A. Garduño[3] and Araceli Contreras-Rodríguez[4]*

[1]Facultad de Ciencias, Universidad Austral de Chile (INCAR), Valdivia, Chile, [2]Interdisciplinary Center for Aquaculture Research (INCAR), Concepción, Chile, [3]Department of Microbiology and Immunology, Dalhousie University and the Canadian Food Inspection Agency, Halifax, NS, Canada, [4]Departamento de Microbiología, Escuela Nacional de Ciencias Biológicas, Instituto Politécnico Nacional, Mexico City, Mexico

KEYWORDS

outer membrane vesicles, OMVs biogenesis, Gram-negative bacteria, OMVs, bacterial vesicles

Editorial on the Research Topic
What is known and what remains to be discovered about bacterial outer membrane vesicles, volume II

Introduction

In 2019–2020, Frontiers in Microbiology published a collection of 13 research articles and five reviews under Volume I of the specialized Research Topic entitled "What is Known and What Remains to be Discovered about Bacterial Outer Membrane Vesicles" (the collection of Volume I articles can be accessed at <What Is known and What Remains To Be Discovered About Bacterial Outer Membrane Vesicles | Frontiers Research Topic (frontiersin.org)>) (References to the 18 publications of Volume I are also given in the references section and grouped under the subsection "Volume I").

Given the success of Volume I of this Research Topic (reflected in a collective total of more than 100,000 online views) and the rapid scientific evolution of the subject area, it was decided in 2020 to launch Volume II. In this editorial, we, the topic editors of both volumes, present a bird's eye view of the seven original research articles and two reviews that compose the research collection published under Volume II in 2020–2021. The collection of Volume II articles can be accessed at <What is known and what remains to be discovered about bacterial outer membrane vesicles, Volume II|Frontiers Research Topic (frontiersin.org)>) (references to the nine publications of Volume II are also given in the references section and grouped under the subsection "Volume II").

Bacterial membrane vesicles at a glance

In the 1960s, some reports described the presence of "blebs" or "vesicles" released from the surface of the outer membrane of Gram-negative bacteria (Bayer and Anderson, 1965). It was then thought that outer membrane vesicles (OMVs) were fragments of lysed cells. However, over time, it was demonstrated that OMVs were actually formed at and released from live whole bacterial cells. Early electron microscopy observations showed the presence of numerous 50- to 300-nm spherical OMVs associated with whole bacterial cells, and their content was initially determined by SDS-PAGE (e.g., Gamazo and Moriyon, 1987). Since OMVs are formed from the outer membrane of Gram-negative bacteria, many components derive from this envelope and from the periplasm, including LPS, outer membrane proteins, and phospholipids. In early years of bacterial membrane vesicle research, no one thought that OMVs were relevant to the physiology and virulence of bacteria. However, historically, investigators have found toxins, hydrolases, and even nucleic acids contained in OMVs, which suggested potential roles of OMVs in pathogenesis and environmental fitness.

With the advent of more refined analytical tools (under the proteomics umbrella), it became possible to evaluate the complete protein composition of OMVs isolated from different bacteria, which in turn contributed to a better understanding of the complexity of these nanostructures (Langlete et al., 2019; Blackburn et al., 2021). One of the main discoveries made possible by the refinement afforded by proteomics is that the presence of proteins in vesicles is not randomly determined but instead proteins are targeted (directed), and their sorting is controlled by still ill-defined mechanisms.

All the new information has brought were new questions. What triggers the release of OMVs? How are proteins in OMVs selected? How does vesicle release occur without altering the integrity of the bacterial cell body? Why do OMVs transport virulence factors? Finally, what is the cell's purpose for releasing "custom-loaded" vesicles? The answers to these questions have been the focus of recent research efforts in different laboratories worldwide. Parts of this research effort constitute the core of the publications of Volume II of "What is Known and What remains to be Discovered about Bacterial Outer Membrane Vesicles", as summarized in the five themes presented below.

Biogenesis and stability of bacterial membrane vesicles

Vesicle formation requires the insertion of hydrophobic molecules into lipid bilayers that act as "wedges" and force the lipid bilayers to curve outward. The type and size of these wedge-type molecules, as well as the number of these molecules that get inserted, determine the size (diameter) and number of membrane vesicles formed. Therefore, a typical approach to determine the involvement of given molecules in the production (or origin/biogenesis) of vesicles is to simply observe changes in these physical properties (vesicle diameter and number of vesicles produced) in the presence or absence of such given molecules. Bacterial strains or mutants that produce an increased number of vesicles are called "hypervesiculating", and several vesicle biogenesis factors have been identified by studying hypervesiculating deletion mutants, for instance lipoproteins, OmpA, LPS, and phospholipids (Nagakubo et al., 2020; Ávila-Calderón et al., 2021). In the case of *Lysobacter* sp. strain XL1, it has been now established that the bacteriolytic enzyme AlpB (which forms part of the OMVs' cargo) plays a role in vesicle biogenesis, since deletion of the *alpB* gene alters the quantity and quality of OMVs produced by this bacterium (Kudryakova et al.). It is important to note here that because AlpB is part of the OMV cargo, it also plays a role in mediating microbe-microbe interactions, as will be explained in the next section.

Besides biomolecules, environmental physical factors can affect the production/biogenesis of OMVs as well as their stability and function. It is thus important to establish how membrane vesicles are affected by (and how stable they are under) different environmental conditions. For instance, it is known that stress factors like pH, temperature, oxidative stress, and even simulated extraterrestrial Mars-like stressors in the international space station, i.e., Martian pressure, atmosphere, and UV illumination, affect the biogenesis and (or) stability of vesicles produced by different bacteria (Klimentova et al., 2019; Podolich et al., 2020; Sarra et al., 2020). Shishpal et al. have demonstrated that in *Gardnerella vaginalis*, extracellular changes in pH result in (i) morphological changes in vesicles (shown by electron microscopy), (ii) altered protein composition of vesicles (showing the presence of protein chaperones), and (iii) loss of cytotoxicity of OMVs toward vaginal epithelial cells.

Finally, for *Shewanella vesiculosa,* a cold-adapted Antarctic bacterium that produces great quantities of vesicles, Baeza et al. performed high resolution flow cytometry, combined with cryo-electron microscopy, to demonstrate the production of several types of membrane vesicles including double-layered vesicles (known as inner-outer membrane vesicles) that contain DNA. These authors also found that the prophage-mediated explosive cell lysis in *S. vesiculosa* is key in mediating the biogenesis and release of single- and double-layered membrane vesicles, and proposed that the vesicles produced as a result of bacteriophage-mediated bacteriolysis have different properties than the vesicles produced by blebbing (Baeza et al.).

Bacterial membrane vesicles as mediators of microbe-microbe and microbe-host interactions

Vesicles are involved in microbe-microbe and microbe-host interactions (reviewed by Caruana and Walper, 2020). Bacteria may interact with other microorganisms playing the role of competitors (Knoke et al., 2020). In such interactions, the production and release of antimicrobial factors (e.g., antibiotics, cytolysins, or toxins) are key. The packaging of these antimicrobial factors into OMVs can increase their effectiveness. That is, instead of secreting free antimicrobials into the extracellular milieu (which can easily diffuse, get diluted, or be degraded), bacteria can keep these factors contained/protected in vesicles, which can then fuse with membranes of other microorganisms to produce effects (van den Berg van Saparoea et al., 2020). One example of this type of interaction is that mediated by membrane vesicles produced by *Lysobacter* sp. This bacterium produces vesicles loaded with the bacteriolytic enzyme AlpB, which besides playing a role in vesicle biogenesis (see previous section), is also responsible for killing competing bacteria (Kudryakova et al.).

The internalization of bacterial membrane vesicles by mammalian host cells is a typical microbe-host interaction mediated by vesicles, as previously demonstrated with vesicles produced by the intestinal commensal *Bacteroides thetaiotamicron* and are internalized by gastrointestinal tract cells (Jones et al., 2020). Now, it has been shown that the unusually shaped tubular OMVs released by the intracellular bacterial pathogen *Francisella tularensis* are internalized by bone-marrow-derived macrophages by micropinocytosis, chlatrin-mediated endocytosis, or lipid raft-dependent endocytosis. These tubular vesicles contain virulence factors and bacterial immunomodulatory proteins but, upon internalization, show no obvious cytotoxity toward macrophages. Instead, the internalized tubular vesicles induced pro-inflammatory responses in macrophages and appeared to somehow mediate the entry of this pathogen into macrophages (Pavkova et al.).

Role of bacterial membrane vesicles as immunogenic antigens

Through proteomics or by the use of specific antibodies, it has been determined that some bacterial protein antigens carried naturally into vesicles are able to elicit a protective immune response in mammalian hosts. Based on this finding, and the fact that the lipidic nature of membrane vesicles makes these nanostructures a natural delivery vehicle for antigens, membrane vesicles have been proposed as a platform for developing novel vaccines. Thus, the vesicles produced by a number of bacterial pathogens have been evaluated as acellular vaccines in animal models (e.g., Araiza-Villanueva et al., 2019; Aispuro et al., 2020; Ávila-Calderón et al., 2020). The flexibility/adaptability of OMV-based vaccines has now been demonstrated in vaccines against pertussis. Since the currently circulating clinical strains of *Bordetella pertussis* (the causal agent of pertussis or whooping cough) have an increased ability to form biofilms, Carriquiriborde et al. used OMVs produced by a clinical *B. pertussis* strain grown in biofilms to develop a 2nd-generation vaccine that not only is more effective than the vaccine based on OMVs produced by the planktonically-grown strain but also induces a tissue-resident memory immune response.

Although OMVs have advantages in the development of novel acellular vaccines, some methodological problems still need to be resolved, especially those related to vesicle yield during the purification process as well as reducing the presence of full-length immunotoxic LPS, which could induce an inflammatory reaction (and even shock) in the human host. Solutions for these imminent problems include the use of rough bacterial mutants (obtained by natural spontaneous mutations or by induced mutagenesis, which produces LPS lacking the O-antigen) (Araiza-Villanueva et al., 2019), and the development of novel production platforms to provide recombinant OMV-based vaccines using the generalized modules for membrane antigens (GMMA) approach, as explained in the thorough review of Mancini et al.

The two opposing roles of bacterial membrane vesicles in relation to infection treatments

Clinical bacterial infections are typically treated by use of antibiotics. Therefore, on the one hand, effective delivery of antibiotics (or alternate natural or synthetic antimicrobials) to bacterial pathogens would aid in treatment of infections. On the other hand, the emergence of antibiotic resistance in bacterial pathogens is a deterrent in treatment of clinical bacterial infections. Interestingly, there have been reports implicating OMVs as effective delivery vehicles of antibiotics like the bacteriocin-loaded OMVs of *Lactobacillus acidophilus* (Dean et al., 2020), as well as reports implicating OMVs in mediating the antibiotic resistance of bacterial pathogens (e.g., Vitse and Devreese, 2020), thereby establishing the opposing roles that OMVs could play in relation to infection treatments.

Now, the subject of using OMVs as delivery vehicles of antibiotics (and other naturally produced antimicrobials) has been reviewed comprehensively, establishing OMVs as tools for treatment of bacterial infections (Collins and Brown).

On the opposite side of the spectrum of bacterial infection treatments, it has now been demonstrated that OMVs from *Salmonella enterica* sv. Typhi can transiently transfer polymyxin

B resistance to susceptible bacteria in cocultures. This finding is relevant since polymyxin is used as a clinical treatment for infections when other antimicrobial treatments fail to eradicate multi-resistant strains (Marchant et al.). The mechanism proposed by Marchant et al. involves sequestration by OMVs of a soluble polymyxin from the extracellular milieu rather than transfer of antimicrobial resistance genes *via* DNA-loaded OMVs.

The diversified cargo of OMVs includes DNA and RNA

As mentioned before, OMVs contain components of the outer membrane, as well as the periplasm. In this respect, proteins that have been secreted across the inner membrane into the periplasm of Gram-negative bacteria constitute a common OMV cargo. However, recently, it has been unequivocally shown that OMVs can carry DNA and(or) RNA (e.g., Ashrafian et al., 2019; Langlete et al., 2019; Ahmadi Badi et al., 2020). The demonstrated presence of DNA in membrane vesicles is indeed intriguing, and the current question researchers in this area are asking is how this large cytoplasmic molecule gets targeted, and transported into OMVs? Now, Aktar et al., using the non-mobilizable, high copy number plasmid pUC19 and hypervesiculating mutants of *Escherichia coli*, observed that defects in peptidoglycan synthesis (intrinsic by genetic defects or externally induced by addition of 1% glycine) are linked to the presence of increased copy numbers of pUC19 in membrane vesicles. These authors proposed that plasmid DNA reaches the bacterial membrane vesicles of peptidoglycan-defective *E. coli via* two possible routes (mechanisms). One route implies increased membrane permeation leading to leakage of cytoplasmic contents without lysis, and the other involves the formation of intermediate inner-outer membrane vesicles (Aktar et al.).

Conclusion

The information presented in this Research Topic regarding bacterial membrane vesicles, provide but a sample of the abundant literature derived from recent research efforts in the field. The five themes that we used to group the nine articles published under Volume II of this Research Topic represent forefront areas of the field, where most of the research activity is currently happening. It is therefore our privilege to present the nine articles of Volume II, which are in combination with the 18 articles published in Volume I and clearly show that this Research Topic is becoming increasingly exciting, touching on many aspects of bacterial physiology and bacteria-eukaryote interactions.

Author contributions

All authors listed have made substantial, direct, and intellectual contributions to the article and approved it for publication.

Funding

AC-R was supported by fellowships from COFAA-IPN, SIP-EDI, and SNI-CONACYT. This study was supported by grant FONDAP INCAR No. 15110027.

Acknowledgments

We sincerely thank all the authors and reviewers who contributed to this topic.

Conflict of interest

The authors declare that the research was conducted in the absence of any commercial or financial relationships that could be construed as a potential conflict of interest.

Publisher's note

References

Ahmadi Badi, S., Bruno, S. P., Moshiri, A., Tarashi, S., Siadat, S. D., and Masotti, A. (2020). Small RNAs in outer membrane vesicles and their function in host-microbe interactions. *Front. Microbiol.* 11, 1209. doi: 10.3389/fmicb.2020.01209

Aispuro, M. P., Ambrosis, N., Zurita, M. E., Gaillard, M. E., Bottero, D., and Hozbor, D. F. (2020). Use of a neonatal-mouse model to characterize vaccines and strategies for overcoming the high susceptibility and severity of pertussis in early life. *Front. Microbiol.* 11, 723. doi: 10.3389/fmicb.2020.00723

Araiza-Villanueva, M., Avila-Calderón, E. D., Flores-Romo, L., Calderón-Amador, J., Sriranganathan, N., Qublan, H. A., et al. (2019). Proteomic analysis of membrane blebs of*Brucella abortus*2308 and RB51 and their evaluation as an acellular vaccine. *Front. Microbiol.* 10, 2714. doi: 10.3389/fmicb.2019.02714

Ashrafian, F., Shahriary, A., Behrouzi, A., Moradi, H. R., Keshavarz Azizi Raftar, S., Lari, A., et al. (2019)*Akkermansiamuciniphila*-derived extracellular vesicles as a mucosal delivery vector for amelioration of obesity in mice. *Front. Microbiol.* 10, 2155. doi: 10.3389/fmicb.2019.02155

Ávila-Calderón, E. D., Medina-Chávez, O., Flores-Romo, L., Hernández-Hernández, J. M., Donis-Maturano, L., López-Merino, A., et al. (2020). Outer membrane vesicles from *Brucella melitensis*modulate immune response and induce cytoskeleton rearrangement in peripheral blood mononuclear cells. *Front. Microbiol.* 11, 556795. doi: 10.3389/fmicb.2020.556795

Ávila-Calderón, E. D., Ruiz-Palma Md, S., Aguilera-Arreola, M. G., Velázquez-Guadarrama, N., Ruiz, E. A., Gomez-Lunar, Z., et al. (2021). Outer membrane vesicles of gram-negative bacteria: an outlook on biogenesis. *Front. Microbiol.* 12, 557902. doi: 10.3389/fmicb.2021.557902

Bayer, M. E., and Anderson, T. F. (1965). The surface structure of *Escherichia coli*. *Proc Natl Acad Sci U S A*. 54, 1592–1599. doi: 10.1073/pnas.54.6.1592

Blackburn, S. A., Shepherd, M., and Robinson, G. K. (2021). Reciprocal packaging of the main structural proteins of type 1 fimbriae and flagella in the outer membrane vesicles of "wild type"*Escherichia coli* strains. *Front. Microbiol.* 12, 557455. doi: 10.3389/fmicb.2021.557455

Caruana, J. C., and Walper, S. A. (2020). bacterial membrane vesicles as mediators of microbe – microbe and microbe – host community interactions. *Front. Microbiol.* 11, 432. doi: 10.3389/fmicb.2020.00432

Dean, S. N., Rimmer, M. A., Turner, K. B., Phillips, D. A., Caruana, J. C., Hervey, W. J. I. V., et al. (2020). *Lactobacillus acidophilus* membrane vesicles as a vehicle of bacteriocin delivery. *Front. Microbiol.* 11, 710. doi: 10.3389/fmicb.2020.00710

Gamazo, C., and Moriyon, I. (1987). Release of outer membrane fragments by exponentially growing *Brucella melitensis* cells. *Infect. Immun.* 55, 609–615. doi: 10.1128/iai.55.3.609-615.1987

Jones, E. J., Booth, C., Fonseca, S., Parker, A., Cross, K., Miquel-Clopés, A., et al. (2020). The uptake, trafficking, and biodistribution of *Bacteroides thetaiotaomicron* generated outer membrane vesicles. *Front. Microbiol.* 11, 57. doi: 10.3389/fmicb.2020.00057

Klimentova, J., Pavkova, I., Horcickova, L., Bavlovic, J., Kofronova, O., Benada, O., et al. (2019). *Francisella tularensis* subsp. *holarctica* releases differentially loaded outer membrane vesicles under various stress conditions. *Front. Microbiol.* 10, 2304. doi: 10.3389/fmicb.2019.02304

Knoke, L. R., Abad Herrera, S., Götz, K., Justesen, B. H., Günther Pomorski, T., Fritz, C., et al. (2020). *Agrobacterium tumefaciens* small lipoprotein Atu8019 is involved in selective outer membrane vesicle (OMV) docking to bacterial cells. *Front. Microbiol.* 11, 1228. doi: 10.3389/fmicb.2020.01228

Langlete, P., Krabberød, A. K., and Winther-Larsen, H. C. (2019). Vesicles from *Vibrio cholera* contain AT-rich DNA and shorter mRNAs that do not correlate with their protein products. *Front. Microbiol.* 10, 2708. doi: 10.3389/fmicb.2019.02708

Nagakubo, T., Nomura, N., and Toyofuku, M. (2020). Cracking open bacterial membrane vesicles. *Front. Microbiol.* 10, 3026. doi: 10.3389/fmicb.2019.03026

Podolich, O., Kukharenko, O., Zaets, I., Orlovska, I., Palchykovska, L., Zaika, L., et al. (2020). Fitness of outer membrane vesicles from *Komagataeibacter intermedius*Is altered under the impact of simulated mars-like stressors outside the international space station. *Front. Microbiol.* 11, 1268. doi: 10.3389/fmicb.2020.01268

Sarra, A., Celluzzi, A., Bruno, S. P., Ricci, C., Sennato, S., Ortore, M. G., et al. (2020). Biophysical characterization of membrane phase transition profiles for the discrimination of outer membrane vesicles (OMVs) from *Escherichia coli* grown at different temperatures. *Front. Microbiol.* 11, 290. doi: 10.3389/fmicb.2020.00290

van den Berg van Saparoea, H. B., Houben, D., Kuijl, C., Luirink, J., and Jong, W. S. P. (2020). Combining protein ligation systems to expand the functionality of semi-synthetic outer membrane vesicle nanoparticles. *Front. Microbiol.* 11, 890. doi: 10.3389/fmicb.2020.00890

Vitse, J., and Devreese, B. (2020). The contribution of membrane vesicles to bacterial pathogenicity in cystic fibrosis infections and healthcare associated pneumonia. *Front. Microbiol.* 11, 630. doi: 10.3389/fmicb.2020.00630

frontiers in Microbiology

ORIGINAL RESEARCH
published: 05 May 2021
doi: 10.3389/fmicb.2021.672467

"One for All": Functional Transfer of OMV-Mediated Polymyxin B Resistance From *Salmonella enterica* sv. Typhi Δ*tolR* and Δ*degS* to Susceptible Bacteria

Pedro Marchant[1], Alexander Carreño[2], Eduardo Vivanco[1], Andrés Silva[1], Jan Nevermann[1], Carolina Otero[3], Eyleen Araya[4], Fernando Gil[5,6], Iván L. Calderón[7]* and Juan A. Fuentes[1]**

[1] Laboratorio de Genética y Patogénesis Bacteriana, Departamento de Ciencias Biológicas, Facultad de Ciencias de la Vida, Universidad Andres Bello, Santiago, Chile, [2] Facultad de Ciencias Exactas, Center of Applied NanoSciences (CANS), Universidad Andres Bello, Santiago, Chile, [3] Escuela de Química y Farmacia, Facultad de Medicina, Universidad Andres Bello, Santiago, Chile, [4] Departamento de Ciencias Químicas, Facultad de Ciencias Exactas, Universidad Andres Bello, Santiago, Chile, [5] Microbiota-Host Interactions and Clostridia Research Group, Universidad Andres Bello, Santiago, Chile, [6] ANID-Millennium Science Initiative Program-Millennium Nucleus in the Biology of the Intestinal Microbiota, Santiago, Chile, [7] Laboratorio de RNAs Bacterianos, Departamento de Ciencias Biológicas, Facultad de Ciencias de la Vida, Universidad Andres Bello, Santiago, Chile

OPEN ACCESS

Edited by:
Alejandro J. Yañez, Austral University of Chile, Chile

Reviewed by:
Yan Zhu, Monash University, Australia
Paola Sperandeo, University of Milan, Italy

***Correspondence:**
Fernando Gil
fernandogil@unab.cl
Iván L. Calderón
lcalderon@unab.cl
Juan A. Fuentes
jfuentes@unab.cl

Specialty section:
This article was submitted to Microbial Physiology and Metabolism, a section of the journal Frontiers in Microbiology

Received: *25 February 2021*
Accepted: *12 April 2021*
Published: *05 May 2021*

Citation:
Marchant P, Carreño A, Vivanco E, Silva A, Nevermann J, Otero C, Araya E, Gil F, Calderón IL and Fuentes JA (2021) "One for All": Functional Transfer of OMV-Mediated Polymyxin B Resistance From Salmonella enterica sv. Typhi ΔtolR and ΔdegS to Susceptible Bacteria. Front. Microbiol. 12:672467. doi: 10.3389/fmicb.2021.672467

The appearance of multi-resistant strains has contributed to reintroducing polymyxin as the last-line therapy. Although polymyxin resistance is based on bacterial envelope changes, other resistance mechanisms are being reported. Outer membrane vesicles (OMVs) are nanosized proteoliposomes secreted from the outer membrane of Gram-negative bacteria. In some bacteria, OMVs have shown to provide resistance to diverse antimicrobial agents either by sequestering and/or expelling the harmful agent from the bacterial envelope. Nevertheless, the participation of OMVs in polymyxin resistance has not yet been explored in *S.* Typhi, and neither OMVs derived from hypervesiculating mutants. In this work, we explored whether OMVs produced by the hypervesiculating strains *Salmonella* Typhi Δ*rfaE* (LPS synthesis), Δ*tolR* (bacterial envelope) and Δ*degS* (misfolded proteins and σ^E activation) exhibit protective properties against polymyxin B. We found that the OMVs extracted from *S.* Typhi Δ*tolR* and Δ*degS* protect *S.* Typhi WT from polymyxin B in a concentration-depending manner. By contrast, the protective effect exerted by OMVs from *S.* Typhi WT and *S.* Typhi Δ*rfaE* is much lower. This effect is achieved by the sequestration of polymyxin B, as assessed by the more positive Zeta potential of OMVs with polymyxin B and the diminished antibiotic's availability when coincubated with OMVs. We also found that *S.* Typhi Δ*tolR* exhibited an increased MIC of polymyxin B. Finally, we determined that *S.* Typhi Δ*tolR* and *S.* Typhi Δ*degS*, at a lesser level, can functionally and transiently transfer the OMV-mediated polymyxin B resistance to susceptible bacteria in cocultures. This work shows that mutants in genes related to OMVs biogenesis can release vesicles with improved abilities to protect bacteria against membrane-active agents. Since mutations affecting OMV biogenesis can involve the bacterial envelope, mutants with increased resistance to

membrane-acting agents that, in turn, produce protective OMVs with a high vesiculation rate (e.g., *S.* Typhi Δ*tolR*) can arise. Such mutants can functionally transfer the resistance to surrounding bacteria via OMVs, diminishing the effective concentration of the antimicrobial agent and potentially favoring the selection of spontaneous resistant strains in the environment. This phenomenon might be considered the source for the emergence of polymyxin resistance in an entire bacterial community.

Keywords: *Salmonella* Typhi, outer membrane vesicles, OMVs, polymyxin, *rfaE*, *degS*, *tolR*, antibiotic resistance

INTRODUCTION

Salmonella enterica serovar Typhi (*S.* Typhi) is the etiologic agent of typhoid fever in humans, a disease producing hundreds of deaths worldwide per year, especially in developing countries (Ajibola et al., 2018; Bhutta et al., 2018; Johnson et al., 2018). *S.* Typhi infection begins with the ingestion of contaminated water or food (Hook et al., 1990). Bacteria reach the small intestine and promote their internalization through intestinal epithelial cells and the M cells of the Peyer's patches, reaching the underlying lymphoid tissue. At this point, bacteria are disseminated to deep organs inside dendritic cells, macrophages, or neutrophils (Galan, 1996; Miao et al., 2003), allowing the systemic bacterial spread (typhoid fever). During the infection, host cells from the innate immune defense respond to bacterial elements [e.g., lipopolysaccharides (LPS)], producing cationic antimicrobial peptides (<100 amino acids), which interact with the anionic bacterial membranes to produce microbial death (Hancock and Scott, 2000; Zasloff, 2002).

The full progression of typhoid fever was commonly observed in the pre-antibiotic era. Nevertheless, the emergence of multi-resistant strains represents a severe problem, with an increased recurrence rate of the disease (Als et al., 2018; Schwartz and Morris, 2018). The appearance of multidrug-resistant strains introduced the use of quinolones (Parry et al., 2013; Karkey et al., 2018), albeit the appearance of quinolone-resistance variants led to increased use of azithromycin and third-generation cephalosporins (Pandit et al., 2007; Karkey et al., 2018). Unfortunately, *S.* Typhi strains that produce extended-spectrum β-lactamase have been increasingly reported (Ahamed Riyaaz et al., 2018; Karkey et al., 2018). This scenario underlines the importance of studying antibiotic resistance in *S.* Typhi.

The appearance of multi-resistant strains (Payne et al., 2007; Kumarasamy et al., 2010; Cornaglia et al., 2011) contributed to reintroducing polymyxins (cationic peptides) as the last-line therapy when more commonly used antibiotics are inefficient (Velkov et al., 2013; Garg et al., 2017). It is generally accepted that polymyxins exert their antimicrobial activity by first interacting with the outer-membrane components of Gram-Negative bacteria. Polymyxins are peptides carrying a hydrophobic acyl tail with positively charged residues (Daugelavicius et al., 2000). Due to their cationic and amphipathic nature, polymyxins electrostatically interact with the negatively charged lipopolysaccharides (LPS). Interestingly, evidence shows that a fluorescent polymyxin derivative can also bind to unspecified outer membrane proteins (van der Meijden and Robinson, 2015), strongly suggesting that polymyxins interact with different kinds of molecules in the outer membrane of Gram-negative bacteria. At this point, the "self-promoted uptake" occurs, a process based on the presence of the hydrophobic acyl tail of polymyxin, enabling polymyxin to insert into the outer membrane by displacing membrane-stabilizing cationic ions, such as Ca^{2+} and Mg^{2+}, and interacting with the lipid A, a recognized polymyxin-binding target in the outer membrane (Velkov et al., 2010; Trimble et al., 2016). Polymyxin insertion in the outer membrane weakens the packing of contiguous lipid A, disrupting the permeability barrier (Falagas and Kasiakou, 2006; Velkov et al., 2013; Trimble et al., 2016). Although subsequent steps are not fully elucidated, the evidence argues for the fusion of the inner membrane's outer leaflets with the outer membrane's inner leaflet to form pores, leading to an osmotic imbalance and a subsequent death (Daugelavicius et al., 2000). At present, an increasing number of reports regarding polymyxin resistance are being published (Li et al., 2019). Some chromosomal mutations have been associated with increased resistance to polymyxins, including modifications of the *pmrCAB* and *phoPQ* operons, among other genes (Li et al., 2019). In *Salmonella enterica* and *Escherichia coli*, many of those mutations lead to LPS modifications, decreasing the anionic charges and diminishing the electrostatic binding of polymyxin to bacterial outer membranes (Li et al., 2019). Nevertheless, the spread of polymyxin resistance has been only associated with the transferable gene *mcr*, which encodes a phosphoethanolamine transferase that modifies the lipid A (Olaitan et al., 2014). Although significant advances in understanding polymyxin-resistance mechanisms have been made, this area needs further research.

OMVs are nanosized proteoliposomes formed and secreted from the outer membrane of Gram-negative bacteria (Kulp and Kuehn, 2010). OMVs biogenesis mainly relies on (1) changes in LPS composition, (2) the dissociation of the outer membrane in specific zones, and (3) accumulation of misfolded proteins in the periplasm (Kulp and Kuehn, 2010; Kulkarni and Jagannadham, 2014). OMVs play different roles in the bacterial life cycle, such as delivering proteins and defense against harmful agents such as phages and antibiotics, among other functions (Kulp and Kuehn, 2010; Jan, 2017). OMVs contribute to resistance to diverse molecules with antimicrobial properties either by sequestering ("decoy") and/or expelling the harmful agent from the bacterial envelope. Some examples include resistance to toluene in *Pseudomonas putida*, chlorhexidine in *Porphyromonas gingivalis,* and polymyxins in *Escherichia coli* (Grenier et al., 1995; Kobayashi et al., 2000; Manning and Kuehn, 2011; Roszkowiak et al., 2019). In this context, the

participation of OMVs in polymyxin resistance has not yet been explored in *S.* Typhi, and neither OMVs derived from hypervesiculating mutants.

A recent study screened 15,000 mutants searching for genes involved in OMVs biogenesis in *S.* Typhi (Nevermann et al., 2019). *S.* Typhi Δ*rfaE*, Δ*tolR*, and Δ*degS* showed some of the most potent hypervesiculation phenotypes compared with the wild type (WT) (Nevermann et al., 2019). In particular, the *rfaE* (*waaE*) gene product is thought to be involved in the formation of ADP-L-glycero-D-manno-heptose of LPS. *Salmonella* Typhimurium Δ*rfaE* mutants synthesize heptose-deficient LPS, exhibiting only lipid A and 3-deoxy-D-manno-octusolonic (KDO) acid (Jin et al., 2001). TolR is an inner membrane protein belonging to the trans-envelope Tol-Pal complex, highly conserved in Gram-negative bacteria (Sturgis, 2001). In *E. coli*, TolR contributes to maintaining the envelope structure and participates in the retrograde phospholipid transport (Muller et al., 1993; Boags et al., 2019). In *E. coli*, DegS is a serine protease harboring a PDZ domain that inhibits the protease activity in the absence of stress (Alba et al., 2001). Under stress, mainly due to overexpression of outer membrane proteins, misfolded proteins accumulate in the periplasm, activate the DegS protease activity to cleave the anti-sigma factor RseA, releasing σ^E. In *Salmonella* Typhimurium, σ^E is required under envelope stress and in the presence of antimicrobial peptides (Testerman et al., 2002; Palmer and Slauch, 2020).

In this work, we explored the protective effect of OMVs produced by *S.* Typhi WT, Δ*rfaE*, Δ*tolR,* and Δ*degS*. Besides, we tested whether the polymyxin resistance can be functionally transferred to polymyxin-susceptible bacteria. We found that *S.* Typhi OMVs protect bacteria against polymyxin B in a concentration-dependent manner by sequestering the antibiotic, where OMVs from *S.* Typhi Δ*tolR* and Δ*degS* showed the highest protection levels. OMVs from *S.* Typhi Δ*tolR* also protected *Candida albicans* against limonene, a membrane-active antimicrobial agent. Finally, we found that *S.* Typhi Δ*tolR* and, at a lesser level, *S.* Typhi Δ*degS* can functionally transfer the OMV-mediated polymyxin B resistance to susceptible bacteria. This study underlines that some mutations affecting vesiculation in a population can increase polymyxin resistance in a bacterial community.

MATERIALS AND METHODS

Bacterial Strains, Media, and Culture Conditions

Salmonella Typhi strain STH2370 (*S.* Typhi WT) was used as parental strain (Valenzuela et al., 2014). *S.* Typhi Δ*rfaE*::FRT, Δ*tolR*::FRT, and Δ*degS*::FRT were previously reported (Nevermann et al., 2019). *S.* Typhimurium LT2 *ompD*::Mu*d*-J (Lac^+) was kindly provided by Dr. Guido Mora (Santiviago et al., 2003). Strains were routinely grown in liquid culture using Luria Bertani medium (Bacto peptone, 10 g/L; Bacto yeast extract, 5 g/L; NaCl, 5 g/L; prepared in phosphate buffer pH 7.0) at 37 °C with shaking. When required, the medium was supplemented with X-gal (5-bromo-4-chloro-3-indolyl-β-D-galactopyranoside) (40 μg/mL) and/or agar (15 g/L). *Candida albicans* corresponds to a clinical isolate from the Hospital Clínico de la Universidad de Chile (Carreno et al., 2018; Carreño et al., 2021). Yeasts were cultured in Sabouraud agar (Bacto peptone, 10 g/L; glucose, 40 g/L; agar, 15 g/L; pH 5.6) at 28°C.

OMV Isolation, Quantification, and Size Measurement

To isolate OMVs (Liu et al., 2016b; Nevermann et al., 2019), bacteria were grown in LB at 37 °C with shaking (OD_{600} = 1.1) before being centrifuged 10 min at 5,400 × *g* at 4°C. The pellet was discarded, and the supernatant was filtered (0.45 μm), ultrafiltered (Ultracel® 100 kDa ultrafiltration discs, Amicon® Bioseparations), and ultracentrifuged 3 h at 150,000 × *g* at 4°C. The supernatant was discarded, and the pellet was resuspended in 1 mL DPBS (Dulbecco's phosphate-buffered saline) (Gibco). OMVs were stored at −20°C until their use. We quantified OMV yield by determining the protein content (BCA assay) and/or the lipid content (FM4-64 molecular probe) (McBroom et al., 2006; Deatherage et al., 2009). We determined OMV size as described (Deatherage et al., 2009; Nevermann et al., 2019). Results were presented as the diameter, classified into the median (P50), and P25 and P75.

Transmission Electron Microscopy (TEM)

OMV extracts were bound to formvar-coated slot grids, stained with 1% aqueous uranyl acetate for 1 min, and viewed with a Philips Tecnai 12 (Biotwin) transmission electron microscope, as described (Nevermann et al., 2019).

Determination of Zeta Potential

The Zeta potential of OMVs was measured at room temperature (25°C) by a Zetasizer Nano series MPT-Z multi Purpose Titrator (Malvern, United Kingdom). The device was equipped with a Helium-Neon laser (633 nm) as a light source. The detection angle of Zetasizer at aqueous media was 173.13° (measurement range: 0.3 nM—10 μm diameter). Capillary cells DTS 1070 were used. To measure the Zeta potential, polymyxin B and OMVs were resuspended in Mili-Q water.

Determination of Minimal Inhibitory Concentration (MIC)

Minimum inhibitory concentration (MIC) was obtained by broth dilution as described (Cuenca-Estrella et al., 2003), with modifications. Briefly, bacteria and yeast were previously cultured as described above. Microorganisms were then diluted in PBS (0.5 McFarland) and then diluted again (1000-fold) in LB for bacteria or Bacto Tryptic Soy broth (Sigma Aldrich) for yeasts, before seeding a 96-well plate. In each well, 180 μL of this dilution was placed, along with 10 μL polymyxin B sulfate (AppliChem GmbH), ciprofloxacin (Sigma Aldrich) or (*R*)-(+)-limonene [(+)-*p*-mentha-1,8-diene,(+)-carvene,(*R*)-4-isopropenyl-1-methyl-1-cyclohexene] (Sigma Aldrich) (stock prepared in 95% ethanol) to achieve a final known concentration, and 10 μL DBPS. When indicated, the 10 μL DBPS were replaced by 10 μL of purified OMVs to achieve a final known

concentration. Alternatively, and when indicated, the 10 μL DBPS were replaced by 10 μL of bacterial supernatant. To obtain the supernatant, bacteria were cultured in LB as stated above (OD_{600} = 1.0–1.3), centrifuged 10 min at 5,400 × *g* at 4°C, the pellet was discarded, and the supernatant fraction was filtered (0.45 μm). The 96-well plates were incubated overnight at 37°C (bacteria) or 24 h at 28°C (yeasts). The MIC was determined by OD_{600} measurement and corroborated by visual inspection and plating onto agar plates.

Estimation of Polymyxin Sequestration by OMVs

To determine Zeta potential changes due to the interaction with polymyxin B, OMV extracts (50 μg/mL) were mixed with 0, 5, 50, or 100 μg/mL polymyxin B and incubated 30 min at 37°C with gentle agitation. The mixture was ultrafiltered in Ultracel® 100 kDa ultrafiltration column (Amicon® Bioseparations) at 5,400 × *g* for 10 min to remove the unbound polymyxin B. The ultrafiltrated obtained with 100 μg/mL polymyxin B was reserved (see below). OMVs were resuspended in 1 volume of Mili-Q water before measuring the Zeta potential. As control of polymyxin B removal, we measured the Zeta potential of water alone (−0.05 ± 0.35 mV), water + 100 μg/mL polymyxin B (5.57 ± 2.98 mV), and water + 100 μg/mL polymyxin ultrafiltered and resuspended in 1 volume of Mili-Q water (0.73 ± 0.43 mV). To estimate the relative amount of polymyxin B sequestered by OMVs, the reserved ultrafiltered was diluted 10 times in LB and then serially diluted in LB to determine the last dilution that inhibited the *S.* Typhi WT growth. As a control, we used a solution with no OMVs.

Protection Assay of a Reporter Strain ("One for All")

Approximately 5 × 10^5 CFU/mL of *S.* Typhi WT or mutant derivatives were mixed with 5 × 10^6 CFU/mL of *S.* Typhimurium *ompD*::Mu*d*-J. Bacteria were previously washed three times with PBS to remove all the accumulated OMVs and resuspended in LB. This mixture was incubated 0 (with no incubation), 1 or 2 h at 37°C with shaking before adding polymyxin B (final concentration: 2.5 μg/mL). Bacterial mixtures were incubated at 37°C with shaking overnight, and CFUs were counted on LB agar with X-gal (*S.* Typhi strains: white colonies, *S.* Typhimurium reporter strain: blue colonies). Alternatively, the serovar was corroborated by PCR (Fuentes et al., 2008) for some colonies. As a control, the strains were tested separately under this same procedure.

Determination of μ and t_d

Bacteria were cultured in LB as described above, and OD_{600} was recorded every 10 min to construct a growth curve. To calculate μ and t_d, we used:

$$\mu = \frac{\ln(N) - \ln(N)_0}{t - t_0}$$

$$t_d = \frac{0.693}{\mu} \times 60$$

Where μ (h^{-1}): growth rate; *N*: bacteria at the end of the logarithmic phase (OD_{600}); N_0 bacteria at the beginning of the logarithmic phase (OD_{600}); *t*: time at the end of the logarithmic phase (h); t_0: time at the end of the logarithmic phase (h); t_d: duplication time (min).

LPS Profile Determination

To observe the LPS profile of OMVs, we followed a protocol previously reported (Kulikov et al., 2019). OMVs were extracted as described above prior to being mixed with 1 volume of lysis buffer (2% w/v of SDS, 4% v/v of 2-mercaptoethanol, 10% v/v glycerol, 1 M Tris-HCl pH 6.8, and 0.05% w/v bromophenol blue). The mixture was incubated at 95 °C for 10 min, cooled to room temperature, and 10 μL of 2.5 mg/mL Proteinase K solution made in the lysis buffer was added before being incubated at 56°C for 1 h in a heating shaker. The preparation obtained was directly loaded on a conventional protein SDS polyacrylamide gel with 12% acrylamide (19:1 acrylamide:bisacrylamide), and it was run at a constant 20 mA current in Tris-glycine-SDS buffer. In order to observe the LPS profile, the gel was treated with fixer-oxidizer solution (40% v/v ethanol, 5% v/v acetic acid, 1% w/v sodium periodate, Milli-Q water up to 1 v) and incubated for 15 min. Then, the gel was washed three times with distilled water (7 min each time). The gel was treated with the stain solution (15 mL Milli-Q water, 1.4 mL 0.1 M NaOH, 100 μL concentrated 35% w/w ammonia, 250 μL of 20% silver nitrate) for 10 min in an orbital shaker (75 rpm). The solution was removed before washing the gel three times with distilled water (15 s each time). After all washes, a pre-warmed 40 °C developer solution (100 μL 3% citric acid, 25 μL 30% formaldehyde, 50 mL Milli-Q water) was added and incubated in darkness. When the bands were visible, the developer solution was removed, and the gel was washed with distilled water.

RESULTS

Characteristic of OMVs Extracted From *S.* Typhi WT and Hypervesiculating Mutant Derivatives

To show some features of the OMVs under study, we characterize them by TEM, showing different morphologies and abundance (**Figure 1**). In addition, we determined their size (**Table 1**), showing that the OMVs from *S.* Typhi Δ*tolR* and Δ*degS* present a bigger size than OMVs from *S.* Typhi WT and Δ*rfaE*. Also, we determined the Zeta potential, where OMVs from *S.* Typhi Δ*degS* showed a more negative value. Previously, it has been reported that these OMVs present different protein content (Nevermann et al., 2019), which could contribute to such differences. All these results show the OMVs under study present distinct features.

OMVs Obtained From *S.* Typhi Mutants Increased the MIC of Polymyxin B in a Concentration-Dependent Manner

OMVs contribute to the resistance against some antimicrobial compounds, including polymyxin in *Escherichia coli* and

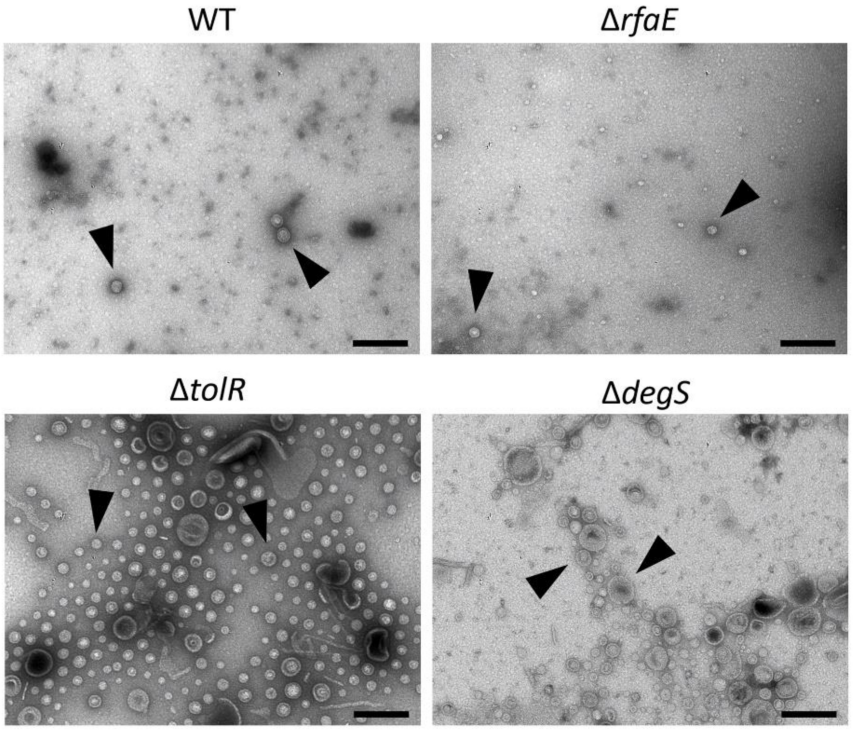

FIGURE 1 | OMVs produced by *S.* Typhi WT, Δ*rfaE*, Δ*tolR*, and Δ*degS* mutants. Bacteria were grown in LB to OD_{600} = 1.0 before extracting OMVs. OMV extracts were observed by transmission electron microscopy (TEM). Arrowheads show OMVs. The black bar corresponds to 200 nm. In all cases, the horizontal field width and the magnification corresponded to 1.5 μm and 60,000×, respectively. In each case, a representative experiment is shown (*n* = at least 3).

Pseudomonas aeruginosa (Grenier et al., 1995; Kobayashi et al., 2000; Manning and Kuehn, 2011; Roszkowiak et al., 2019). In this context, we determined the MIC of polymyxin B for *S.* Typhi WT in the presence OMVs extracted from *S.* Typhi WT, Δ*rfaE*, Δ*tolR*, or Δ*degS*. As shown in **Figures 2A,B**, the presence of OMVs from *S.* Typhi Δ*tolR* or Δ*degS* increased the MIC of polymyxin B for *S.* Typhi WT (˜0.3125 μg/mL) 3–8 times. Nevertheless, OMVs extracted from *S.* Typhi WT or *S.* Typhi Δ*rfaE* did not significantly increase the MIC of polymyxin B. As a control, we tested whether purified OMVs could protect against ciprofloxacin, a quinolone that inhibits DNA gyrase and topoisomerase IV (Zhang et al., 2018), i.e., it is not a membrane-active antibiotic. As shown in **Figure 2C**, the presence of OMVs did not increase the MIC of ciprofloxacin for *S.* Typhi WT. To determine whether the OMVs can protect against other membrane-acting antimicrobials, we tested the limonene's antifungal effect. Limonene is a monoterpene that induces membrane stress in *Candida albicans*, producing oxidative stress leading to DNA damage and apoptosis (Thakre et al., 2021). **Figure 2D** shows that only the presence of OMVs extracted from *S.* Typhi Δ*tolR* increased the MIC of limonene. The other OMV extracts showed no effect in this case. All these results show that OMVs from *S.* Typhi Δ*tolR* and Δ*degS* protect *S.* Typhi WT against polymyxin B, and OMVs *S.* Typhi Δ*tolR* protects *Candida albicans* against limonene.

TABLE 1 | Some characteristics of OMVs used in this study.

Source of OMVs	OMV diameter (nm) Median (P50)[a]	OMV diameter (nm) P25	OMV diameter (nm) P75	Zeta potential (mV)[b]
S. Typhi WT	25	20	28	−13.50 ± 2.07
S. Typhi Δ*rfaE*	22	19	28	−12.35 ± 1.44
S. Typhi Δ*tolR*	41***	36	45	−11.30 ± 1.22
S. Typhi Δ*degS*	54***	43	65	−20.15 ± 0.89*

n = at least 3.
*[a]Kruskal-Wallis, Dunn as a post hoc test, ***p < 0.001. The analysis refers to differences in the size among different OMVs, not only to the median.*
*[b]One-way ANOVA, Tukey as a post hoc test, *p < 0.05.*

To establish whether OMVs offer concentration-dependent protection against polymyxin B, we tested the MIC in the presence of increasing concentrations of OMVs. As shown in **Figure 3**, augmenting the concentration of OMVs from *S.* Typhi WT or *S.* Typhi Δ*rfaE* bearly increased the MIC of polymyxin B, even with the highest concentrations tested. By contrast, the presence of OMVs from *S.* Typhi Δ*tolR* or *S.* Typhi Δ*degS* showed a high protective effect, increasing almost linearly the protection under the range of concentration tested. The concentration-dependence protection against polymyxin B

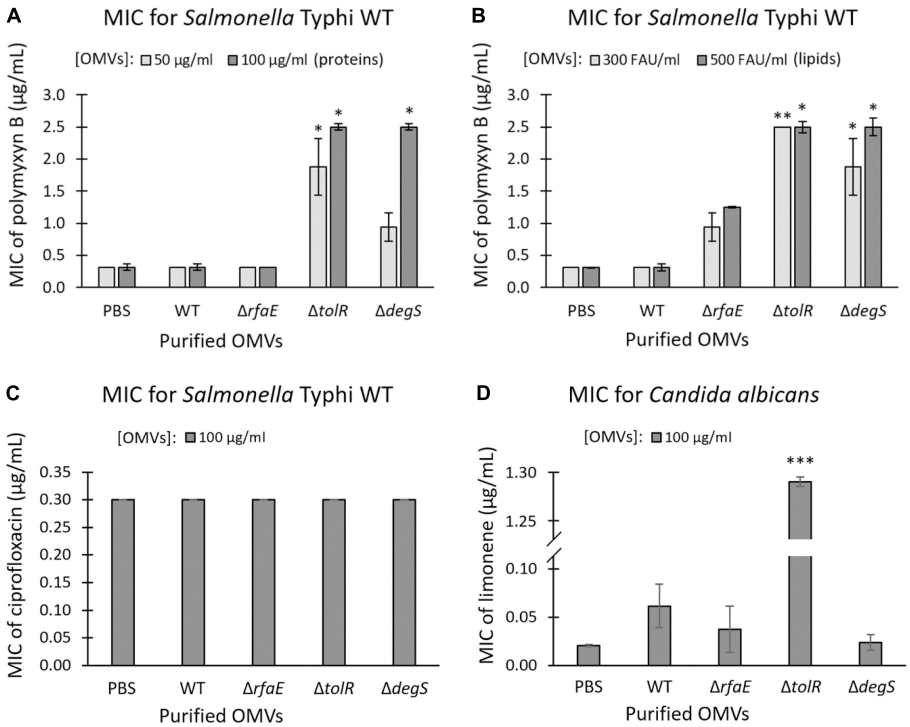

FIGURE 2 | Purified OMVs from *S.* Typhi mutant derivatives contributed to the resistance of polymyxin B and limonene. MIC of polymyxin B for *S.* Typhi WT supplemented with OMVs extracted from *S.* Typhi WT, Δ*rfaE*, Δ*tolR,* or Δ*degS* **(A,B)**. OMV concentration was standardized as protein **(A)** or lipide content **(B)** and expressed as the final concentration. **(C)** MIC of ciprofloxacin for *S.* Typhi WT supplemented with OMVs extracted from *S.* Typhi WT, Δ*rfaE*, Δ*tolR,* or Δ*degS*. OMVs were standardized by protein content. **(D)** MIC of limonene for a clinical isolate of *Candida albicans* supplemented with OMVs extracted from *S.* Typhi WT, Δ*rfaE*, Δ*tolR,* or Δ*degS*. OMVs were standardized by protein content. In all cases, PBS was used as the negative control. FAU: Fluorescent arbitrary units obtained with the FM4-64 probe (Nevermann et al., 2019) as a measure of lipid concentration. (*n* = at least 4; bars represent the standard error; One-way ANOVA, Tukey as a *post hoc* test, $*p < 0.05$; $**p < 0.01$; $***p < 0.001$; compared with PBS).

offered by OMVs (especially OMVs extracted from *S.* Typhi Δ*tolR* and Δ*degS*) is consistent with the role of OMVs capturing polymyxin B and decreasing its effective concentration.

OMVs From *S.* Typhi Exert Their Protective Effect by Sequestering Polymyxin B

Previous works showed that OMVs from *Escherichia coli* and *Pseudomonas aeruginosa* sequester polymyxin B, decreasing the free concentration of the antibiotic (Kulkarni et al., 2015; Roszkowiak et al., 2019). The Zeta potential has been used as an indicator of interaction between bacterial membranes or OMVs with polymyxin B (Halder et al., 2015; Roszkowiak et al., 2019). Usually, OMVs present a negative Zeta potential, which can be depolarized by the interaction with cationic peptides such as polymyxin B. Thus, we mixed 50 µg/mL OMVs obtained from *S.* Typhi WT or mutant derivatives with polymyxin B. The mixture was incubated for 30 min at 37°C, and then ultrafiltered to remove any unbound polymyxin B prior to determining the Zeta potential of OMVs. As shown in **Figure 4**, the presence of polymyxin B tended to neutralize the Zeta potential of OMVs in a concentration-dependent manner, showing that the antibiotic remained retained by the vesicles. Interestingly, only OMVs from *S.* Typhi Δ*tolR* showed a significant depolarization with the lowest concentration tested. In all other cases, significant depolarization was achieved only with 50 µg/mL polymyxin B. This result suggests that OMVs from *S.* Typhi Δ*tolR* have a higher affinity for polymyxin B, plausibly removing more efficiently the polymyxin B from the medium and lowering the effective concentration.

To estimate the relative amount of polymyxin B sequestered by OMVs, we mixed 50 µg/mL OMVs extracted by *S.* Typhi WT or mutant derivatives with 100 µg/mL polymyxin B. We incubated for 30 min at 37 °C with gentle shaking before discarding the OMVs by ultrafiltration. To determine the relative amount of the unbound polymyxin B, the ultrafiltered fraction was diluted 10-fold in LB and then serially diluted in LB prior to being seeded with *S.* Typhi WT. The inhibition of bacterial growth was used as an indicator for the presence of polymyxin B. **Table 2** shows that all the OMVs decreased the effective concentration of polymyxin B compared to the control. Furthermore, OMVs showed differential polymyxin-B sequestration abilities, in decreasing order: OMVs from Δ*tolR*, Δ*degS*, Δ*rfaE*, and WT. These results agree with those showing the protective effect of OMVs (**Figure 3**) and the Zeta potential determination (**Figure 4**). We obtained similar results when we

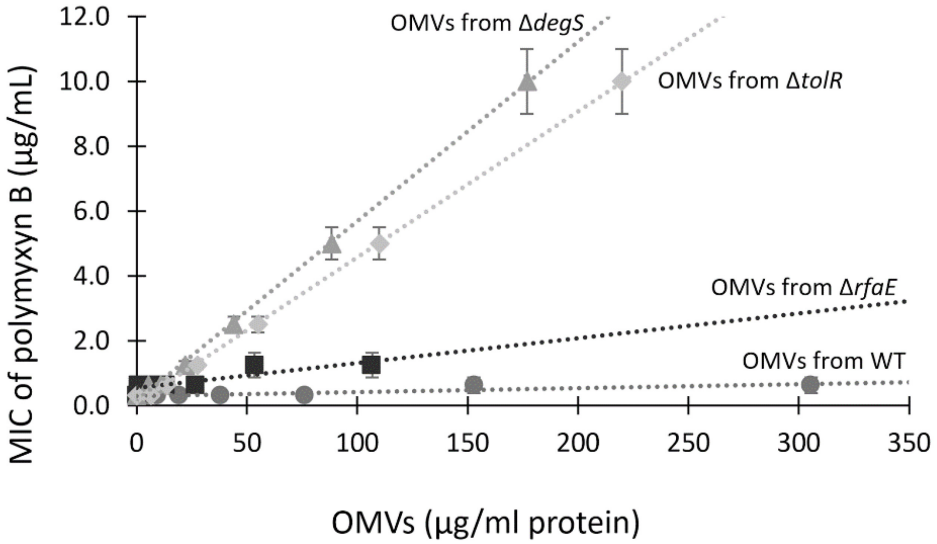

FIGURE 3 | The MIC of polymyxin B depends on the concentration of OMVs. MIC of polymyxin B for *S.* Typhi WT was determined in the presence of different known concentrations of OMVs. Linear trend lines are represented by dotted lines (n = at least 4; bars represent the standard error).

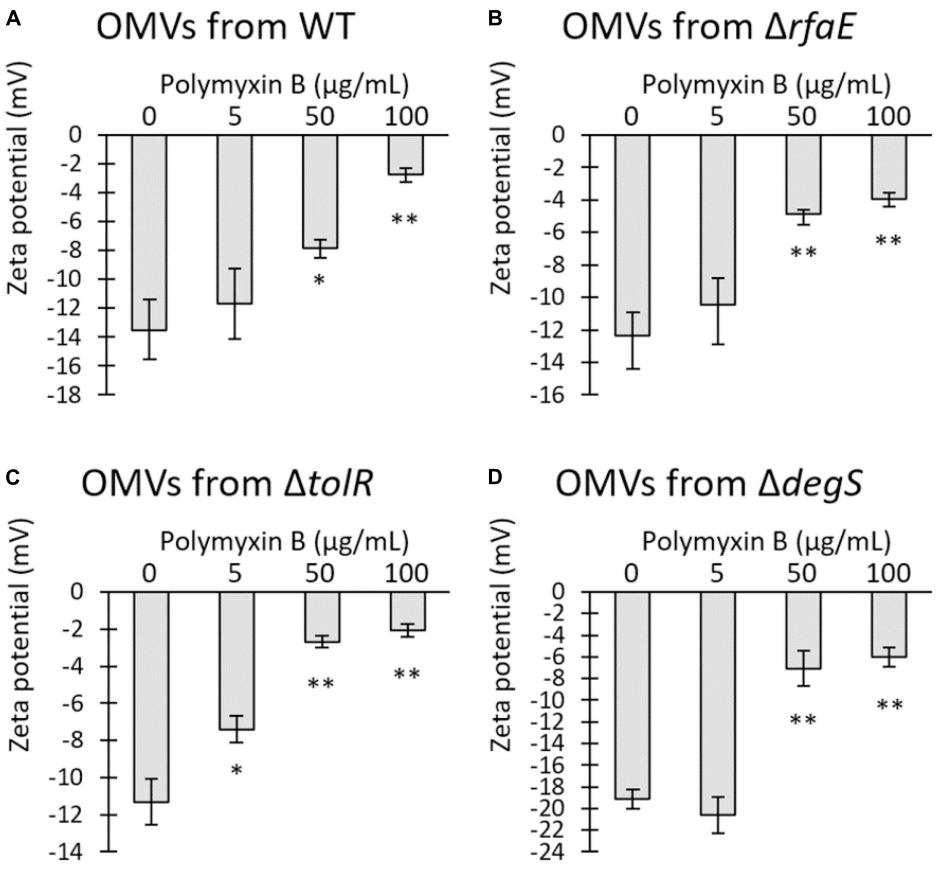

FIGURE 4 | Polymyxin B interacts with OMVs from *S.* Typhi, depolarizing the Zeta potential of OMVs. Increasing concentrations of polymyxin B were mixed with 50 µg/mL OMVs obtained from *S.* Typhi WT **(A)**, Δ*rfaE* **(B)**, Δ*tolR* **(C)**, or Δ*degS* **(D)**. The mixture was incubated for 30 min at 37 °C and ultrafiltered to remove the unbound polymyxin B prior to determining the Zeta potential. (n = 3, bars represent standard error, One-way ANOVA, Tukey as a *post hoc* test, $^{*}p < 0.05$; $^{**}p < 0.01$; compared the control with no polymyxin B).

determined the sequestration of polymyxin B by *S.* Typhi WT and mutant derivatives instead of OMVs (**Supplementary Figure 1**).

Thus, all these results together show that OMVs from *S.* Typhi exert their protective effect against polymyxin B by sequestering the antibiotic. Moreover, the OMVs from *S.* Typhi WT and mutant derivative are not equivalent, showing that mutations affecting different processes associated with OMV biogenesis generate OMVs with diverse properties.

S. Typhi Δ*tolR* and Δ*degS* Can Functionally Transfer Their Polymyxin Resistance to Polymyxin-Susceptible Bacteria

Our results show that purified OMVs from *S.* Typhi Δ*tolR* and Δ*degS* exert the highest protective effect against polymyxin B. In this context, we wondered whether the amount of OMVs present in the supernatant of these mutants is sufficient to protect against polymyxin B. Thus, we determined the MIC of polymyxin B for *S.* Typhi WT in the presence of supernatant from *S.* Typhi WT, Δ*rfaE*, Δ*tolR,* or Δ*degS*. We added 10 μL of the corresponding filtered supernatant to a final volume of 200 μL to determine the MIC of polymyxin B. As shown in **Figure 5A**, the supernatant of *S.* Typhi Δ*tolR* and Δ*degS*, diluted 20 times, was sufficient to increase two-fold the MIC of polymyxin B. By contrast, the supernatant obtained from *S.* Typhi WT or Δ*rfaE* showed no noticeable effects. Since OMVs are produced and released to the supernatant fraction during the normal bacterial growth (Kulp and Kuehn, 2010), we hypothesized that the *S.* Typhi Δ*tolR* and *S.* Δ*degS* mutants might protect surrounding bacteria against polymyxin B by producing and releasing protective OMVs. However, to exert a protective effect, OMV-producing bacteria should present an increased MIC to polymyxin B in order to reproduce and release sufficient OMVs to achieve the OMV-mediated protection. Thus, we determined the MIC of polymyxin B for the strains under study. As shown in **Figure 5B** (light gray bars), *S.* Typhi Δ*rfaE* and Δ*degS* exhibited a diminished MIC of polymyxin B (30% and 20% the MIC of the *S.* Typhi WT, respectively) (see a summary in **Table 3**). By contrast, *S.* Typhi Δ*tolR* showed a twofold increased MIC of polymyxin B. When we determined the MIC of polymyxin B but using 10-fold less diluted bacteria (dark gray bars), we found an increased resistance in all cases. Nevertheless, we observed a higher increase with the *S.* Typhi Δ*tolR* strain, which exhibited 10.7 times the MIC of the WT under the same conditions. Since polymyxin B can remain attached to biological membranes exerting a detergent-like effect (Velkov et al., 2013; Roszkowiak et al., 2019), it was expected that the MIC of polymyxin B would increase with a higher bacterial concentration. However, we postulate that the more notorious MIC rise showed by *S.* Typhi Δ*tolR*, compared with the WT, can also be explained by protective OMVs in the bacterial inoculum.

TABLE 2 | Bioassay to determine the relative amount of polymyxin B in a solution previously incubated with OMVs extracted from *S.* Typhi WT or derivatives.

Source of OMVs	Last dilution that inhibited the *S.* Typhi WT growth (% v/v)[a]
No OMVs (control)	0.3
S. Typhi WT	1.3
S. Typhi Δ*rfaE*	2.5
S. Typhi Δ*tolR*	10.0
S. Typhi Δ*degS*	5.0

[a] *50 μg/mL OMVs were mixed with 100 μg/mL polymyxin B, incubated 30 min at 37°C with gentle shaking. OMVs were removed by ultrafiltration. Then, the filtrated was serially diluted in LB before being seeded with S. Typhi WT as a bioindicator for the presence of polymyxin B. n = 3 (this is a representative experiment).*

To test the resistance of *S.* Typhi and the most potent hypervesiculating strains (*S.* Typhi Δ*tolR* and Δ*degS*) with an alternative procedure, we performed a challenge with a high polymyxin B concentration (2.5 μg/mL, corresponding to 8 times the MIC of the WT). To that aim, the strains (OD_{600} = ∼1.2) were washed three times and diluted in fresh LB to remove all OMVs previously accumulated in the supernatant (input). Then, bacteria were resuspended directly in LB supplemented with 2.5 μg/mL polymyxin B (time 0 h) or incubated in LB alone for 1 or 2 h at 37 °C with shaking to allow OMVs accumulation, before adding 2.5 μg/mL polymyxin. Bacteria were then incubated overnight at 37 °C with shaking prior to determining the final CFU/mL (output). As shown in **Figure 6A**, we were unable to recover colonies when we added polymyxin B immediately after washing (0 h), plausibly due to the absence of OMVs exerting a protective effect. However, when bacteria were incubated in LB for 1 or 2 h before adding polymyxin B, we could recover *S.* Typhi Δ*tolR*. We also recovered *S.* Typhi Δ*degS* but only after 2 h of incubation in LB before the polymyxin-B challenge. This result could be explained by accumulating protective OMVs during the incubation in LB prior to adding polymyxin B. The differences between *S.* Typhi Δ*tolR* and Δ*degS* strains can be attributed to their MIC of polymyxin B. By contrast, we could not recover *S.* Typhi WT after the challenge with polymyxin B, even after 2 h of incubation in LB.

If the growth of *S.* Typhi Δ*tolR* and Δ*degS* after the challenge with polymyxin B involves OMVs, this resistance should be functionally and transiently transferred to susceptible bacteria since OMVs are diffusible elements. Thus, we tested whether mutants can protect a polymyxin-susceptible strain (*S.* Typhimurium *ompD*::Mu*d*-J, Lac^+) in an assay that we denominated "one for all." *S.* Typhimurium *ompD*::Mu*d*-J has a MIC of polymyxin B corresponding to around twice the MIC exhibited by *S.* Typhi WT (∼0.625 μg/mL, **Figure 5**). In addition, we could not recover colonies of this strain in the challenge with 2.5 μg/mL, even after 2 h of incubation in LB before adding the antibiotic (**Figure 6A**), demonstrating its susceptibility to polymyxin B under the tested conditions. To perform the protection assay, *S.* Typhi WT, Δ*tolR*, or Δ*degS* were cultured, washed and diluted as described above, and mixed with *S.* Typhimurium *ompD*::Mu*d*-J (also washed and diluted) before the challenge with 2.5 μg/mL polymyxin B. The output was determined by plating onto LB with X-gal (white colonies: *S.* Typhi WT or mutant derivatives, blue colonies: *S.* Typhimurium *ompD*::Mu*d*-J). As shown in **Figure 6B**, *S.* Typhi WT could not protect the reporter strain even after 2 h of incubation in LB before adding polymyxin B and vice-versa.

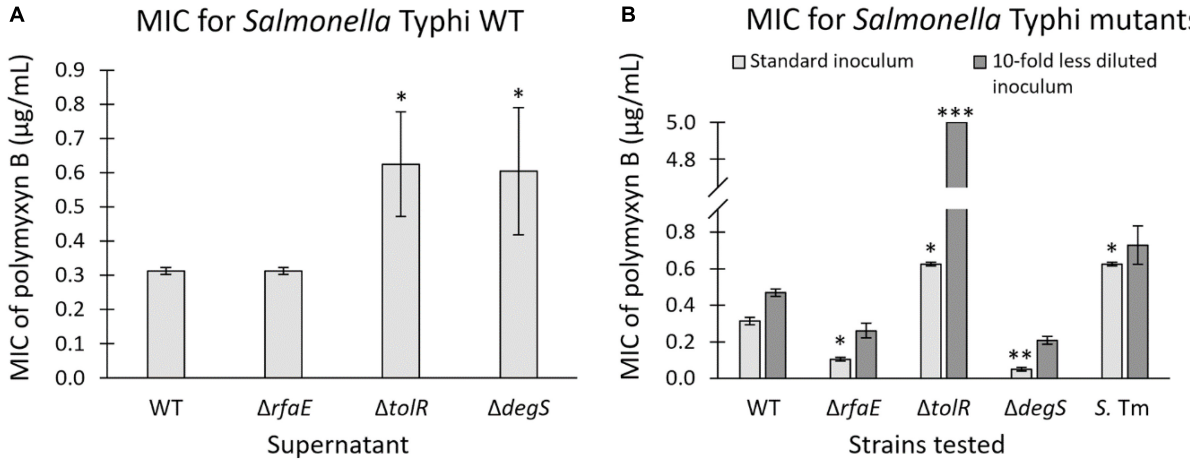

FIGURE 5 | (A) MIC of polymyxin B for *S.* Typhi WT in the presence of supernatant (1:20 v/v) of *S.* Typhi WT, Δ*rfaE*, Δ*tolR,* or Δ*degS*. Supernatants were obtained from bacteria grown in LB at 37°C with shaking (OD_{600}: 1.0–1.3). (*n* = at least 4). **(B)** MIC of polymyxin B of strains *S.* Typhi WT, Δ*rfaE*, Δ*tolR* or Δ*degS*, and *S.* Typhimurium LT2 *ompD*::Mu*dJ* (*S.* Tm). We used two bacterial concentrations to seed the wells for the MIC determination (*n* = at least 4). In all cases, bars represent the standard error; One-way ANOVA, Tukey as a *post hoc* test, *$p < 0.05$; **$p < 0.01$; ***$p < 0.001$; compared with *S.* Typhi WT under the same condition.

In the *S.* Typhi Δ*tolR* + *S.* Typhimurium *ompD*::Mu*d*-J mixture, we observed that *S.* Typhi Δ*tolR* could resist the polymyxin challenge after 1 o 2 h of preincubation in LB. Accordingly, only the presence of *S.* Typhi Δ*tolR* efficiently protected the susceptible reporter strain since no colonies were seen with no preincubation (0 h) (**Figure 6C**). Consistent with a higher accumulation of protective OMVs, the mixture incubated for 2 h before the challenge with polymyxin B showed the highest protection for *S.* Typhi Δ*tolR* and *S.* Typhimurium *ompD*::Mu*d*-J.

Finally, the mixture of *S.* Typhi Δ*degS* + *S.* Typhimurium *ompD*::Mu*d*-J showed colonies of both bacteria only after 2 h of preincubation in LB (**Figure 6D**). Again, we attribute this result to the accumulation of protective OMVs. Despite the high degree of protection provided by OMVs from *S.* Typhi Δ*degS*, the lower protective effect of such mutant is consistent with its lower MIC of polymyxin B, compared with *S.* Typhi Δ*tolR*.

S. Typhimurium *ompD*::Mu*d*-J recovered after the challenge showed an unaffected MIC of polymyxin (∼0.625 µg/mL), showing that the protection received by *S.* Typhi Δ*tolR* or Δ*degS* is transient and could not be attributed to genetic changes (**Table 3**). Besides, it is important to state that the obtained results cannot be attributed to a faster-growing phenotype of *S.* Typhi Δ*tolR* or *S.* Typhi Δ*degS* (**Table 4**).

At this point, OMVs extracted from *S.* Typhi Δ*tolR* and Δ*degS* showed the most noticeable protective effect against polymyxin B. This result suggests that their compositions are different from the OMVs produced by the WT. Previously, it has been reported that the protein cargo of OMVs from *S.* Typhi WT, Δ*tolR*, and Δ*degS* are different among them (Nevermann et al., 2019). Since LPS is crucial regarding polymyxin interaction, we assessed the LPS profile in these OMVs to complement this information. As shown in **Figure 7** and **Supplementary Figure 2**, the LPS profile of OMVs extracted from *S.* Typhi Δ*tolR* and Δ*degS* present a distinct pattern. These differences could also be contributing to the protective effect of these OMVs against polymyxin B.

All these results show that a susceptible strain efficiently can grow in the presence of a high amount of polymyxin B when is cocultured with a hypervesiculating strain producing protective OMVs. We observed this protective effect even with *S.* Typhi Δ*degS*, which presents a very low MIC of polymyxin B when this mutant encounters conditions that allow OMVs accumulation. This protective effect is more potent with a strain exhibiting a higher MIC of polymyxin B, as shown with *S.* Typhi Δ*tolR*.

DISCUSSION

In this work, we found that the OMVs from *S.* Typhi WT and mutant derivatives exert a protective effect against polymyxin B, albeit the OMVs from *S.* Typhi Δ*tolR* and Δ*degS* were much more protective. Furthermore, we found that *S.* Typhi Δ*tolR* (and at a lesser degree, *S.* Typhi Δ*degS*) can functionally transfer the polymyxin-resistance to susceptible bacteria, plausibly via OMVs. To our knowledge, this is the first report exploring

TABLE 3 | MIC of polymyxin B for strains used in this study.

Strain	MIC of polymyxin B (µg/mL) ± SE
S. Typhi WT	0.31 ± 0.03
S. Typhi Δ*rfaE*	0.10 ± 0.05
S. Typhi Δ*tolR*	0.63 ± 0.08
S. Typhi Δ*degS*	0.05 ± 0.03
S. Typhimurium *ompD*::Mu*dJ*	0.63 ± 0.05
S. Typhimurium *ompD*::Mu*dJ* colonies recovered after de "one for all assay" (representative data of one colony)	0.63 ± 0.07

SE, Standard error; n = at least 4.

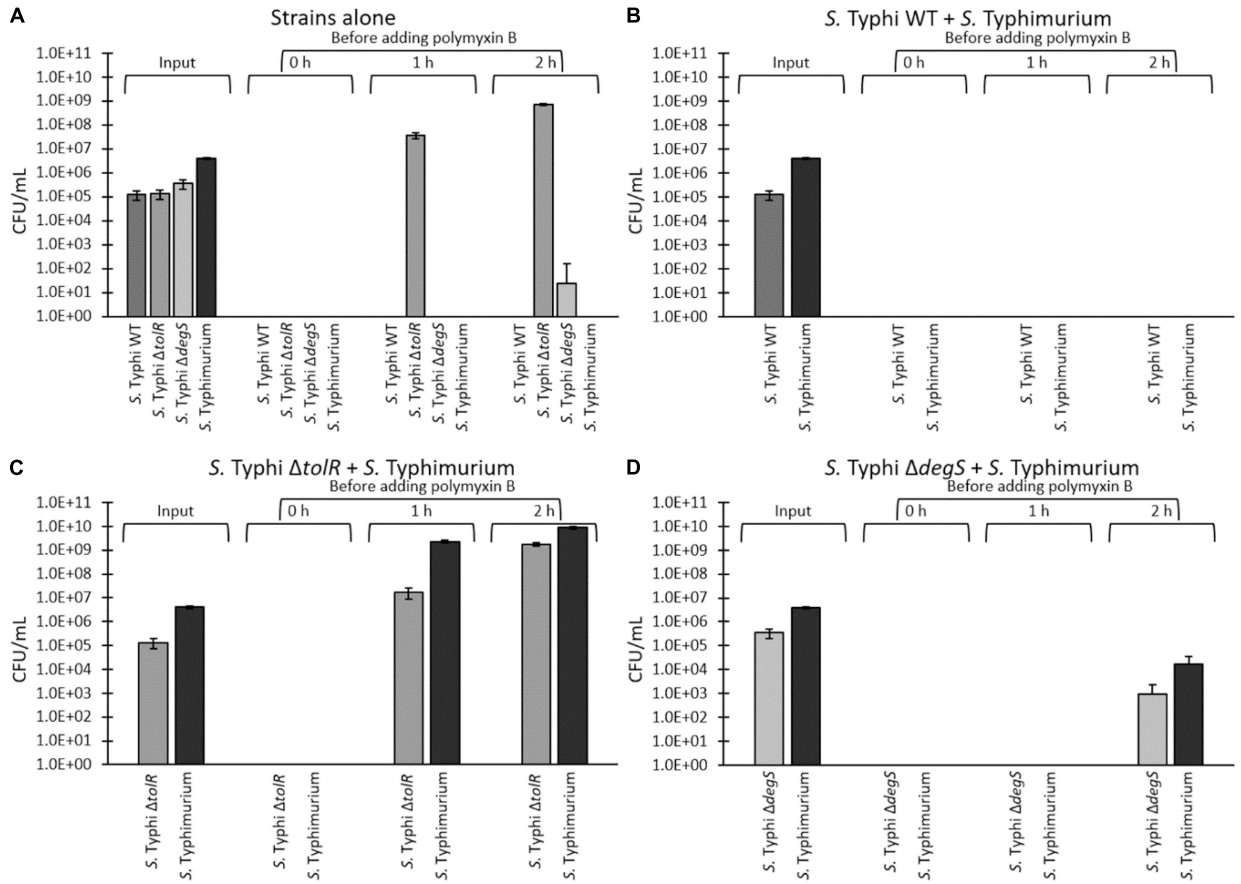

FIGURE 6 | "One for all" assay of a challenge with 2.5 μg/mL polymyxin B. *S.* Typhi WT, Δ*tolR*, Δ*degS,* and *S.* Typhimurium *ompD*::Mu*d*-J (Lac$^+$) were washed and diluted in LB to remove OMVs, and incubated in LB at 37°C with shaking for 0, 1, or 2 h at 37°C to allow OMVs accumulation, before adding polymyxin B (final concentration of 2.5 μg/mL, corresponding to 8 times the MIC of *S.* Typhi WT). Bacteria were incubated with polymyxin B overnight at 37°C with shaking prior to determining the CFU/mL (output). **(A)** Strains were challenged separately. **(B)** *S.* Typhi WT and *S.* Typhimurium *ompD*::Mu*d*-J were mixed (1:10) before the challenge. **(C)** *S.* Typhi Δ*tolR* and *S.* Typhimurium *ompD*::Mu*d*-J were mixed (1:10) before the challenge. **(D)** *S.* Typhi Δ*degS* and *S.* Typhimurium *ompD*::Mu*d*-J were mixed (1:10) before the challenge. To determine the CFU/mL, bacteria were plated onto LB supplemented with X-gal (white colonies: *S.* Typhi WT or derivatives, blue colonies: *S.* Typhimurium *ompD*::Mu*dJ*). Alternatively, the serovar was corroborated by a PCR for the SPI-18 as previously described (Fuentes et al., 2008). (In all cases, *n* = at least 4).

OMVs from *S.* Typhi as protective agents against antimicrobial agents. Furthermore, this is the first study showing that OMVs obtained by different genetic backgrounds exhibit, in turn, different protective effects.

We found that the presence of purified OMVs exerted a protective effect against polymyxin B and limonene but not against ciprofloxacin. Both polymyxin B and limonene exert their antimicrobial effect by interacting with biological membranes, while ciprofloxacin targets gyrase and topoisomerase IV (Velkov et al., 2013; Zhang et al., 2018; Thakre et al., 2021). OMVs from *E. coli* can protect against membrane-active antibiotics, i.e., polymyxin B, colistin (polymyxin E) and melittin, but no against antibiotics with other targets, such as ciprofloxacin, streptomycin and trimethoprim (Manning and Kuehn, 2011; Kulkarni et al., 2015). Although polymyxin B and limonene do not share structural similarities, their modes of action require the interaction with biological membranes, suggesting that the protection exerted by *S.* Typhi OMVs is based on an unspecific mechanism involving membranes. In this sense, this work showed that OMVs from *S.* Typhi and mutant derivatives sequester polymyxin B and remove it from the solution. The fact

TABLE 4 | Growth rate (μ) and duplication time (t_d) of *S.* Typhi strains used in this study.

Strain	μ (h^{-1}) ± SE[a]	t_d (min) ± SE[a]	p^b
S. Typhi WT	1.532 ± 0.052	27.246 ± 0.967	–
S. Typhi Δ*rfaE*	1.539 ± 0.049	27.090 ± 0.846	ns
S. Typhi Δ*tolR*	1.480 ± 0.085	28.393 ± 1.765	ns
S. Typhi Δ*degS*	1.432 ± 0.067	29.235 ± 1.437	ns

Strains were cultured in LB at 37°C with shaking. Bacterial growth was assessed by measuring OD_{600} over time.

[a]*n = 4 (with 8 technical replicates). SE, standard error.*

[b]*One-way ANOVA, with Tukey as post hoc test. ns = non-significative compared with S. Typhi WT.*

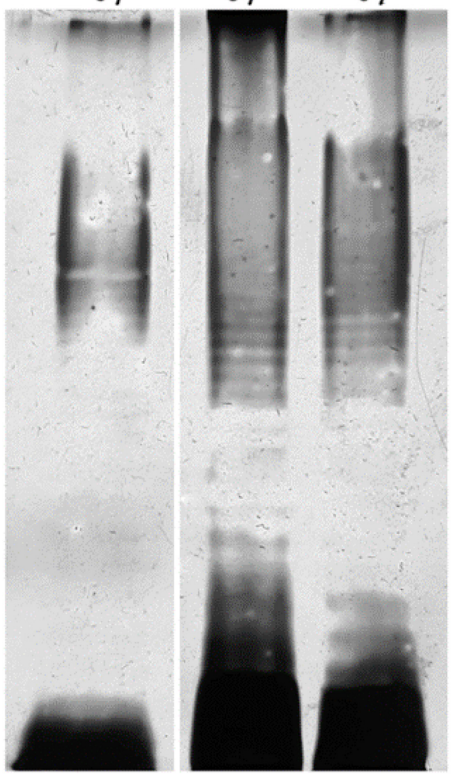

FIGURE 7 | LPS of OMVs extracted from *S.* Typhi WT, Δ*tolR*, and Δ*degS*. OMVs were extracted as described, and the LPS profile was resolved as described in section "Materials and Methods." In each lane, 40 μg/mL (proteins) of OMVs were loaded.

that OMVs increased the MIC of polymyxin B in a concentration-dependent manner supports this assertion. Furthermore, in the present manuscript, the sequestration of polymyxin B by OMVs was shown by measuring the Zeta potential of OMVs exposed to polymyxin B and determining the polymyxin B activity that remained after coincubating with OMVs. A similar strategy was previously used to demonstrate the sequestration of polymyxin B by *Pseudomonas aeruginosa* OMVs (Roszkowiak et al., 2019), and this same mechanism was also shown in *E. coli* (Kulkarni et al., 2015). The data that we obtained with the Zeta potential agrees with the bioassay designed to assess the polymyxin B removed by OMVs, where we found that all OMVs tested showed the ability to decrease the amount of effective polymyxin B. According to our results and previous works showing the sequestration of polymyxin B by OMVs from other bacteria (Kulkarni et al., 2015; Roszkowiak et al., 2019), the most straightforward explanation is that OMVs from *S.* Typhi sequester polymyxin B. However, we cannot rule out that other mechanisms were also acting. Kulkarni et al. (2015) showed that OMVs from *Escherichia coli* sequester both colistin and melittin. Furthermore, they demonstrated that the OMVs from *Escherichia coli* also degrade melittin, but not colistin (Kulkarni et al., 2015). Thus, determining whether OMVs from *S.* Typhi can degrade polymyxin B, as an additional mechanism, remains to be elucidated.

A previous study showed that OMVs from *S.* Typhi WT, Δ*rfaE*, Δ*tolR*, and Δ*degS* present different features, such as size and protein content (Nevermann et al., 2019). Besides, *rfaE*, *tolR,* and *degS* are genetic determinants of three different processes involved in OMV biogenesis (Schwechheimer and Kuehn, 2015; Nevermann et al., 2019). It has been shown that mutations affecting different OMV biogenesis processes produce OMVs with different cargo (Altindis et al., 2014; Bonnington and Kuehn, 2014; Murphy et al., 2014; Schwechheimer and Kuehn, 2015). For these reasons, it was postulated that OMVs from *S.* Typhi WT, Δ*rfaE*, Δ*tolR*, and Δ*degS* should present different properties regarding biological functions (Nevermann et al., 2019). As stated above, polymyxin B, a cationic amphipathic peptide, can interact with negatively charged LPS, as well as with proteins, to get inserted into the outer membrane, interacting with the lipid A (Daugelavicius et al., 2000; Falagas and Kasiakou, 2006; Velkov et al., 2013; van der Meijden and Robinson, 2015; Trimble et al., 2016). Since OMVs are discharged from the outer membrane, mutations affecting the bacterial envelope also affect the OMV content, including both LPS and proteins (Kim et al., 2009; Liu et al., 2016a), potentially affecting the polymyxin—OMVs interaction or affinity. In the present manuscript, we found apparent differences among mutants, where OMVs can be sorted in decreasing protective effect as OMVs from *S.* Typhi Δ*tolR*, Δ*degS*, Δ*rfaE*, and WT. Why OMVs from *S.* Typhi Δ*tolR* showed the most potent protective effect against polymyxin B could be attributed to their higher affinity by polymyxin B as the Zeta potential measurement suggests and the sequestration bioassay showed.

Previously published works support the high affinity showed by OMVs from *S.* Typhi Δ*tolR* shown in the present study. The *tolR* gene encodes an inner membrane protein of the trans-envelope Tol-Pal complex (Sturgis, 2001). In *E. coli and S.* Typhimurium, TolR participates in maintaining the envelope structure and retrograde phospholipid transport (Muller et al., 1993; Masilamani et al., 2018; Boags et al., 2019). Furthermore, *E. coli* mutants in genes encoding Tol-Pal components showed defective O-antigen polymerization (Vinés et al., 2005), while *Pseudomonas aeruginosa* defective in a Tol-Pal component (TolA) showed membranes with high affinity for cationic compounds, including polymyxin B, due to changes in the LPS (Rivera et al., 1988). Furthermore, the hypervesiculating *Shigella flexneri* Δ*tolR* produces OMVs with alterations in the LPS O-chain (Pastor et al., 2018). Thus, we propose that OMVs from *S.* Typhi Δ*tolR* present a higher affinity for polymyxin B than the other OMVs tested due to changes in their membrane profile. On the other hand, we observed an increased MIC of polymyxin B for *S.* Typhi Δ*tolR* than the WT. Nevertheless, when the *S.* Typhi Δ*tolR* was washed, it was necessary, at

least, to incubate bacteria for 1 h to obtain CFU after the challenge with 2.5 μg/mL polymyxin B, or to protect susceptible bacteria in a coculture. From these results, we inferred that the increased MIC of polymyxin B exhibited by *S.* Typhi Δ*tolR* can be attributed to OMVs. Nevertheless, other mechanisms can also be contributing to this phenotype. According to the Zeta potential experiments and sequestering of polymyxin B, OMVs from *S.* Typhi Δ*tolR* have the highest affinity by polymyxin B. In this sense, the bioassay of the polymyxin B activity after incubation with bacteria strongly suggests that the *S.* Typhi Δ*tolR* envelope has increased affinity for polymyxin B than the WT (**Supplementary Figure 1**). In this case, a membrane with a high affinity for polymyxin B might also increase antibiotic resistance via OMV production. *S.* Typhi Δ*tolR* presents one of the most hypervesiculating phenotypes in *S.* Typhi, showing a high release of OMVs when grown under standard conditions (LB, 37°C with shaking), without the need for additional stimuli (Nevermann et al., 2019). Thus, the polymyxin B bound to bacterial membranes might be rapidly discharged from the cells by the hyperproduction of OMVs. Supporting this point, it has been described a toluene elimination system in *Pseudomonas putida*, where the toluene adhered to the outer membrane is rapidly eliminated by shedding OMVs, rendering this strain resistant to such compound (Kobayashi et al., 2000). The role of OMVs to eliminate toxic compounds from the bacterial envelope has already been reviewed (Schwechheimer and Kuehn, 2015).

We also found that OMVs from *S.* Typhi Δ*degS* protect bacteria against polymyxin B. DegS regulates σ^E activation under membrane stress (Alba et al., 2001). In *Salmonella* Typhimurium, σ^E is required under oxidative stress, envelope stress, and the presence of antimicrobial peptides (Testerman et al., 2002; Palmer and Slauch, 2020). Crosstalk between outer membrane protein and LPS biogenesis with the activation of σ^E has been reported (Kim, 2015), suggesting a different composition in the lipidic components in OMVs from *S.* Typhi Δ*degS*, as found in **Figure 7** and **Supplementary Figure 2**. The most negative Zeta potential in these OMVs could support this hypothesis. On the other hand, σ^E is necessary for resistance to cationic peptides in *S.* Typhimurium (Crouch et al., 2005). The lack of DegS may be impairing the σ^E activation, explaining the low MIC exhibited by the *S.* Typhi Δ*degS* mutant. In addition, although the *S.* Typhi Δ*degS* envelope seems to present a similar affinity for polymyxin B than *S.* Typhi Δ*tolR*, as inferred by **Supplementary Figure 1**, the OMV release by *S.* Typhi Δ*tolR* is 1,000 times more than the OMV release by *S.* Typhi Δ*degS* (measured as protein content). Thus, an envelope with increased affinity for polymyxin B but insufficient OMVs production could be considered detrimental regarding polymyxin resistance.

OMVs from *S.* Typhi WT and Δ*rfaE* showed low protection levels against polymyxin B. Nevertheless, the *S.* Typhi Δ*rfaE* strain exhibited a much lower MIC of polymyxin B than the WT strain. In *Salmonella* Typhimurium, it has been reported that Δ*rfaE* and other mutants involved in the LPS synthesis present an increased membrane permeability, decreasing the resistance to diverse antimicrobial compounds, including polymyxin B (Vaara, 1993; Acuna et al., 2016). In particular, *rfaP* (*waaP*), whose product is responsible for phosphorylation of the first heptose residue of the LPS inner core region, is necessary for polymyxin resistance in *E. coli*. The authors concluded that the absence of phosphoryl modifications in the LPS core region leads to an increased polymyxin susceptibility, despite the more depolarized membrane (Yethon et al., 2000). *Salmonella* Typhimurium Δ*rfaE* mutants synthesize heptose-deficient LPS (Jin et al., 2001) (i.e., no phosphorylation by WaaP would be possible), providing a possible explanation of the phenotype found with *S.* Typhi Δ*rfaE*.

Polymyxin mode of action requires two main kinds of interactions to get inserted into the bacterial outer membrane. (1) Electrostatic interaction between the cationic moiety of polymyxin and negatively charged LPS, and (2) hydrophobic interaction between the aliphatic acyl tail of polymyxin and hydrophobic segments of the membrane, including lipid A (Velkov et al., 2010; Trimble et al., 2016). The evidence also suggests polymyxin interaction with outer membrane proteins (van der Meijden and Robinson, 2015). In this sense, OMV from *S.* Typhi Δ*tolR* shows the highest sequestering ability (**Figure 4** and **Table 2**), albeit their Z potential is similar to that observed with OMVs from the WT (**Table 1**). This result suggests that the hydrophobic interaction might be most important concerning the increased protection ability of OMVs from *S.* Typhi Δ*tolR*. On the other hand, OMVs from Δ*degS* could be exerting their protective effect by increasing the electrostatic interactions with polymyxin B, as their more negative Z potential suggests (**Table 1**). Nevertheless, since OMVs are complex supramacromolecular entities, both the hydrophobicity and the negative charge can be achieved by a complex interaction of protein and lipid cargo. Accordingly, OMVs from *S.* Typhi Δ*tolR* and Δ*degS* showed a pattern of protein cargo that is different from OMVs extracted from the WT (Nevermann et al., 2019), where preliminary proteomic analyses show that OMVs from *S.* Typhi Δ*tolR* and Δ*degS* have approximately 180 and 500 proteins, respectively, absent from OMVs from the WT (unpublished results). Furthermore, OMVs from *S.* Typhi WT and mutant derivatives show different LPS profiles (**Figure 7** and **Supplementary Figure 2**), strongly suggesting that increased affinity for polymyxin B is multifactorial.

At present, the role of OMVs as protective agents against polymyxin, or other antimicrobial compounds, has been assessed by extracting OMVs and adding them to axenic reporter cultures to determine the degree of protection (Manning and Kuehn, 2011; Kulkarni et al., 2015; Roszkowiak et al., 2019). However, studies showing the participation of OMVs in more physiological conditions are less common. In this study, we tested whether the hypervesiculating strains could protect a susceptible strain from a challenge with a high amount of polymyxin B in a coculture. We found that, when the strains were washed to remove OMVs, no colonies were observed after the challenge. Nevertheless, when the culture was incubated for 1 h to allow the bacterial growth and OMV accumulation, we found that *S.* Typhi Δ*tolR* could resist the challenge with polymyxin B. Longer incubation times allowed even the *S.* Typhi Δ*degS* growth. We inferred that the survival of *S.* Typhi Δ*tolR* and, at a lesser level, *S.* Typhi Δ*degS*, depends on the OMV accumulation. Consistently, both

strains could transiently transfer their polymyxin B resistance to a susceptible reporter strain. Since the reporter strains did not show an increased MIC of polymyxin B after the challenge, we ruled out any genetic change. Altogether, these results argue for a functional and transient transfer of OMV-mediated polymyxin B resistance from *S.* Typhi Δ*tolR* and Δ*degS* to susceptible bacteria in more physiological conditions, i.e., in a coculture. The most potent protective effect shown by *S.* Typhi Δ*tolR* is consistent with the high protection level of its OMVs, the apparent higher affinity of its OMVs for polymyxin B, and the increased MIC of polymyxin B. It has been reported that mutations leading to changes in the bacterial envelope can increase the resistance to polymyxin B by decreasing the anionic charges (Olaitan et al., 2014; Li et al., 2019). Nevertheless, this kind of resistance could be considered "selfish" since it is not generally thought to be shared, except for the *mcr* genes (Olaitan et al., 2014). However, in this study, we showed that it is possible to transfer the polymyxin resistance via OMVs to the bacterial community without genetic exchange.

This work showed that mutants in genes related to OMVs biogenesis can release vesicles with improved abilities to protect bacteria against membrane-active agents such as polymyxin B. Since mutations affecting OMV biogenesis can involve the bacterial envelope (Kulp and Kuehn, 2010; Kulkarni and Jagannadham, 2014; Nevermann et al., 2019), it is possible to obtain mutant bacteria with increased resistance to membrane-acting agents that, in turn, produce protective OMVs with a high vesiculation rate (e.g., S. Typhi Δ*tolR*). Such mutants can functionally transfer the resistance to surrounding bacteria via OMVs, diminishing the effective concentration of the antimicrobial agent and potentially favoring the selection of spontaneous resistant strains in the environment. Finally, since OMVs can also protect against other agents such as antimicrobial peptides, which can be produced by the innate immune system (Urashima et al., 2017), the possible role of vesicles in bacterial pathogenesis as protective agents is progressively gaining attention.

DATA AVAILABILITY STATEMENT

The original contributions presented in the study are included in the article/**Supplementary Material**, further inquiries can be directed to the corresponding author/s.

AUTHOR CONTRIBUTIONS

PM: experiments, support, and discussion. AC: facilities, Zeta potential experiments, and discussion. EV: experiments and support. AS: TEM and support. JN: mutant construction and support. CO: manuscript edition. EA: facilities, supervision of Zeta potential experiments. FG: facilities, discussion, and manuscript edition. IC: facilities, discussion, and manuscript edition. JF: conception of the study, data curation, figures, facilities, funding acquisition, manuscript writing, and editing. All authors contributed to the article and approved the submitted version.

FUNDING

This work was funded by FONDECYT 1181638 (ANID).

ACKNOWLEDGMENTS

AC thanks FONDECYT de Inicio 11170637 (ANID). FG thanks to FONDECYT 1171397. IC thanks to FONDECYT 1171655. We thank the Center of Applied Nanoscience (CANS) for instrumental facilities.

SUPPLEMENTARY MATERIAL

The Supplementary Material for this article can be found online at: https://www.frontiersin.org/articles/10.3389/fmicb.2021.672467/full#supplementary-material

REFERENCES

Acuna, L. G., Barros, M. J., Penaloza, D., Rodas, P. I., Paredes-Sabja, D., Fuentes, J. A., et al. (2016). A feed-forward loop between SroC and MgrR small RNAs modulates the expression of *eptB* and the susceptibility to polymyxin B in *Salmonella typhimurium*. *Microbiology* 162, 1996–2004. doi: 10.1099/mic.0.000365

Ahamed Riyaaz, A. A., Perera, V., Sivakumaran, S., and De Silva, N. (2018). Typhoid fever due to extended spectrum beta-lactamase-producing *Salmonella enterica* serovar Typhi: a case report and literature review. *Case Rep. Infect. Dis.* 2018:4610246.

Ajibola, O., Mshelia, M. B., Gulumbe, B. H., and Eze, A. A. (2018). Typhoid fever diagnosis in endemic countries: a clog in the wheel of progress? *Medicina (Kaunas)* 54:23. doi: 10.3390/medicina54020023

Alba, B. M., Zhong, H. J., Pelayo, J. C., and Gross, C. A. (2001). *degS* (*hhoB*) is an essential *Escherichia coli* gene whose indispensable function is to provide sigma (E) activity. *Mol. Microbiol.* 40, 1323–1333. doi: 10.1046/j.1365-2958.2001.02475.x

Als, D., Radhakrishnan, A., Arora, P., Gaffey, M. F., Campisi, S., Velummailum, R., et al. (2018). Global trends in typhoidal salmonellosis: a systematic review. *Am. J. Trop. Med. Hyg.* 99(3_Suppl), 10–19. doi: 10.4269/ajtmh.18-0034

Altindis, E., Fu, Y., and Mekalanos, J. J. (2014). Proteomic analysis of *Vibrio cholerae* outer membrane vesicles. *Proc. Natl. Acad. Sci. U.S.A.* 111, E1548–E1556.

Bhutta, Z. A., Gaffey, M. F., Crump, J. A., Steele, D., Breiman, R. F., Mintz, E. D., et al. (2018). Typhoid fever: way forward. *Am. J. Trop. Med. Hyg.* 99, 89–96.

Boags, A. T., Samsudin, F., and Khalid, S. (2019). Binding from both sides: TolR and full-length OmpA bind and maintain the local structure of the *E. coli* cell wall. *Structure* 27, 713–724e712.

Bonnington, K. E., and Kuehn, M. J. (2014). Protein selection and export via outer membrane vesicles. *Biochim. Biophys. Acta.* 1843, 1612–1619. doi: 10.1016/j.bbamcr.2013.12.011

Carreño, A., Páez-Hernández, D., Zúñiga, C., Ramírez-Osorio, A., Pizarro, N., Vega, A., et al. (2021). Exploring rhenium (I) complexes as potential fluorophores for walled-cells (yeasts and bacteria): photophysics, biocompatibility, and confocal microscopy. *Dyes Pigm.* 184:108876. doi: 10.1016/j.dyepig.2020.108876

Carreno, A., Rodriguez, L., Paez-Hernandez, D., Martin-Trasanco, R., Zuniga, C., Oyarzun, D. P., et al. (2018). Two new fluorinated phenol derivatives pyridine schiff bases: synthesis, spectral, theoretical characterization, inclusion in epichlorohydrin-beta-cyclodextrin polymer, and antifungal effect. *Front. Chem.* 6:312. doi: 10.3389/fchem.2018.00312

Cornaglia, G., Giamarellou, H., and Rossolini, G. M. (2011). Metallo-beta-lactamases: a last frontier for beta-lactams? *Lancet Infect. Dis.* 11, 381–393. doi: 10.1016/s1473-3099(11)70056-1

Crouch, M. L., Becker, L. A., Bang, I. S., Tanabe, H., Ouellette, A. J., and Fang, F. C. (2005). The alternative sigma factor sigma is required for resistance of *Salmonella enterica* serovar Typhimurium to anti-microbial peptides. *Mol. Microbiol.* 56, 789–799. doi: 10.1111/j.1365-2958.2005.04578.x

Cuenca-Estrella, M., Moore, C. B., Barchiesi, F., Bille, J., Chryssanthou, E., Denning, D. W., et al. (2003). Multicenter evaluation of the reproducibility of the proposed antifungal susceptibility testing method for fermentative yeasts of the antifungal susceptibility testing subcommittee of the european committee on antimicrobial susceptibility testing (AFST-EUCAST). *Clin. Microbiol. Infect.* 9, 467–474. doi: 10.1046/j.1469-0691.2003.00592.x

Daugelavicius, R., Bakiene, E., and Bamford, D. H. (2000). Stages of polymyxin B interaction with the *Escherichia coli* cell envelope. *Antimicrob. Agents Chemother.* 44, 2969–2978. doi: 10.1128/aac.44.11.2969-2978.2000

Deatherage, B. L., Lara, J. C., Bergsbaken, T., Rassoulian Barrett, S. L., Lara, S., and Cookson, B. T. (2009). Biogenesis of bacterial membrane vesicles. *Mol. Microbiol.* 72, 1395–1407.

Kim, D. Y. (2015). Two stress sensor proteins for the expression of sigmaE regulon: DegS and RseB. *J. Microbiol.* 53, 306–310. doi: 10.1007/s12275-015-5112-6

Falagas, M. E., and Kasiakou, S. K. (2006). Toxicity of polymyxins: a systematic review of the evidence from old and recent studies. *Crit. Care* 10:R27.

Fuentes, J. A., Villagra, N., Castillo-Ruiz, M., and Mora, G. C. (2008). The *Salmonella typhi hlyE* gene plays a role in invasion of cultured epithelial cells and its functional transfer to *S. typhimurium* promotes deep organ infection in mice. *Res. Microbiol.* 159, 279–287. doi: 10.1016/j.resmic.2008.02.006

Galan, J. E. (1996). Molecular genetic bases of *Salmonella* entry into host cells. *Mol. Microbiol.* 20, 263–271. doi: 10.1111/j.1365-2958.1996.tb02615.x

Garg, S. K., Singh, O., Juneja, D., Tyagi, N., Khurana, A. S., Qamra, A., et al. (2017). Resurgence of polymyxin B for MDR/XDR gram-negative infections: an overview of current evidence. *Crit. Care Res. Pract.* 2017:3635609.

Grenier, D., Bertrand, J., and Mayrand, D. (1995). *Porphyromonas gingivalis* outer membrane vesicles promote bacterial resistance to chlorhexidine. *Oral Microbiol. Immunol.* 10, 319–320. doi: 10.1111/j.1399-302x.1995.tb00161.x

Halder, S., Yadav, K. K., Sarkar, R., Mukherjee, S., Saha, P., Haldar, S., et al. (2015). Alteration of Zeta potential and membrane permeability in bacteria: a study with cationic agents. *Springerplus* 4:672.

Hancock, R. E., and Scott, M. G. (2000). The role of antimicrobial peptides in animal defenses. *Proc. Natl. Acad. Sci. U.S.A.* 97, 8856–8861. doi: 10.1073/pnas.97.16.8856

Hook, M., Mcgavin, M. J., Switalski, L. M., Raja, R., Raucci, G., Lindgren, P. E., et al. (1990). Interactions of bacteria with extracellular matrix proteins. *Cell Differ. Dev.* 32, 433–438.

Jan, A. T. (2017). Outer Membrane Vesicles (OMVs) of gram-negative bacteria: a perspective update. *Front. Microbiol.* 8:1053. doi: 10.3389/fmicb.2017.01053

Jin, U. H., Chung, T. W., Lee, Y. C., Ha, S. D., and Kim, C. H. (2001). Molecular cloning and functional expression of the *rfaE* gene required for lipopolysaccharide biosynthesis in *Salmonella typhimurium*. *Glycoconjugate journal* 18, 779–787.

Johnson, R., Mylona, E., and Frankel, G. (2018). Typhoidal *Salmonella*: distinctive virulence factors and pathogenesis. *Cell. Microbiol.* 20:e12939. doi: 10.1111/cmi.12939

Karkey, A., Thwaites, G. E., and Baker, S. (2018). The evolution of antimicrobial resistance in *Salmonella typhi*. *Curr. Opin. Gastroenterol.* 34, 25–30. doi: 10.1097/mog.0000000000000406

Kim, S. H., Kim, K. S., Lee, S. R., Kim, E., Kim, M. S., Lee, E. Y., et al. (2009). Structural modifications of outer membrane vesicles to refine them as vaccine delivery vehicles. *Biochim. Biophys. Acta* 1788, 2150–2159. doi: 10.1016/j.bbamem.2009.08.001

Kobayashi, H., Uematsu, K., Hirayama, H., and Horikoshi, K. (2000). Novel toluene elimination system in a toluene-tolerant microorganism. *J. Bacteriol.* 182, 6451–6455. doi: 10.1128/jb.182.22.6451-6455.2000

Kulikov, E. E., Golomidova, A. K., Prokhorov, N. S., Ivanov, P. A., and Letarov, A. V. (2019). High-throughput LPS profiling as a tool for revealing of bacteriophage infection strategies. *Sci. Rep.* 9:2958.

Kulkarni, H. M., and Jagannadham, M. V. (2014). Biogenesis and multifaceted roles of outer membrane vesicles from Gram-negative bacteria. *Microbiology* 160, 2109–2121. doi: 10.1099/mic.0.079400-0

Kulkarni, H. M., Nagaraj, R., and Jagannadham, M. V. (2015). Protective role of *E. coli* outer membrane vesicles against antibiotics. *Microbiol. Res.* 181, 1–7. doi: 10.1016/j.micres.2015.07.008

Kulp, A., and Kuehn, M. J. (2010). Biological functions and biogenesis of secreted bacterial outer membrane vesicles. *Annu. Rev. Microbiol.* 64, 163–184. doi: 10.1146/annurev.micro.091208.073413

Kumarasamy, K. K., Toleman, M. A., Walsh, T. R., Bagaria, J., Butt, F., Balakrishnan, R., et al. (2010). Emergence of a new antibiotic resistance mechanism in India, Pakistan, and the UK: a molecular, biological, and epidemiological study. *Lancet Infect. Dis.* 10, 597–602. doi: 10.1016/s1473-3099(10)70143-2

Li, Z., Cao, Y., Yi, L., Liu, J. H., and Yang, Q. (2019). Emergent polymyxin resistance: end of an Era? *Open Forum. Infect. Dis.* 6:ofz368.

Liu, Q., Liu, Q., Zhao, X., Liu, T., Yi, J., Liang, K., et al. (2016a). Immunogenicity and cross-protective efficacy induced by outer membrane proteins from *Salmonella typhimurium* mutants with truncated LPS in mice. *Int. J. Mol. Sci.* 17:416. doi: 10.3390/ijms17030416

Liu, Q., Yi, J., Liang, K., Liu, T., Roland, K. L., Jiang, Y., et al. (2016b). Outer membrane vesicles derived from *Salmonella typhimurium* mutants with truncated LPS induce cross-protective immune responses against infection of *Salmonella enterica* serovars in the mouse model. *Int. J. Med. Microbiol.* 306, 697–706. doi: 10.1016/j.ijmm.2016.08.004

Manning, A. J., and Kuehn, M. J. (2011). Contribution of bacterial outer membrane vesicles to innate bacterial defense. *BMC Microbiol.* 11:258. doi: 10.1186/1471-2180-11-258

Masilamani, R., Cian, M. B., and Dalebroux, Z. D. (2018). *Salmonella* Tol-Pal reduces outer membrane glycerophospholipid levels for envelope homeostasis and survival during bacteremia. . *Infect. Immun.* 86, e00173-e00218.

McBroom, A. J., Johnson, A. P., Vemulapalli, S., and Kuehn, M. J. (2006). Outer membrane vesicle production by *Escherichia coli* is independent of membrane instability. *J. Bacteriol.* 188, 5385–5392. doi: 10.1128/jb.00498-06

Miao, E. A., Brittnacher, M., Haraga, A., Jeng, R. L., Welch, M. D., and Miller, S. I. (2003). *Salmonella* effectors translocated across the vacuolar membrane interact with the actin cytoskeleton. *Mol. Microbiol.* 48, 401–415. doi: 10.1046/j.1365-2958.2003.t01-1-03456.x

Muller, M. M., Vianney, A., Lazzaroni, J. C., Webster, R. E., and Portalier, R. (1993). Membrane topology of the *Escherichia coli* TolR protein required for cell envelope integrity. *J. Bacteriol.* 175, 6059–6061. doi: 10.1128/jb.175.18.6059-6061.1993

Murphy, K., Park, A. J., Hao, Y., Brewer, D., Lam, J. S., and Khursigara, C. M. (2014). Influence of O polysaccharides on biofilm development and outer membrane vesicle biogenesis in *Pseudomonas aeruginosa* PAO1. *J. Bacteriol.* 196, 1306–1317. doi: 10.1128/jb.01463-13

Nevermann, J., Silva, A., Otero, C., Oyarzun, D. P., Barrera, B., Gil, F., et al. (2019). Identification of genes involved in biogenesis of outer membrane vesicles (OMVs) in *Salmonella enterica* serovar Typhi. *Front. Microbiol.* 10:104. doi: 10.3389/fmicb.2019.00104

Olaitan, A. O., Morand, S., and Rolain, J. M. (2014). Mechanisms of polymyxin resistance: acquired and intrinsic resistance in bacteria. *Front. Microbiol.* 5:643. doi: 10.3389/fmicb.2014.00643

Palmer, A. D., and Slauch, J. M. (2020). Envelope stress and regulation of the *Salmonella* pathogenicity Island 1 type III secretion system. *J. Bacteriol.* 202:e00272-20.

Pandit, A., Arjyal, A., Day, J. N., Paudyal, B., Dangol, S., Zimmerman, M. D., et al. (2007). An open randomized comparison of gatifloxacin versus cefixime for the treatment of uncomplicated enteric fever. *PLoS One* 2:e542. doi: 10.1371/journal.pone.0000542

Parry, C. M., Basnyat, B., and Crump, J. A. (2013). The management of antimicrobial-resistant enteric fever. *Exp. Rev. Anti Infect. Ther.* 11, 1259–1261. doi: 10.1586/14787210.2013.858019

Pastor, Y., Camacho, A. I., Zuniga-Ripa, A., Merchan, A., Rosas, P., Irache, J. M., et al. (2018). Towards a subunit vaccine from a *Shigella flexneri* Δ*tolR* mutant. *Vaccine* 36, 7509–7519. doi: 10.1016/j.vaccine.2018.10.066

Payne, D. J., Gwynn, M. N., Holmes, D. J., and Pompliano, D. L. (2007). Drugs for bad bugs: confronting the challenges of antibacterial discovery. *Nat. Rev. Drug Discov.* 6, 29–40. doi: 10.1038/nrd2201

Rivera, M., Hancock, R. E., Sawyer, J. G., Haug, A., and McGroarty, E. J. (1988). Enhanced binding of polycationic antibiotics to lipopolysaccharide from an aminoglycoside-supersusceptible, tolA mutant strain of *Pseudomonas aeruginosa*. *Antimicrob. Agents Chemother.* 32, 649–655. doi: 10.1128/aac.32.5.649

Roszkowiak, J., Jajor, P., Gula, G., Gubernator, J., Zak, A., Drulis-Kawa, Z., et al. (2019). Interspecies Outer Membrane Vesicles (OMVs) modulate the sensitivity of pathogenic bacteria and pathogenic yeasts to cationic peptides and serum complement. *Int. J. Mol. Sci.* 20:5577. doi: 10.3390/ijms20225577

Santiviago, C. A., Toro, C. S., Hidalgo, A. A., Youderian, P., and Mora, G. C. (2003). Global regulation of the *Salmonella enterica* serovar typhimurium major porin. OmpD. *J. Bacteriol.* 185, 5901–5905. doi: 10.1128/jb.185.19.5901-5905.2003

Schwartz, K. L., and Morris, S. K. (2018). Travel and the spread of drug-resistant bacteria. *Curr. Infect. Dis. Rep.* 20:29.

Schwechheimer, C., and Kuehn, M. J. (2015). Outer-membrane vesicles from Gram-negative bacteria: biogenesis and functions. *Nat. Rev. Microbiol.* 13, 605–619. doi: 10.1038/nrmicro3525

Sturgis, J. N. (2001). Organisation and evolution of the *tol-pal* gene cluster. *J. Mol. Microbiol. Biotechnol.* 3, 113–122.

Testerman, T. L., Vazquez-Torres, A., Xu, Y., Jones-Carson, J., Libby, S. J., and Fang, F. C. (2002). The alternative sigma factor sigmaE controls antioxidant defences required for *Salmonella* virulence and stationary-phase survival. *Mol. Microbiol.* 43, 771–782. doi: 10.1046/j.1365-2958.2002.02787.x

Thakre, A., Zore, G., Kodgire, S., Kazi, R., Mulange, S., Patil, R., et al. (2021). Limonene inhibits *Candida albicans* growth by inducing apoptosis. *Med. Mycol.* 56, 565–578.

Trimble, M. J., Mlynarcik, P., Kolar, M., and Hancock, R. E. (2016). Polymyxin: alternative mechanisms of action and resistance. *Cold Spring Harb. Perspect. Med.* 6:a025288. doi: 10.1101/cshperspect.a025288

Urashima, A., Sanou, A., Yen, H., and Tobe, T. (2017). Enterohaemorrhagic *Escherichia coli* produces outer membrane vesicles as an active defence system against antimicrobial peptide LL-37. *Cell. Microbiol.* 19:e12758. doi: 10.1111/cmi.12758

Vaara, M. (1993). Outer membrane permeability barrier to azithromycin, clarithromycin, and roxithromycin in gram-negative enteric bacteria. *Antimicrob. Agents Chemother.* 37, 354–356. doi: 10.1128/aac.37.2.354

Valenzuela, C., Ugalde, J. A., Mora, G. C., Alvarez, S., Contreras, I., and Santiviago, C. A. (2014). Draft genome sequence of *Salmonella enterica* serovar Typhi strain STH2370. *Genome Announc.* 2:e00104-14.

van der Meijden, B., and Robinson, J. A. (2015). Synthesis of a polymyxin derivative for photolabeling studies in the gram-negative bacterium *Escherichia coli*. *J. Pept. Sci.* 21, 231–235. doi: 10.1002/psc.2736

Velkov, T., Roberts, K. D., Nation, R. L., Thompson, P. E., and Li, J. (2013). Pharmacology of polymyxins: new insights into an 'old' class of antibiotics. *Future Microbiol.* 8, 711–724. doi: 10.2217/fmb.13.39

Velkov, T., Thompson, P. E., Nation, R. L., and Li, J. (2010). Structure–activity relationships of polymyxin antibiotics. *J. Med. Chem.* 53, 1898–1916. doi: 10.1021/jm900999h

Vinés, E. D., Marolda, C. L., Balachandran, A., and Valvano, M. A. (2005). Defective O-antigen polymerization in tolA and pal mutants of *Escherichia coli* in response to extracytoplasmic stress. *J. Bacteriol.* 187, 3359–3368. doi: 10.1128/jb.187.10.3359-3368.2005

Yethon, J. A., Gunn, J. S., Ernst, R. K., Miller, S. I., Laroche, L., Malo, D., et al. (2000). *Salmonella enterica* serovar Typhimurium waaP mutants show increased susceptibility to polymyxin and loss of virulence In vivo. *Infect. Immun.* 68, 4485–4491. doi: 10.1128/iai.68.8.4485-4491.2000

Zasloff, M. (2002). Antimicrobial peptides of multicellular organisms. *Nature* 415, 389–395. doi: 10.1038/415389a

Zhang, G. F., Liu, X., Zhang, S., Pan, B., and Liu, M. L. (2018). Ciprofloxacin derivatives and their antibacterial activities. *Eur. J. Med. Chem.* 146, 599–612. doi: 10.1016/j.ejmech.2018.01.078

Conflict of Interest: The authors declare that the research was conducted in the absence of any commercial or financial relationships that could be construed as a potential conflict of interest.

frontiers in Immunology

REVIEW
published: 03 August 2021
doi: 10.3389/fimmu.2021.715393

GMMA-Based Vaccines: The Known and The Unknown

Francesca Mancini, Francesca Micoli, Francesca Necchi, Mariagrazia Pizza, Francesco Berlanda Scorza and Omar Rossi*

GlaxoSmithKline (GSK) Vaccines Institute for Global Health (GVGH), Siena, Italy

Generalized Modules for Membrane Antigens (GMMA) are outer membrane vesicles derived from Gram-negative bacteria engineered to provide an over-vesiculating phenotype, which represent an attractive platform for the design of affordable vaccines. GMMA can be further genetically manipulated to modulate the risk of systemic reactogenicity and to act as delivery system for heterologous polysaccharide or protein antigens. GMMA are able to induce strong immunogenicity and protection in animal challenge models, and to be well-tolerated and immunogenic in clinical studies. The high immunogenicity could be ascribed to their particulate size, to their ability to present to the immune system multiple antigens in a natural conformation which mimics the bacterial environment, as well as to their intrinsic self-adjuvanticity. However, GMMA mechanism of action and the role in adjuvanticity are still unclear and need further investigation. In this review, we discuss progresses in the development of the GMMA vaccine platform, highlighting successful applications and identifying knowledge gaps and potential challenges.

Keywords: Generalized modules for membrane antigens, GMMA, OMV, vaccine, mode of action, reactogenicity

OPEN ACCESS

Edited by:
Rafael A. Garduno, Retired, Fredericton, NB, Canada

Reviewed by:
Lisa A. Morici, Tulane University, United States
Stefan Schild, University of Graz, Austria

****Correspondence:***
Francesca Mancini
francesca.x.mancini@gsk.com

Specialty section:
This article was submitted to Vaccines and Molecular Therapeutics, a section of the journal Frontiers in Immunology

Received: *26 May 2021*
Accepted: *19 July 2021*
Published: *03 August 2021*

Citation:
Mancini F, Micoli F, Necchi F, Pizza M, Berlanda Scorza F and Rossi O (2021) GMMA-Based Vaccines: The Known and The Unknown. Front. Immunol. 12:715393. doi: 10.3389/fimmu.2021.715393

INTRODUCTION

Both pathogenic and nonpathogenic Gram-negative bacteria are able to spontaneously release 25–250 nm vesicles during growth, especially during the end of log phase (1). Since they originate from the bacterial outer membrane, these vesicles reflect the membrane composition and are then named outer membrane vesicles (OMVs). They contain bacterial antigens such as lipopolysaccharides (LPS) and proteins in their original environment, and additional immunostimulatory molecules (i.e. lipoproteins, peptidoglycans). Because of their composition, they raise high scientist interest and have been widely investigated as a promising vaccine platform (2, 3).

However, bacteria naturally release OMV but in relatively low amounts, and contain endotoxins in the natural form, which might cause systemic reactogenicity in humans depending on the vaccine dose used. Hence, in order to overcome issues of limited yield and to reduce the levels of endotoxicity, bacterial strains have been genetically modified to increase outer membrane vesiculation (4–6) and reduce LPS endotoxicity (7–9). We named the resulting vesicles, deriving from the over-vesiculating strain and with mutations in the LPS genes, Generalized Modules for Membrane Antigens (GMMA) whereas others called them mutant-derived or genetically detoxified OMV. Through a three-step process consisting on fermentation of the GMMA-producing strain coupled with two consecutive tangential flow filtration steps (4), GMMA can be produced at high

yield and purity through a simple process. Indeed, the entire production process from fermentation to final purified GMMA lasts 3 days and thus, depending on the size of the vaccine dose, a relatively small manufacture facility with a 500 L fermenter could produce 100 000 000 doses of vaccines per year at a manufacturing cost of approximately $1 per dose (10). GMMA from *Shigella* (4, 5, 7, 9, 11–13), *Salmonella* (8, 14, 15), and *Neisseria* (16, 18) species have been already generated using this approach, which is shown to be flexible enough to be potentially extended with minimal adjustments to any Gram-negative bacterial species. Indeed multiple industrial (17–19) and research (20–22) approaches based on genetic engineering of bacteria for hyper-vesiculating and surface-expression of a variety of homologous and heterologous antigens, including bacterial (20–22), viral (23), parasitic (24) and even cancer antigens (25) have been described.

In this review, we will refer to genetically modified OMV as GMMA, and will focus our attention on GMMA-based vaccines that are in an advanced stage of the development and already moved or are approaching to move in clinical trials rather than on research vaccines. We will discuss progress in the development of the GMMA vaccine platform, highlighting successful applications, gaps and potential challenges.

GMMA AS A VACCINE PLATFORM

GMMA constitute a straightforward technology based on low-cost of production and high purification yields and is therefore suitable for the development of vaccines against bacterial pathogens and particularly of affordable vaccines targeting low- and middle-income countries (LMICs).

GMMA resemble faithfully the outer membrane of the bacterial pathogen they shed from but lack the ability to cause the associated disease. They present to the immune system key antigens in their natural environment and conformation, facilitating uptake by immune cells and inducing strong immune response (26). The GMMA outer membrane also displays several Pathogen Associated Molecular Patterns (PAMPs), small molecular motifs well conserved in bacteria which are recognized by Patter Recognition Receptors (PRRs) expressed on mammalian cells (27). PAMPs interaction with PRRs rapidly activates the complex signaling pathway, with the induction of pro-inflammatory cytokines and chemokines, and that may be the basis of GMMA self-adjuvanticity. However, while activation of the innate immune system can result in a high immune response to an antigen, it may also induce local and severe adverse effects in humans, from febrile response to septic shock (28). Thus, fine tuning the balance between immune stimulation and reactogenicity is key for an acceptable GMMA-based vaccine.

LPS, the most abundant component of GMMA, is a key antigen in Gram-negative bacteria, but it is also the main component for systemic reactogenicity (29). Intrinsic LPS endotoxicity can be reduced by genetically modifying the lipid A structure. Lipid A is the endotoxic component of LPS which mediates the binding to toll like receptor (TLR) 4 inducing innate immune activation. TLR4 recognition of LPS is strongly influenced by the structure of its lipid A component which, in most Gram-negative bacteria (i.e., *E. coli*, *Shigella*, *Salmonella*), is composed of a β-1',6-linked disaccharide of glucosamine phosphorylated at the 1 and 4' positions and acylated at 2, 3, 2' and 3' position with R-3-hydroxymyristate (called lipid IV A). This scaffold is then decorated in various positions with fatty acids differing in length and saturation level or with substituents of phosphoryl groups of glucosamines (30). The most reactogenic form of lipid A is the bis-phosphorylated and hexa-acylated with 12 to 14 carbon acyl chains and an asymmetric (4/2) distribution, whereas the penta-acylated lipid A is much less active than the hexa-acylated form in activating human TLR4 (31–33). Bacteria use lipid A modifications as immune evasion mechanism and to adapt to environmental changes (e.g., temperature, nutrient, osmolarity) (30, 34). The selection of the appropriate modified lipid A structure, depending on the structure present in the parent bacteria, is key to balance immunogenicity and reactogenicity of GMMA-based vaccines. Indeed, the selection of the modifications on the lipid A acylation status are critical, as most of the genes implicated in LPS biosynthesis are necessary to preserve bacterial membrane stability and therefore viability. Genes that encode for acyltransferases such as HtrB or MsbB in *Shigella* (4, 5, 7, 9), MsbB and PagP in *Salmonella* (8), or LpxL1 in *N. meningitidis* (16, 17, 35) have been mutated to generate GMMA with different penta-acylated lipid A forms.

In addition to LPS, other molecules contained in GMMA, like lipoproteins, are able to stimulate the innate immune system through the activation of TLR2. Indeed, GMMA from *Shigella* and *Salmonella* were able to stimulate peripheral blood mononuclear cells (PBMCs) and induce interleukin (IL)-6 release, which was almost completely abolished when a combination of antibodies blocking TLR4 and TLR2 was used (7, 8), indicating that they are the PRRs mostly involved in GMMA mediated cytokine release.

GMMA act as effective adjuvant and carrier, thus having an intrinsic ability to improve immunogenicity of protein and carbohydrate antigens. The glycoconjugate approach is the gold standard for enhancing immunogenicity, particularly for polysaccharides (36). Bacterial polysaccharides are T-cell-independent antigens which are generally not able to elicit germinal center (GC) formation and therefore immunological memory, persistence of antibody response, and affinity maturation of B cell receptors. Covalent linkage to a suitable carrier protein confers to saccharide antigens the ability to elicit a T-cell-dependent response, overcoming the limitation listed above. Consequently, vaccination with conjugates enhances polysaccharide immunogenicity and protective efficacy, especially in infants and children under 2 years of age (37, 38). As carriers for polysaccharides, GMMA can be somehow considered multi-valent antigens, as they may present multiple polysaccharide molecules and proteins in natural conformation (39). GMMA was shown to be superior to traditional glycoconjugate vaccines in animal models, likely due to the

nano-sized particle properties, ability to present multiple saccharide epitopes and self-adjuvanticity. GMMA from *S.* Typhimurium and *S.* Enteritidis strains elicited levels of anti-O polysaccharide-specific immunoglobulins (Ig)G comparable to those observed after vaccination with corresponding CRM_{197} glycoconjugates formulated with Alhydrogel, but showed an increased IgG antibody isotype profile and improved complement-mediated bactericidal activity and protective ability in challenge model (40). Similarly, GMMA from *S. flexneri* 6 strain induced higher anti-O-antigen IgG titers compared to CRM_{197} glycoconjugate when both were administered to mice without Alhydrogel (13).

GMMA can also be carriers for heterologous antigens, which renders them even a more powerful vaccine platform. Bacterial strains can be engineered for overexpression in GMMA of key homologous and heterologous antigens or multiple antigenic variants (6, 41–43). In alternative to genetic manipulation, decoration of GMMA with heterologous polysaccharide or protein antigens can also be achieved through chemical conjugation (44).

SUCCESSFUL APPLICATIONS OF GMMA VACCINE PLATFORM

Safe, cost-effective and affordable technologies such as GMMA constitute ideal vaccine candidates to prevent diseases prevalent in LMICs (10). Indeed, many GMMA-based vaccines targeting several bacterial pathogens are in development (45, 46). Currently, the most advanced GMMA-based vaccine is the *Shigella sonnei* 1790GAHB that has been extensively tested in preclinical (5) and clinical studies (47–49). *Shigella sonnei* GMMA formulated with Alhydrogel were highly immunogenic in mice and rabbits and had low stimulatory activity in the *in vitro* monocyte activation test. The low reactogenicity was also confirmed by two *in vivo* models: a modified rabbit pyrogenicity test based on the intramuscular administration of the full human dose and a multiple dose toxicology study in rabbits using intramuscular, intranasal, and intradermal administration routes (5). Moreover, *Shigella sonnei* GMMA elicited in the animal model antibodies not only against the key antigen LPS, but also against GMMA proteins (9). In phase I and II clinical studies, the vaccine was well tolerated up to 100 μg following intramuscular (two or three doses), intradermal or intranasal administrations (48). Moreover, the vaccine induced anti-LPS specific antibodies in healthy adults in Europe and in Kenya, where shigellosis is endemic (47, 48). In addition, immune response was significantly increased following a booster dose, administered two-three years after the primary immunization (49). Antibodies elicited were able to induce complement mediated bactericidal killing in a dose dependent manner (50). The promising results obtained with *Shigella sonnei* GMMA vaccine corroborated the ability of GMMA to be an ideal delivery system for *Shigella* LPS, and to induce high levels of anti-*Shigella* LPS IgG considered as the most promising correlate of protection against shigellosis (51). However, based on recent results not yet published from a controlled human infection model (CHIM) study, it seems that *Shigella* LPS amount is critical to induce a level of IgG antibodies able to protect from *Shigella* infection and additional work has been done for improving the design of a 4-component *Shigella* GMMA-based vaccine that is entering clinical testing.

An additional GMMA-based vaccine in an advanced stage of development is the HOPS-G meningococcal vaccine adjuvanted with aluminum hydroxide. GMMA were derived from an engineered meningococcal B strain, containing the deletion of the *lpxL*1 and *synX* genes to remove the expression of capsular polysaccharide and reduce LPS reactogenicity, over-expressing factor H binding protein, two PorAs and the stabilized OpcA (17). When tested in a human clinical trial as a three doses vaccine, it resulted to be safe and immunogenic. Sera form 79% of volunteers, collected two weeks after third dose had a fourold or greater increase in bactericidal activity against the homologous strain by which the GMMA were derived. 68% of volunteers showed cross-protection against strains carrying the L3-5,7-5 phase variant of the parent strain. Similar results were obtained with a vaccine differing only for the strategy used to detoxify the lipo-oligosaccharide: lipid A acylation status was indeed modified through disabling the *lpxL2* gene instead of the *lpxL*1 (18).

The results obtained so far with the GMMA-based vaccines tested in clinical trials paved the way for other GMMA-based vaccines. Indeed multi component GMMA-based vaccines consisting in GMMA derived from the key disease-causing *invasive* nontyphoidal *Salmonellae* (*Salmonella* Typhimurium and *Salmonella* Enteritidis) strains, either alone or in combination with the recently licensed Vi-CRM conjugate vaccines are moving to Phase I/II clinical studies. Results in mice showed that *S.* Typhimurium and *S.* Enteritidis GMMA were able to elicit strong and functional bactericidal anti-LPS O-antigen antibodies and a broad IgG range of antibodies. Moreover, induced antibodies were able to protect in an *in vivo* mouse challenge model (40).

GAPS ON UNDERSTANDING THE BASIS OF GMMA IMMUNOGENICITY AND POTENTIAL CHALLENGES

Recent clinical trials not only showed good immunogenicity data but highlighted a satisfactory tolerability profile of GMMA. However, due to differences in maturation of TLR in children and adults (52), the risk of systemic reactogenicity in different age groups needs to be further evaluated, and age-de-escalation clinical trials will be necessary, especially for GMMA vaccines targeting diseases mainly affecting children.

Moreover, Alhydrogel has been used in preclinical and clinical studies in *S. sonnei* GMMA vaccine formulation as absorbent agent with the solely purpose of reducing GMMA reactogenicity, mainly due to results observed after intramuscular immunization of rabbits (29). Indeed, intramuscular immunization of rabbits with 100 μg of 1790GAHB caused only a low and transient temperature rise, comparable to what observed with 5 μg of *S. sonnei* GMMA

delivered alone. However, no results in humans comparing non-adjuvanted and Alhydrogel-adsorbed GMMA are yet available. Similar preclinical results have been obtained when OMV from *Neisseria meningitidis* (*Nm*) were tested in a rabbit pyrogenicity study alone or adsorbed to aluminum hydroxide. Differently from GMMA which display a modified LPS, *Nm* OMV were obtained by extraction with deoxycholate detergent and therefore wild type LPS was largely removed. When OMV were adsorbed to aluminum hydroxide, the pyrogenicity was reduced four-fold in rabbits and this reduction was also observed in the Limulus Amebocyte Lysate (LAL) test. However, when reactogenicity was evaluated in human volunteers, the adsorbed vaccine gave more local side effects and longer duration of tenderness at the site of injection than the unadsorbed vaccine, whereas no differences were observed between the two formulations in terms of minimal, unspecific systemic reactions (53). Therefore, more studies in humans are needed to better elucidate the contribution of Alhydrogel to reactogenicity.

Preclinical studies in mice showed that immunization with *S.* Typhimurium GMMA not adjuvanted with Alhydrogel elicited antigen-specific IgG titers higher than after immunization with GMMA with adjuvant. For *S.* Enteritidis and *S. flexneri* 6 GMMA, addition of Alhydrogel did not increase or decreased anti-O-antigen-specific IgG response (13, 40). On the opposite, a preclinical study with *Nm* OMV showed that the addition of aluminum hydroxide improved antigen-specific IgG levels and bactericidal activity (54). Differences in the LPS content and structure in GMMA and detergent extracted OMV can have an impact on innate immunity activation and therefore on self-adjuvanticity. More studies will be needed to evaluate the added value of Alhydrogel or alternative adjuvants on GMMA immunogenicity.

GMMA vaccines are highly immunogenic, but there are no many insights into their mechanism of action. Few experiments have been performed so far to understand what happens at the injection site and after injection, and to identify the factors which influence the cellular and humoral responses elicited.

It has been shown that after injection, nanoparticles are coated by proteins present in the interstitial fluid (55). The nature and amount of these proteins is influenced by their particle size and physico-chemical properties that may result in augmented or reduced interaction with immune cells. No information is available so far for GMMA, and it may be important to consider that GMMA from different bacteria can display LPS with different charge, which can in turn influence the quality of the interstitial fluid proteins binding on their surface. Indeed, net charge and hydrophobicity are some of the several physical–chemical features of nanoparticles which influence their interactions with plasma proteins (56).

At the injection site, GMMA encounter tissue resident immune cells and dendritic cells (DCs) recruited at the site through the inflammation process (**Figure 1A-I**). GMMA uptake by DCs should favor DC maturation, allowing trafficking to the lymph node (LN), but this interaction has not been proven so far. It is known that OMV are able to drive DC maturation. Indeed, native OMV derived from the facultative-intracellular bacterium *Burkholderia pseudomallei* were shown to favor DC maturation and activation both *in vitro* and *in vivo* in a mouse model (57). Moreover, Schetters et al. demonstrated that the LPS present on OMV was able to induce, through the myeloid differentiation primary response 88 (Myd88) adapter protein, maturation of human monocyte-derived DCs, murine bone marrow-derived DCs and CD11c+ splenic DCs (58).

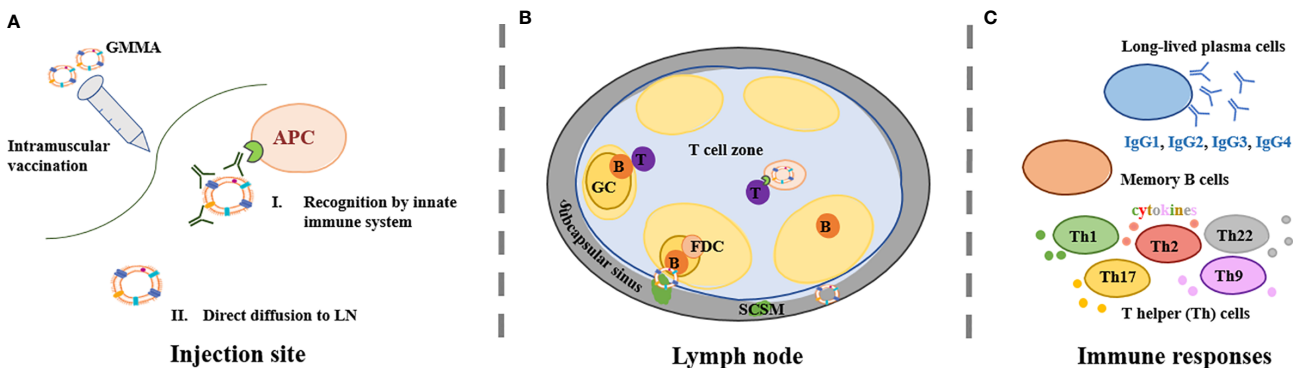

FIGURE 1 | GMMA mechanism of action. **(A)** GMMA vaccines have been administered intramuscularly. At the injection site, GMMA may be coated by proteins present in the interstitial fluid. The kind and amount of these proteins is influenced by GMMA size and physico-chemical properties. GMMA trafficking to the lymph node (LN) may require cellular transport from antigen presenting cells (APCs) **(A-I)** but GMMA can also be able to drain freely to the LN **(A-II)**. **(B)** Upon arrival into the LN, GMMA and APCs circulate into the LN subcapsular sinus where subcapsular sinus macrophages (SCSM) reside. SCSM can uptake GMMA in complex with IgG and can reach the LN follicular area where they transfer the antigen to B cells. B cell receptor crosslinking and B cell activation is facilitated by repetitive display of optimally spaced antigen on GMMA. Also follicular dendritic cells (FDCs) play a major role in germinal center (GC) kinetics and in the development of humoral responses. GMMA delivered to the LN *via* active transport are presented to naïve T cells with antigen-cognate T cell receptors in the T cell zone. T cells also interact with activated B cells, that present them antigen-derived peptides thus providing T cell 'help' to B cells, sustaining their activation and driving the formation of GCs. **(C)** GMMA drive the selection of B cell clones with high antigen affinity into long-lasting memory B cells and/or long-lived antibody-producing plasma cells and possibly the differentiation of T cells in different subsets of T helper (Th) cells.

Since GMMA are 25-250 nm vesicles, their size should allow them direct diffusion into lymphatic vessels (**Figure 1A-II**). It has been shown that nanoparticles of 20–200 nm and 30 nm virus-like particles (VLPs) are detected in LN resident CD8+ DCs and macrophages two hours after vaccination, thus indicating that they can be rapidly drained to the LN without active transport by antigen presenting cells (APCs) (59). As particle size increases over 200 nm, antigens are likely to require APCs for trafficking to the LNs.

Upon arrival into the LN, nanoparticulated antigens like GMMA and cells circulate into the LN subcapsular sinus where subcapsular sinus macrophages (SCSM) reside (**Figure 1B**). SCSM can uptake GMMA in complex with IgG and can reach the LN follicular area where they transfer the antigen to B cells *via* CR2 (60). The GMMA-IgG complexes allow B cell receptor crosslinking with the CR2 complex thus lowering the affinity threshold for B cell activation (61). B cell receptor crosslinking is facilitated by repetitive display of optimally spaced antigen on GMMAs. The antigen is also transferred to follicular dendritic cells (FDCs), which play a major role in the development of humoral responses. Indeed, FDCs secrete the B cell attracting chemokine CXCL13 which induces activated B cell migration into the GC, produce B-cell activating factor (BAFF), which regulates GC B cell survival and retain the antigen for long time, thus enabling persistent GC reactions and resulting in long-lasting plasma cells that secrete high affinity antibodies (62). VLPs rapid delivery to FDCs was proven to be dependent on natural IgM and complement (60), and their ability to facilitate antigen persistence in the LN shown in comparison to soluble antigens (63). Besides many similarities between VLPs and GMMA, no data are available so far for GMMA. If GMMA are delivered to the LN *via* active DC transport, the outer membrane antigens are presented to naïve T cells with antigen-cognate T cell receptors in the T cell zone. Moreover, T cells also interact with activated B cells, presenting them antigen-derived peptides thus providing T cell 'help' to B cells, sustaining their activation and driving the formation of GCs (64).

Preclinical and clinical studies conducted with GMMA-based vaccines have addressed humoral responses but poorly the cellular response (**Figure 1C**). Baker and co-authors demonstrated that OMV could induce robust cellular immune responses that exceeded those induced by a live-attenuated strain (65).

GMMA could also be used as adjuvants and as alternative carrier. When OMV have been tested as adjuvants for heterologous peptides or ovalbumin, they elicited broad antigen-specific immune responses, including antibody, B cells, CD4 T cells, and CD8 T cells. Humoral immune responses to ovalbumin elicited upon immunization with OMV were higher compared to those induced by ovalbumin adjuvanted with Alhydrogel and CpG DNA (57). When used as carrier, GMMA have shown superior immunogenicity compared with conventional carrier proteins such as CRM_{197} (13, 40, 44). It will be interesting to understand the immunological mechanisms behind this superiority.

FUTURE DIRECTIONS

GMMA is recognized as a powerful vaccine technology. It has the unique advantage to be a multivalent vaccine with a straightforward production process and simple purification steps to generate high yield, and which does not need the addition of detergents as in the case of classical OMV purification which may alter vaccine composition and antigen conformation. The presentation of multiple antigens in their natural environment and the inherent GMMA characteristics are the driving force of the high immunogenic profile.

However, there are still many immunogenicity aspects that need to be unraveled for a deep understanding of the full potential of GMMA-based vaccines. We have recently started to investigate more in depth the impact that GMMA structural features may have on the immune response. One of these features is the saccharide length, a well-known parameter that can modulate the intensity and quality of immune response elicited by glycoconjugate vaccines. In contrast with what observed for traditional glycoconjugates, O-antigen length did not result to be a critical parameter for GMMA immunogenicity, independently by the pathogen and by the sugar structural characteristics (11). Moreover, we demonstrated that exposure of GMMA to high-temperature (100°C for 40 min) did not impact GMMA stability and immunogenicity in mice, whereas milder temperatures for a longer period of time did (37°C or 50°C for 4 weeks). Major differences were related to O-antigen O-acetylation and its release from vesicles (66). Although what makes GMMA a unique antigen and delivery system is known, the mechanism of action *in vivo* is still unknown. Therefore, more efforts should be directed towards the dissection of what happens at the GMMA injection site and afterwards and the mechanisms which mediate the immune response, either in presence or absence of an adjuvant. Unravelling such mechanisms will allow to improve the design of GMMA-based vaccines. Clinical studies conducted so far with GMMA-based vaccines have confirmed the good immunogenicity and safety profile observed in preclinical studies. However, even though GMMA technology has been applied to several bacterial targets in preclinical studies, only few of them have progressed into clinical trials in adults but none in children and infants. More clinical data will be needed to corroborate the preclinical findings, and further evaluation of GMMA-based *Shigella* and *Salmonella* vaccines are expected to provide a better understanding of the immunological potential of this platform.

AUTHOR CONTRIBUTIONS

All authors contributed to the article and approved the submitted version.

FUNDING

This work was undertaken at the request of and sponsored by GlaxoSmithKline Biologicals SA.

REFERENCES

1. Schwechheimer C, Kuehn MJ. Outer-Membrane Vesicles From Gram-negative Bacteria: Biogenesis and Functions. *Nat Rev Microbiol* (2015) 3 (0):605–9. doi: 10.1038/nrmicro3525
2. Collins BS. Gram-Negative Outer Membrane Vesicles in Vaccine Development. *Discovery Med* (2011) 12(62):7–15.
3. Micoli F, MacLennan CA. Outer Membrane Vesicle Vaccines. *Semin Immunol* (2020) 50:101433. doi: 10.1016/j.smim.2020.101433
4. Berlanda Scorza F, Colucci AM, Maggiore L, Sanzone S, Rossi O, Ferlenghi I, et al. High Yield Production Process for Shigella Outer Membrane Particles. *PloS One* (2012) 7(6):e35616–e. doi: 10.1371/journal.pone.0035616
5. Gerke C, Colucci AM, Giannelli C, Sanzone S, Vitali CG, Sollai L, et al. Production of a Shigella Sonnei Vaccine Based on Generalized Modules for Membrane Antigens (Gmma), 790gahb. *PloS One* (2015) 10(8):e0134478–e. doi: 10.1371/journal.pone.0134478
6. Berlanda Scorza F, Doro F, Rodríguez-Ortega MJ, Stella M, Liberatori S, Taddei AR, et al. Proteomics Characterization of Outer Membrane Vesicles From the Extraintestinal Pathogenic Escherichia Coli DeltatolR IHE3034 Mutant. *Mol Cell Proteomics MCP* (2008) 7(3):473–85. doi: 10.1074/mcp.M700295-MCP200
7. Rossi O, Pesce I, Giannelli C, Aprea S, Caboni M, Citiulo F, et al. Modulation of Endotoxicity of Shigella Generalized Modules for Membrane Antigens (GMMA) by Genetic Lipid A Modifications: Relative Activation of TLR4 and TLR2 Pathways in Different Mutants. *J Biol Chem* (2014) 289(36):24922–35. doi: 10.1074/jbc.M114.566570
8. Rossi O, Caboni M, Negrea A, Necchi F, Alfini R, Micoli F, et al. Toll-Like Receptor Activation by Generalized Modules for Membrane Antigens From Lipid A Mutants of <Span Class="Named-Content Genus-Species" Id="Named-Content-">Salmonella Enterica Serovars Typhimurium and Enteritidis. *Clin Vaccine Immunol* (2016) 23(4):304–14. doi: 10.1128/CVI.00023-16
9. Mancini F, Gasperini G, Rossi O, Aruta MG, Raso MM, Alfini R, et al. Dissecting the Contribution of O-Antigen and Proteins to the Immunogenicity of Shigella Sonnei Generalized Modules for Membrane Antigens (GMMA). *Sci Rep* (2012) 11(1):906. doi: 10.1038/s41598-020-80421-y
10. Kis Z, Shattock R, Shah N, Kontoravdi C. Emerging Technologies for Low-Cost, Rapid Vaccine Manufacture. *Biotechnol J* (2019) 14(7):1–2. doi: 10.1002/biot.201970055
11. Gasperini G, Raso MM, Arato V, Aruta MG, Cescutti P, Necchi F, et al. Effect of O-Antigen Chain Length Regulation on the Immunogenicity of Shigella and Salmonella Generalized Modules for Membrane Antigens (Gmma). *Int J Mol Sci* (2012) 22(3):1309. doi: 10.3390/ijms22031309
12. Richardson NI, Ravenscroft N, Arato V, Oldrini D, Micoli F, Kuttel MM. Conformational and Immunogenicity Studies of the Shigella Flexneri Serogroup 6 O-Antigen: The Effect of O-Acetylation. *Vaccines (Basel)* (2012) 9(5):432. doi: 10.3390/vaccines9050432
13. Raso MM, Gasperini G, Alfini R, Schiavo F, Aruta MG, Carducci M, et al. GMMA and Glycoconjugate Approaches Compared in Mice for the Development of a Vaccine Against Shigella Flexneri Serotype 6. *Vaccines* (2020) 8: (2):60. doi: 10.3390/vaccines8020160
14. De Benedetto G, Alfini R, Cescutti P, Caboni M, Lanzilao L, Necchi F, et al. Characterization of O-antigen Delivered by Generalized Modules for Membrane Antigens (GMMA) Vaccine Candidates Against Nontyphoidal Salmonella. *Vaccine* (2017) 35(3):419–26. doi: 10.1016/j.vaccine.2016.11.089
15. Schager AE, Dominguez-Medina CC, Necchi F, Micoli F, Goh YS, Goodall M, et al. Igg Responses to Porins and Lipopolysaccharide Within an Outer Membrane-Based Vaccine Against Nontyphoidal Salmonella Develop at Discordant Rates. *mBio* (2018) 9(2). doi: 10.1128/mBio.02379-17
16. Koeberling O, Ispasanie E, Hauser J, Rossi O, Pluschke G, Caugant DA, et al. A Broadly-Protective Vaccine Against Meningococcal Disease in Sub-Saharan Africa Based on Generalized Modules for Membrane Antigens (GMMA). *Vaccine* (2014) 32(23):2688–95. doi: 10.1016/j.vaccine.2014.03.068
17. Keiser PB, Biggs-Cicatelli S, Moran EE, Schmiel DH, Pinto VB, Burden RE, et al. A Phase Study of a Meningococcal Native Outer Membrane Vesicle Vaccine Made From a Group B Strain With Deleted Lpxl and synX, Over-Expressed Factor H Binding Protein, Two PorAs and Stabilized OpcA Expression. *Vaccine* (2011) 29(7):1413–20. doi: 10.1016/j.vaccine.2010.12.039
18. Keiser PB, Gibbs BT, Coster TS, Moran EE, Stoddard MB, Labrie JE3rd, et al. A Phase Study of a Group B Meningococcal Native Outer Membrane Vesicle Vaccine Made From a Strain With Deleted lpxL2 and Synx and Stable Expression of Opca. *Vaccine* (2010) 28(43):6970–6. doi: 10.1016/j.vaccine.2010.08.048
19. van de Waterbeemd B, Streefland M, van der Ley P, Zomer B, van Dijken H, Martens D, et al. Improved OMV Vaccine Against Neisseria Meningitidis Using Genetically Engineered Strains and a Detergent-Free Purification Process. *Vaccine* (2010) 28(30):4810–6. doi: 10.1016/j.vaccine.2010.04.082
20. Bartolini E, Ianni E, Frigimelica E, Petracca R, Galli G, Berlanda Scorza F, et al. Recombinant Outer Membrane Vesicles Carrying Chlamydia Muridarum HtrA Induce Antibodies That Neutralize Chlamydial Infection In Vitro. *J Extracell Vesicles* (2013) 2(1):20181. doi: 10.3402/jev.v2i0.208
21. Daleke-Schermerhorn MH, Felix T, Soprova Z, ten Hagen-Jongman CM, Vikström D, Majlessi L, et al. Decoration of Outer Membrane Vesicles With Multiple Antigens by Using an Autotransporter Approach. *Applied Environ Microbiol* (2014) 80: (18):5854–65. doi: 10.1128/AEM.01941-14
22. Gasperini G, Alfini R, Arato V, Mancini F, Aruta MG, Kanvatirth P, et al. Salmonella Paratyphi A Outer Membrane Vesicles Displaying Vi Polysaccharide as a Multivalent Vaccine Against Enteric Fever. *Infect Immun* (2012) 89: (4):e00699–20. doi: 10.1128/IAI.00699-20
23. Watkins HC, Rappazzo CG, Higgins JS, Sun X, Brock N, Chau A, et al. Safe Recombinant Outer Membrane Vesicles That Display M2e Elicit Heterologous Influenza Protection. *Mol Ther* (2017) 25(4):989–1002. doi: 10.1016/j.ymthe.2017.01.010
24. Scaria PV, Rowe CG, Chen BB, Muratova OV, Fischer ER, Barnafo EK, et al. Outer Membrane Protein Complex as a Carrier for Malaria Transmission Blocking Antigen Pfs230. *NPJ Vaccines* (2019) 4:24. doi: 10.1038/s41541-019-0121-9
25. Grandi A, Tomasi M, Zanella I, Ganfini L, Caproni E, Fantappiè L, et al. Synergistic Protective Activity of Tumor-Specific Epitopes Engineered in Bacterial Outer Membrane Vesicles. *Front Oncol* (2017) 7:253. doi: 10.3389/fonc.2017.00253
26. van der Pol L, Stork M, van der Ley P. Outer Membrane Vesicles as Platform Vaccine Technology. *Biotechnol J* (2015) 10: (11):1689–706. doi: 10.1002/biot.201400395
27. Mancini F, Rossi O, Necchi F, Micoli F. Omv Vaccines and the Role of TLR Agonists in Immune Response. *International J Mol Sci* (2020) 2: (2):446. doi: 10.3390/ijms21124416
28. Bishop RE. Polymorphic Regulation of Outer Membrane Lipid A Composition. *mBio* (2016) 7:(6):e01903–16. doi: 10.1128/mBio.01903-16
29. Rossi O, Citiulo F, Mancini F. Outer Membrane Vesicles: Moving Within the Intricate Labyrinth of Assays That can Predict Risks of Reactogenicity in Humans. *Hum Vaccines Immunotherapeutics* (2012) 17(2):601–13. doi: 10.1080/21645515.2020.1780092
30. Raetz CR, Reynolds CM, Trent MS, Bishop RE. Lipid A Modification Systems in Gram-Negative Bacteria. *Annu Rev Biochem* (2007) 76:295–329. doi: 10.1146/annurev.biochem.76.010307.145803
31. Rietschel ET, Kirikae T, Schade FU, Mamat U, Schmidt G, Loppnow H, et al. Bacterial Endotoxin: Molecular Relationships of Structure to Activity and Function. *FASEB J* (1994) 8: (2):217–25. doi: 10.1096/fasebj.8.2.8119492
32. Schromm AB, Brandenburg K, Loppnow H, Moran AP, Koch MHJ, Rietschel ET, et al. Biological Activities of Lipopolysaccharides are Determined by the Shape of Their Lipid. *A portion* (2000) 267(7):2008–13. doi: 10.1046/j.1432-1327.2000.01204.x
33. Seydel U, Oikawa M, Fukase K, Kusumoto S, Brandenburg K. Intrinsic Conformation of Lipid A Is Responsible for Agonistic and Antagonistic Activity. *Eur J Biochem* (2000) 267: (10):3032–9. doi: 10.1046/j.1432-1033.2000.01326.x
34. Trent MS, Stead CM, Tran AX, Hankins JV. Diversity of Endotoxin and its Impact on Pathogenesis. *J endotoxin Res* (2006) 2(4):205–23. doi: 10.1179/096805106X118825
35. Dowling DJ, Sanders H, Cheng WK, Joshi S, Brightman S, Bergelson I, et al. A Meningococcal Outer Membrane Vesicle Vaccine Incorporating Genetically Attenuated Endotoxin Dissociates Inflammation From Immunogenicity. *Front Immunol* (2016) 7:562. doi: 10.3389/fimmu.2016.00562
36. Schneerson R, Barrera O, Sutton A, Robbins JB. Preparation, Characterization, and Immunogenicity of Haemophilus Influenzae Type B

Polysaccharide-Protein Conjugates. *J Exp Med* (1980) 152(2):361–76. doi: 10.1084/jem.152.2.361
37. Pollard AJ, Perrett KP, Beverley PC. Maintaining Protection Against Invasive Bacteria With Protein-Polysaccharide Conjugate Vaccines. *Nat Rev Immunol* (2009) 9(3):213–20. doi: 10.1038/nri2494
38. Rappuoli R. Glycoconjugate Vaccines: Principles and Mechanisms. *Sci Trans Med* (2018) 10(456):eaat4615. doi: 10.1126/scitranslmed.aat4615
39. Berti F, Micoli F. Improving Efficacy of Glycoconjugate Vaccines: From Chemical Conjugates to Next Generation Constructs. *Curr Opin Immunol* (2020) 65:42–9. doi: 10.1016/j.coi.2020.03.015
40. Micoli F, Rondini S, Alfini R, Lanzilao L, Necchi F, Negrea A, et al. Comparative Immunogenicity and Efficacy of Equivalent Outer Membrane Vesicle and Glycoconjugate Vaccines Against Nontyphoidal Salmonella. *Proc Natl Acad Sci United States America* (2018) 115(41):10428–33. doi: 10.1073/pnas.1807655115
41. Gnopo YMD, Watkins HC, Stevenson TC, DeLisa MP, Putnam D. Designer Outer Membrane Vesicles as Immunomodulatory Systems – Reprogramming Bacteria for Vaccine Delivery. *Advanced Drug Delivery Rev* (2017) 114:132–42. doi: 10.1016/j.addr.2017.05.003
42. Stevenson TC, Cywes-Bentley C, Moeller TD, Weyant KB, Putnam D, Chang Y-F, et al. Immunization With Outer Membrane Vesicles Displaying Conserved Surface Polysaccharide Antigen Elicits Broadly Antimicrobial Antibodies. *PNAS* (2018) 115: (14):E3106–15. doi: 10.1073/pnas.1718341115
43. Marini A, Rossi O, Aruta MG, Micoli F, Rondini S, Guadagnuolo S, et al. Contribution of Factor H-Binding Protein Sequence to the Cross-Reactivity of Meningococcal Native Outer Membrane Vesicle Vaccines With Over-Expressed fHbp Variant Group 1. *PloS One* (2017) 12(7):e0181508. doi: 10.1371/journal.pone.0181508
44. Micoli F, Alfini R, Di Benedetto R, Necchi F, Schiavo F, Mancini F, et al. Gmma Is a Versatile Platform to Design Effective Multivalent Combination Vaccines. *Vaccines (Basel)* (2020) 8(3):540. doi: 10.3390/vaccines8030540
45. Liu Y, Hammer LA, Liu W, Hobbs MM, Zielke RA, Sikora AE, et al. Experimental Vaccine Induces Th-driven Immune Responses and Resistance to Neisseria Gonorrhoeae Infection in a Murine Model. *Mucosal Immunol* (2017) 10(6):1594–608. doi: 10.1038/mi.2017.11
46. Valguarnera E, Feldman MF. Chapter Ten - Glycoengineered Outer Membrane Vesicles as a Platform for Vaccine Development. In: B Imperiali, editor. *Methods in Enzymology*. (Cambridge, Massachusetts: Academic Press). (2017). p. 285–310.
47. Obiero CW, Ndiaye AGW, Sciré AS, Kaunyangi BM, Marchetti E, Gone AM, et al. A Phase 2a Randomized Study to Evaluate the Safety and Immunogenicity of the 790GAHB Generalized Modules for Membrane Antigen Vaccine Against Shigella Sonnei Administered Intramuscularly to Adults From a Shigellosis-Endemic Country. *Front Immunol* (2017) 8:1884–. doi: 10.3389/fimmu.2017.01884
48. Launay O, Lewis DJM, Anemona A, Loulergue P, Leahy J, Sciré AS, et al. Safety Profile and Immunologic Responses of a Novel Vaccine Against Shigella Sonnei Administered Intramuscularly, Intradermally and Intranasally: Results From Two Parallel Randomized Phase Clinical Studies in Healthy Adult Volunteers in Europe. *EBioMedicine* (2017) 22:164–72. doi: 10.1016/j.ebiom.2017.07.013
49. Launay O, Ndiaye AGW, Conti V, Loulergue P, Sciré AS, Landre AM, et al. Booster Vaccination With GVGH Shigella Sonnei 790GAHB GMMA Vaccine Compared to Single Vaccination in Unvaccinated Healthy European Adults: Results From a Phase Clinical Trial. *Front Immunol* (2019) 10:335–. doi: 10.3389/fimmu.2019.00335
50. Micoli F, Rossi O, Conti V, Launay O, Sciré AS, Aruta MG, et al. Antibodies Elicited by the Shigella Sonnei GMMA Vaccine in Adults Trigger Complement-Mediated Serum Bactericidal Activity: Results From a Phase Dose Escalation Trial Followed by a Booster Extension. *Front Immunol* (2012) 12: (1607):1607. doi: 10.3389/fimmu.2021.671325
51. Cohen D, Meron-Sudai S, Bialik A, Asato V, Goren S, Ariel-Cohen O, et al. Serum IgG Antibodies to Shigella Lipopolysaccharide Antigens – a Correlate of Protection Against Shigellosis. *Hum Vaccines Immunotherapeutics* (2019) 15(6):1401–8. doi: 10.1080/21645515.2019.1606971
52. Li YP, Yu SL, Huang ZJ, Huang J, Pan J, Feng X, et al. An Impaired Inflammatory Cytokine Response to Gram-Negative LPS in Human Neonates Is Associated With the Defective TLR-mediated Signaling Pathway. *J Clin Immunol* (2015) 35(2):218–26. doi: 10.1007/s10875-015-0128-6
53. Rosenqvist E, Høiby E, Bjune G, Aase A, Halstensen A, Lehmann A, et al. Effect of Aluminium Hydroxide and Meningococcal Serogroup C Capsular Polysaccharide on the Immunogenicity and Reactogenicity of a Group B Neisseria Meningitidis Outer Membrane Vesicle Vaccine. *Developments Biol standardization* (1998) 92:323–33.
54. Tunheim G, Arnemo M, Næss LM, Norheim G, Garcia L, Cardoso D, et al. Immune Responses of a Meningococcal A + W Outer Membrane Vesicle (OMV) Vaccine With and Without Aluminium Hydroxide Adjuvant in Two Different Mouse Strains. *APMIS* (2016) 124: (11):996–1003. doi: 10.1111/apm.12589
55. Kelly HG, Kent SJ, Wheatley AK. Immunological Basis for Enhanced Immunity of Nanoparticle Vaccines. *Expert Rev Vaccines* (2019) 18(3):269–80. doi: 10.1080/14760584.2019.1578216
56. Zhang H, Burnum KE, Luna ML, Petritis BO, Kim J-S, Qian W-J, et al. Quantitative Proteomics Analysis of Adsorbed Plasma Proteins Classifies Nanoparticles With Different Surface Properties and Size. *Proteomics* (2011) 11: (23):4569–77. doi: 10.1002/pmic.201100037
57. Prior JT, Davitt C, Kurtz J, Gellings P, McLachlan JB, Morici LA. Bacterial-Derived Outer Membrane Vesicles are Potent Adjuvants That Drive Humoral and Cellular Immune Responses. *Pharmaceutics* (2012) 3(2):131. doi: 10.3390/pharmaceutics13020131
58. Schetters STT, Jong WSP, Horrevorts SK, Kruijssen LJW, Engels S, Stolk D, et al. Outer Membrane Vesicles Engineered to Express Membrane-Bound Antigen Program Dendritic Cells for Cross-Presentation to CD8(+) T Cells. Acta Biomaterialia. *Acta Biomaterialia* (2019) 91:248–57. doi: 10.1016/j.actbio.2019.04.033
59. Manolova V, Flace A, Bauer M, Schwarz K, Saudan P, Bachmann MF. Nanoparticles Target Distinct Dendritic Cell Populations According to Their Size. *Eur J Immunol* (2008) 38: (5):404–3. doi: 10.1002/eji.200737984
60. Phan TG, Grigorova I, Okada T, Cyster JG. Subcapsular Encounter and Complement-Dependent Transport of Immune Complexes by Lymph Node B Cells. *Nat Immunol* (2007) 8(9):992–000. doi: 10.1038/ni1494
61. Carter RH, Fearon DT. CD9: Lowering the Threshold for Antigen Receptor Stimulation of B Lymphocytes. *Sci (New York NY)* (1992) 256(5053):105–7. doi: 10.1126/science.1373518
62. Kranich J, Krautler NJ. How Follicular Dendritic Cells Shape the B-Cell Antigenome. *Front Immunol* (2016) 7:225. doi: 10.3389/fimmu.2016.00225
63. Hu X, Deng Y, Chen X, Zhou Y, Zhang H, Wu H, et al. Immune Response of A Novel ATR-AP205-00 Conjugate Anti-hypertensive Vaccine. *Sci Rep* (2017) 7 (1):12580. doi: 10.1038/s41598-017-12996-y
64. Bennett NR, Zwick DB, Courtney AH, Kiessling LL. Multivalent Antigens for Promoting B and T Cell Activation. *ACS Chem Biol* (2015) 10(8):1817–24. doi: 10.1021/acschembio.5b00239
65. Baker SM, Settles EW, Davitt C, Gellings P, Kikendall N, Hoffmann J, et al. Burkholderia Pseudomallei OMVs Derived From Infection Mimicking Conditions Elicit Similar Protection to a Live-Attenuated Vaccine. *NPJ Vaccines* (2012) 6(1):18. doi: 10.1038/s41541-021-00281-z
66. Palmieri E, Arato V, Oldrini D, Ricchetti B, Aruta MG, Pansegrau W, et al. Stability of Outer Membrane Vesicles-Based Vaccines, Identifying the Most Appropriate Methods to Detect Changes in Vaccine Potency. *Vaccines (Basel)* (2021) 9(3):229. doi: 10.3390/vaccines9030229

Conflict of Interest: This work was undertaken at the request of and sponsored by GlaxoSmithKline Biologicals SA. GSK Vaccines Institute for Global Health Srl is an affiliate of GlaxoSmithKline Biologicals SA. All authors are employed by the GSK group of companies.

frontiers in Microbiology

ORIGINAL RESEARCH
published: 16 August 2021
doi: 10.3389/fmicb.2021.715802

Deletion of *alpB* Gene Influences Outer Membrane Vesicles Biogenesis of *Lysobacter* sp. XL1

*Irina V. Kudryakova[1], Alexey S. Afoshin[1], Tanya V. Ivashina[2], Natalia E. Suzina[3], Elena A. Leontyevskaya[1] and Natalia V. Leontyevskaya (Vasilyeva)[1]**

[1] Laboratory of Microbial Cell Surface Biochemistry, Pushchino Center for Biological Research, G. K. Skryabin Institute of Biochemistry and Physiology of Microorganisms, Russian Academy of Sciences, Pushchino, Russia, [2] Laboratory of Molecular Microbiology, Pushchino Center for Biological Research, G. K. Skryabin Institute of Biochemistry and Physiology of Microorganisms, Russian Academy of Sciences, Pushchino, Russia, [3] Laboratory of Microbial Cytology, Pushchino Center for Biological Research, G. K. Skryabin Institute of Biochemistry and Physiology of Microorganisms, Russian Academy of Sciences, Pushchino, Russia

Outer membrane vesicles (OMVs) produced by Gram-negative bacteria constitute important factors in defining interactions with the extracellular milieu. *Lysobacter* sp. XL1 produces OMVs capable of lysing microbial cells due to the presence in their cargo of bacteriolytic protease L5 (AlpB). Although protein L5 has been functionally and biochemically characterized (including aspects of its packing into OMVs), its role in vesicle biogenesis through genetic deletion of *alpB* had not been studied previously. Here, we have successfully deleted *alpB* by allelic replacement and show that the *alpB* deletion mutant produces a significantly lower amount of OMVs that lack bacteriolytic activity and display altered ultrastructural characteristics in relation to the OMVs produced by the wild-type strain. These results confirm that, as previously proposed, protein L5 participates in OMV production through a mechanism that is not yet fully understood.

Keywords: biogenesis of vesicles, *Lysobacter* sp. XL1, antimicrobial potency of vesicles, deletion in gene *alpB*, bacteriolytic protease L5

OPEN ACCESS

Edited by:
Alejandro J. Yañez, Austral University of Chile, Chile

Reviewed by:
Yoshihiro Ojima, Osaka City University, Japan
Meta J. Kuehn, Duke University, United States

****Correspondence:***
Natalia V. Leontyevskaya (Vasilyeva)
vasilyevanv@rambler.ru

Specialty section:
This article was submitted to Microbial Physiology and Metabolism, a section of the journal Frontiers in Microbiology

Received: *27 May 2021*
Accepted: *16 July 2021*
Published: *16 August 2021*

Citation:
Kudryakova IV, Afoshin AS, Ivashina TV, Suzina NE, Leontyevskaya EA and Leontyevskaya (Vasilyeva) NV (2021) Deletion of alpB Gene Influences Outer Membrane Vesicles Biogenesis of Lysobacter sp. XL1. Front. Microbiol. 12:715802. doi: 10.3389/fmicb.2021.715802

INTRODUCTION

Outer membrane vesicles (OMVs) are structures 50–300 nm in diameter that all Gram-negative bacteria form from their outer membrane (OM). OMVs perform a number of vital activities in relation to nutrient uptake, microbe–microbe interactions (including horizontal gene transfer), pathogen–host interactions, symbiotic interactions, and cell protection like phage and toxin release (Mashburn-Warren and Whiteley, 2006; Avila-Calderón et al., 2015; Schwechheimer and Kuehn, 2015; Guerrero-Mandujano et al., 2017; Nagakubo et al., 2020). In light of this, the topicality of vesicle studies is evident.

At present, one of the most intriguing issues in vesicle subject matter is OMV biogenesis. At first, vesicles were considered to form due to spontaneous evagination of the OM, followed by the release of these fragments (Knox et al., 1966). Later on, three models of vesicle biogenesis were formulated. According to the first model, vesicles form in the region of a decreased concentration of lipoproteins (Hoekstra et al., 1976; Deatherage et al., 2009; Schwechheimer et al., 2014). The second model explains the presence of cell debris [misfolded proteins, peptidoglycan

and lipopolysaccharide (LPS) fragments] in vesicles (Zhou et al., 1998; Hayashi et al., 2002; Schwechheimer et al., 2014). According to the third model, the formation of vesicles occurs under the action of curvature-inducing molecules (B-type LPS, signalling molecule 2-heptyl-3-hydroxy-4-quinolone (PQS) (Kadurugamuwa and Beveridge, 1995; Mashburn-Warren and Whiteley, 2006; Schertzer and Whiteley, 2012). Thus, all these models indicate that vesicles form from OM destabilization loci, and their contents are periplasmic components randomly captured in the process of vesicle formation.

With time, the view of vesicle biogenesis began to change. Data supporting a model for the specific sorting of vesicle components emerged (Horstman and Kuehn, 2000; Kato et al., 2002; Haurat et al., 2011, 2015; Schwechheimer and Kuehn, 2015). This contributed to the emergence of the theory of the formation of various vesicle groups (subpopulations) produced by one cell type (Olofsson et al., 2010; Rompikuntal et al., 2012; Kunsmann et al., 2015; Kudryakova et al., 2015; Afoshin et al., 2020). It should be noted that this theory enables understanding the ability of vesicles to perform various vital activities of the bacterial cell. It is evident that a relation between vesicle biogenesis processes and component sorting is bound to exist. It is hypothesized that these components themselves are factors contributing to vesicle biogenesis. We addressed this hypothesis by studying of vesicle biogenesis in *Lysobacter* sp. XL1.

The Gram-negative bacterium *Lysobacter* sp. XL1 has been studied at our laboratory for about 45 years. This bacterium is a potent producer of a complex of extracellular bacteriolytic enzymes. To date, five bacteriolytic enzymes (L1–L5) have been isolated and partially characterized. By the specificity of their action on bacterial peptidoglycans, the lytic enzymes of *Lysobacter* sp. XL1 are endopeptidases (L1, L4, L5), amidase (L2), and a muramidase (L3). The bacteriolytic complex is highly efficient in breaking down competitive cells of bacteria, yeasts, mycelial fungi and some protozoa (Kulaev et al., 2006). This property makes *Lysobacter* sp. XL1 an active participant of microbial biocenoses in nature and a biotechnologically promising strain producing novel antimicrobial agents. In 2008, we found *Lysobacter* sp. XL1 to form vesicles that lysed cells of Gram-positive bacteria, yeasts, mycelial fungi and possessed a curative action with respect to staphylococcal and anthrax infections. The lytic action of vesicles is determined by bacteriolytic enzyme L5, which is a component of their cargo (Vasilyeva et al., 2008, 2014). Research into the OMV biogenesis of *Lysobacter* sp. XL1 found their formation to occur in OM segments enriched with cardiolipin (Kudryakova et al., 2017). Fractionation of vesicles revealed a group/subpopulation of vesicles containing protein L5. Electron immunocytochemistry of *Lysobacter* sp. XL1 cell sections established protein L5 to concentrate in certain loci of the periplasm at the inner leaflet of the OM; it is from these loci that vesicles form (Kudryakova et al., 2015). We hypothesized that protein L5 could participate in vesicle biogenesis. To study this, the gene of protein L5 (*alpB*) was expressed in cells of a phylogenetically close genus *Pseudomonas fluorescens* Q2-87/B. It was found that in the recombinant strain, protein L5 was contained in vesicles. Cells of the recombinant strain were shown to form a larger number of vesicles as compared with the parent strain (Kudryakova et al., 2017). All these data indirectly confirmed the involvement of bacteriolytic protein L5 in the biogenesis of that group of vesicles by means of which it was released into the extracellular milieu. To substantiate this model, the goal of the present study to investigate OMV production by an *alpB* mutant strain compared with that of the wild-type strain. We have deleted *alpB* in *Lysobacter* sp. XL1, which in itself is an important experimental accomplishment mainly because the ill-developed molecular tools available for conducting genetic studies on *Lysobacter* had not previously permitted gene knockouts. Here, we report that the quantity of vesicles produced by the mutant strain was significantly lower than that of the wild-type strain and the lytic properties of mutant strain vesicles were lost practically completely, confirming that protein L5 influences OMV formation.

MATERIALS AND METHODS

Bacterial Strains, Plasmids, and Growth Conditions

All bacterial strains and plasmids used are listed in **Table 1**.

Escherichia coli strain XL1-Blue used for molecular cloning was grown in a Luria–Bertani (LB) medium containing (g/l): tryptone, 10; yeast extract, 5; NaCl, 10; pH 7.0 at 37°C. Wild-type *Lysobacter* sp. XL1, *Lysobacter* sp. XL1Δ*alpB*::*tet*, and *Lysobacter* sp. XL1Δ*alpB*::*alpB* strains were grown at 29°C in modified LB (LB-M) broth (in g/l: peptone, 5; yeast extract, 5; NaCl, 5; pH 7.5). *Lysobacter* cultures were grown for 20 h, which corresponds to the end of the exponential growth phase. Antibiotics were added as necessary at the following final concentrations (μg/ml): for *E. coli*: tetracycline (Tc), 10; gentamicin (Gm), 10; ampicillin (Ap), 100; for *Lysobacter* sp. XL1: Tc, 10; Gm, 20. For screening clones that had undergone double crossover events, sucrose was added to a final concentration of 10%. When plates of solid media were required, agar at a concentration of 15 g/L was added to the corresponding broths.

Bacterial cultures used in lysis tests (*Staphylococcus aureus* 209P, *Micrococcus luteus* B-1813, *Micrococcus roseus* B-1236, and *Bacillus cereus* B-454) were grown at 29°C as confluent lawns on plates of IBPM RAS medium (in g/l: yeast extract, 1; soybean extract, 30; tryptone, 5; aminopeptide, 60; agar, 15; pH 7.2).

DNA Manipulations

DNA recombinant techniques were performed according to standard procedures (Sambrook and Russell, 2001). All restriction endonucleases, T4 polynucleotide kinase, shrimp alkaline phosphatase, and T4 DNA ligase were obtained from Thermo Fisher Scientific (United States) and used according to the manufacturer's recommendations. TaqSE DNA polymerase was from SybEnzyme (Russia), and Q5 high-fidelity DNA polymerase was purchased from New England Biolabs (United States). Plasmid DNA was isolated and purified using a Quantum Prep Plasmid Miniprep Kit (Bio-Rad, United States). The PCR reactions (total volume is 50 μl) were conducted in the following conditions: 200 μM dNTPs, 0.5 μM forward and reverse primers, 0.05 ng/μl *Lysobacter* sp. XL1 genomic DNA

TABLE 1 | Strains and plasmid used in this study.

Strains and plasmids	Characteristics	References
Lysobacter sp. XL1	Wild-type	Kulaev et al., 2006
Lysobacter sp. XL1 Δ*alpB::tet*	Deletion in *alpB* gene (mutant form)	This study
Lysobacter sp. XL1 Δ*alpB::alpB*	Complementation of mutant strain (complemented form)	This study
S. aureus 209P	Wild-type	*
M. roseus B-1236^T	Wild-type	VKM B-1236
M. luteus B-1813^T	Wild-type	VKM B-1813
B. cereus B-454^T	Wild-type	VKM B-454
E. coli XL1-Blue	*recA1 endA1 gyrA96 thi hsdR17 supE44 relA1 lac/[*F′:Tn10 *proAB + lacI^q lacZ*Δ*M15 traD36]*	Bullock et al., 1987
pJQ200SK	Suicide vector with a *sacB* gene, Gm^R	Quandt and Hynes, 1993
pBR322	Source of Tc^R cassette	Balbás et al., 1986
pJQ200SKΔ*5′alpB*	pJQ200SK with 924-bp DNA fragment containing 3′ end of *alpB* and downstream region	This study
pJQ200SKΔ*alpB*	pJQ200SK with 880-bp deletion in *alpB*	This study
pJQ200SKΔ*alpB::tet*	pJQ200SK carrying deletion in *alpB* marked with 1.43-kb Tc^R cassette	This study
pJQ200SKΔ*alpB::alpB*	pJQ200SK carrying the full-length *alp*B with downstream and upstream genome sequences	This study

**Kindly provided by Federal Budget Institution of Science «State Research Center for Applied Microbiology and Biotechnology».*

(for amplification of a 924-bp DNA fragment containing the 3′ end of *alpB* and downstream region, an 825-bp DNA fragment containing the 5′ end of *alpB* and upstream region and the full-length *alpB* gene with downstream and upstream genome sequences) or 7 ng/μl pBR322 plasmid (for amplification of 1.43 kb Tc^R cassette), 0.02 U/μl Q5 high-fidelity DNA polymerase (New England Biolabs) in 1 × reaction buffer containing 2 mM $MgCl_2$. The thermo cycles were programmed according to the manufacturer's protocol: initial denaturation at 98°C for 30 s, followed by 30 cycles of 98°C for 10 s, annealing temperature 60°C for 20 s, 72°C for time that was determined by amplicon length (extension times are 30 s per kb), and a final extension at 72°C for 2 min. Amplicons were separated in gels of 0.8% agarose (Merck, Germany) in Tris-acetate-ethylenediaminetetraacetic acid (TAE) buffer containing 0.5 μg/ml ethidium bromide, visualized in a Bio-Print ST4 gel documentation system (Vilber lourmat, France), at 354 nm, and purified by QIAquick spin-column (Qiagen, United States). The concentration of DNA was measured using NanoPhotometer P360 (IMLEN, Germany) and by electrophoretic assay in 0.8% agarose gel.

Plasmid Constructions

Deletion of *alpB* was done by allelic replacement using a suicide plasmid construct (**Figure 1**). Briefly, a 924-bp DNA fragment containing the 3′ end of *alpB* and its downstream region was amplified from the genomic DNA of *Lysobacter* sp. XL1 with a pair of primers L5_*Sac*I(for) and L5_*Sma*I(rev). All primers are listed in **Supplementary Table 1**. The resulting amplicon was ligated into *Sac*I/*Sma*I-digested suicide vector pJQ200SK to form pJQ200SKΔ5′*alpB*. Subsequently, an 825-bp DNA fragment containing the 5′ end of *alpB* and its upstream region was amplified with primers L5_*Sma*I(for) and L5_*Xho*I(rev) and ligated into *Sma*I/*Xho*I-digested pJQ200SKΔ5′*alpB* to give pJQ200SKΔ*alpB*. In pJQ200SKΔ*alpB*, the *alpB* gene carries an 880-bp deletion in its central region. Finally, the deletion allele was marked by the insertion of a 1.43-kb Tc^R cassette amplified from pBR322 with primers Tc(for) and Tc(rev), which was phosphorylated with T4 polynucleotide kinase and ligated into *Sma*I-digested pJQ200SKΔ*alpB* pretreated with shrimp alkaline phosphatase to produce the suicide vector plasmid pJQ200SKΔ*alpB*::*tet* (**Figure 1** and **Supplementary Figure 1A**).

To replace the *alpB*::*tet* allele in the deletion mutant with the wild-type *alpB* gene, the full-length *alpB* gene (which is 1,200 bp long) plus its immediate downstream and upstream sequences was amplified using primers L5_*Sac*I(for) and L5_*Xho*I(rev) followed by ligation of the amplicon into the *Sac*I/*Xho*I-digested pJQ200SK to yield pJQ200SKΔ*alpB::alpB* (**Supplementary Figure 1B**). All cloned DNA fragments were sequenced at the Evrogen JSC (Russia) to confirm the correctness of inserts and the absence of random mutations.

Bacterial Transformation and Electroporation

E. coli cells were transformed by the RbCl method according to Hanahan (1983). *Lysobacter* sp. XL1 electro-competent cells were prepared according to Lin and McBride (1996). Briefly, 20-μl aliquots of *Lysobacter* sp. competent cells in 10% ice-cold glycerol were mixed with 250 ng of pJQ200SKΔ*alpB*::*tet* or pJQ200SKΔ*alpB::alpB* plasmid DNA in 2-mm gapped cuvettes (Bio-Rad, United States). Electroporation was performed using a Gene Pulser apparatus (Bio-Rad, United States) under conditions at 12.5 kV/cm. Immediately after the electric pulse, 1 ml of an LB-M medium was added to the pulsed bacterial cell suspension, which was then incubated for 3 h at 29°C without agitation, and subsequently plated on solid medium containing the appropriate antibiotics.

Selection of *Lysobacter* sp. XL1Δ*alpB::tet* Deletion Strain and Complementation of Mutation

After electroporation of pJQ200SKΔ*alpB*::*tet* into *Lysobacter* sp. XL1 (or of pJQ200SKΔ*alpB*::*alpB* into the *Lysobacter* sp. XL1 *alpB*::*tet* mutant), single crossover (SCO) clones with

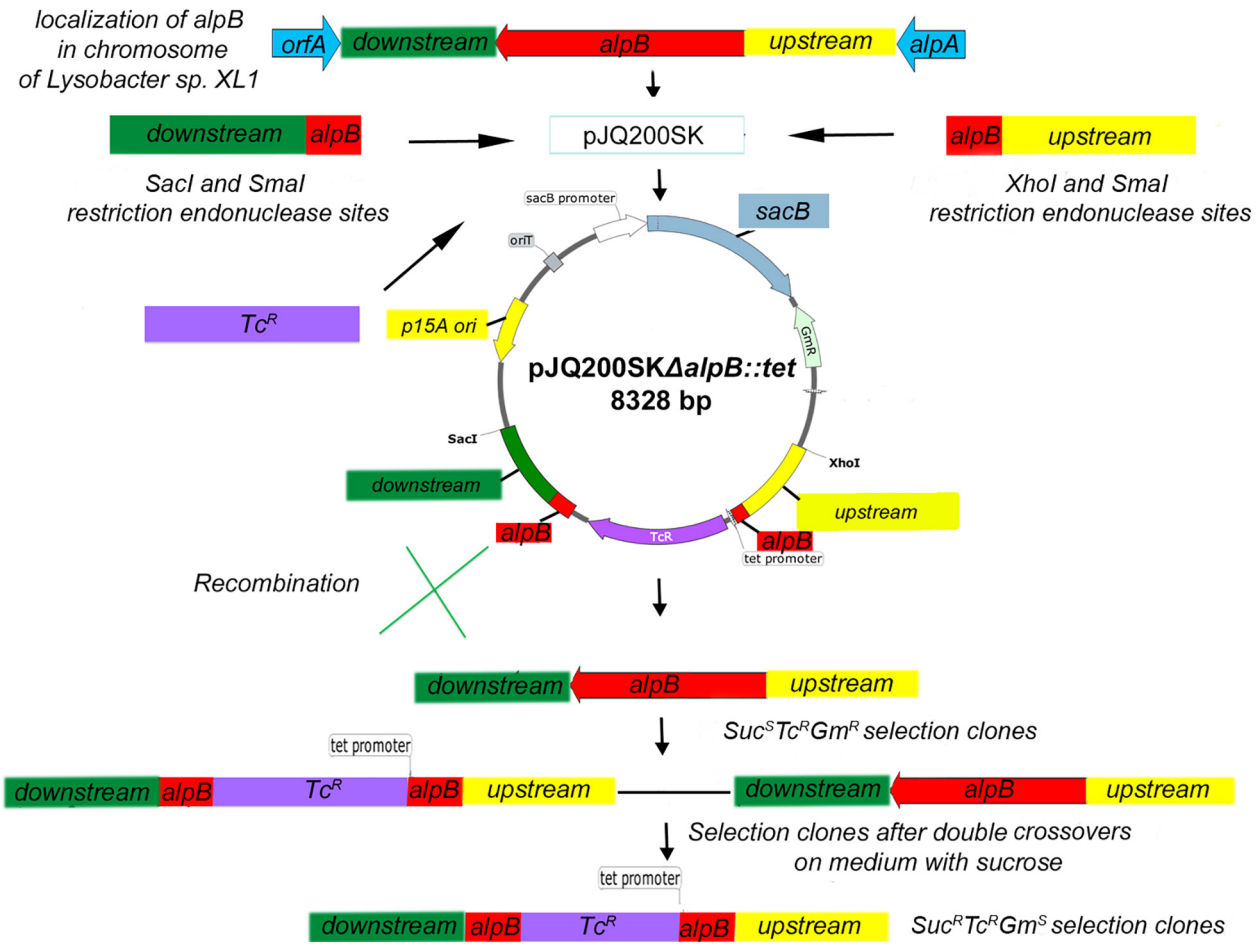

FIGURE 1 | Scheme of inserting a mutation into the *alpB* gene of *Lysobacter* sp. XL1. The pJQ200SKΔ*alpB::tet* recombinant plasmid was introduced into cells of *Lysobacter* sp. XL1 *via* electroporation. Integration of the plasmid into the chromosome was testified by the resistance of transformants to gentamicin (plasmid marker) and tetracycline (cassette marker inserted into the deletion locus) and by the sensitivity to sucrose. As a result of merodiploid resolution, $Suc^{R}Tc^{R}Gm^{S}$ clones with double crossovers between the mutant and wild-type alleles of the *alpB* gene were selected.

the $Suc^{S}Tc^{R}Gm^{R}$ phenotype were screened (**Figure 1**). Double crossover clones (DCOs) with the $Suc^{R}Tc^{R}Gm^{S}$ phenotype were counter-selected after growing one SCO clone in LB-M broth containing sucrose for 3 h at 29°C, followed by plating and cultivation for 72 h at 29°C on LB-M agar containing Tc. DCOs were confirmed by PCR for the presence of the wild-type or deletion allele using primers in **Supplementary Table 1**, which amplify a 2.62-kb product from the wild-type allele, or a 3.17-kb product from the mutant allele. The sites of recombination in DCOs were confirmed by sequencing.

Obtaining Outer Membrane Vesicles

OMVs were isolated by ultracentrifugation from equal volumes of the culture liquids of *Lysobacter* sp. XL1, *Lysobacter* sp. XL1Δ*alpB*::*tet*, and *Lysobacter* sp. XL1Δ*alpB*::*alpB* strains grown in LB-M liquid medium. Briefly, cells from a 0.3-L culture were pelleted by centrifugation at 7,500 × *g* for 20 min at 4°C, and the supernatant was recovered. Vesicles were then pelleted from 300-ml supernatants by centrifugation in an L5-50 ultracentrifuge (Beckman, United States) at 113,000 × *g* for 2 h at 4°C. The OMV pellet was washed once with 50 mM Tris-HCl, pH 8.0, by resuspension and centrifugation at the same speed for 1 h. The washed vesicle pellet was resuspended in 600 μl of 50 mM Tris-HCl, pH 8.0, and stored at –20°C.

Sodium Dodecyl Sulfate–Polyacrylamide Gel Electrophoresis

For the electrophoretic assay, preparations of wild-type *Lysobacter* sp. XL1 OMVs and *Lysobacter* sp. XL1Δ*alpB::tet* OMVs were sedimented with trichloroacetic acid at a final concentration of 10%. Preparations of OMVs were equal and contained 0.04 mg of total proteins. Protein residues were analyzed by electrophoresis with 0.1% sodium dodecyl sulfate (SDS) in 12.5% polyacrylamide gel (PAG). Electrophoresis in stacking gel was run at 60 V; in separating gel, at 180 V. Protein bands in gels were revealed by staining with a solution of Coomassie Brilliant Blue R-250 (Serva, Germany). As molecular weight markers, we used SM0431 (Thermo Fisher Scientific,

United States): β-galactosidase (116 kDa), bovine serum albumin (66.2 kDa), ovalbumin (45 kDa), lactate dehydrogenase (35 kDa), REase Bsp981 (25 kDa), β-lactoglobulin (18.4 kDa), and lysozyme (14.4 kDa).

Thin-Layer Chromatography

Preparations of wild-type *Lysobacter* sp. XL1 OMVs and *Lysobacter* sp. XL1Δ*alpB*::*tet* OMVs were aligned by mass of protein (20 μg) for phospholipid extraction. Phospholipids were extracted from both preparations with chloroform–methanol mixture (1:2 v/v) according to the method of Ames (1968). Individual phospholipids were separated by two-dimensional chromatography on silica gel plates 60 F254 (HPTLC; Merck, Germany) using $CHCl_3$–CH_3OH–H_2O (65:25:4 v/v) mixture as the first-dimension separation system and $CHCl_3$–CH_3OH–CH_3COOH–H_2O (40:7.5:6:1.8 v/v) as the second-dimension separation system. Phospholipids were visualized using molybdenum blue solution.

Quantitation of Outer Membrane Vesicles by Biochemical Analysis

The total protein concentration in OMV preparations was measured by the Lowry method (Lowry et al., 1951) against a standard curve done with bovine serum albumin (Sigma, United States) in the 2–20 μg/ml range.

The concentration of 2-Keto-3-deoxyoctanate (Kdo, a core LPS component) was determined by the reaction with thiobarbituric acid, exactly as described by Karkhanis et al. (1978). The standard curve was done with an aqueous solution of Kdo (Sigma, United States) in the 1.85–29.60 μg/ml range.

Measurement of Lytic Activity

The total bacteriolytic activities of culture supernatants were determined by turbidimetry as previously reported (Vasilyeva et al., 2014). Briefly, liquid cultures of *Lysobacter* strains in LB-M were centrifuged at 7,500 × *g* for 20 min at 4°C to pellet bacterial cells. Then, 25 μl of the clear supernatant were added to 975 μl of heat-killed cells of *S. aureus* 209P suspended to an OD_{540} = 0.5 in 10 mM Tris-HCl, pH 8.0, and incubated at 37°C for 5 min. The reaction was arrested by placing test tubes on ice, and the OD_{540} of the suspension was measured in a Beckman DU 730 (United States) spectrophotometer. A decrease in 0.01 optical units/min (at 37°C) was taken as a lytic unit (LU). Therefore, LUs were calculated by the following formula: {[0.5 (initial OD_{540} of suspension) – final OD_{540}] × 1,000 μl (total reaction volume)}/[5 min (time of reaction) × 25 μl (volume of sample) × 0.01 (correction coefficient for OD reduction per minute)].

The lytic action of OMVs against live Gram-positive bacteria was determined by the spot assay with *S. aureus* 209P, *M. roseus* B-1236, *M. luteus* B-1813, and *B. cereus* B-454 (Vasilyeva et al., 2014). Three independent experiments were carried out. Vesicle preparations (as 12-μl aliquots) were applied on a pre-grown lawn of the target bacterium on an agar plate after the concentration of OMVs had been adjusted to have identical amounts (0.09 μg) of Kdo. Applied OMV samples were allowed to absorb into the lawn for 30 min, and plates were then incubated at 29°C overnight (16 h). The lytic action of the preparations was then assessed by simple observation where the presence of a clear lysis zone indicated strong activity, a hazy lysis zone indicated weak activity, and the absence of a lysis zone indicated no activity.

Transmission Electron Microscopy

Samples of OMVs (obtained from two independent isolation runs) of *Lysobacter* sp. XL1, *Lysobacter* sp. XL1Δ*alpB*::*tet*, and *Lysobacter* sp. XL1Δ*alpB*::*alpB* were diluted fivefold in 50 mM Tris-HCl, pH 8.0, and 10 μl were placed on top of a formvar-coated copper grid. The applied sample was allowed to adsorb for 2 min, and sample excess was then removed using filter paper. After air-drying, the samples were stained with 10 μl of 0.3% aqueous solution of uranyl acetate (pH 4.0), placed on the grids, and immediately removed using filter paper. Negatively stained preparations were examined with a JEM-1400 transmission electron microscope (JEOL, Japan) at an accelerating voltage of 80 kV, and random images of representative fields of observation were captured with an 11-Megapixel TEM Camera MORADA G2 (EMSIS GmbH, Germany). All micrographs were done with 25,000 magnification. The six micrographs were obtained from each experiment. All vesicles of wild-type *Lysobacter* sp. XL1, *Lysobacter* sp. XL1Δ*alpB*::*tet*, and *Lysobacter* sp. XL1Δ*alpB*::*alpB* in all obtained micrographs were studied. Ultrastructural observations, including various degrees of density (full and empty vesicles), and measurements were done on the acquired images. The ratio of full/empty vesicles was estimated by visual analysis of micrographs: full OMVs have compact packaging or local crystal packing, and in the case of the empty OMVs, it was possible to distinguish the backing film of the grid.

Statistical Analysis

All experiments were in triplicates. Statistical analysis was done using GraphPad Prism (version 9.1.0; GraphPad Software, San Diego, CA). The analytical results were compared by Student's *t*-test. Data are presented as the mean ± standard deviation. Statistical significance was considered at $p < 0.05$.

RESULTS

alpB Is Not an Essential Gene in *Lysobacter* sp. XL1

The deletion of *alpB* in *Lysobacter* sp. XL1Δ*alpB*::*tet* was genetically confirmed by the production of a 3,177-bp PCR amplicon (**Figure 2**) that was subsequently sequenced to show that the Tc^R cassette had indeed replaced, as expected, the region between 117 and 997 bp of the *alpB* gene. *Lysobacter* sp. XL1Δ*alpB*::*tet* grew well in LB-M (**Table 2**), indicating that *alpB* is not an essential gene and does not affect the gross overall physiology of the bacterium. The mutation was confirmed biochemically and functionally by the reduction in bacteriolytic activity of the mutant strain (**Table 2** and **Supplementary Figure 4**). Since the total lytic activity of *Lysobacter* sp. XL1 is attributed to several secreted bacteriolytic enzymes (reviewed

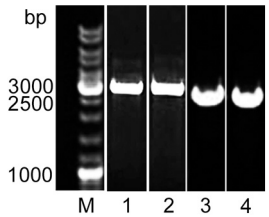

FIGURE 2 | Molecular evidence of the deletion of *alpB* in *Lysobacter* XL1. Agarose gel stained with ethidium bromide after the electrophoresis of PCR amplicons produced with primers L5_*Sac*I(for) and L5_*Xho*I(rev). The PCR amplicon for the mutant allele is 3,177 bp long (including *alpB* flanking sequences + the TcR cassette), whereas the wild-type allele produces a 2,623-bp product (including the full-length *alpB* gene + adjacent regions). M, SM0331 GeneRuler DNA Ladder Mix (Thermo Fisher Scientific, United States) (lane taken from **Supplementary Figure 3**); **(1)** *Lysobacter* sp. XL1 Δ*alpB::tet* clone (from **Supplementary Figure 2**); **(2)** pJQ200SK Δ*alpB::tet* plasmid (from **Supplementary Figure 2**); **(3)** *Lysobacter* sp. XL1 Δ*alpB::alpB* clone (from **Supplementary Figure 3**); and **(4)** *Lysobacter* sp. XL1 clone (from **Supplementary Figure 3**).

TABLE 2 | Effect of *alpB* gene knockout on *Lysobacter* sp. XL1 growth and bacterial activity.

Strains	OD_{540}	LU/ml
Lysobacter sp. XL1 Δ*alpB::tet*[a]	4.65 ± 0.09	115.68 ± 18.82
Wild-type *Lysobacter* sp. XL1[b]	3.81 ± 0.81[ns]	149.00 ± 14.85***
Lysobacter sp. XL1 Δ*alpB::alpB*[c]	4.59 ± 0.28[ns]	140.00 ± 0.92*

*Results are shown as mean ± standard deviation. The mean values were obtained in three independent experiments, each with two technical replicates (n = 6). [ns] Not statistically significant = $p > 0.05$ when comparing the means of the two groups ([a] and [b]—OD_{540}; [a] and [c]—OD_{540}) by the Student's t-test. *** $p < 0.001$ when comparing the means of the two groups ([a] and [b]−LU/ml) by the Student's t-test. *$p < 0.05$ when comparing the means of the two groups ([a] and [c]—LU/ml) by the Student's t-test.*

by Vasilyeva et al., 2013), it seems reasonable to surmise that the observed difference in lytic activities between *Lysobacter* sp. XL1 and *Lysobacter* sp. XL1 Δ*alpB::tet* corresponds to the activity contributed by protein L5 (AlpB).

Effect of *alpB* Gene Knockout on Vesicle Formation of *Lysobacter* sp. XL1

Vesicle preparations obtained from equal volumes of the culture liquids of the wild-type, complemented strain, and mutant strains were analyzed by TEM and characterized biochemically.

In the preparation of mutant strain vesicles, the predominant species are larger vesicles 100–150 nm (47%) and 150–190 nm (30%) in diameter (**Figure 3B** and **Supplementary Figure 5A**). Vesicles 50–100 nm in diameter are few (14%). Vesicles in the preparation produced from the wild-type culture liquid are predominantly 50–100 nm (73%) and 100–150 nm (24%) in diameter (**Figure 3A** and **Supplementary Figure 5B**). Large vesicles 150–190 nm in diameter are 3% of the total number of vesicles occurring in all fields of vision. Vesicles in the preparation produced from the complemented strain are two groups as wild-type: 100–150 nm (46%) and 50–100 nm (33%) (**Figure 3C** and **Supplementary Figure 5C**). Vesicles 150–190 nm and 190–250 nm in diameter are few (17 and 4%, respectively).

The main distinction of the preparations is the various degrees of density (full and empty vesicles). The micrographs in **Figures 3D–G** show OMVs with representative ultrastructures observed in all preparations. Vesicles with clear-cut dense cores of polygonal shapes occur (**Figure 3D**). Such structures bear resemblance to crystals and may form as a result of a dense packing of their contents. Besides these, vesicles with diffusely distributed contents of low densities (**Figure 3E**) and with small contents in the form of a small loose granule at the periphery inside the vesicle (**Figure 3F**) occur, as well as broken vesicles with their contents released outside (**Figure 3G**). Although all these types of vesicles were observed in all preparations, they were present in very different proportions. TEM obtained that the preparations of wild-type OMVs and complemented strain OMVs contain more full vesicles than that of mutant strain vesicles. Thus, the ratio of full/empty vesicles in the wild-type strain and complemented strain is 2, whereas in the mutant strain, it is 0.7. This analysis considered only intact vesicles.

The main components of vesicles are proteins, lipids, and LPS. By the content of protein and Kdo (the essential constituent of LPS) in the preparations, we can assess the quantity of formed vesicles. The general analysis of protein revealed that its content in the vesicle preparation of the mutant strain is 2.4 times and 1.6 times lower than that in the vesicle preparation of the wild-type strain and complemented strain, respectively (**Table 3** and **Supplementary Figure 6**). The content of Kdo in the vesicle preparation of the mutant strain is 2.1 times and 1.6 times lower than in the vesicle preparation of the wild-type strain and complemented strain, respectively (**Table 3** and **Supplementary Figure 7**).

The general electrophoretic pattern for the distribution of major proteins in the vesicle preparation of the mutant strain did not differ from that in the wild-type strain. The phospholipid composition of mutant strain vesicles did not change either (**Supplementary Figure 8**). The main phospholipid of vesicles of the wild-type and mutant strains is cardiolipin.

In summary, the knockout of the *alpB* gene led to a decrease of the quantity of formed vesicles and to a change in the degree to which they are filled.

The obtained results confirm the influence of protein L5 on vesicle biogenesis of *Lysobacter* sp. XL1.

Effect of *alpB* Gene Knockout on the Lytic Properties of Vesicles

To study the effect of *alpB* gene knockout on the lytic activity of vesicles, as test cultures, we used living cells of several bacteria (**Table 4** and **Figure 4**).

As seen in the figure and table, vesicles of the mutant strain practically lost their ability to lyse living target cells, whereas vesicles of the wild-type and complemented strains possess a strong lytic action. Thus, knockout of the *alpB* gene was accompanied by a significant decrease of vesicles' lytic properties, in addition to the reduction of the antimicrobial potential of *Lysobacter* sp. XL as a whole.

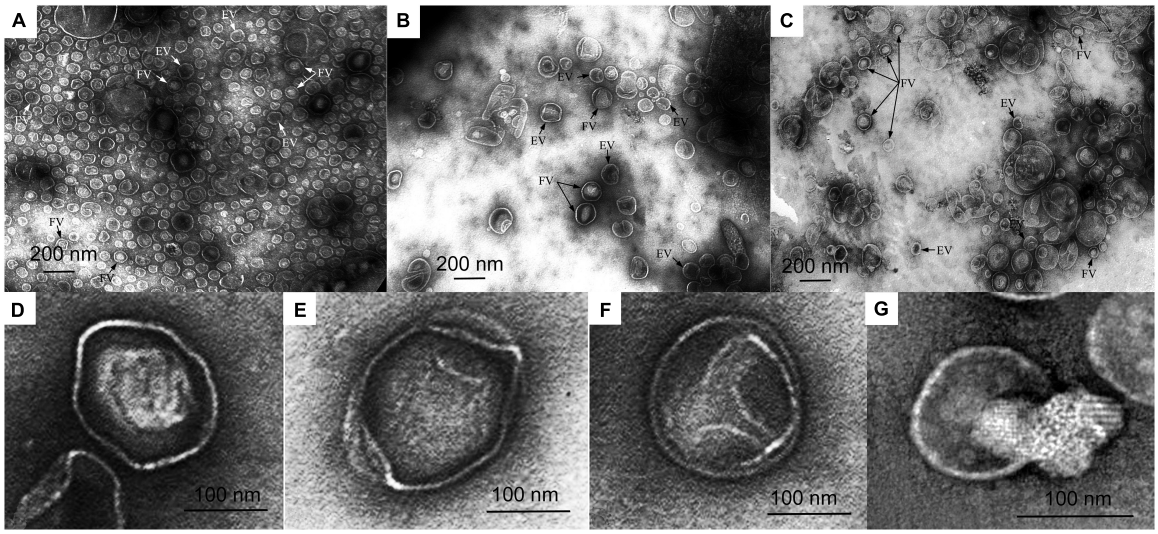

FIGURE 3 | Electron microscopy of vesicle preparations. **(A)** Wild-type *Lysobacter* sp. XL1 vesicles. **(B)** *Lysobacter* sp. XL1Δ*alpB::tet* mutant strain vesicles. **(C)** *Lysobacter* sp. XL1Δ*alpB::alpB* complemented strain vesicles. **(D)** Representative outer membrane vesicle (OMV) with a clear-cut dense polygonal core. **(E)** Representative OMV with diffusely distributed low-density contents. **(F)** Representative OMV with small contents in the form of a small loose granule at the periphery inside the vesicle. **(G)** Representative empty (or broken) vesicle that seems to have spilled its contents. Vesicles from **(D–G)** are from the mutant strain. EV, empty vesicle; FV, full vesicle.

DISCUSSION

The results presented in this work continue the investigation of the influence of bacteriolytic enzyme L5 on the vesicle biogenesis in the Gram-negative bacterium *Lysobacter* sp. XL1.

Based on our earlier work, we proposed that protein L5 could be involved in the biogenesis of the subpopulation of vesicles by means of which it was released into the extracellular milieu and proposed a model of the process. Immediately, a question arose how enzyme L5 could initiate the formation of vesicles. One of the existing models of vesicle biogenesis in Gram-negative bacteria assumes a pressure of cell debris (misfolded proteins, peptidoglycan, and LPS fragments) on the inner leaflet of the OM, which provokes vesicle formation (Zhou et al., 1998; Hayashi et al., 2002; Schwechheimer et al., 2014). At some point, we assumed that vesicle biogenesis in *Lysobacter* sp. XL1 could occur according to that model. However, on the premise that the OM is a dynamic and well-regulated cell structure of complex organization, it is impossible to imagine that a pressure caused by accumulation of protein at the inner leaflet of the OM

TABLE 3 | Content of protein and Kdo in OMV preparations.

OMVs	Total protein content, mg/ml	Concentration of Kdo (μg/ml)
Lysobacter sp. XL1Δ*alpB::tet*[a]	0.39 ± 0.07	8.25 ± 2.49
Wild-type *Lysobacter* sp. XL1[b]	0.95 ± 0.04***	17.35 ± 3.73***
Lysobacter sp. XL1Δ*alpB::alpB*[c]	0.62 ± 0.07***	12.84 ± 2.68*

*Results are shown as mean ± standard deviation. The mean values were obtained in three independent experiments, each with two technical replicates (n = 6). *** $p < 0.001$ when comparing the means of the two groups ([a] and [b]—total protein content and Kdo concentration; [a] and [c]—total protein content) by the Student's t-test. * $p < 0.05$ when comparing the means of the two groups ([a] and [c]—Kdo concentration) by the Student's t-test.*

TABLE 4 | Lytic action of vesicles.

Bacteria	OMV preparations		
	Wild-type *Lysobacter* sp. XL1	*Lysobacter* sp. XL1Δ*alpB::tet*	*Lysobacter* sp. XL1Δ*alpB::alpB*
S. aureus 209P	++	±	++
M. luteus B-1813	++	±	++
M. roseus B-1236	++	±	++
B. cereus B-454	++	±	++

++, strong lytic effect;±, weak lytic effect.

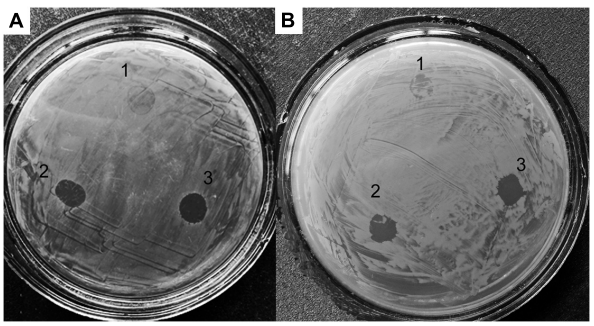

FIGURE 4 | Lytic activities of *Lysobacter* sp. XL1Δ*alpB::tet* **(1)**, *Lysobacter* sp. XL1Δ*alpB::alpB* **(2)**, and wild-type *Lysobacter* sp. XL1 **(3)** vesicle preparations with respect to live test cultures. **(A)** *S. aureus* 209P. **(B)** *M. luteus* B-1813.

could evoke vesicle formation. In our view, this single condition is insufficient.

Further investigation of the biogenesis revealed that the main phospholipid of *Lysobacter* sp. XL1 vesicles was cardiolipin (Kudryakova et al., 2017). That meant that vesicles formed from OM loci enriched with this phospholipid. The hydrophilic head of cardiolipin carries two negative charges, and, due to their intermolecular repulsion, the rigidity of the OM can be disturbed in loci enriched in this phospholipid, which leads to the emergence of a destabilization locus. According to two more known models, vesicles form from certain loci of OM destabilization, which can emerge due to a decreased lipoprotein content (Hoekstra et al., 1976; Deatherage et al., 2009; Schwechheimer et al., 2014) or an increased content of curvature-inducing molecules (B-type LPS, signaling molecule PQS) (Kadurugamuwa and Beveridge, 1995; Mashburn-Warren and Whiteley, 2006; Schertzer and Whiteley, 2012). We note here once again that the cell envelope has a complex organization, and the occurrence of destabilization loci leading to spontaneous evagination and release of OM fragments is not probable. Thus, it is also hard to consider that destabilization loci in the OM are the sole condition for vesicle formation.

Instead, we showed that *Lysobacter* sp. XL1 vesicles formed from cardiolipin-enriched OM loci, and a particular subpopulation contained bacteriolytic protein L5 (**Figure 5**). Based on these results, we suggested that vesicle formation was due to a set of several factors. An obligatory factor is the occurrence of an OM destabilization locus, and a factor initiating vesicle formation is a component of the inner contents; in the case of *Lysobacter* sp. XL1, it is bacteriolytic enzyme L5. We should single out here one more vesicle biogenesis model based on specific sorting of vesicles' inner components, proposed by American scientists Amanda Horstman and Meta Kuehn (Horstman and Kuehn, 2000). Their idea is intensively developed now (Haurat et al., 2011, 2015; Evans et al., 2012; Elhenawy et al., 2014; Schwechheimer and Kuehn, 2015). In our opinion, at present, this model can be considered to be the most significant for understanding vesicle biogenesis. It is proposed to be supplemented by the idea that vesicles form in the OM destabilization locus, and additionally, a vesicle-formation initiator is a sorted vesicle component. Other results can be taken to be in favor of this concept. Haurat et al. (2011) present possible models of selective protein sorting due to the occurrence of domains, which can interact with B-type LPS (from which destabilization loci form). The work considers the selective sorting of gingipain into *Porphyromonas gingivalis* vesicles. Besides, the same authors assume the occurrence of a sorting factor, which binds protein directed into vesicles to B-type LPS (Haurat et al., 2015). In this model, they draw an analogy with the role of galectin in protein sorting in the formation of eukaryotic exosomes. Those authors were the first to show a relation of the prospective vesicle component (the sorting component)

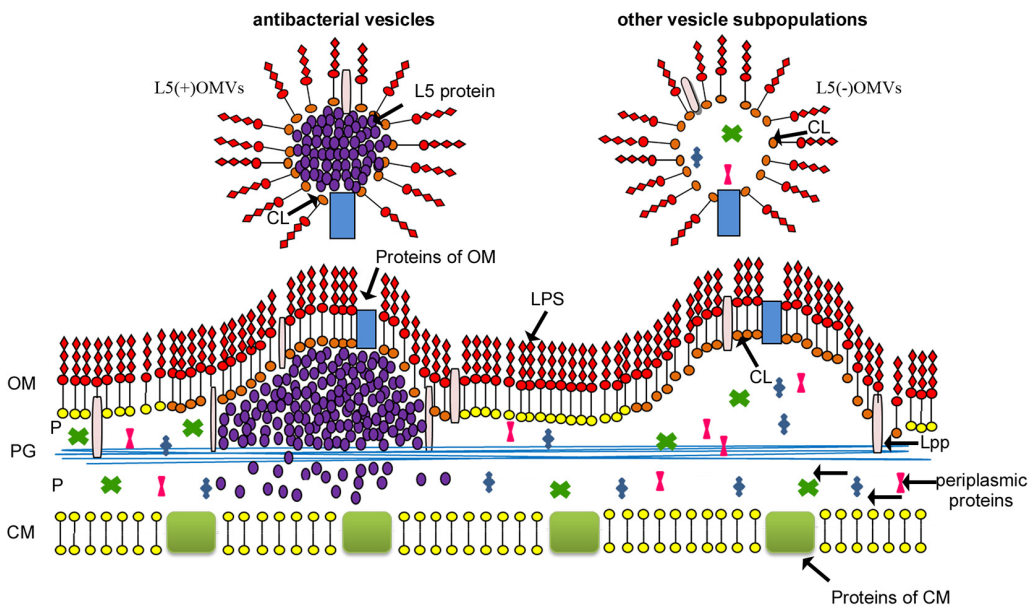

FIGURE 5 | Model of *Lysobacter* sp. XL1 vesicle biogenesis (Kudryakova et al., 2015) with modification. *Lysobacter* sp. XL1 forms several subpopulations of vesicles from OM loci enriched with CL. The hydrophilic head of cardiolipin carries two negative charges, and, due to their intermolecular repulsion, the rigidity of the OM can be disturbed in loci enriched with this phospholipid, which leads to the initiation of vesicle formation (Kudryakova et al., 2017). One of the vesicle subpopulations contains bacteriolytic enzyme L5. In the process of its topogenesis, this protein accumulates in the periplasm at the inner leaflet of the OM (Kudryakova et al., 2015) in the form of amyloid-like structures (Kudryakova et al., 2018). This may lead to a pressure on the cardiolipin-enriched inner leaflet of the OM (the destabilization locus) and contribute to the formation of a subpopulation of antibacterial vesicles containing protein L5. This vesicle subpopulation is a "bacterial bomb" for competitive bacteria and is involved in invasion expansion of ecological niches for *Lysobacter* sp. XL1. L5(+)OMVs, antibacterial subpopulation of vesicles containing protein L5; L5(–)OMVs, other subpopulations of vesicles; LPS, lipopolysaccharide; OM, outer membrane; P, periplasm; CM, cytoplasmic membrane; Lpp, lipoprotein; PG, peptidoglycan; CL, cardiolipin.

with B-type LPS, which leads to OM destabilization. Our model assumes that alkaline protein L5 possesses some affinity to the acid cardiolipin. Notably, studies of the structural and functional features of this enzyme have revealed the formation of amyloid-like structures with increased concentration. It has been found that, in vesicles, this enzyme is namely in its amyloid-like form (Kudryakova et al., 2018). This property can be assumed to be important for initiating the formation of vesicle in the destabilization locus. However, proof of this requires integrated molecular, genetic, and structural studies, which will enable understanding the accurate mechanism of the process.

Additional confirmation that protein L5 possesses an ability to initiate vesicle formation is the result of the expression of enzyme L5 in the recombinant strain *P. fluorescens* Q2-87/B (Kudryakova et al., 2017). As the result of expression of this protein gene, the recombinant strain formed a larger number of vesicles, which produced enzyme L5 and acquired lytic properties.

To confirm the role of protein L5 in *Lysobacter* sp. XL1 vesicle biogenesis, we lacked genetic studies, in particular, of the knockout of a corresponding gene. The generation of gene knockouts in *Lysobacter* spp. constitutes a very recent development, as the availability of molecular genetic tools for this bacterium has evolved slowly. Only a few investigations to date are known to involve the deletion of *Lysobacter* genes, like the chitinase gene and the genes responsible for the biosynthesis of antibiotics and for regulation of this process in *L. enzymogenes* OH11 (Qian et al., 2012; Xu et al., 2015; Wang et al., 2016, 2017). Therefore, the successful deletion of *alpB* represents an important contribution to this field of genetic investigation.

In this work, we present the results of research into the effect of bacteriolytic enzyme L5 gene knockout on vesicle formation in *Lysobacter* sp. XL1. As a result of this gene knockout, the total bacteriolytic activity of the culture liquid in the mutant strain decreased. The following results became crucial for our hypothesis: the mutant strain formed fewer vesicles, the degree of their filling decreased, the lytic properties of vesicles were lost practically completely. The latter result indicates that, in the mutant strain, there is no subpopulation of vesicles containing enzyme L5. However, other subpopulations of vesicles continued to form.

Thus, we conclude that bacteriolytic enzyme L5 influences the formation of vesicle subpopulations that contain it. The molecular mechanisms of this effect are yet to be established by future research.

DATA AVAILABILITY STATEMENT

The raw data supporting the conclusions of this article will be made available by the authors without undue reservation.

AUTHOR CONTRIBUTIONS

IK, AA, and NL contributed to planning the experiments. IK, AA, and TI contributed to the experimental work. EL contributed to the purification of vesicles. NS contributed to the electron microscopy. NL contributed to the project administration. IK contributed to the funds acquisition. IK and NL contributed to the writing the manuscript. All authors contributed to the article and approved the submitted version.

FUNDING

This research was funded by the Russian Science Foundation (Project No. 19-74-00086).

ACKNOWLEDGMENTS

We are grateful to Victor Selivanov for professional English translation. Electron microscopy was carried out at the UNIQEM Collection (Research Center of Biotechnology, Russian Academy of Sciences, Moscow, Russia).

SUPPLEMENTARY MATERIAL

The Supplementary Material for this article can be found online at: https://www.frontiersin.org/articles/10.3389/fmicb.2021.715802/full#supplementary-material

REFERENCES

Afoshin, A. S., Kudryakova, I. V., Borovikova, A. O., Suzina, N. E., Toropygin, I. Y., Shishkova, N. A., et al. (2020). Lytic potential of *Lysobacter capsici* VKM B-2533^T: bacteriolytic enzymes and outer membrane vesicles. *Sci. Rep*. 10:9944. doi: 10.1038/s41598-020-67122-2

Ames, G. F. (1968). Lipids of *Salmonella typhimurium* and *Escherichia coli*: structure and metabolism. *J. Bacteriol.* 95:833843. doi: 10.1128/jb.95.3.833-843.1968

Avila-Calderón, E. D., Araiza-Villanueva, M. G., Cancino-Diaz, J. C., López-Villegas, E. O., Sriranganathan, N., Boyle, S. M., et al. (2015). Roles of bacterial membrane vesicles. *Arch. Microbiol.* 197, 1–10. doi: 10.1007/s00203-014-1042-7

Balbás, P., Soberón, X., Merino, E., Zurita, M., Lomeli, H., Valle, F., et al. (1986). Plasmid vector pBR322 and its special-purpose derivatives – a review. *Gene* 50, 3–40. doi: 10.1016/0378-1119(86)90307-0

Bullock, W. O., Fernandez, J. M., and Short, J. M. (1987). XL1-Blue: a high efficiency plasmid transforming *recA Escherichia coli* strain with β-galactosidase selection. *BioTechniques* 5, 376–378.

Deatherage, B. L., Lara, J. C., Bergsbaken, T., Rassoulian Barrett, S. L., Lara, S., and Cookson, B. T. (2009). Biogenesis of bacterial membrane vesicles. *Mol. Microbiol.* 72, 1395–1407. doi: 10.1111/j.1365-2958.2009.06731.x

Elhenawy, W., Debelyy, M. O., and Feldman, M. F. (2014). Preferential packing of acidic glycosidases and proteases into *Bacteroides* outer membrane vesicles. *mBio* 5, e909–e914. doi: 10.1128/mBio.00909-14

Evans, A. G. L., Davey, H. M., Cookson, A., Currinn, H., Cooke-Fox, G., Stanczyk, P. J., et al. (2012). Predatory activity of *Myxococcus xanthus* outer-membrane vesicles and properties of their hydrolase cargo. *Microbiology* 158, 2742–2752. doi: 10.1099/mic.0.060343-0

Guerrero-Mandujano, A., Hernández-Cortez, C., Ibarra, J. A., and Castro-Escarpulli, G. (2017). The outer membrane vesicles: secretion system type zero. *Traffic* 18, 425–432. doi: 10.1111/tra.12488

Hanahan, D. (1983). Studies on transformation of *Escherichia coli* with plasmids. *J. Mol. Biol.* 166, 557–580. doi: 10.1016/s0022-2836(83)80284-8

Haurat, M. F., Aduse-Opoku, J., Rangarajan, M., Dorobantu, L., Gray, M. R., Curtis, M. A., et al. (2011). Selective sorting of cargo proteins into bacterial membrane vesicles. *J. Biol. Chem.* 286, 1269–1276. doi: 10.1074/jbc.M110.185744

Haurat, M. F., Elhenawy, W., and Feldman, M. F. (2015). Prokaryotic membrane vesicles: new insights on biogenesis and biological roles. *Biol. Chem.* 396, 95–109. doi: 10.1515/hsz-2014-0183

Hayashi, J., Hamada, N., and Kuramitsu, H. K. (2002). The autolysin of *Porphyromonas gingivalis* is involved in outer membrane vesicle release. *FEMS Microbiol. Lett.* 216, 217–222. doi: 10.1111/j.1574-6968.2002.tb11438.x

Hoekstra, D., van der Laan, J. W., de Leij, L., and Witholt, B. (1976). Release of outer membrane fragments from normally growing *Escherichia coli*. *Biochim. Biophys. Acta* 455, 889–899. doi: 10.1016/0005-2736(76)90058-4

Horstman, A. L., and Kuehn, M. J. (2000). Enterotoxigenic *Escherichia coli* secretes active heat-labile enterotoxin via outer membrane vesicles. *J. Biol. Chem.* 275, 12489–12496. doi: 10.1074/jbc.275.17.12489

Kadurugamuwa, J. L., and Beveridge, T. J. (1995). Virulence factors are released from *Pseudomonas aeruginosa* in association with membrane vesicles during normal growth and exposure to gentamicin: a novel mechanism of enzyme secretion. *J. Bacteriol.* 177, 3998–4008. doi: 10.1128/jb.177.14.3998-4008.1995

Karkhanis, Y. D., Zeltner, J. Y., Jackson, J. J., and Carlo, D. J. (1978). A new and improved microassay to determine 2-keto-3-deoxyoctonate in lipopolysaccharide of Gram-negative bacteria. *Anal. Biochem.* 85, 595–601. doi: 10.1016/0003-2697(78)90260-9

Kato, S., Kowashi, Y., and Demuth, D. R. (2002). Outer membrane-like vesicles secreted by *Actinobacillus actinomycetemcomitans* are enriched in leukotoxin. *Microb. Pathog.* 32, 1–13. doi: 10.1006/mpat.2001.0474

Knox, K. W., Vesk, M., and Work, E. (1966). Relation between excreted lipopolysaccharide complexes and surface structures of a lysine-limited culture of *Escherichia coli*. *J. Bacteriol.* 92, 1206–1217. doi: 10.1128/JB.92.4.1206-1217.1966

Kudryakova, I. V., Gabdulkhakov, A. G., Tishchenko, S. V., Lysanskaya, V. Y., Suzina, N. E., Tsfasman, I. M., et al. (2018). Structural and functional properties of antimicrobial protein L5 of *Lysîbacter sp.* XL1. *Appl. Microbiol. Biotechnol.* 102, 10043–10053. doi: 10.1007/s00253-018-9364-z

Kudryakova, I. V., Suzina, N. E., and Vasilyeva, N. V. (2015). Biogenesis of *Lysobacter* sp. XL1 vesicles. *FEMS Microbiol. Lett.* 362:fnv137. doi: 10.1093/femsle/fnv137

Kudryakova, I. V., Suzina, N. E., Vinokurova, N. G., Shishkova, N. A., and Vasilyeva, N. V. (2017). Studying factors involved in biogenesis of *Lysobacter* sp. XL1 outer membrane vesicles. *Biochemistry* 82, 501–509. doi: 10.1134/S0006297917040125

Kulaev, I. S., Stepnaya, O. A., Tsfasman, I. M., Tchermenskaja, T. S., Ledova, L. A., Zubrizkaja, L. G., et al. (2006). Bacteriolytic complex, method for producing said complex and strain for carrying out said method. *PatentNo: US 7,150,985 B2*.

Kunsmann, L., Rüter, C., Bauwens, A., Greune, L., Glüder, M., Kemper, B., et al. (2015). Virulence from vesicles: novel mechanisms of host cell injury by *Escherichia coli* O104:H4 outbreak strain. *Sci. Rep.* 5:13252. doi: 10.1038/srep13252

Lin, D., and McBride, M. J. (1996). Development of techniques for the genetic manipulation of the gliding bacteria *Lysobacter enzymogenes* and *Lysobacter brunescens*. *Can. J. Microbiol.* 42, 896–902. doi: 10.1139/m96-115

Lowry, O. H., Rosebrough, N. J., Farr, A. L., and Randall, R. J. (1951). Protein measurement with the Folin phenol reagent. *J. Biol. Chem.* 193, 265–275.

Mashburn-Warren, L. M., and Whiteley, M. (2006). Special delivery: vesicle trafficking in prokaryotes. *Mol. Microbiol.* 61, 839–846. doi: 10.1111/j.1365-2958.2006.05272.x

Nagakubo, T., Nomura, N., and Toyofuku, M. (2020). Cracking open bacterial membrane vesicles. *Front. Microbiol.* 10:3026. doi: 10.3389/fmicb.2019.03026

Olofsson, A., Vallström, A., Petzold, K., Tegtmeyer, N., Schleucher, J., Carlsson, S., et al. (2010). Biochemical and functional characterization of *Helicobacter pylori* vesicles. *Mol. Microbiol.* 77, 1539–1555. doi: 10.1111/j.1365-2958.2010.07307.x

Qian, G., Wang, Y., Qian, D., Fan, J., Hu, B., and Liu, F. (2012). Selection of available suicide vectors for gene mutagenesis using *chiA* (a chitinase encoding gene) as a new reporter and primary functional analysis of *chiA* in *Lysobacter enzymogenes* strain OH11. *World J. Microbiol. Biotechnol.* 28, 549–557. doi: 10.1007/s11274-011-0846-8

Quandt, J., and Hynes, M. F. (1993). Versatile suicide vectors which allow direct selection for gene replacement in gram-negative bacteria. *Gene* 127, 15–21. doi: 10.1016/0378-1119(93)90611-6

Rompikuntal, P. K., Thay, B., Khan, M. K., Alanko, J., Penttinen, A. M., Asikainen, S., et al. (2012). Perinuclear localization of internalized outer membrane vesicles carrying active cytolethal distending toxin from *Aggregatibacter actinomycetemcomitans*. *Infect. Immun.* 80, 31–42. doi: 10.1128/IAI.06069-11

Sambrook, J., and Russell, D. W. (2001). *Molecular Cloning: A Laboratory Manual*. New York: Cold Spring Harbor Laboratory Press.

Schertzer, J. W., and Whiteley, M. (2012). A bilayer-couple model of bacterial outer membrane vesicle biogenesis. *mBio* 3, e297–e211. doi: 10.1128/mBio.00297-11

Schwechheimer, C., and Kuehn, M. J. (2015). Outer-membrane vesicles from Gram-negative bacteria: biogenesis and functions. *Nat. Rev. Microbiol.* 13, 605–619. doi: 10.1038/nrmicro3525

Schwechheimer, C., Kulp, A., and Kuehn, M. J. (2014). Modulation of bacterial outer membrane vesicle production by envelope structure and content. *BMC Microbiol.* 14:324. doi: 10.1186/s12866-014-0324-1

Vasilyeva, N. V., Shishkova, N. A., Marinin, L. I., Ledova, L. A., Tsfasman, I. M., Muranova, T. A., et al. (2014). Lytic peptidase L5 of *Lysobacter* sp. XL1 with broad antimicrobial spectrum. *J. Mol. Microbiol. Biotechnol.* 24, 59–66. doi: 10.1159/000356838

Vasilyeva, N. V., Tsfasman, I. M., Suzina, N. E., Stepnaya, O. A., and Kulaev, I. S. (2008). Secretion of bacteriolytic endopeptidase L5 of *Lysobacter* sp. XL1 into the medium by means of outer membrane vesicles. *FEBS J.* 275, 3827–3835. doi: 10.1111/j.1742-4658.2008.06530.x

Vasilyeva, N. V., Tsfasman, I. M., Kudryakova, I. V., Suzina, N. E., Shishkova, N. A., Kulaev, I. S., et al. (2013). The role of membrane vesicles in secretion of *Lysobacter* sp. bacteriolytic enzymes. *J. Mol. Microbiol. Biotechnol.* 23, 142–151. doi: 10.1159/000346550

Wang, R., Xu, H., Du, L., Chou, S. H., Liu, H., Liu, Y., et al. (2016). TonB-dependent receptor regulates antifungal HSAF biosynthesis in *Lysobacter*. *Sci. Rep.* 6:26881. doi: 10.1038/srep26881

Wang, R., Xu, H., Zhao, Y., Zhang, J., Yuen, G. Y., Qian, G., et al. (2017). Lsp family proteins regulate antibiotic biosynthesis in *Lysobacter enzymogenes* OH11. *AMB Express* 7:123. doi: 10.1186/s13568-017-0421-2

Xu, G., Zhao, Y., Du, L., Qian, G., and Liu, F. (2015). Hfq regulates antibacterial antibiotic biosynthesis and extracellular lytic-enzyme production in *Lysobacter enzymogenes* OH11. *Microb. Biotechnol.* 8, 499–509. doi: 10.1111/1751-7915.12246

Zhou, L., Srisatjaluk, R., Justus, D. E., and Doyle, R. J. (1998). On the origin of membrane vesicles in gram-negative bacteria. *FEMS Microbiol. Lett.* 163, 223–228. doi: 10.1111/j.1574-6968.1998.tb13049.x

Conflict of Interest: The authors declare that the research was conducted in the absence of any commercial or financial relationships that could be construed as a potential conflict of interest.

Publisher's Note: All claims expressed in this article are solely those of the authors and do not necessarily represent those of their affiliated organizations, or those of the publisher, the editors and the reviewers. Any product that may be evaluated in this article, or claim that may be made by its manufacturer, is not guaranteed or endorsed by the publisher.

frontiers in Immunology

ORIGINAL RESEARCH
published: 15 September 2021
doi: 10.3389/fimmu.2021.730434

Pertussis Vaccine Candidate Based on Outer Membrane Vesicles Derived From Biofilm Culture

*Francisco Carriquiriborde[1], Pablo Martin Aispuro[1], Nicolás Ambrosis[1], Eugenia Zurita[1], Daniela Bottero[1], María Emilia Gaillard[1], Celina Castuma[1], Erika Rudi[1], Aníbal Lodeiro[2] and Daniela F. Hozbor[1]**

[1] Laboratorio VacSal, Instituto de Biotecnología y Biología Molecular (IBBM), Facultad de Ciencias Exactas, Universidad Nacional de La Plata, CCT-CONICET La Plata, La Plata, Argentina, [2] Instituto de Biotecnología y Biología Molecular (IBBM), Facultad de Ciencias Exactas, Universidad Nacional de La Plata, CCT-CONICET La Plata, La Plata, Argentina

OPEN ACCESS

Edited by:
Araceli Contreras-Rodriguez, Instituto Politécnico Nacional (IPN), Mexico

Reviewed by:
Tomasz Niedziela, Hirszfeld Institute of Immunology and Experimental Therapy (PAN), Poland
Virgilio Bocanegra-Garcia, Instituto Politécnico Nacional, Mexico
Scott Allen Walper, United States Naval Research Laboratory, United States

***Correspondence:**
Daniela F. Hozbor
hozbor.daniela@gmail.com;
hozbor@biol.unlp.edu.ar

Specialty section:
This article was submitted to Vaccines and Molecular Therapeutics, a section of the journal Frontiers in Immunology

Received: 24 June 2021
Accepted: 27 August 2021
Published: 15 September 2021

Citation:
Carriquiriborde F, Martin Aispuro P, Ambrosis N, Zurita E, Bottero D, Gaillard ME, Castuma C, Rudi E, Lodeiro A and Hozbor DF (2021) Pertussis Vaccine Candidate Based on Outer Membrane Vesicles Derived From Biofilm Culture. Front. Immunol. 12:730434. doi: 10.3389/fimmu.2021.730434

Outer membrane vesicles (OMV) derived from *Bordetella pertussis*—the etiologic agent of the resurgent disease called pertussis—are safe and effective in preventing bacterial colonization in the lungs of immunized mice. Vaccine formulations containing those OMV are capable of inducing a mixed Th1/Th2/Th17 profile, but even more interestingly, they may induce a tissue-resident memory immune response. This immune response is recommended for the new generation of pertussis-vaccines that must be developed to overcome the weaknesses of current commercial acellular vaccines (second-generation of pertussis vaccine). The third-generation of pertussis vaccine should also deal with infections caused by bacteria that currently circulate in the population and are phenotypically and genotypically different [in particular those deficient in the expression of pertactin antigen, PRN(-)] from those that circulated in the past. Here we evaluated the protective capacity of OMV derived from bacteria grown in biofilm, since it was observed that, by difference with older culture collection vaccine strains, circulating clinical *B. pertussis* isolates possess higher capacity for this lifestyle. Therefore, we performed studies with a clinical isolate with good biofilm-forming capacity. Biofilm lifestyle was confirmed by both scanning electron microscopy and proteomics. While scanning electron microscopy revealed typical biofilm structures in these cultures, BipA, fimbria, and other adhesins described as typical of the biofilm lifestyle were overexpressed in the biofilm culture in comparison with planktonic culture. OMV derived from biofilm (OMVbiof) or planktonic lifestyle (OMVplank) were used to formulate vaccines to compare their immunogenicity and protective capacities against infection with PRN(+) or PRN(-) *B. pertussis* clinical isolates. Using the mouse protection model, we detected that OMVbiof-vaccine was more immunogenic than OMVplank-vaccine in terms of both specific antibody titers and quality, since OMVbiof-vaccine induced antibodies with higher avidity. Moreover, when OMV were administered at suboptimal quantity for protection,

OMVbiof-vaccine exhibited a significantly adequate and higher protective capacity against PRN(+) or PRN(-) than OMVplank-vaccine. Our findings indicate that the vaccine based on *B. pertussis* biofilm-derived OMV induces high protection also against pertactin-deficient strains, with a robust immune response.

Keywords: *Bordetella pertussis*, outer membrane vesicles, biofilm, planktonic, protection, vaccine

INTRODUCTION

Pertussis, a highly contagious respiratory disease mainly caused by the Gram-negative bacterium *Bordetella pertussis*, has resurged in many countries even in those with high vaccination coverage (1–5). In order to confront this worrying epidemiological situation in the short term, vaccination schedules have been modified in many countries by implementing additional boosters (6–8). Currently, whole cell vaccines (wP) based on standardized cultures of *B. pertussis* strains and acellular vaccines (aP) composed of two (pertussis toxin and filamentous hemagglutinin), three (pertussis toxin, filamentous hemagglutinin and pertactin) or five (pertussis toxin, filamentous hemagglutinin, pertactin and fimbriae-2 and -3) immunogens are available. However, these vaccines manifest some weaknesses, such as the reactogenicity associated to wP or the faster waning immunity induced by aP (9, 10). This situation requires a third generation of vaccines with the capacity to overcome such weaknesses in the medium-long term (11). Thus, this new generation of vaccines must be i) safer than wP, ii) able to induce an immune response profile that is mostly Th1 and Th17 (12) with proliferation of the memory cell population resident in tissues (13, 14), iii) made up of multiple epitopes to minimize the selection pressure that it may exert on the circulating bacterial population, iv) able to protect against the circulating bacterial population, and v) biotechnologically easy to produce, ensuring accessibility to the entire population (5, 15).

The World Health Organization recommends, in Annex 6 of vaccines production against pertussis, that the strain used (hereafter referred to as vaccine strain) must be characterized and have a known history (https://www.who.int/biologicals/publications/trs/areas/vaccines/whole_cell_pertussis/Annex%206%20whole%20cell%20pertussis.pdf?ua=1visited on June 15 of 2021). Under this context, we designed a novel acellular vaccine candidate based on OMV derived from *B. pertussis*. This candidate was obtained from the strain *B. pertussis* Tohama phase I from the Collection of the Pasteur Institute in Paris (France), whose genome was sequenced and whose genotypic and phenotypic characteristics were widely studied by different laboratories (16–18). This strain was isolated in 1954 in Japan and since then, it has been used to produce wP and more recently to obtain immunogens that constitute aP. We already showed that OMV derived from *B. pertussis* Tohama phase I are safe and effective in preventing bacterial colonization in the lungs of immunized animals (19, 20). Furthermore, we have shown that vaccine formulations containing OMV derived from *B. pertussis* are capable of inducing a mixed Th1, Th2 and Th17 profile, but even more interestingly, they may induce a tissue-resident memory immune response (13). More recently, we described that these OMV induce inflammasome by the canonical and non- canonical ways (21). In addition, the OMV-based vaccine may protect against modern circulating isolates that possess the *ptx*P3, *prn*2 and *ptx*A1 genotypes (10, 22). The current challenge, however, is generating protection against strains that do not express the pertactin (PRN) vaccine antigen. PRN-deficient *B. pertussis* strains have recently been detected as prevalent bacteria in countries using aP vaccines (e.g. United States: 85%, Australia:> 80%, Sweden: 69%, etc.) (23–25). On the contrary, the prevalence of PRN-deficient *B. pertussis* strains in countries that switched to aP vaccines that exclude pertactin in their composition or use wP vaccine to cover the primary vaccination series, is low. As examples, Japan reduced the prevalence of PRN-deficient *B. pertussis* strains from 41% to 8% (26) and Argentina has very rare detection of PRN-deficient *B. pertussis* strains (27). All these observations provide a strong correlation between the use of aP vaccines containing PRN and a higher prevalence of PRN-deficient strains, suggesting a lower protective capacity of such aP vaccines against PRN-deficient *B. pertussis* in comparison with that conferred by wP vaccine. Furthermore, experiments using the murine model of protection have shown that PRN-deficient strains are more resistant to the immunity induced by aP vaccines than those expressing PRN (28, 29).

To further improve the protective capacity of OMV against the newest PRN(-) genotypes, one possible strategy is to obtain OMV from currently circulating clinical isolates. Since bacteria continue to evolve with a bottleneck caused by vaccines selective pressure, this strategy would force us not only to continuously select a representative clinical isolate but also to establish the frequency of this change. A rational alternative strategy is to identify a common and specific characteristic among the clinical isolates not present in the strains used for vaccine production. After decades of laboratory adaptation, vaccine strains evolved for planktonic growth in culture media under controlled conditions. By contrast, biofilm growth is detected in a much larger extent in clinical isolates—which present the characteristic of having recent contact with the host—than in laboratory-adapted strains (30). The formation of biofilms has been shown to increase the virulence and persistence of *B. pertussis* in the human nasopharynx (31). Furthermore, it has been shown that membrane proteins derived from the *B. pertussis* biofilm have immunogenic characteristics with protective capacity against virulent infection by *B. pertussis* in the murine protection model (32–34). At this point it is important to underscore that all currently available pertussis vaccines are formulated with antigens derived from planktonic bacterial cells. Under this context, we turned our efforts towards the

investigation of OMV obtained from *B. pertussis* biofilms as an improved vaccine candidate. In this study we have evaluated whether a vaccine formulated with those OMV is capable of overcoming the deficiencies of commercial vaccines in both controlling infections caused by the PRN(-) isolate/strain and inducing the recommended immunity for protection.

MATERIALS AND METHODS

Animals

Animal experiments were performed using female BALB/c mice 3 to 4 weeks of age, obtained from Faculty of Veterinary Sciences of the National University of La Plata (UNLP, Argentina). The studies have been approved by the Ethical Committee for Animal Experiments of the Faculty of Science of UNLP (Argentina, approval number 004-06-15 and 003-06-15).

Bacterial Strains and Growth Conditions

B. pertussis Tohama phase I strain, the Argentinian clinical isolate BpAR106 collected in 2001 from an infant patient residing in Buenos Aires (35), and PRN-deficient clinical isolates from both 2012 Washington (US) outbreak (36) and Argentinian collection of our Reference Laboratory (27) were used throughout this study. PRN deficiency in this isolate was caused by IS481 insertion in its *prn* gene, and its MLVA-MLST type is the most prevalent among the isolates from that outbreak (*ptx*P3, *ptx*A1, *prn*2).

Bacteria were grown on Bordet-Gengou agar (BGA, Difco) supplemented with 10% defibrinated sheep blood at 36.5°C for 72 h and plated again in the same medium for 24 h before each infection.

To carry out the planktonic culture of *B. pertussis*, the biomass obtained after replating for 24 h on BGA was used as inoculum for the Stainer-Scholte (37, 38) liquid medium supplemented with 1% casaminoacids (SSC). This inoculated medium was incubated at 36.5°C with shaking at 160 rpm until the optical density at 650 nm reached 1.2. For biofilm cultures, a planktonic culture was used as starting biomass and petri dishes as abiotic support. These petri dishes containing SSC medium were incubated at 36.5°C under static conditions for 96 h. To evaluate the biofilm formation, a modified version of the crystal violet assay described by O`Toole (39) was performed. At the incubation endpoint, the plates were washed out using PBS (pH 7.2) to remove the planktonic bacteria. Attached bacteria were then stained with 1 mL of 0.1% crystal violet solution (Biopack). The stain was dissolved by adding 1000 µL of 33% acetic acid solution. One-hundred µL of the stain solution was transferred to flat bottom microplates and quantified by measuring at 595 nm.

The biomasses from both planktonic and biofilm cultures were used to obtain outer membrane vesicles (OMV) as described below.

Isolation and Characterization of Outer Membrane Vesicles (OMV)

OMV were produced and characterized as previously described (40). Briefly, samples from the decelerating growth phase in liquid medium or 96 h-biofilm cultures were centrifuged and the bacterial pellets were resuspended in 20 mM Tris–HCl, 2 mM EDTA, pH 8.5. The suspension was sonicated (ultrasonic bath) in cool water for 20 min. After two centrifugations at 10,000 ×*g* for 20 min at 4°C, the supernatant was pelleted at 100,000 ×*g* for 2 h at 4°C. This pellet was resuspended in 20 mM Tris–HCl, pH 7.2. The samples obtained were negatively stained for electron microscope examination and size estimation. Protein content was estimated by the Bradford method using bovine serum albumin as standard (41). The presence of the main immunogenic proteins in the OMV was corroborated by immunoblot assays using specific antibodies as previously described (20, 42).

Scanning Electron Microscopy

The biomass obtained in the biofilm culture was fixed on the abiotic support by adding 2.5% glutaraldehyde. Increasing alcohol solutions ranging from 20 to 100% were used for dehydration. For observation, the sample was dried by the critical point technique and coated in gold. This procedure was performed by the microscopy service of the Metallurgical Physical Research Laboratory Ing. Gregorio Cusminsky (LIMF) from the Faculty of Engineering of UNLP, the equipment used for the observation was the FEI Quanta 200.

Transmission Electron Microscopy - Negative Staining

Transmission electron microscopy was carried out with a suspension of OMV in 0.1 mM ammonium acetate, pH 7.0. A drop of this suspension was placed on a grid covered with a reinforced carbon film. After 30 seconds, the excess liquid was gently removed with a filter paper and the grid was stained with a 2% phosphotungstic acid, pH 5.2. Observations were done with a Jeol JEM 1200EX Microscope.

Sodium Dodecylsulfate-Polyacrylamide Gel Electrophoresis (SDS-PAGE)

Samples of OMV obtained from *B. pertussis* cells were treated with Laemmli sample buffer and run on 12.5% SDS gels as previously described (42). Electrophoresis was performed at room temperature and constant voltage. Polypeptides and lipo-oligosaccharides were visualized by Coommassie Blue- and the BioRad silver-staining techniques, respectively.

Comparative Proteomic Study Between Samples Obtained From Planktonic and Biofilm Cultures

For this study, the methodology described by Nilsson et al. (43) was performed with the BpAR106 isolate. Briefly, 3 biological replicates of a bacterial lysate from a biofilm culture and another 3 from a planktonic culture were used. To obtain the samples, a bacterial suspension of OD650nm = 20 was started, which was then subjected to rupture using a Rybolizer Precellys equipment. After eliminating the cellular debris, a precipitation was carried out with 100% trichloroacetic acid at 4°C ON. The sediments obtained from this precipitation were resuspended in 50 mM

ammonium bicarbonate and treated with trypsin (Promega V5111). The trypsinized samples were desalted with Zip-Tip C18 columns (Millipore) and injected on a Nanoflow Ultrahigh-performance Liquid Chromatography (Thermo Scientific, model EASYnLC 1000) with an Easy-spray column (P/N ES801, C18, 2 μm, 100 Å, 50 μm × 15 cm, serial number: 10433446, temperature 50°C, Thermo Scientific) coupled to a quad Orbitrap mass spectrometer (Thermo Scientific, model Q-Exactive). The threshold for ion precursor selection was 10,000. The number of precursors chosen in each scan cycle was 15, and the accepted mass window for this selection was 1.6 m/z. The collision energy was normalized at 27. These analyzes were carried out at the Center for Chemical and Biological Studies by Mass Spectrometry (CEQUIBIEM), of the University of Buenos Aires (UBA).

For the analysis of the mass spectra and the identification of the peptides, the Max Quant software (version 1.5.3.30) was used. The search was carried out using the information on the genomic sequences of *B. pertussis* present in the Uni-Prot database. The identification of the peptides was carried out with a falsehood range (FDR) of 1% and the peptides thus selected were linked to a protein with a FDR also of 1%. The search parameters allowed up to 2 erroneous cuts with trypisin/P in the sequence and oxidation of methionine. In the identification of the proteins, a minimum of 2 peptides was used; the quantification of unlabeled proteins was performed as found with the MaxQuant software (version 1.5.3.30). All biological replicas of both culture conditions were included in the experimental design of the quantification of the level of label free proteins (LFQ) and normalization was carried out with 0.01 and 0.05 FDR filters for peptides and proteins respectively. For the statistical analysis, the Perseus program (version 1.5.6.0, from the Max Planck Institute of Germany) was used. The significance of the changes between biofilm and planktonic growth was determined with the Student's *t*-test with a p value <0.05.

Formulation of OMV-Based Vaccine

The characterized OMV from planktonic or biofilm growth conditions that range in size from approximately 50 to 200 nm in diameter were used to formulate the vaccine in suboptimal quantity for protection (0.75 μg total protein per dose) with tetanus (5 to 7 Lf/dose with a power greater than or equal to 2 UIA/ml serum) and diphtheria (1 to 3 Lf/dose with an output of 0.1 UIA/ml serum) toxoids as previously described. The safety of this vaccine was confirmed by human whole-blood IL-6–release assays. The results were presented in **Figure S1** of **Supplementary Material**.

Immunization of Mice

Groups of 4-5 female BALB/c mice were immunized with OMV-based vaccine formulated as previously described (0.75 μg total protein per dose) using a two-dose schedule. For protection assays mice were challenged with sublethal doses (10^7-10^8 CFU/40 μl) of *B. pertussis* BpAR106 PRN(+), USA PRN(-) *B. pertussis* clinical isolate, or Argentinian PRN(-) *B. pertussis* clinical isolate. Mice were sacrificed 1 week after challenge and bacterial counts from the lungs of treated animals were performed as we previously described (20).

Enzyme-Linked Immunosorbent Assay (ELISA)

As we previously described (44), plates (Nunc A/S, Roskilde, Denmark) were coated with sonicated *B. pertussis* BpAR106 (whole-cell lysates) at 3 μg/ml in 0.5 M carbonate buffer, pH 9.5, by means of an overnight incubation at 4°C. The rinsed plates were then blocked with 3% milk in PBS (2 h at 37°C) and incubated with serially diluted samples of mouse serum (1 h at 37°C). In the experiments described above, blood samples were collected and the sera were obtained after leaving the blood samples to clot for 1 h at 37°C followed by centrifuging for 10 min at 7,000 × *g*. IgG from individual serum or pooled sera bound to the plates were detected after a 2-h incubation with goat anti–mouse-IgG–linked horseradish peroxidase (1:8,000 Invitrogen, USA). For measuring IgG isotypes, detection of bound antibodies was performed using HRP labeled subclass-specific anti-mouse IgG1 (1:8,000) or IgG2a (1:1,000) (Sigma, Aldrich). As substrate, 1.0 mg/ml o-phenylendiamine (OPD, Bio Basic Canada Inc) in 0.1 M citrate-phosphate buffer, pH 5.0 containing 0.1% hydrogen peroxide was used. Optical densities (ODs) were measured with Titertek Multiskan Model 340 microplate reader (ICN, USA) at 492 nm, and the OD was plotted as a function of the log of the inverse of serum dilution factor. A successful assay produced, for each antibody sample, a sigmoidal curve in this type of plot. The titer of each antibody sample was determined from this curve by identifying the concentration by GraphPad Prism® software (expressed as the inverse of the dilution factor of the antibody) that provokes a half-way between the basal and maximal responses.

From the experimental protocol performed in triplicate, one representative experiment is presented in the Results.

Avidity Assay

Avidity was measured by an ELISA elution assay as the overall strength of binding between antibody and antigen, using plates incubated for 15 min with increasing concentration of ammonium thiocyanate (NH_4SCN) from 0 to 0.375 M. Antibody avidity was defined as the amount (percentage) of antibody eluted for each increment of NH_4SCN concentration.

Statistical Analysis

For the analysis of CFU counts in animal lungs, we evaluated the normality of the data by using Shapiro-Wilk test (http://scistatcalc.blogspot.com.ar/2013/10/shapiro-wilk-test-calculator.html) before applying the statistical methods described below. After verifying that our CFU data follows a normal distribution, we analyzed them by one-way analysis of variance (ANOVA) followed by Bonferroni´s multiple comparison test. Differences were considered to be significant when $p<0.05$. All statistical analyses were performed using GraphPadPrism® version 6.00 for Windows, GraphPad® Software.

RESULTS

B. pertussis BpAR106 Growth in Biofilm Culture Condition

Based on a relatively recent report on the higher capacity of Argentinian *B. pertussis* clinical isolates to form biofilms in comparison with reference strains adapted to laboratory growth condition (30) we decided to perform this study with the BpAR106 clinical isolate, which was sequenced and characterized by our group, possesses the *ptx*P3, *ptx*A1, *prn*2 genotype, and expresses pertactin (45). We evaluated the ability of BpAR106 to form biofilm in petri dishes in comparison with the reference strain *B. pertussis* Tohama phase I. Negative controls consisted of uninoculated petri dishes containing sterile medium only. In agreement with a previous report (30) BpAR106 exhibited more than twofold mature biofilm biomass after 96 h of culture compared with the reference strain *B. pertussis* Tohama I (**Figure 1**).

The formation of a biofilm (pellicle) at the air-liquid interface for BpAR106 was analyzed by scanning electron microscope observations. While at 24 h of incubation bacteria looked dispersed on the surface (**Figure 2A**), at 96 h of culture the bacteria adhered to each other, forming a complex internal architecture characteristic of biofilm growth. In addition, bacteria were stacked forming three-dimensional towers separated by bacteria-free furrows. Through these electron microscopic observations, the presence of OMV in the biofilm condition was detected (**Figure 2B**).

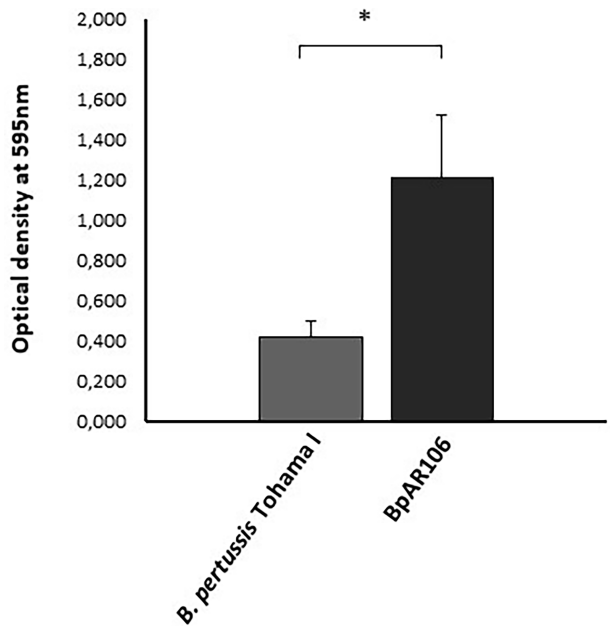

FIGURE 1 | Biofilm formation by *B. pertussis* Tohama I strain (gray column) and the clinical isolate BpAR106 (black column) on an abiotic surface. Biofilm biomass was quantified at 96 h of growth by staining with crystal violet and absorbance was measurement at OD 595 nm. Each value represents the mean from three independent experiments and the bars indicate standard deviation. Statistically significant differences in Student's t-test between the clinical isolate and *B. pertussis* Tohama I biomass absorbance are indicated by * ($p < 0.05$).

To add evidence that the starting bacteria from which OMV were isolated actually came from biofilm lifestyle, we conducted a proteomic study to detect those differential proteins that were reported as characteristic of this lifestyle. Perseus software (version 1.5.6.0, Max Planck Institute, Germany) was used for the statistical analysis and visualization of the differences and common proteins obtained from biofilm or from planktonic cultures. The statistical significance of the relative quantitative changes between the growth conditions in biofilm *vs* planktonic cultures was determined by Student's *t*-test at $p < 0.05$. To assign a location to each protein in the respective routes, the Kyoto Encyclopedia of Genes and Genomes (KEGG) and STRING version 9.1 were used, in addition to protein-by-protein searches. In total, 1144 proteins were detected, of which 402 were found as differential between the two culture conditions analyzed. From these 402 proteins (the list of proteins is presented in **Table 1** of the **Supplementary Material**), 316 were overexpressed in biofilm, and 86 were overexpressed in planktonic culture (**Figure 3A**). Among the overexpressed proteins, BipA, fimbria, and other adhesins reported as marker of biofilm culture condition were detected (31, 46). In agreement to the findings reported by de Gouw et al. (32) and Dorji et al. (33), functional analysis using *B. pertussis* database showed that proteins involved in cell envelope, energy metabolism and protein synthesis were significantly overproduced in biofilm cells compared to planktonic cells (**Figure 3B**).

Isolation and Immunogenic Characterization of OMV Derived From BpAR106 Grown in Biofilm

We obtained OMV from BpAR106 in biofilm (OMVbiof) or planktonic (OMVplank) cultures using the protocol described by our group (20, 42). Similar unidimensional SDS-PAGE profiles of proteins (**Figure 4A**) and lipo-oligosaccharides (**Figure 4B**) were observed in extracts from OMVbiof and OMVplank. When observed under transmission electron microscopy, the sizes of both OMV were similar, and consistently with previously reported, had a size range between 50 and 250 nm (**Figure 4C**) (42). Then, we proceeded to the vaccine formulation of OMVbiof or OMVplank following the protocol described in the *Materials and Methods* section. To evaluate whether OMVbiof improved the protective capacity of OMVplank we used suboptimal protective OMV doses 0.75 μg of OMV (as total protein) per animal instead of the previously described protective dose of 3 μg (42, 44). This suboptimal protective dose was determined by the dose-response experiment showed in the **Supplementary Material** (**Figure S2**).

First, we evaluated the effect of a schedule consisting in 2 doses of vaccine on inducing specific IgG against *B. pertussis* (**Figure 5**). IgG2a and IgG1 levels were also evaluated after the second dose of each OMV. Higher values of IgG titers were detected in OMVbiof-immunized mice in comparison with OMVplank-immunized mice ($p<0.05$, **Figure 5A**). An interesting observation was the higher proportion of anti-Bp

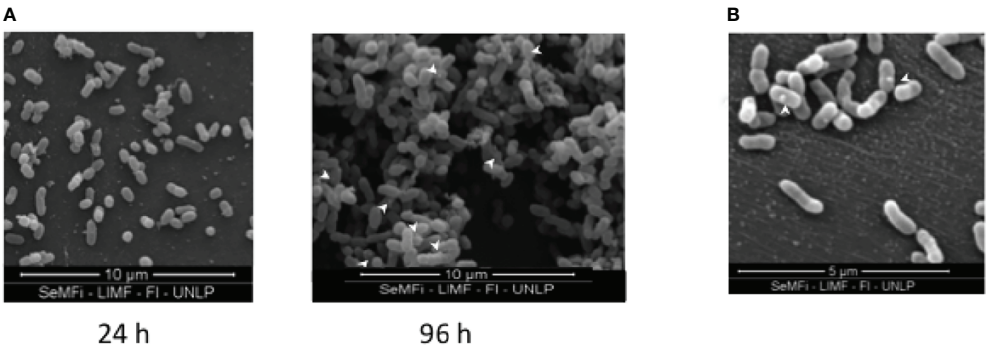

FIGURE 2 | **(A)** Scanning electron microscopy of *B. pertussis* BpAR106 biofilm culture on abiotic surface at 24h and 96h of growth. For observation through the FEI Quanta 200 electron microscope (24,000 x magnification), the samples were dried by the critical point technique and coated in gold. **(B)** To visualize the OMV, an electronic zoom of panel **(A)** is shown. White arrows were used to mark the presence of OMV.

IgG with high avidity detected in the sera of OMVbiof-immunized mice (**Figure 5B**). In addition, we observed differential recognition patterns in blots from SDS-PAGE probed with the tested vaccine-induced sera (**Figure 5C**). When sera induced by OMVbiof are confronted with BpAR106 lysates obtained from biofilm or planktonic cultures, more complex recognition profiles were detected in comparison with the patterns detected with OMVplank-induced sera. As expected, the recognition of naïve animal sera was null (data not shown). Both OMVbiof and OMVplank-induced sera recognized the 2 characteristic electrophoretic bands (Band A and Band B) of the LOS extracted from both culture conditions (**Figure 5D**).

Moreover, both OMV triggered murine antibody responses with an IgG2a/IgG1 > 1.2 (**Figure 5A**) suggesting that both OMV skewed the immune response to a Th1 profile.

Protective Capacity of OMVbiof Against Current Circulating Bacteria

To compare the protective capacity of OMVbiof and OMVplank vaccines, mice were immunized twice with each formulation and challenged with a sublethal dose of *B. pertussis* 2 weeks after the second immunization. For the first challenge we used BpAR106 bacteria expressing *prn* gene (*ptx*P3, *ptx*A1 and *prn*2, PRN+). As negative control of protection we used mice treated with PBS. Significant differences in lung CFU between immunized animals and negative controls were observed ($p<0.001$) (**Figure 6A**). While almost 2.5 $\log_{10}$ differences between OMVplank-vaccinated and non-immunized mice were detected, more than 4 $\log_{10}$ differences were observed between OMVbiof-vaccinated and non-immunized mice (**Figure 6A**).

When the challenge was performed with a PRN(-) clinical isolate obtained during an outbreak in USA (*ptx*P3, *ptx*A1 and *prn*2, PRN-), again the protective capacity of OMVbiof vaccine was significantly higher than that of OMVplank vaccine (**Figure 6B**). Mice immunized with the OMVbiof had more than 4 $\log_{10}$ reduction in lung CFU 7 days after challenge with *B. pertussis* PRN(-) compared with the non-immunized mice, whereas in the lungs of mice immunized with the OMVplank vaccine the reduction was only 2.5 $\log_{10}$ ($p < 0.05$, **Figure 6B**). Similar results were found against another PRN(-) clinical isolate obtained in Argentina: while OMVbiof reduced the number of lung CFU by 3 $\log_{10}$, OMVplank did it by 1.9 $\log_{10}$ ($p < 0.05$, **Figure 6C**).

DISCUSSION

In response to the need of a safer pertussis vaccine, a second generation of vaccine consisting in purified *B. pertussis* immunogens (aP vaccines) was developed. Thus, the first aP vaccines containing only pertussis toxin or pertussis toxin and filamentous hemagglutinin were licensed in the 80s (47). Current aP vaccines contain between two and five immunogens. These aP vaccines mainly induce Th2 response with poor induction of memory B-cells (48). On the other hand, T-cell responses were detected mainly in wP-primed children boosted by aP or natural infections but not in aP-primed children (49). The high concentration of immunogens in aP vaccines and their immune response not very robust seem to have contributed to the selection of *B. pertussis* strains more resistant to vaccination, favoring the emergence of genetically and phenotypically distinct *B. pertussis* strains (50). A novel P3 linage antigenically distinct from vaccine strains that produces higher levels of pertussis toxin is now common in most countries (51, 52). *B. pertussis* strains that are deficient in the production of the pertactin immunogen are prevalent in countries where only aP vaccines are used. In many of these countries the number of pertussis cases was increasing during the last decades (23, 53, 54).

To improve the epidemiological situation of pertussis, a third generation of acellular vaccines that stimulate a potent T-cell response, confer long lasting immunity and do not generate a selection pressure on the circulating bacterial population is necessary (10). In this context, our group has designed an OMV-based vaccine candidate that overcomes the weaknesses of current acellular vaccines (55). Preclinical tests in mice have shown that our vaccine candidate is safe and effective in avoiding the colonization of animals caused by different genotypes of *B. pertussis* (13, 44). We have also found that our candidate improves protection against

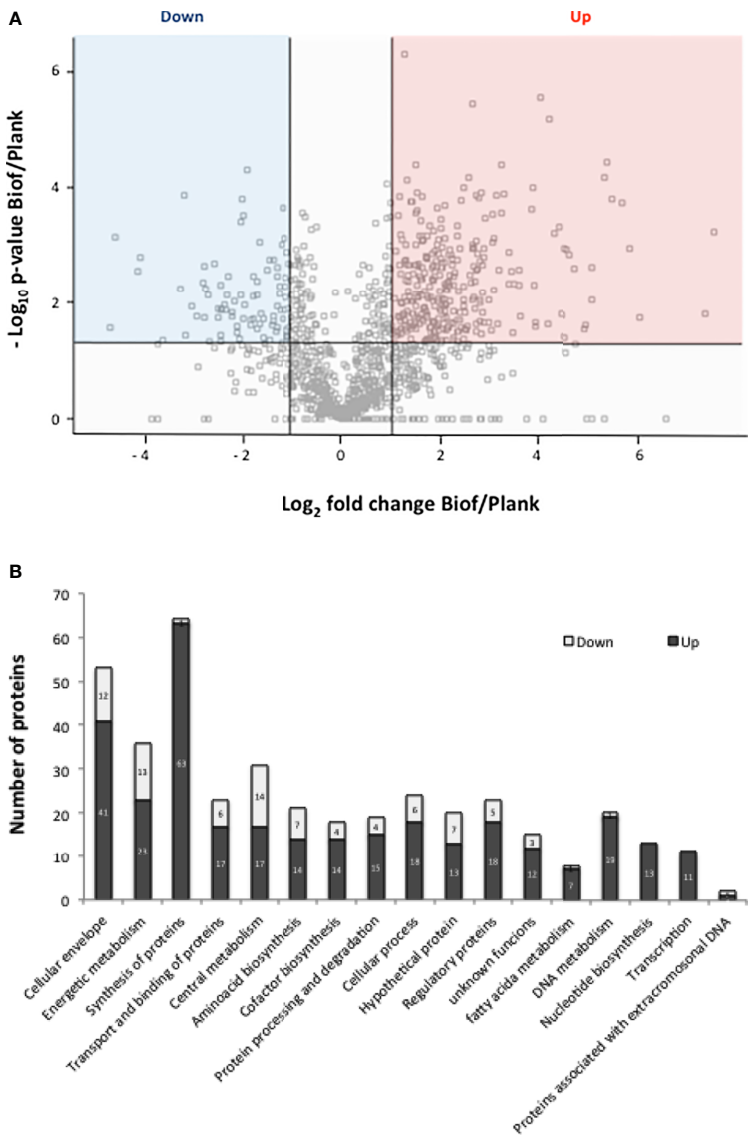

FIGURE 3 | **(A)** Volcano plot of protein samples from the clinical isolate *B. pertussis* BpAR106 grown in biofilm (Biof) or planktonic (Plank) condition. -Log_{10} of the *p*-value associated with the magnitude of the fold-change of a given protein between the biofilm and planktonic growth conditions is plotted on the ordinate as a function of the log_2 of that fold change on the abscissa. M = log_2(fold-change). The overexpressed proteins are indicated in red (M ≥ 1), and the underexpressed proteins in blue (M ≤ −1) based on $p<0.05$. The proteins located on the 0 line correspond to the ON/OFF proteins since those proteins did not have an associated *p*-value. **(B)** Representation of the different clusters of orthologous groups (COGs) containing the proteins differentially expressed under biofilm culture condition of *B. pertussis* BpAR106. In the figure, the bar length represents the number of overexpressed (black) or underexpressed (gray) proteins within each COG among the total differentially expressed proteins.

pertactin-deficient isolates as compared to current commercial aP vaccines (13). The levels of protection detected for the OMV-based vaccine against these PRN(-) *B. pertussis* isolates are high; however, improvements to increase the reduction of pathogen colonization are still required to achieve protection levels similar as those detected for the PRN(+) *B. pertussis* isolates (13). Based on the knowledge that current circulating *B. pertussis* isolates form biofilms more readily than the strains used for vaccine production, and that all currently available pertussis vaccines are formulated with antigens derived from planktonic bacterial cells, an attractive improvement could be the obtaining of OMV from clinical isolate grown in biofilm culture. This hypothesis is also supported by the fact that proteins that are expressed only when bacteria grow in biofilms are immunogenic and possess immunoprotective capacity in the murine model (32). We prepared biofilms with a *B. pertussis* clinical isolate obtained in Argentina since these isolates were reported as good biofilm producers (30). This growth capability was evidenced here for BpAR106 clinical strain. Proteomic studies carried out with this strain comparing bacteria grown in biofilm with those obtained from planktonic culture showed that 316

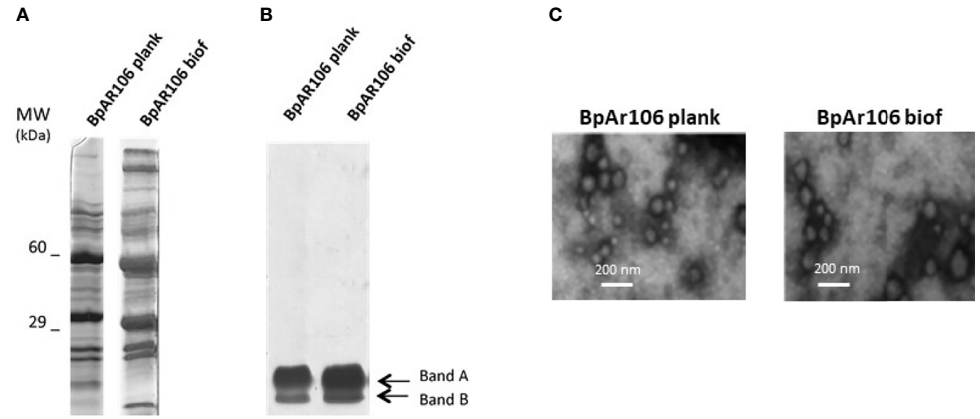

FIGURE 4 | **(A)** SDS-PAGE (12.5%) of OMV derived from *B. pertussis* BpAR106 grown under planktonic or biofilm culture conditions. Molecular weights are indicated at the left. **(B)** Lipo-oligosaccharides content in OMVplank and OMVbiof suspensions normalized by total protein content. **(C)** Scanning electron micrographs of negative stained OMV obtained from *B. pertussis* BpAR106 grown under planktonic or biofilm culture conditions (scale bar: 200 nm).

A

Treatment	Total IgG	IgG2a	IgG1	IgG2a/IgG1
OMVbiof	377.14 ± 14.55	282.2 ± 12.09	231.4 ± 73.7	1.21
OMVplank	175.2 ± 12.52	137.1 ±11.12	111.7 ± 1.7	1.23
Non immunized	18.6 ± 29.9	ND	ND	ND

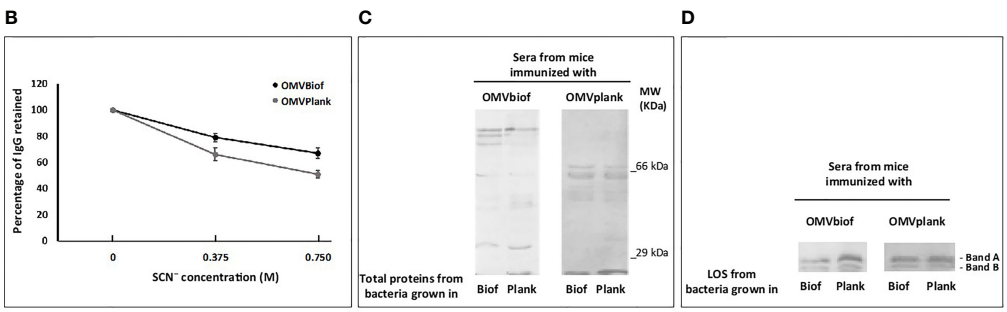

FIGURE 5 | Anti-*B. pertussis* antibodies induced by 2-dose vaccination schedules. **(A)** Anti-*B. pertussis* IgG titers as well as the IgG isotypes were measured 14 days after the second vaccination dose. The titers are expressed as the geometric mean of the data from each group. **(B)** The avidity of IgG antibodies was also measured 14 days after the second dose and is represented as percentages of eluted *B. pertussis*-specific antibodies after treatment with increasing concentrations of ammonium thiocyanate (NH_4SCN). The asterisk indicates statistically significant difference with $p < 0.05$. **(C)** Immunoblotting of total proteins of *B. pertussis* BpAR106 separated by 12.5% (w/v) SDS-PAGE and probed with the polyclonal antiserum obtained from immunized mice. The sera are designated according to the OMV-based vaccine used to immunize the mice. **(D)** Immunoblotting of BpAR106 LOS from both culture condition here tested separated by 12.5% (w/v) SDS-PAGE and probed with the polyclonal antiserum obtained from immunized mice. The sera are designated according to the OMV-based vaccine used to immunize the mice.

proteins were overexpressed in the biofilm culture, among them BipA, fimbria, and other adhesins reported as biofilm markers (31, 46). In addition, we detected OMV within the *B. pertussis* biofilm, with a size range similar to OMV obtained from *B. pertussis* planktonic cultures. This finding raises questions about the OMV formation mechanism and its role within the biofilm, as well as about biofilm formation *in vivo*. Though these topics are interesting, they were not addressed in this work since our objective was focused on obtaining OMVbiof to improve our vaccine candidate protective capacity.

The vaccine formulated with OMVbiof obtained from *B. pertussis* BpAR106 was more immunogenic than the OMVplank vaccine candidate not only in terms of specific antibody titers but also in their quality (higher avidity). Furthermore, the formulation based on OMVbiof induced a mixed Th1 and Th2 profile according to the IgG2a/IgG1 ratio detected and was more protective in mice

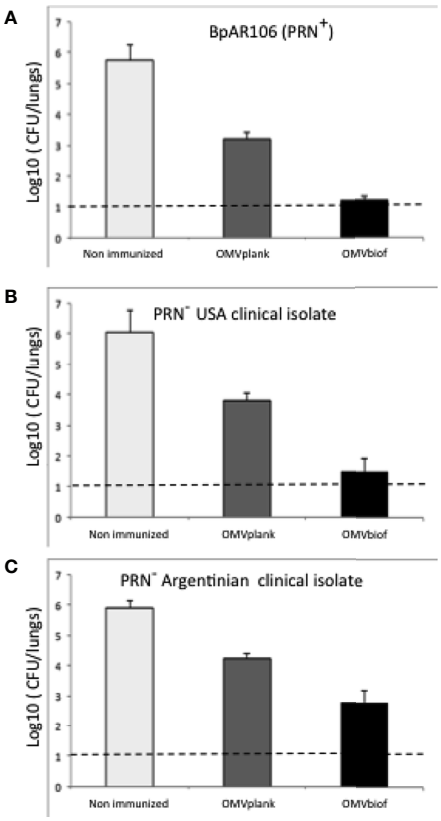

FIGURE 6 | Protection against *B. pertussis* PRN(-) isolates induced with OMVbiof- or OMVplank-based vaccines in a mouse model. BALB/c mice were immunized (i.m) twice, 2 weeks apart. Mice were challenged with sublethal doses (5 x 10^7 CFU/40 µl) of *B. pertussis* BpAR106 PRN(+) **(A)**, USA PRN(-) *B. pertussis* clinical isolate **(B)** or Argentinian PRN(-) B. pertussis clinical isolate **(C)**, 2 weeks after the second immunization with OMV-based vaccine. Non-immunized animals were included as negative control of protection. Three independent experiments were performed for each strain/isolate. Results from one representative experiment are shown. Results depicted are means of 5 mice per group sacrificed at 7 days post-challenge. The dashed line indicates the lower limit of detection. The number of bacteria recovered from mouse lungs is expressed as the average $\log_{10}$ CFU ± SEM (error bars) per lung. Data obtained were analyzed statistically by using one-way analysis of variance (ANOVA) followed by Bonferroni´s multiple comparison test (GraphPadPrism®). For panel **(A)** significant differences among the treatments with $p < 0.001$ were detected. For panels **(B, C)** significant differences among the treatments with $p < 0.05$ were detected.

assays challenged with the PRN(+) *B. pertussis* clinical isolate. This higher immunogenicity is in agreement with earlier findings by Dorji et al. (34) who demonstrated in mice model that proteins typical of bacteria grown in biofilm led to a more Th1-type response profile when added to commercial aP vaccines and additionally, retained lower bacterial loads than mice vaccinated with aP alone (34). Moreover, de Gouw et al. also shown that BipA, a biofilm characteristic protein, induces a significant reduction in colonization of mice lungs (56). These authors also detected that membrane proteins derived from biofilm bacteria induced protection against respiratory *B. pertussis* infection. Lipoproteins and Fim chaperones, in addition to the LOS adjuvant action, are also expected to play a role in the induction of protection. Regarding the LOS molecule, here we detected LOS specific antibodies induced by OMV-based vaccines as was previously reported by Raeven et al. (57). Previous results showed that antibodies against LOS, detected in the sera from individuals convalescing from natural infection, have bactericidal activity (58). These results showed the importance of LOS presence in the new generation of pertussis vaccines in lower quantities than in the wP vaccine, as occurred in the case of OMV-based formulation. Other non-excluding alternative might be the use of formulation with LOS containing modified lipid A (42) since antibodies to the terminal trisaccharide appear to be sufficient to elicit bactericidal activity (58).

The boundary condition of suboptimal OMV amounts to induce protection allowed us to detect the impact of OMVbiof on improvement in vaccine design. With this approach, we also showed that OMVbiof are superior in terms of protective capacity against PRN(-) isolates, which are currently prevalent in countries that use only aP vaccines in their calendars. Thus, protection level detected of OMVbiof against both PRN(-) clinical isolates (obtained in USA or in Argentina) not only were higher than those observed for OMVplank but also were within the accepted protection standard for a pertussis vaccine.

The representativeness of a given *B. pertussis* isolate from which a new vaccine is generated might be narrow and, above all, limited in time. The attempt to overcome this is that the growth in biofilm by itself has characteristics that seem to go beyond the specificity of each isolate and that may cushion the differences. The broad protective capacity shown in **Figure 6** would be in line with this idea. An alternative might be the use of a mixture of OMV from different strains.

Undoubtedly, all these data position OMVbiof as an interesting approach to overcome the weaknesses of current commercial vaccines formulated with immunogens obtained from planktonic cultures, which do not necessarily reflect the composition and physiology of the pathogen during the *in vivo* infection.

DATA AVAILABILITY STATEMENT

The raw data supporting the conclusions of this article will be made available by the authors, without undue reservation.

ETHICS STATEMENT

The animal study was reviewed and approved by Ethical Committee for Animal Experiments of the Faculty of Exact Sciences of UNLP (Argentina, approval number 004-06-15 and 003-06-15).

AUTHOR CONTRIBUTIONS

DH planned the study, made the laboratory analysis, interpreted data, and drafted manuscript. DB, EG, EZ, and AL interpreted data, and revised figures and the manuscript. FC, PA, NA, CC, and ER

performed certain experiments and laboratory analyses. All authors contributed to the article and approved the submitted version.

FUNDING

This work was supported by ANCPyT (PICT 2014-3617, PICT 2017- 2365), CONICET grants to DH. DH, EG, EZ, DB, and AL are members of the Scientific Career of CONICET. FC, PA, and ER are fellows from CONICET. NA is a fellow from ANPCyT and CC is a full-time Professor at Universidad Nacional de La Plata.

ACKNOWLEDGMENTS

Luciana Cayuela provided excellent technical assistance.

SUPPLEMENTARY MATERIAL

The Supplementary Material for this article can be found online at: https://www.frontiersin.org/articles/10.3389/fimmu.2021.730434/full#supplementary-material

REFERENCES

1. Tan T, Dalby T, Forsyth K, Halperin SA, Heininger U, Hozbor D, et al. Pertussis Across the Globe: Recent Epidemiologic Trends From 2000 to 2013. *Pediatr Infect Dis J* (2015) 34:e222–32. doi: 10.1097/INF.0000000000000795
2. Syed MA, Bana NF. Pertussis. A Reemerging and an Underreported Infectious Disease. *Saudi Med J* (2014) 35:1181–7.
3. Jakinovich A, Sood SK. Pertussis: Still a Cause of Death, Seven Decades Into Vaccination. *Curr Opin Pediatr* (2014) 26:597–604. doi: 10.1097/MOP.0000000000000139
4. Domenech de Cellès M, Magpantay FMG, King AA, Rohani P. The Pertussis Enigma: Reconciling Epidemiology, Immunology and Evolution. *Proc Biol Sci* (2016) 283:2015–309. doi: 10.1098/rspb.2015.2309
5. Damron FH, Barbier M, Dubey P, Edwards KM, Gu X-X, Klein NP, et al. Overcoming Waning Immunity in Pertussis Vaccines: Workshop of the National Institute of Allergy and Infectious Diseases. *J Immunol (Baltimore Md: 1950)* (2020) 205:877–82. doi: 10.4049/jimmunol.2000676
6. de Miranda Lopes KA, Baptista PN, de Medeiros Nascimento R, Pimentel A, de Alencar Ximenes RA. Clinical Repercussions in Pertussis Infants Post-Tdpa Vaccination of Pregnant Woman: An Immunization Success? *Vaccine* (2021) 39:2555–60. doi: 10.1016/j.vaccine.2021.03.069
7. Riccò M, Vezzosi L, Gualerzi G, Bragazzi NL, Balzarini F. Pertussis Immunization in Healthcare Workers Working in Pediatric Settings: Knowledge, Attitudes and Practices (KAP) of Occupational Physicians. Preliminary Results From a Web-Based Survey (2017). *J Prev Med Hygiene* (2020) 61:E66–75. doi: 10.15167/2421-4248/jpmh2020.61.1.1155
8. Saadatian-Elahi M, Plotkin S, Mills KHG, Halperin SA, McIntyre PB, Picot V, et al. Pertussis: Biology, Epidemiology and Prevention. *Vaccine (Elsevier Ltd)* (2016) 5819–26. doi: 10.1016/j.vaccine.2016.10.029
9. Mills KHG, Ross PJ, Allen AC, Wilk MM. Do We Need a New Vaccine to Control the Re-Emergence of Pertussis? *Trends Microbiol* (2016) 22:49–52. doi: 10.1016/j.tim.2013.11.007
10. Hozbor D. New Pertussis Vaccines: A Need and a Challenge. In: *Advances in Experimental Medicine and Biology*. Springer (2019). p. 115–26. doi: 10.1007/5584_2019_407
11. Locht C. Pertussis: Where did We Go Wrong and What can We do About it? *J Infect* (2016) 72 Suppl:S34–40. doi: 10.1016/j.jinf.2016.04.020
12. Brummelman J, Wilk MM, Han WGH, van Els CACM, Mills KHG. Roads to the Development of Improved Pertussis Vaccines Paved by Immunology. *Pathog Dis* (2015) 73:ftv067. doi: 10.1093/femspd/ftv067
13. Zurita ME, Wilk MM, Carriquiriborde F, Bartel E, Moreno G, Misiak A, et al. A Pertussis Outer Membrane Vesicle-Based Vaccine Induces Lung-Resident Memory CD4 T Cells and Protection Against Bordetella Pertussis, Including Pertactin Deficient Strains. *Front Cell Infection Microbiol* (2019) 9:125. doi: 10.3389/fcimb.2019.00125
14. Wilk MM, Misiak A, Mcmanus RM, Allen AC, Lynch MA, Mills KHG. Lung CD4 Tissue-Resident Memory T Cells Mediate Adaptive Immunity Induced by Previous Infection of Mice With Bordetella Pertussis. *J Immunol* (2017) 199:233–43. doi: 10.4049/jimmunol.1602051
15. Diavatopoulos DA, Mills KHG, Kester KE, Kampmann B, Silerova M, Heininger U, et al. PERISCOPE: Road Towards Effective Control of Pertussis. *Lancet Infect Dis* (2019) 19:e179–86. doi: 10.1016/S1473-3099(18)30646-7
16. Bottero D, Gaillard ME, Basile LA, Fritz M, Hozbor DF. Genotypic and Phenotypic Characterization of Bordetella Pertussis Strains Used in Different Vaccine Formulations in Latin America. *J Appl Microbiol* (2012) 112:1266–76. doi: 10.1111/j.1365-2672.2012.05299.x
17. Parkhill J, Sebaihia M, Preston A, Murphy LD, Thomson N, Harris DE, et al. Comparative Analysis of the Genome Sequences of Bordetella Pertussis, Bordetella Parapertussis and Bordetella Bronchiseptica. *Nat Genet* (2003) 35:32–40. doi: 10.1038/ng1227
18. Caro V, Bouchez V, Guiso N. Is the Sequenced Bordetella Pertussis Strain Tohama I Representative of the Species? *J Clin Microbiol* (2008) 46:2125–8. doi: 10.1128/JCM.02484-07
19. Hozbor DF. Outer Membrane Vesicles: An Attractive Candidate for Pertussis Vaccines. *Expert Rev Vaccines* (2017) 16:193–6. doi: 10.1080/14760584.2017.1276832
20. Roberts R, Moreno G, Bottero D, Gaillard ME, Fingermann M, Graieb A, et al. Outer Membrane Vesicles as Acellular Vaccine Against Pertussis. *Vaccine* (2008) 26:4639–46. doi: 10.1016/j.vaccine.2008.07.004
21. Elizagaray ML, Gomes MTR, Guimaraes ES, Rumbo M, Hozbor DF, Oliveira SC, et al. Canonical and Non-Canonical Inflammasome Activation by Outer Membrane Vesicles Derived From Bordetella Pertussis. *Front Immunol* (2020) 11:1879. doi: 10.3389/fimmu.2020.01879
22. Gaillard ME, Bottero D, Errea A, Ormazábal M, Zurita ME, Moreno G, et al. Acellular Pertussis Vaccine Based on Outer Membrane Vesicles Capable of Conferring Both Long-Lasting Immunity and Protection Against Different Strain Genotypes. *Vaccine* (2014) 32:931–7. doi: 10.1016/j.vaccine.2013.12.048
23. Martin SW, Pawloski L, Williams M, Weening K, Debolt C, Qin X, et al. Pertactin-Negative Bordetella Pertussis Strains: Evidence for a Possible Selective Advantage. *Clin Infect Dis* (2015) 60:223–7. doi: 10.1093/cid/ciu788
24. S B, AT S. Analysis of Bordetella Pertussis Pertactin and Pertussis Toxin Types From Queensland, Australia, 1999-2003. *BMC Infect Dis* (2006) 6:53–61. doi: 10.1186/1471-2334-6-53
25. Weigand MR, Williams MM, Peng Y, Kania D, Pawloski LC, Tondella ML, et al. Genomic Survey of Bordetella Pertussis Diversity, United States, 2000–2013. *Emerging Infect Dis* (2019) 25:780–3. doi: 10.3201/eid2504.180812
26. Zomer A, Otsuka N, Hiramatsu Y, Kamachi K, Nishimura N, Ozaki T, et al. Bordetella Pertussis Population Dynamics and Phylogeny in Japan After Adoption of Acellular Pertussis Vaccines. *Microbial Genomics* (2018) 4:180–93. doi: 10.1099/mgen.0.000180
27. Carriquiriborde F, Regidor V, Aispuro PM, Magali G, Bartel E, Bottero D, et al. Rare Detection of Bordetella Pertussis Pertactin-Deficient Strains in Argentina. *Emerging Infect Dis* (2019) 25:2048–54. doi: 10.3201/eid2511.190329
28. Safarchi A, Octavia S, Luu LDW, Tay CY, Sintchenko V, Wood N, et al. Pertactin Negative Bordetella Pertussis Demonstrates Higher Fitness Under Vaccine Selection Pressure in a Mixed Infection Model. *Vaccine* (2015) 33:6277–81. doi: 10.1016/j.vaccine.2015.09.064
29. Hegerle N, Dore G, Guiso N. Pertactin Deficient Bordetella Pertussis Present a Better Fitness in Mice Immunized With an Acellular Pertussis Vaccine. *Vaccine* (2014) 32:6597–600. doi: 10.1016/j.vaccine.2014.09.068
30. Arnal L, Grunert T, Cattelan N, de Gouw D, Villalba MI, Serra DO, et al. Bordetella Pertussis Isolates From Argentinean Whooping Cough Patients Display Enhanced Biofilm Formation Capacity Compared to Tohama I Reference Strain. *Front Microbiol* (2015) 6:1352. doi: 10.3389/fmicb.2015.01352

31. Cattelan N, Jennings-Gee J, Dubey P, Yantorno OM, Deora R. Hyperbiofilm Formation by Bordetella Pertussis Strains Correlates With Enhanced Virulence Traits. *Infection Immun* (2017) 85:373–15. doi: 10.1128/IAI.00373-17
32. de Gouw D, Serra DO, de Jonge MI, Hermans PW, Wessels HJ, Zomer A, et al. The Vaccine Potential of Bordetella Pertussis Biofilm-Derived Membrane Proteins. *Emerging Microbes infections* (2014) 3:e58. doi: 10.1038/emi.2014.58
33. Dorji D, Graham RM, Richmond P, Keil A, Mukkur TK. Biofilm Forming Potential and Antimicrobial Susceptibility of Newly Emerged Western Australian Bordetella Pertussis Clinical Isolates. *Biofouling* (2016) 32:1141–52. doi: 10.1080/08927014.2016.1232715
34. Dorji D, Graham RM, Singh AK, Ramsay JP, Price P, Lee S. Immunogenicity and Protective Potential of Bordetella Pertussis Biofilm and Its Associated Antigens in a Murine Model. *Cell Immunol* (2019) 337:42–7. doi: 10.1016/j.cellimm.2019.01.006
35. Bottero D, Gaillard ME, Fingermann M, Weltman G, Fernández J, Sisti F, et al. Pulsed-Field Gel Electrophoresis, Pertactin, Pertussis Toxin S1 Subunit Polymorphisms, and Surfaceome Analysis of Vaccine and Clinical Bordetella Pertussis Strains. *Clin Vaccine Immunol* (2007) 14:1490–8. doi: 10.1128/CVI.00177-07
36. Pawloski LC, Queenan AM, Cassiday PK, Lynch AS, Harrison MJ, Shang W, et al. Prevalence and Molecular Characterization of Pertactin-Deficient Bordetella Pertussis in the United States. *Clin Vaccine Immunol* (2014) 21:119–25. doi: 10.1128/CVI.00717-13
37. Von Koenig CHW, Tacken A, Finger H. Use of Supplemented Stainer-Scholte Broth for the Isolation of Bordetella Pertussis From Clinical Material. *J Clin Microbiol* (1988) 26:2558–60. doi: 10.1128/jcm.26.12.2558-2560.1988
38. Stainer DW, Scholte MJ. A Simple Chemically Defined Medium for the Production of Phase I Bordetella Pertussis. *J Gen Microbiol* (1970) 63:211–20. doi: 10.1099/00221287-63-2-211
39. O'Toole GA. Microtiter Dish Biofilm Formation Assay. *J Visualized Experiments* (2010) 47:2437–8. doi: 10.3791/2437
40. Hozbor D, Rodriguez ME, Fernández J, Lagares A, Guiso N, Yantorno O. Release of Outer Membrane Vesicles From Bordetella Pertussis. *Curr Microbiol* (1999) 38:273–8. doi: 10.1007/PL00006801
41. Kielkopf CL, Bauer W, Urbatsch IL. Bradford Assay for Determining Protein Concentration. *Cold Spring Harbor Protoc* (2020) 2020:136–8. doi: 10.1101/pdb.prot102269
42. Asensio CJA, Gaillard ME, Moreno G, Bottero D, Zurita E, Rumbo M, et al. Outer Membrane Vesicles Obtained From Bordetella Pertussis Tohama Expressing the Lipid a Deacylase PagL as a Novel Acellular Vaccine Candidate. *Vaccine* (2011) 29:1649–56. doi: 10.1016/j.vaccine.2010.12.068
43. Nilsson JF, Castellani LG, Draghi WO, Pérez-Giménez J, Torres Tejerizo GA, Pistorio M. Proteomic Analysis of Rhizobium Favelukesii LPU83 in Response to Acid Stress. *J Proteome Res* (2019) 18:3615–29. doi: 10.1021/acs.jproteome.9b00275
44. Bottero D, Gaillard ME, Zurita E, Moreno G, Martinez DS, Bartel E, et al. Characterization of the Immune Response Induced by Pertussis OMVs-Based Vaccine. *Vaccine* (2016) 34:3303–9. doi: 10.1016/j.vaccine.2016.04.079
45. Bart MJ, Harris SR, Advani A, Arakawa Y, Bottero D, Bouchez V, et al. Global Population Structure and Evolution of Bordetella Pertussis and Their Relationship With Vaccination. *mBio* (2014) 5:e01074-14. doi: 10.1128/mBio.01074-14
46. Serra DO, Lücking G, Weiland F, Schulz S, Görg A, Yantorno OM, et al. Proteome Approaches Combined With Fourier Transform Infrared Spectroscopy Revealed a Distinctive Biofilm Physiology in Bordetella Pertussis. *Proteomics* (2008) 8:4995–5010. doi: 10.1002/pmic.200800218
47. Sato Y, Kimura M, Fukumi H. Development of a Pertussis Component Vaccine In Japan. *Lancet* (1984) 323:122–6. doi: 10.1016/S0140-6736(84)90061-8
48. Edwards KM, Berbers GAM. Immune Responses to Pertussis Vaccines and Disease. *J Infect Dis* (2014) 209:s10-5. doi: 10.1093/infdis/jit560
49. Schure RM, Hendrikx LH, de Rond LGH, Öztürk K, Sanders EAM, Berbers GAM, et al. Differential T- and B-Cell Responses to Pertussis in Acellular Vaccine-Primed *Versus* Whole-Cell Vaccine-Primed Children 2 Years After Preschool Acellular Booster Vaccination. *Clin Vaccine Immunol* (2013) 20:1388–95. doi: 10.1128/CVI.00270-13
50. Octavia S, Maharjan RP, Sintchenko V, Stevenson G, Reeves PR, Gilbert GL, et al. Insight Into Evolution of Bordetella Pertussis From Comparative Genomic Analysis: Evidence of Vaccine-Driven Selection. *Mol Biol Evol* (2011) 28:707–15. doi: 10.1093/molbev/msq245
51. Loconsole D, de Robertis AL, Morea A, Metallo A, Lopalco PL, Chironna M. Resurgence of Pertussis and Emergence of the Ptx P3 Toxin Promoter Allele in South Italy. *Pediatr Infect Dis J* (2018) 37:E126–31. doi: 10.1097/INF.0000000000001804
52. Armstrong ME, Loscher CE, Lynch MA, Mills KHG. IL-1β-Dependent Neurological Effects of the Whole Cell Pertussis Vaccine: A Role for IL-1-Associated Signalling Components in Vaccine Reactogenicity. *J Neuroimmunology* (2003) 136:25–33. doi: 10.1016/S0165-5728(02)00468-X
53. Barkoff AM, He Q. Molecular Epidemiology of Bordetella Pertussis. In: *Advances in Experimental Medicine and Biology*. Springer (2019). p. 19–33. doi: 10.1007/5584_2019_402
54. Fingermann M, Fernández J, Sisti F, Rodríguez ME, Gatti B, Bottero D, et al. Differences of Circulating Bordetella Pertussis Population in Argentina From the Strain Used in Vaccine Production. *Vaccine* (2006) 24:3513–21. doi: 10.1016/j.vaccine.2006.02.026
55. Rumbo M, Hozbor D. Development of Improved Pertussis Vaccine. *Hum Vaccines Immunotherapeutics* (2014) 10:2450–3. doi: 10.4161/hv.29253
56. de Gouw D, de Jonge MI, Hermans PWM, Wessels HJCT, Zomer A, Berends A, et al. Proteomics-Identified Bvg-Activated Autotransporters Protect Against Bordetella Pertussis in a Mouse Model. *PloS One* (2014) 9:e105011-19. doi: 10.1371/journal.pone.0105011
57. RH R, van der LM, T W, U JP, B TH, K B, et al. Immunoproteomic Profiling of Bordetella Pertussis Outer Membrane Vesicle Vaccine Reveals Broad and Balanced Humoral Immunogenicity. *J Proteome Res* (2015) 14:2929–42. doi: 10.1021/ACS.JPROTEOME.5B00258
58. Weiss AA, Mobberley PS, Fernandez RC, Mink CM. Characterization of Human Bactericidal Antibodies to Bordetella Pertussis. *Infection Immun* (1999) 67:1424. doi: 10.1128/IAI.67.3.1424-1431.1999

Conflict of Interest: The authors declare that the research was conducted in the absence of any commercial or financial relationships that could be construed as a potential conflict of interest.

frontiers in Immunology

REVIEW
published: 20 September 2021
doi: 10.3389/fimmu.2021.733064

Bacterial Outer Membrane Vesicles as Antibiotic Delivery Vehicles

Shannon M. Collins and Angela C. Brown *

Department of Chemical and Biomolecular Engineering, Lehigh University, Bethlehem, PA, United States

Bacterial outer membrane vesicles (OMVs) are nanometer-scale, spherical vehicles released by Gram-negative bacteria into their surroundings throughout growth. These OMVs have been demonstrated to play key roles in pathogenesis by delivering certain biomolecules to host cells, including toxins and other virulence factors. In addition, this biomolecular delivery function enables OMVs to facilitate intra-bacterial communication processes, such as quorum sensing and horizontal gene transfer. The unique ability of OMVs to deliver large biomolecules across the complex Gram-negative cell envelope has inspired the use of OMVs as antibiotic delivery vehicles to overcome transport limitations. In this review, we describe the advantages, applications, and biotechnological challenges of using OMVs as antibiotic delivery vehicles, studying both natural and engineered antibiotic applications of OMVs. We argue that OMVs hold great promise as antibiotic delivery vehicles, an urgently needed application to combat the growing threat of antibiotic resistance.

Keywords: outer membrane vesicles, antibiotics, antibiotic resistance, drug delivery, Gram-negative bacteria

OPEN ACCESS

Edited by:
Alejandro J. Yañez, Austral University of Chile, Chile

Reviewed by:
Natalie Jane Bitto, La Trobe University, Australia
Araceli Contreras-Rodriguez, Instituto Politécnico Nacional (IPN), Mexico

***Correspondence:**
Angela C. Brown
acb313@lehigh.edu

Specialty section:
This article was submitted to Vaccines and Molecular Therapeutics, a section of the journal Frontiers in Immunology

Received: *29 June 2021*
Accepted: *31 August 2021*
Published: *20 September 2021*

Citation:
Collins SM and Brown AC (2021) Bacterial Outer Membrane Vesicles as Antibiotic Delivery Vehicles. Front. Immunol. 12:733064. doi: 10.3389/fimmu.2021.733064

1 INTRODUCTION

The treatment of bacterial infections continues to be more difficult due to the growing number of antibiotic-resistant organisms and the slow pace of antibiotic discovery. Recently, the United States Centers for Disease Control and Prevention (CDC) reported that annually, almost three million people develop antibiotic-resistant infections in the United States, and more than 35,000 die as a result (1). Gram-negative bacteria, in particular, are extremely difficult to treat with many classes of antibiotics due to their complex, dual-membrane cell envelopes (2). A majority of the CDC's biggest antibiotic resistant threats are Gram-negative bacteria, including carbapenem-resistant *Acinetobacter* and Enterobacterales, and drug-resistant *Neisseria gonorrhoeae* (1). Gram-negative bacteria have been reported to be responsible for more than 30% of nosocomial infections, including 70% of infections acquired in intensive care units (ICUs) in the United States (3). In order to combat Gram-negative-associated infections, research has focused on developing new types of drugs as well as new delivery strategies to overcome the limitations of currently available drugs.

Like most other cells, Gram-negative bacteria release membrane vesicles, often referred to as outer membrane vesicles (OMVs) to aid in numerous cellular processes. OMVs are biological spheres that are naturally produced by many, if not all, bacterial species. These bilayered vesicles are derived from the outer membrane of the Gram-negative bacteria, range in size from 50-250 nm in diameter, and contain many of the same components as the outer membrane of the bacterial cell (4–7) (**Figure 1**). In recent years, the role of OMVs in intracellular communication, both between bacterial cells and the host as well as between bacterial cells, has been established (5, 8). This communication is possible due to the ability of the OMVs to deliver a wide range of biomolecules,

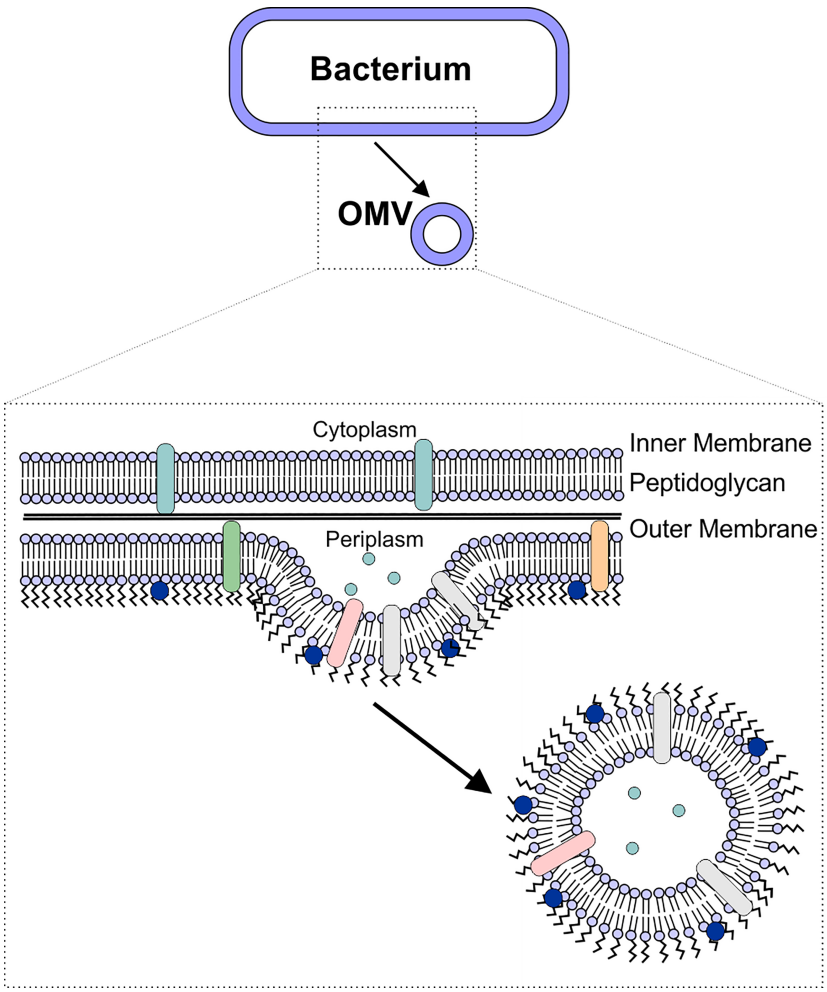

FIGURE 1 | OMV Biogenesis. OMVs are formed due to blebbing of the bacterial outer membrane. The vesicle contains outer membrane-associated proteins and lipids (including lipopolysaccharide), as well as periplasmic components such as peptidoglycan.

including proteins, lipids, nucleic acids, peptidoglycan, and small molecules to other cells (8–15). In particular, the unique ability of OMVs to deliver molecules across the Gram-negative cell envelope (10, 14, 16–19) suggests that OMVs have potential as natural antibiotic delivery vehicles to overcome the limitations of antibiotic delivery to these difficult-to-treat bacteria (20–23).

In this paper, we describe the intrinsic delivery functions of OMVs in relation to their potential use as antibiotic delivery vehicles. We provide examples demonstrating successful application of these vehicles for therapeutic purposes and discuss the limitations that remain to be addressed to enable the translation of OMVs as antibiotic delivery vehicles.

2 NATURAL FUNCTIONS OF OMVs

Derived from the outer membrane of Gram-negative bacteria, OMVs contain many similar components, including lipids, proteins, peptidoglycan, and nucleic acids, though not necessarily in the same proportions as in the donor cell (14, 24–27). One of the primary functions of OMVs is to transport these molecules to other cells, including both host and bacterial cells. While much focus has been placed on understanding OMV-mediated virulence factor delivery to host cells to understand the role of OMVs in the host-pathogen interaction, it has become clear that OMVs are also used by bacteria to communicate with neighboring bacterial cells by delivering proteins, genetic material, and quorum sensing molecules. In this section, we describe several specific natural functions of OMVs that provide them with advantages that could be harnessed for the delivery of antibiotics.

2.1 Transport Across the Bacterial Cell Envelope

The primary advantage of using OMVs as antibiotic delivery vehicles is their inherent ability to deliver their cargo across the cell envelope of Gram-negative bacteria. With a cell envelope that consists of two membranes, Gram-negative bacteria are

inherently resistant to many antibiotics (2). Several reports of the OMV-mediated delivery of active proteins or genes across the Gram-negative cell envelope highlight the potential utility of OMVs to enhance antibiotic delivery to these cells. Although detailed mechanisms of this process remain elusive, future work to better understand this delivery processes will further enhance research into the use of OMVs as antibiotic delivery vehicles to overcome current transport limitations.

The first reports of OMV-mediated transport across the Gram-negative cell membrane focused on the delivery of peptidoglycan-degrading hydrolases (19, 22). These "predatory" OMVs were hypothesized to fuse with the target cell's outer membrane, delivering their enzyme cargo to the periplasm of the target cells (22). This hypothesis was supported by subsequent experiments demonstrating that components of *Shigella flexneri* and *Pseudomonas aeruginosa* OMVs are incorporated into the membranes of other bacterial cells (*Salmonella typhi*, *Salmonella typhimurium*, and *Escherichia coli*) (18). More recently, myxobacteria, small Gram-negative soil-dwelling bacteria (28), have been found to produce OMVs encapsulating hydrolytic enzymes (29, 30), which exhibited lytic activity against *E. coli* (14, 31). Together, these findings demonstrate that OMVs are able to deliver cargo to the periplasm of certain bacteria (**Figure 2A**).

In addition to the delivery of intact, functional proteins, OMVs have been observed to facilitate delivery of DNA to bacterial cells (**Figure 2B**). The first evidence of DNA in OMVs was uncovered in 1995, when Kadurugamuwa and Beveridge observed its presence in the OMVs produced by two strains of *P. aeruginosa* (H103 and ATCC 19660) (32). Kolling and Matthews later demonstrated the presence of DNA in OMVs produced by *E. coli* O157:H7. They observed that these OMVs contained DNA encoding certain virulence genes, including *stx1* and *stx2*, which encode for Shiga toxins 1 and 2, respectively. These genes were delivered to noncompetent recipient cells, *E. coli* JM109 (33). Yaron et al. later demonstrated that *E. coli* O157:H7 OMVs transfer DNA to *E. coli* JM109 and *Salmonella* cells, and the recipient cells were shown to express the virulence proteins encoded in the genes (34).

The role of OMVs in the horizontal transfer of antibiotic resistance genes has also been demonstrated. Rumbo et al. observed that two clinical strains of *Acinetobacter baumannii* that were resistant to carbapenem released OMVs containing the *blaOXA-24* gene, which encodes for a β-lactamase. When these *blaOXA-24*-containing OMVs were incubated with a carbapenem-susceptible strain of *A. baumannii*, resistance to several β-lactam drugs was observed. Importantly, this previously susceptible strain was subsequently found to express *blaOXA-24* and to release *blaOXA-24*-containing OMVs (35). Similarly, OMV-mediated horizontal gene transfer has also been identified in the oral pathogen *Porphyromonas gingivalis* (36), *E. coli* O104:H4 (37), and *S. typhi* (38).

Delivery of functional genes and the important role of OMVs in horizontal gene transfer indicates that the OMVs enable delivery of their DNA cargo into the bacterial cytosol. This process was first visualized by Fulsunder et al. by using immunogold labeling of double-stranded DNA to observe movement of DNA from the donor bacterial cells (*Acinetobacter bayli*, JV26) into OMVs and then recipient cells (both *E. coli* DH5α and *A. bayli* JV26) (15).

Together, these observations of OMV-mediated protein and DNA delivery demonstrate that OMVs are able to deliver functional cargo across the Gram-negative cell envelope. This behavior is particularly appealing for the delivery of antibiotics as

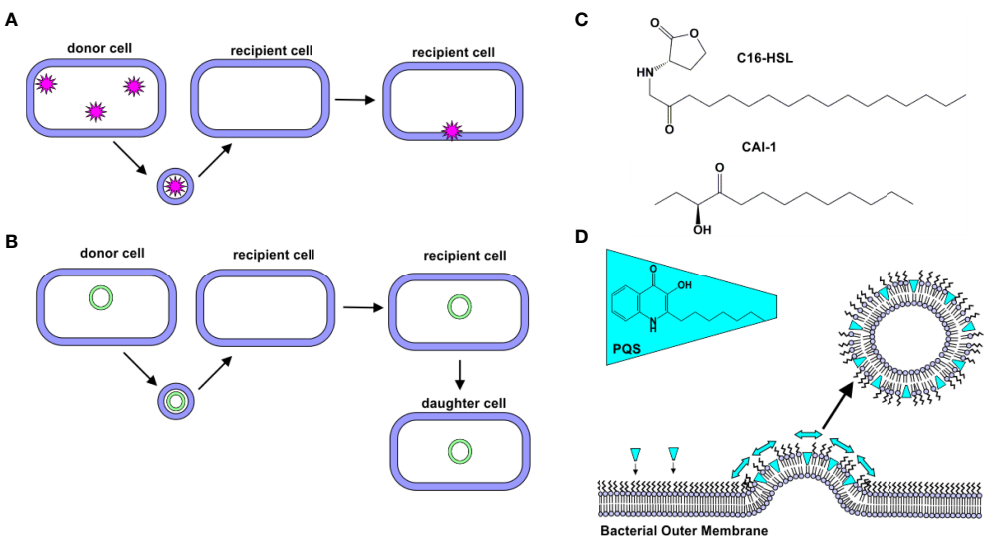

FIGURE 2 | Natural Delivery Functions of OMVs. **(A)** Protein Delivery. Proteins derived from a donor cell are encapsulated within OMVs and delivered to recipient cells. **(B)** Gene Delivery. DNA (plasmid, chromosomal, and/or phage-associated) is encapsulated within OMVs and delivered to recipient cells. In some cases, this new gene is expressed by daughter cells. **(C)** C16-HSL and CAI-1. Hydrophobic quorum sensing molecules, such as C16-HSL and CAI-1, have been observed to be delivered to bacterial cells *via* OMVs. **(D)** Quorum sensing. PQS is a hydrophobic quorum sensing molecule. As it intercalates into the outer leaflet of the bacterial membrane, a wedge-like force promotes the formation of PQS-containing OMVs.

it suggests that encapsulation of the drugs within OMVs might decrease the transport issues that limit the efficacy of many antibiotics against Gram-negative bacteria.

2.2 Delivery of Hydrophobic Molecules

With their membrane structure, OMVs have a unique property of being able to transport both hydrophilic and hydrophobic molecules simultaneously. This property has been demonstrated in the natural delivery processes of OMVs and holds great importance in the future development of OMVs for antibiotic delivery.

Quorum sensing is the process by which bacteria sense cell population density and as a result, alter gene expression. In bacteria, this process occurs through the release of certain molecules; as cell density increases, the concentration of these quorum sensing molecules increases correspondingly, thus serving as a signal of high population density (39). N-acyl-homoserine lactones (AHLs) are the most common quorum sensing molecules employed by Gram-negative bacteria (40). A long-standing question in the quorum sensing field was how hydrophobic, long-chain containing AHLs were delivered through the aqueous extracellular environment. Toyofuku demonstrated that N-hexadecanoyl-L-homoserine lactone (C16-HSL, **Figure 2C**), produced by *Paracoccus denitrificans*, is packaged into outer membrane vesicles to promote solubility of the molecule (41). Similarly, CAI-1, a long-chain ketone QS molecule (**Figure 2C**), was observed to be released in association with OMVs produced by *Vibrio harveyi.* The OMV-associated CAI-1 was able to be delivered in an active form to non-CAI-1-producing cells, including *Vibrio cholerae* (42).

P. aeruginosa produces several quorum sensing molecules, including 2-heptyl-3-hydroxy-4-quinolone (*Pseudomonas* quinolone signal, PQS). Mashburn and Whiteley demonstrated that a majority of the produced PQS was released in association with OMVs, while less hydrophobic signaling molecules were not. Interestingly, the authors observed that the PQS molecule itself promotes OMV formation (43). Subsequent work by this group found that PQS intercalates into the outer membrane to induce membrane curvature, thereby promoting OMV formation (42, 44, 45) (**Figure 2D**).

Recently, Choi et al. demonstrated that *Chromobacterium violaceum* delivers the hydrophobic molecule, violacein, to bacterial cells by packaging it in OMVs (46). This process appeared to be regulated, as the OMVs were found to contain more violacein than protein. The OMV-encapsulated violacein retained its activity against the Gram positive organism, *Staphylococcus aureus* (46).

Thus, the natural ability of OMVs to solubilize hydrophobic molecules could enable improved delivery of lipophilic antibiotics, which often exhibit low bioavailability due to poor solubility, limited absorption, and rapid metabolism (47).

2.3 Selective Delivery of OMVs to Specific Bacterial Cells

OMVs have been observed to naturally interact with other bacterial cells, both from the same and different species. Selective delivery of their cargo has been observed, but the processes mediating this phenomenon remain unclear.

Tashiro et al. used a classical colloidal science theory, the Derjaguin-Landau-Verwey-Overbeek (DLVO) theory in an attempt to explain the interaction of certain OMVs with specific bacterial cells. This group observed that OMVs produced by *Buttiauxella agrestis* selectively associated with *B. agrestis* cells, enabling delivery of plasmid DNA and gentamicin specifically to *B. agrestis* cells. Because this selective association of OMVs with the bacterial cells did not require the cells to be viable, the authors hypothesized that interaction energies, as calculated using the DLVO theory, might explain this behavior. In this theory, the interaction energy is defined as the sum of the attractive London-van der Waals forces, which depend on OMV radius, and the repulsive electric force, which is a function of the surface charge (zeta potential) of the OMV. The authors observed a correlation between interaction energies and OMV association, which was not entirely linear; therefore, they proposed that this interaction energy is only one factor that regulates OMV specificity for certain bacterial cells, and they hypothesized that surface proteins on both the OMV and bacterial cell surface likely play an additional role in this specific delivery process (48).

Tran and Boedicker investigated whether OMV-mediated DNA transfer is regulated by the relatedness of the OMV donor and recipient cells. The authors observed that *E. coli* is able to encapsulate plasmids with different replication origins within its OMVs and deliver this genetic cargo to recipient cells. *Aeromonas veronii* and *Enterobacter cloacae* exhibited similar behavior. The rate of gene transfer between the three types of OMVs and five types of cells: *E. coli*, *A. veronii*, *E. cloacae*, *C. violaceum*, and *P. aeruginosa* was studied, but no relation between the rates of uptake and the relatedness of the donor and recipient cells was observed (49). The authors did observe that the rates of delivery differed depending on the origin of the OMVs, with *A. veronii* OMVs being the most efficient (49).

Recently, some evidence of the involvement of an OMV surface protein in selective delivery of OMVs was reported. *Agrobacterium tumefaciens* is a phytopathogen that releases OMVs containing a small lipoprotein called Atu8019. The authors of this study observed that OMVs produced by a Δ*Atu8019* deletion mutant were similar in properties to the OMVs released by wildtype cells; however, OMVs from the deletion mutant exhibited an inhibited propensity for cell association, suggesting a role for this protein in selective OMV delivery (50).

The naturally targeted delivery of OMVs to specific bacterial cells holds exciting promise in their development for drug delivery. However, the details of this process have yet to be elucidated. Future research to identify the biological determinants enabling this specificity will enhance the design of targeted delivery systems, both natural and synthetic, for improved antibiotic function.

2.4 OMV Stability

A final advantage of using OMVs for antibiotic delivery is their extreme stability and their ability to protect their luminal content from enzymatic degradation, thus promoting long-distance delivery.

The inherent ability of OMVs to protect their cargo from degradation has been widely reported, particularly in the transfer of β-lactamases between bacteria. This process has been observed in a number of organisms, including *A. baumanii*, *Moraxella catarrhalis*, *Stenotrophomonas maltophilia*, *E. coli*, and *P. aeruginosa* (51–55). The luminal location of these antibiotic resistance enzymes has been demonstrated to protect the proteins from enzymatic degradation (54) as well as serum IgG-mediated neutralization (56). In addition, transfer of various protein toxins *via* OMVs has been reported to protect them from enzymatic degradation (12, 57–60), which has been hypothesized to enable long-distance delivery *in vivo* (12).

OMVs are also able to protect their nucleic acid cargo from enzymatic degradation. Koeppen et al. observed that inclusion of RNA within the OMV lumen protected it from RNase digestion (61). Similarly, OMV-encapsulated genes were protected from DNase digestion (34, 35, 62).

In addition to protecting their cargo from enzymatic degradation, OMVs appear to protect their cargo from degradation due to handling and storage. In a systematic study of the stability of OMV-encapsulated cargo, Alves et al. packaged an enzyme, phosphotriesterase (PTE) into the lumen of *E. coli* OMVs. The authors observed increased stability of the protein cargo relative to free PTE against multiple freeze-thaw cycles (63). Later work by this group demonstrated that encapsulation within OMVs protected long-term enzyme activity under multiple storage conditions, including freezing, heating, and lyophilization (64).

Together these observations demonstrate that encapsulation within the OMV lumen is able to protect the cargo from degradation, both *in vivo* and during storage. This property is likely to enhance the activity of encapsulated antibiotics, enabling delivery of reduced dosages.

3 NATURAL ANTIBIOTIC PROPERTIES OF OMVs

OMVs play important roles in the interactions of the microbiota, including interspecies competition. This innate antibiotic property has inspired some groups to propose the use of native OMVs as natural antibiotics (65). These "predatory OMVs" have been observed in many different systems, showing a conservation of this trait across bacterial species.

P. aerguinosa OMVs have a well-documented ability to interact with foreign bacteria. Kadurugamuwa and Beveridge observed fusion between native OMVs from strain PAO1 and both Gram-positive and Gram-negative bacteria. Electron micrographs demonstrated the degradation of the bacterial peptidoglycan after incubation with PAO1 OMVs, leading the authors to hypothesize that the OMVs may be carrying autolysins that act to disintegrate the wall of other bacteria cells. Interestingly, the authors found that when the cells were grown in the presence of a sub-inhibitory concentration of gentamicin, the resulting OMVs were even more potent. These antibiotic-loaded OMVs contained less gentamicin than what would normally be used for treatment, but with the added protection from the OMVs, and the additional lytic ability of the OMVs, the antibiotic loaded OMVs were effective in killing the gentamicin-resistant strain, *P. aeruginosa* 8803 (22).

Li et al. investigated the lytic behavior of OMVs produced by 15 different strains of Gram-negative bacteria against 17 different species of Gram-positive and Gram-negative bacteria. They observed significant and broad lytic activity in *P. aeruginosa* PAO1 OMVs, particularly against *E. coli* K12 cells and other cells with similar peptidoglycan structures. Not all OMVs demonstrated lytic activity; those from *Enterobacter agglomerans*, *Klebsiella pneumoniae*, *Citrobacter freundii*, and *Morganella morganii* had very little activity. No OMVs were able to lyse cells of the parent strain (19). This group had previously demonstrated that *P. aeruginosa* OMVs contain a murein hydrolase that is capable of degrading peptidoglycan (66). Additionally, this group has shown that OMVs from *P. aeruginosa* are able to break open the S-layer, the planar paracrystalline structures on some Gram-negative and Gram-positive bacteria that protects the peptidoglycan, and release a peptidoglycan hydrolase (67). They therefore hypothesized that the lytic behavior of the OMVs was due to the presence of these peptidoglycan-degrading enzymes in the OMVs (19).

More recently, OMVs from the soil bacterium, *Myxococcus xanthus*, were demonstrated to lyse *E. coli* cells. The authors observed that the addition of glyceraldehyde-3-phosphate dehydrogenase (GAPDH), an enzyme that enhances membrane fusion, increased the cytotoxicity of the *M. xanthus* OMVs; as a result, the authors concluded that the predatory activity of *M. xanthus* OMVs arises from fusion of the OMVs with the target cell membrane (14). Proteomic analysis demonstrated that *M. xanthus* OMVs contain numerous putative hydrolytic enzymes (30), which may be responsible for this predatory activity. OMVs produced by two additional myxobacterial strains, SBSr073 and Cbv34, were also shown to inhibit *E. coli* growth, a property the authors attributed to the presence of cystobactamids (myxobacterial-derived inhibitors of bacterial gyrase) within the OMVs (68). This group subsequently showed that OMVs produced by CBv34 and Cbfe23 (another myxobacterial strain) were taken up by host cells and inhibited intracellular growth of *Staphylococcus aureus* cells (69).

In addition to encapsulation of anti-bacterial molecules, some OMVs have been observed to naturally encapsulate anti-fungal molecules. Meers et al. demonstrated that *Lysobacter enzymogenes* OMVs exhibit chitinase activity and are able to inhibit the growth of the fungi, *Saccharomyces cerevisiae* and *Fusarium subglutinans*. Importantly, the OMVs were responsible for almost all of the anti-fungal activity of the *L. enzymogenes* supernatant, demonstrating that OMV-mediated transfer of these molecules is the primary pathway for this anti-fungal activity (70).

4 METHODS OF ENGINEERING OMVs TO IMPROVE THEIR POTENTIAL AS DRUG DELIVERY VEHICLES

The ability of OMVs to deliver functional molecules, including proteins, nucleic acids, and small molecules, combined with their natural selectivity has increased interest in their potential as

natural delivery vehicles. In particular, OMVs have an intrinsic ability to protect cargo from enzymatic degradation, and with their hydrophobic membrane and hydrophilic lumen, they have the ability to encapsulate a range of drug types. OMVs have been reported to be highly stable (12, 63), and they are readily functionalized to enhance targeted delivery. Despite these numerous advantages, several issues must first be address to enable the translational potential of OMVs as drug delivery vehicles. These challenges include increasing the vesicle yield, reducing the immunogenicity of the OMVs, incorporating specific molecules, and promoting targeting of specific cell types. Continued advancement of these techniques will improve the therapeutic potential of OMVs, particularly as antibiotic delivery vehicles.

4.1 Strategies to Increase Vesicle Yield

OMVs are naturally produced throughout bacterial growth; however, the resulting yields are too low for biotechnological applications. To overcome this challenge, many groups have looked towards genetic modifications that result in increased vesiculation. Mutations in the Tol-Pal system have been particularly appealing for this purpose. The *tol-pal* operon consists of seven genes, including the five genes comprising the Tol-Pal system: *tolQ*, *tolR*, *tolA*, *tolB*, and *pal*. These genes express proteins that together, form a complex linking the inner membrane, peptidoglycan, and outer membrane (71) (**Figure 3A**). Mutation of any one of the genes results in increased vesiculation in *E. coli* (72, 73). A similar approach that included mutation of the *tolR* gene along with the *galU* gene, which is involved in LPS biogenesis, was found to increase vesiculation in *Shigella sonnei* (74). In *Helicobacter pylori*, deletion of *tolB* but not *pal* increased vesiculation (75).

Building on the finding of the importance of the Tol-Pal system in vesiculation, Henry et al. demonstrated that genetic modifications to promote production of certain protein domains that interact with elements of the Tol-Pal system can likewise increase OMV production. Specifically, they found that periplasmic production of a TolR domain induced a high level of vesiculation in *E. coli*. Additionally, periplasmic production of the translocation domain of colicin A, colicin E3, and minor coat protein g3p also increased vesiculation. Finally, the authors demonstrated that the approach could be used in other bacteria, including *Shigella flexneri* and *Salmonella enterica* (76).

These multiple genetic approaches to increase OMV production have already enabled the use of OMVs for biotechnological purposes, particularly as vaccines and are likely to enable future development of OMVs as natural antibiotic delivery vehicles.

4.2 Engineering to Decrease LPS Toxicity

Another important limitation in the use of OMVs as drug delivery vehicles is their inflammatory nature. Derived from the outer membrane, the surface of OMVs is primarily composed of lipopolysaccharide (LPS). LPS consists of a hydrophobic lipid A molecule, which is tethered to the membrane *via* six acyl chains, core oligosaccharides, and the O-antigen (77) (**Figure 3B**). The lipid A portion, also called endotoxin, is responsible for the inflammatory response induced by LPS (78). Thus, to use OMVs as drug delivery vehicles, it is imperative that the toxicity of the LPS be reduced.

One strategy to reduce the toxicity of LPS is to genetically modify the genes leading to full acylation of the lipid A moiety. Nine enzymes are required for the biosynthesis of lipid A (77) and knockout of certain genes encoding these enzymes, in

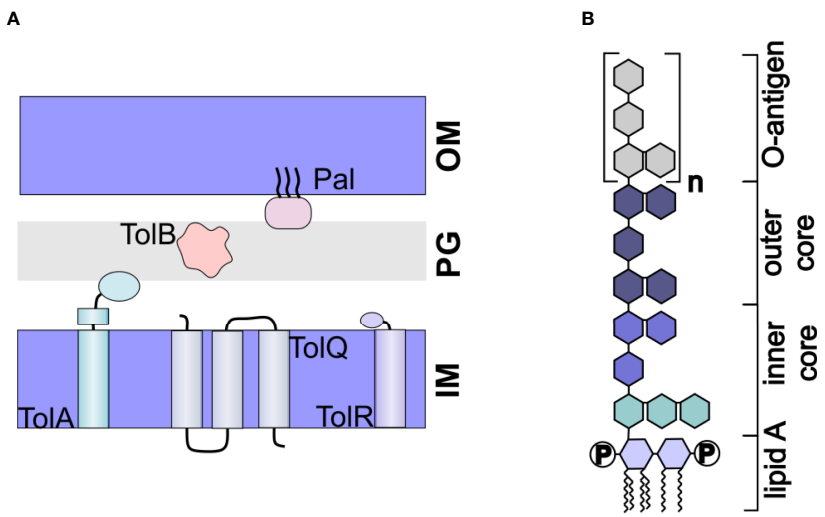

FIGURE 3 | Engineered OMVs. **(A)** The Tol-Pal System. The Tol-Pal system consists of five proteins, TolA, TolQ, and TolR located in the inner membrane (IM), TolB located in the peptidoglycan layer, and Pal located in the outer membrane. Mutation of any of these components has been shown to affect vesiculation. **(B)** Structure of LPS. LPS consists of a hydrophobic lipid A, which is commonly hexaacylated and di-phosphorylated (P). The polysaccharide portion of the molecule consists of a well conserved inner and outer core and a nonconserved O-antigen.

particular *lpxL* and *lpxM* (also known as *msbB*) have been demonstrated to result in under-acylated strains with reduced endototoxicity (79–81).

Alternatively, modification of the phosphorylation of the lipid A moiety can be an effective strategy to reduce endotoxicity of LPS. Lipid A is usually diphosphorylated (82). Edgar Ribi observed that monophosphorylated lipid A is significantly less immunogenic (83), and since then, monophosphoryl lipid A (MPL) has been FDA-approved as an adjuvant (84). A promising strategy to create OMVs consisting of monophosphorylated lipid A is to express the *Helicobacter pylori* Hp0021 gene in the OMV-producing organism. This enzyme removes the 1-phosphate of the lipid A moiety, resulting in monophosphorylated lipid A (85). When this gene was heterologously expressed in *E. coli*, the 1-phosphate group of lipid A was removed (86). While promising, this approach has not yet been used to develop OMVs for biotechnological purposes.

While LPS toxicity remains a serious concern with using OMVs as drug delivery vehicles, multiple promising approaches have demonstrated the potential to reduce the inflammatory response, thus enabling their future use as antibiotic delivery vehicles.

4.3 Strategies for Drug Loading

While certain OMVs naturally possess some antibiotic properties, additional work has focused on encapsulating specific molecules within the OMV lumen to expand on the potential of OMVs as delivery vehicles. Several methods to encapsulate different molecules, including antibiotics, have been explored, as described below. Further optimization of these approaches will enable full realization of the potential of OMVs as drug delivery vehicles.

4.3.1 Antibiotic Export *via* OMVs

The role of OMVs in removing unwanted material from the cell has been employed as a method to load OMVs with antibiotics. In this passive loading approach, bacterial cells are grown in the presence of the desired drug. The resulting antibiotic-containing OMVs are collected and tested to measure drug loading efficiencies (**Figure 4A**).

Kadurugamuwa and Beveridge first discovered that bacteria grown in the presence of antibiotics release vesicles containing some drug (22). The authors cultured *P. aeruginosa* strain PAO1 in gentamicin and discovered that the OMVs contained 4 ng of drug per μg of protein. These gentamicin-containing OMVs killed *S. aureus*, *E. coli*, and *P. aeruginosa* (strains PAO1 and Pa8803). Importantly, the authors observed that in Pa8803, which is a permeability mutant, OMV encapsulation enhanced gentamicin delivery significantly, demonstrating the potential of OMV-mediated drug delivery to overcome this mechanism of resistance (22). However, the Beveridge group later demonstrated that OMV-mediated delivery is unable to overcome all mechanisms of resistance. The group observed that *Burkholderia cepacia* strain CEP0248 was susceptible to both free and OMV-associated gentamicin, but the highly resistant strain C5424 was not. The OMVs were able to deliver gentamicin; however, the cells were not sensitive to the drug. The authors therefore hypothesized that this strain must possess another mechanism of resistance beyond inhibition of drug uptake (87). Gentamicin-containing *P. aeruginosa* OMVs were also found to be effective in killing some Gram-positive organisms as well, including *Bacillus subtilis* and *S. aureus* (23).

Tashiro et al. hypothesized that the selective delivery of *B. agrestis* OMVs to *B. agrestis* cells (as described in Section 2.4) could enable OMV-mediated selective antibiotic delivery. To test this, the authors grew *B. agrestis* until the late stationary phase, then added gentamicin at a concentration four times higher than the MIC for 30 mins. The purified OMVs were found to contain gentamicin, and selective delivery of gentamicin to *B. agrestis* cells was observed (48).

Huang et al. grew *A. baumanii* in sub-MIC concentrations of levofloxacin and observed that the resulting OMVs contained a high concentration of levofloxacin (20). They demonstrated that OMV encapsulation increased the stability of levofloxacin under a number of storage conditions. The levofloxacin-containing OMVs were able to kill enterotoxigenic *E. coli* (ETEC) cells, and at a low dose, the levofloxacin-containing OMVs were more effective than free levofloxacin. The authors also demonstrated that these levofloxacin-containing OMVs were effective in killing

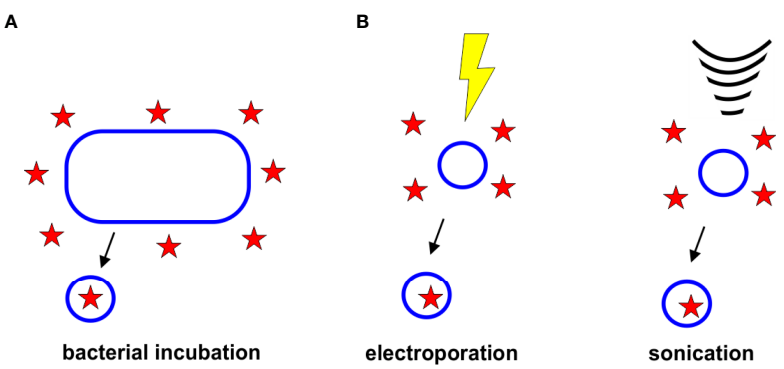

FIGURE 4 | Strategies for Drug Loading. **(A)** Bacterial Incubation. Bacteria grown in the presence of antibiotics have been found to release antibiotic-containing OMVs. **(B)** Electroporation and Sonication. Electroporation and sonication can enhance drug loading within the OMV lumen.

K. pneumoniae and *P. aeruginosa* as well, and the procedure for loading could be accomplished with other antibiotics, demonstrating a broad potential of the approach. In a mouse model of ETEC infection, the levofloxacin-containing OMVs were more effective than free drug. Finally, the authors observed that the levofloxacin-containing OMVs were biocompatible (20).

4.3.2 Active Loading Techniques

To enhance the incorporation of drugs and other therapeutics in OMVs and other extracellular vesicles, several active incorporation techniques have been proposed, including electroporation and sonication, (**Figure 4B**). Although none of these techniques have yet been used specifically to load antibiotics into OMVs, it is likely that these approaches could improve the encapsulation efficiencies of antibiotics, as has been observed with other drugs and vesicle types.

4.3.2.1 Electroporation

Electroporation involves the use of a strong electric field to induce the formation of transient pores in a biological membrane (88). This technique has long been used to enhance DNA uptake by bacterial cells (88), and more recently has been used to promote loading of content into human-derived extracellular vesicles (89–93). Gujrati et al. demonstrated that the approach could also be used with OMVs, when they loaded OMVs with siRNA against kinesin spindle protein (KSP) to develop anti-cancer therapeutics. To accomplish loading, the authors electroporated the OMVs in the presence of the siRNA using an empirical approach to identify the optimal conditions (700 V, 50 μF) that promoted loading but did not affect OMV integrity (94). Similarly, Ayed et al. optimized electroporation conditions to load gold nanoparticles (7 nm) into *P. aeruginosa* PAO1 OMVs. The authors observed that one pulse of 0.47 kV was sufficient to encapsulate 55% of the nanoparticles without disrupting OMV integrity (95). These results suggest that electroporation is an effective method for loading a variety of cargo into the OMV lumen, and could have great potential for improving the encapsulation efficiencies of antibiotics.

4.3.2.2 Sonication

Sonication is the use of ultrasonic energy to increase the fluidity of a membrane to enhance drug diffusion. While this technique has not yet been reported as a means of loading drug into bacterial vesicles, it has been used to improve loading efficiencies within human-derived vesicles (96, 97). The primary drawback of this approach is that it may permanently disrupt the integrity of the vesicles (98).

4.3.3 OMV Coating Approach

Wu et al. took advantage of the natural delivery properties of OMVs to enhance delivery of rifampicin-loaded mesoporous silica nanoparticles (MSNs). Rifampicin is a hydrophobic antibiotic with limited effectiveness against Gram-negative bacteria due to its inability to cross the cell envelope. Incorporation of rifampicin within MSNs improves drug solubility, but uptake by Gram-negative bacteria is low. The authors observed that coating the rifampicin-loaded MSNs with *E. coli* OMVs extended the release of drug and the OMV-coated MSNs were taken up by *E. coli* cells more effectively than uncoated MSNs or free drugs. The OMV-coated nanoparticles also displayed good biocompatibility (99).

4.4 Surface Engineering

In order to enhance targeting or functionality of OMVs, several approaches to display particular moieties on the vesicle surface have been employed. These genetic approaches involve the development of fusions between the desired protein and certain surface-localized proteins (42, 100–102), or the use of the SpyCatcher/Tag or SnoopCatcher/Tag systems to promote isopeptide bond formation between the desired protein and a surface-localized protein (103, 104) (**Figure 5**). These approaches have been primarily developed for vaccine technology; however, targeted delivery of antibiotics specifically to pathogenic cells could likely be accomplished using similar approaches.

The ClyA toxin expressed by many *E. coli* strains and enriched in OMVs (27) has been commonly employed as a fusion partner to localize specific proteins to the OMV surface. Kim et al. first demonstrated the power of this approach by creating a series of chimeric ClyA fusion proteins, using green fluorescent protein (GFP), β-lactamase, β-galactosidase, organophosphorous hydrolase (OPH), and a single chain Fv antibody fragment (100). The authors observed that each fusion partner retained its activity and was located on the surface of the vesicles (100). In engineering their siRNA-containing OMVs, Gujrati et al. genetically fused a targeting affibody to the ClyA protein and demonstrated that this approach enabled targeted delivery of the siRNA-containing OMVs to HER2-expressing cells (94).

Another fusion protein approach that has been shown to be successful takes advantage of the autotransporter (AT) Hbp. *Mycobacterium tuberculosis* antigens were localized to the surface of *E. coli* or *Salmonella enterica* OMVs through fusion to Hbp. Hbp is one of the most abundant proteins detected in *E. coli* and *S. enterica* OMVs, making it a strong fusion partner candidate. In addition, the authors exploited the dispensability of certain side domains of Hbp to simultaneously display multiple heterologous antigens on the OMV surface (101). In subsequent work, the authors developed a strategy to overcome limitations in the size and complexity of proteins that can be displayed on the surface of the OMVs *via* fusion to Hbp. In this approach, the authors fused the SpyTag protein (105) to Hbp. Upon translocation of the Hbp across the outer membrane, the SpyTag protein was found to be displayed on the surface of the OMVs. Large protein antigens or nanobodies were then conjugated to the SpyCatcher protein to enable efficient ligation to the OMV. The SnoopTag/SnoopCatcher system (106) was used in tandem to facilitate surface display of heterologous proteins (103, 104).

Chen et al. developed an approach to simultaneously localize proteins of interest within and on the surface of *E. coli* OMVs. To target the OMV lumen, the authors created a fusion protein with SlyB, a native lipoprotein that is localized at the inner leaflet (periplasmic side) of the outer membrane (107). At the same time, they localized an antibody on the surface of the OMV using

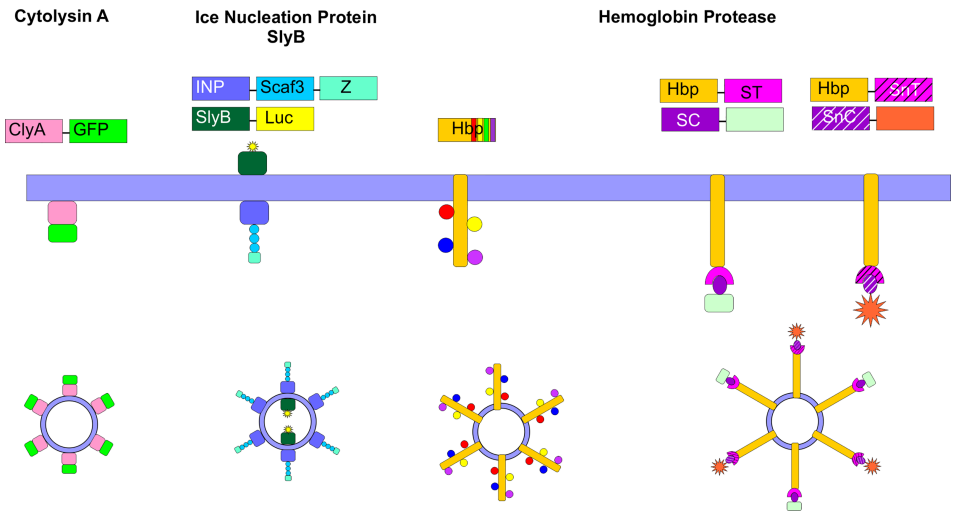

FIGURE 5 | Surface Engineering of OMVs. Several genetic strategies have been used to localize certain proteins on the surface of OMVs. Fusion proteins between cytolysin A (ClyA) and several cargos, including GFP have been created in *E. coli*. Ice nucleation protein (INP) was used to tether an antibody on the surface of the OMV by creating a fusion between INP, a cohesin-containing Scaf3 domain, and an antibody-binding Z-domain. Simultaneously, SlyB was used to localize luciferase to the OMV lumen. Up to four bacterial antigens were tethered to the surface of OMVs using the hemoglobin protease (Hbp). This protein was also used in combination with the SpyCatcher/Tag and SnoopCatcher/Tag systems to display heterologous proteins on the OMV surface.

an ice nucleation protein (INP) anchor (108) tethered to an antibody-binding Z domain *via* a scaffold assembly consisting of 3 cohesin domains (Scaf3). As proof of concept, the authors encapsulated nanoluciferase for detection purposes and tethered IgG to the surface to target thrombin (102).

The ability to functionalize the surface of the OMV to enable selective delivery holds great promise for the targeted delivery of antibiotics. Although not yet commonly employed, targeted delivery of antibiotics represents a promising approach to limit the development of antibiotic resistance, as it would limit exposure of the healthy microbiota to the drug.

5 FUTURE DIRECTIONS

OMVs have several properties that make them promising antibiotic delivery vehicles as described above, including overcoming the entry limitation of certain antibiotics for Gram-negative bacteria. However, while the potential is strong, a number of limitations and challenges remain to be addressed before the use of this novel delivery system can be fully realized.

The mechanisms by which OMVs deliver cargo to bacterial cells remains understudied. While great advances have been made in our understanding of OMV delivery to host cells, little work has focused on delivery to bacterial cells. Additionally, the factors leading to targeted delivery to certain cell types remain unclear. As a more detailed understanding of mechanisms leading to inter-bacterial delivery emerges, researchers will be well-equipped to engineer better performing OMVs or to incorporate specific OMV features into synthetic (liposome) systems to enhance delivery.

In order to realize OMVs as biotechnological devices, several manufacturing advances are necessary. OMV purification remains time-consuming and inefficient, relying on long ultracentrifugation runs as well as filtration and other slow processes. Although OMVs are produced throughout growth, the yield remains low, even for hypervesiculating strains. Thus, more advanced techniques to scale-up these systems are needed. In addition, the heterogeneity of OMVs has recently been established (57, 109–111). For biotechnological applications, it will be essential to develop optimized strategies to purify more homogeneous OMV populations. Furthermore, while some work has demonstrated stability of OMVs under certain storage conditions (63), additional research to identify and/or develop optimal processing and storage conditions that do not affect OMV integrity are necessary.

Finally, standardization of techniques and analyses has been lacking in the OMV field. To overcome this issue, the International Society for Extracellular Vesicles (ISEV) has worked diligently towards developing a set of standards to be applied to all EV studies (112–114). Full adoption of such standards in the OMV field would greatly advance the rate of development of OMVs for biotechnological applications.

6 CONCLUSIONS

Despite these challenges, the potential of OMVs for antibiotic delivery remains a promising approach to treat Gram-negative bacterial infections, which are otherwise difficult to treat. The field has advanced rapidly over the past 10 years, and it is expected that new discoveries will further advance the biotechnological applications of OMVs, particularly as antibiotic delivery vehicles.

AUTHOR CONTRIBUTIONS

SC and AB conceived the concept of the review, and wrote and edited the manuscript. AB prepared the figures, and acquired funding. All authors contributed to the article and approved the submitted version.

FUNDING

This research was funded by the National Science Foundation, grant number 1554417 and the National Institutes of Health, grant number DE027769.

REFERENCES

1. U.S.Department of Health and Human Services Centers for Disease Control and Prevention. *Antibiotic Resistance Threats in the United States*. Atlanta, GA:U.S. Department of Health and Human Services, CDC (2019). doi: 10.15620/cdc:82532
2. Denyer SP, Maillard JY. Cellular Impermeability and Uptake of Biocides and Antibiotics in Gram-Negative Bacteria. *J Appl Microbiol* (2002) 92(s1):35S–45S. doi: 10.1046/j.1365-2672.92.5s1.19.x
3. Peleg AY, Hooper DC. Hospital-Acquired Infections Due to Gram-Negative Bacteria. *N Engl J Med* (2010) 362(19):1804–13. doi: 10.1056/NEJMra0904124
4. Bonnington KE, Kuehn MJ. Protein Selection and Export *via* Outer Membrane Vesicles. *Biochim Biophys Acta (BBA) - Mol Cell Res* (2014) 1843(8):1612–9. doi: 10.1016/j.bbamcr.2013.12.011
5. Kuehn MJ, Kesty NC. Bacterial Outer Membrane Vesicles and the Host-Pathogen Interaction. *Genes Dev* (2005) 19:2645–55. doi: 10.1101/gad.1299905
6. Kulp A, Kuehn MJ. Biological Functions and Biogenesis of Secreted Bacterial Outer Membrane Vesicles. *Annu Rev Microbiol* (2010) 64:163–84. doi: 10.1146/annurev.micro.091208.073413
7. Schwechheimer C, Kuehn MJ. Outer-Membrane Vesicles From Gram-Negative Bacteria: Biogenesis and Functions. *Nat Rev Microbiol* (2015) 13:605–19. doi: 10.1038/nrmicro3525
8. Ellis TN, Kuehn MJ. Virulence and Immunomodulatory Roles of Bacterial Outer Membrane Vesicles. *Microbiol Mol Biol Rev* (2010) 74:81–94. doi: 10.1128/MMBR.00031-09
9. Amano A, Takeuchi H, Furata N. Outer Membrane Vesicles Function as Offensive Weapons in Host-Parasite Interactions. *Microbes Infect* (2010) 12:791–8. doi: 10.1016/j.micinf.2010.05.008
10. Berleman J, Auer M. The Role of Bacterial Outer Membrane Vesicles for Intra- and Interspecies Delivery. *Environ Microbiol* (2012) 15(2):347–54. doi: 10.1111/1462-2920.12048
11. Bitto NJ, Chapman R, Pidot S, Costin A, Lo C, Choi J, et al. Bacterial Membrane Vesicles Transport Their DNA Cargo Into Host Cells. *Sci Rep* (2017) 7:7072. doi: 10.1038/s41598-017-07288-4
12. Bomberger JM, MacEachran DP, Coutermarsh BA, Ye S, O'Toole GA, Stanton BA. Long-Distance Delivery of Bacterial Virulence Factors by *Pseudomonas aeruginosa* Outer Membrane Vesicles. *PloS Pathog* (2009) 5 (4):e1000382. doi: 10.1371/journal.ppat.1000382
13. Donato GM, Goldsmith CS, Paddock CD, Eby JC, Gray MC, Hewlett EL. Delivery of *Bordetella pertussis* Adenylate Cyclase Toxin to Target Cells via Outer Membrane Vesicles. *FEBS Lett* (2012) 586:459–65. doi: 10.1016/j.febslet.2012.01.032
14. Evans AGL, Davey HM, Cookson A, Currinn H, Cooke-Fox G, Stanczyk PJ, et al. Predatory Activity of *Myxococcus xanthus* Outer-Membrane Vesicles and Properties of Their Hydrolase Cargo. *Microbiology* (2012) 158 (11):2742–52. doi: 10.1099/mic.0.060343-0
15. Fulsundar S, Harms K, Flaten GE, Johnsen PJ, Chopade BA, Nielsen KM. Gene Transfer Potential of Outer Membrane Vesicles of *Acinetobacter baylyi* and Effects of Stress on Vesiculation. *Appl Environ Microbiol* (2014) 80 (11):3469–83. doi: 10.1128/AEM.04248-13
16. Chiura HX, Kogure K, Hagemann S, Ellinger A, Velimirov B. Evidence for Particle-Induced Horizontal Gene Transfer and Serial Transduction Between Bacteria. *FEMS Microbiol Ecol* (2011) 76(3):576–91. doi: 10.1111/j.1574-6941.2011.01077.x
17. Domingues S, Nielsen KM. Membrane Vesicles and Horizontal Gene Transfer in Prokaryotes. *Curr Opin Microbiol* (2017) 38:16–21. doi: 10.1016/j.mib.2017.03.012
18. Kadurugamuwa JL, Beveridge TJ. Membrane Vesicles Derived From *Pseudomonas aeruginosa* and *Shigella flexneri* Can Be Integrated Into the Surfaces of Other Gram-Negative Bacteria. *Microbiology* (1999) 145 (8):2051–60. doi: 10.1099/13500872-145-8-2051
19. Li Z, Clarke AJ, Beveridge TJ. Gram-Negative Bacteria Produce Membrane Vesicles Which Are Capable of Killing Other Bacteria. *J Bacteriol* (1998) 180 (20):5478–83. doi: 10.1128/JB.180.20.5478-5483.1998
20. Huang W, Zhang Q, Li W, Yuan M, Zhou J, Hua L, et al. Development of Novel Nanoantibiotics Using an Outer Membrane Vesicle-Based Drug Efflux Mechanism. *J Controlled Release* (2020) 317:1–22. doi: 10.1016/j.jconrel.2019.11.017
21. Jain S, Pillai J. Bacterial Membrane Vesicles as Novel Nanosystems for Drug Delivery. *Int J Nanomedicine* (2017) 12:6329–41. doi: 10.2147/IJN.S137368
22. Kadurugamuwa JL, Beveridge TJ. Bacteriolytic Effect of Membrane Vesicles From *Pseudomonas aeruginosa* on Other Bacteria Including Pathogens: Conceptually New Antibiotics. *J Bacteriol* (1996) 178(10):2767–74. doi: 10.1128/jb.178.10.2767-2774.1996
23. MacDonald KL, Beveridge TJ. Bactericidal Effect of Gentamicin-Induced Membrane Vesicles Derived From *Pseudomonas Aeruginosa* PAO1 on Gram-Positive Bacteria. *Can J Microbiol* (2002) 48(9):810–20. doi: 10.1139/w02-077
24. Haurat MF, Aduse-Opoku J, Rangarajan M, Dorobantu L, Gray MR, Curtis MA, et al. Selective Sorting of Cargo Proteins Into Bacterial Membrane Vesicles. *J Biol Chem* (2011) 286:1269–71. doi: 10.1074/jbc.M110.185744
25. Horstman AL, Kuehn MJ. Enterotoxigenic *Escherichia coli* Secretes Active Heat-Labile Enterotoxin via Outer Membrane Vesicles. *J Biol Chem* (2000) 275:12489–96. doi: 10.1074/jbc.275.17.12489
26. Kato S, Kowashi Y, Demuth DR. Outer Membrane-Like Vesicles Secreted by *Actinobacillus actinomycetemcomitans* are Enriched in Leukotoxin. *Microb Pathog* (2002) 32(1):1–13. doi: 10.1006/mpat.2001.0474
27. Wai SN, Lindmark B, Soderblom T, Takade A, Westermark M, Oscarsson J, et al. Vesicle-Mediated Export and Assembly of Pore-Forming Oligomers of the Enterobacterial ClyA Cytotoxin. *Cell* (2003) 115(1):25–35. doi: 10.1016/S0092-8674(03)00754-2
28. Shimkets L, Woese CR. A Phylogenetic Analysis of the Myxobacteria: Basis for Their Classification. *Proc Natl Acad Sci* (1992) 89(20):9459–63. doi: 10.1073/pnas.89.20.9459
29. Kahnt J, Aguiluz K, Koch J, Treuner-Lange A, Konovalova A, Huntley S, et al. Profiling the Outer Membrane Proteome During Growth and Development of the Social Bacterium *Myxococcus xanthus* by Selective Biotinylation and Analyses of Outer Membrane Vesicles. *J Proteome Res* (2010) 9(10):5197–208. doi: 10.1021/pr1004983
30. Berleman JE, Allen S, Danielewicz MA, Remis JP, Gorur A, Cunha J, et al. The Lethal Cargo of *Myxococcus Xanthus* Outer Membrane Vesicles. *Front Microbiol* (2014) 5:474. doi: 10.3389/fmicb.2014.00474
31. Whitworth DE. Chapter 1 - Myxobacterial Vesicles: Death at a Distance? In: AI Laskin, S Sariaslani, GM Gadd, editors. *Advances in Applied Microbiology*, vol. 75. 525 B Street, Suite 1900, San Diego, CA 92101-4495, USA 225 Wyman Street, Waltham, MA 02451, USA 32, Jamestown Road, London NW1 7BY, UK:Academic Press (2011). p. 1–31.
32. Kadurugamuwa JL, Beveridge TJ. Virulence Factors are Released From *Pseudomonas aeruginosa* in Association With Membrane Vesicles During Normal Growth and Exposure to Gentamicin: A Novel Mechanism of Enzyme Secretion. *J Bacteriol* (1995) 177(14):3998–4008. doi: 10.1128/jb.177.14.3998-4008.1995
33. Kolling GL, Matthews KR. Export of Virulence Genes and Shiga Toxin by Membrane Vesicles of *Escherichia coli* O157:H7. *Appl Environ Microbiol* (1999) 65(5):1843–8. doi: 10.1128/AEM.65.5.1843-1848.1999
34. Yaron S, Kolling GL, Simon L, Matthews KR. Vesicle-Mediated Transfer of Virulence Genes From *Escherichia Coli* O157:H7 to Other Enteric Bacteria. *Appl Environ Microbiol* (2000) 66(10):4414–20. doi: 10.1128/AEM.66.10.4414-4420.2000

35. Rumbo C, Fernández-Moreira E, Merino M, Poza M, Mendez JA, Soares NC, et al. Horizontal Transfer of the OXA-24 Carbapenemase Gene via Outer Membrane Vesicles: A New Mechanism of Dissemination of Carbapenem Resistance Genes in *Acinetobacter Baumannii*. *Antimicrob Agents Chemother* (2011) 55(7):3084–90. doi: 10.1128/AAC.00929-10
36. Ho M-H, Chen C-H, Goodwin JS, Wang B-Y, Xie H. Functional Advantages of *Porphyromonas Gingivalis* Vesicles. *PloS One* (2015) 10(4):e0123448–e0123448. doi: 10.1371/journal.pone.0123448
37. Bielaszewska M, Daniel O, Karch H, Mellmann A. Dissemination of the *blaCTX-M-15* Gene Among Enterobacteriaceae *via* Outer Membrane Vesicles. *J Antimicrob Chemother* (2020) 75(9):2442–51. doi: 10.1093/jac/dkaa214
38. Marchant P, Carreño A, Vivanco E, Silva A, Nevermann J, Otero C, et al. "One for All": Functional Transfer of OMV-Mediated Polymyxin B Resistance From *Salmonella Enterica* Sv. Typhi Δ*tolR* and Δ*degS* to Susceptible Bacteria. *Front Microbiol* (2021) 12:1068. doi: 10.3389/fmicb.2021.672467
39. Miller MB, Bassler BL. Quorum Sensing in Bacteria. *Annu Rev Microbiol* (2001) 55(1):165–99. doi: 10.1146/annurev.micro.55.1.165
40. Wagner-Döbler I, Thiel V, Eberl L, Allgaier M, Bodor A, Meyer S, et al. Discovery of Complex Mixtures of Novel Long-Chain Quorum Sensing Signals in Free-Living and Host-Associated Marine Alphaproteobacteria. *ChemBioChem* (2005) 6(12):2195–206. doi: 10.1002/cbic.200500189
41. Toyofuku M, Morinaga K, Hashimoto Y, Uhl J, Shimamura H, Inaba H, et al. Membrane Vesicle-Mediated Bacterial Communication. *ISME J* (2017) 11(6):1504–9. doi: 10.1038/ismej.2017.13
42. Cooke AC, Nello AV, Ernst RK, Schertzer JW. Analysis of *Pseudomonas aeruginosa* Biofilm Membrane Vesicles Supports Multiple Mechanisms of Biogenesis. *PloS One* (2019) 14(2):e0212275. doi: 10.1371/journal.pone.0212275
43. Mashburn LM, Whiteley M. Membrane Vesicles Traffic Signals and Facilitate Group Activities in a Prokaryote. *Nature* (2005) 437(7057):422–5. doi: 10.1038/nature03925
44. Mashburn-Warren L, Howe J, Garidel P, Richter W, Steiniger F, Roessle M, et al. Interaction of Quorum Signals With Outer Membrane Lipids: Insights Into Prokaryotic Membrane Vesicle Formation. *Mol Microbiol* (2008) 69(2):491–502. doi: 10.1111/j.1365-2958.2008.06302.x
45. Schertzer JW, Whiteley M. A Bilayer-Couple Model of Bacterial Outer Membrane Vesicle Biogenesis. *mBio* (2012) 3(2):e00297–11. doi: 10.1128/mBio.00297-11
46. Choi SY, Lim S, Cho G, Kwon J, Mun W, Im H, et al. *Chromobacterium Violaceum* Delivers Violacein, a Hydrophobic Antibiotic, to Other Microbes in Membrane Vesicles. *Environ Microbiol* (2020) 22(2):705–13. doi: 10.1111/1462-2920.14888
47. Kirkpatrick P. Pressures in the Pipeline. *Nat Rev Drug Discov* (2003) 2(5):337–7. doi: 10.1038/nrd1095
48. Tashiro Y, Hasegawa Y, Shintani M, Takaki K, Ohkuma M, Kimbara K, et al. Interaction of Bacterial Membrane Vesicles With Specific Species and Their Potential for Delivery to Target Cells. *Front Microbiol* (2017) 8(571):13. doi: 10.3389/fmicb.2017.00571
49. Tran F, Boedicker JQ. Genetic Cargo and Bacterial Species Set the Rate of Vesicle-Mediated Horizontal Gene Transfer. *Sci Rep* (2017) 7(1):8813. doi: 10.1038/s41598-017-07447-7
50. Knoke LR, Abad Herrera S, Götz K, Justesen BH, Günther Pomorski T, Fritz C, et al. *Agrobacterium Tumefaciens* Small Lipoprotein Atu8019 Is Involved in Selective Outer Membrane Vesicle (OMV) Docking to Bacterial Cells. *Front Microbiol* (2020) 11:1228. doi: 10.3389/fmicb.2020.01228
51. Ciofu O, Beveridge TJ, Kadurugamuwa J, Walther-Rasmussen J, Hoiby N. Chromosomal Beta-Lactamase is Packaged Into Membrane Vesicles and Secreted From *Pseudomonas aeruginosa*. *J Antimicrob Chemother* (2000) 45:9–13. doi: 10.1093/jac/45.1.9
52. Schaar V, Nordstrom T, Morgelin M, Riesbeck K. *Moraxella catarrhalis* Outer Membrane Vesicles Carry {Beta}-Lactamase and Promote Survival of *Streptococcus pneumoniae* and *Haemophilus influenzae* by Inactivating Amoxicillin. *Antimicrob Agents Chemother* (2011) 55:3845–53. doi: 10.1128/AAC.01772-10
53. Schaar V, Uddbäck I, Nordström T, Riesbeck K. Group A Streptococci are Protected From Amoxicillin-Mediated Killing by Vesicles Containing β-Lactamase Derived From *Haemophilus influenzae*. *J Antimicrob Chemother* (2013) 69(1):117–20. doi: 10.1093/jac/dkt307
54. Liao Y-T, Kuo S-C, Chiang M-H, Lee Y-T, Sung W-C, Chen Y-H, et al. *Acinetobacter baumannii* Extracellular OXA-58 Is Primarily and Selectively Released *via* Outer Membrane Vesicles After Sec-Dependent Periplasmic Translocation. *Antimicrob Agents Chemother* (2015) 59(12):7346–54. doi: 10.1128/AAC.01343-15
55. Kim SW, Park SB, Im SP, Lee JS, Jung JW, Gong TW, et al. Outer Membrane Vesicles From β-Lactam-Resistant *Escherichia Coli* Enable the Survival of β-Lactam-Susceptible E. Coli in the Presence of β-Lactam Antibiotics. *Sci Rep* (2018) 8(1):5402. doi: 10.1038/s41598-018-23656-0
56. Schaar V, Paulsson M, Mörgelin M, Riesbeck K. Outer Membrane Vesicles Shield *Moraxella Catarrhalis* β-Lactamase From Neutralization by Serum IgG. *J Antimicrob Chemother* (2012) 68(3):593–600. doi: 10.1093/jac/dks444
57. Nice JB, Balashova NV, Kachlany SC, Koufos E, Krueger E, Lally ET, et al. *Aggregatibacter actinomycetemcomitans* Leukotoxin Is Delivered to Host Cells in an LFA-1-Independent Manner When Associated With Outer Membrane Vesicles. *Toxins* (2018) 10(10):414. doi: 10.3390/toxins10100414
58. Rasti ES, Schappert ML, Brown AC. Association of *Vibrio Cholerae* 569B Outer Membrane Vesicles With Host Cells Occurs in a GM1-Independent Manner. *Cell Microbiol* (2018) 20:e12828. doi: 10.1111/cmi.12828
59. Elluri S, Enow C, Vdovikova S, Rompikuntal PK, Dongre M, Carlsson S, et al. Outer Membrane Vesicles Mediate Transport of Biologically Active *Vibrio cholerae* Cytolysin (VCC) From V. *Cholerae strains*. *PloS One* (2014) 9(9):e106731. doi: 10.1371/journal.pone.0106731
60. Mondal A, Tapader R, Chatterjee NS, Ghosh A, Sinha R, Koley H, et al. Cytotoxic and Inflammatory Responses Induced by Outer Membrane Vesicle-Associated Biologically Active Proteases From *Vibrio cholerae*. *Infect Immun* (2016) 84(5):1478–90. doi: 10.1128/IAI.01365-15
61. Koeppen K, Hampton TH, Jarek M, Scharfe M, Gerber SA, Mielcarz DW, et al. A Novel Mechanism of Host-Pathogen Interaction Through sRNA in Bacterial Outer Membrane Vesicles. *PloS Pathog* (2016) 12(6):e1005672. doi: 10.1371/journal.ppat.1005672
62. Renelli M, Matias V, Lo RY, Beveridge TJ. DNA-Containing Membrane Vesicles of *Pseudomonas Aeruginosa* PAO1 and Their Genetic Transformation Potential. *Microbiology* (2004) 150:2161–9. doi: 10.1099/mic.0.26841-0
63. Alves NJ, Turner KB, Daniele MA, Oh E, Medintz IL, Walper SA. Bacterial Nanobioreactors–Directing Enzyme Packaging Into Bacterial Outer Membrane Vesicles. *ACS Appl Mater Interfaces* (2015) 7(44):24963–72. doi: 10.1021/acsami.5b08811
64. Alves NJ, Turner KB, Medintz IL, Walper SA. Protecting Enzymatic Function Through Directed Packaging Into Bacterial Outer Membrane Vesicles. *Sci Rep* (2016) 6(1):24866. doi: 10.1038/srep24866
65. Pérez J, Contreras-Moreno FJ, Marcos-Torres FJ, Moraleda-Muñoz A, Muñoz-Dorado J. The Antibiotic Crisis: How Bacterial Predators Can Help. *Comput Struct Biotechnol J* (2020) 18:2547–55. doi: 10.1016/j.csbj.2020.09.010
66. Li Z, Clarke AJ, Beveridge TJ. A Major Autolysin of *Pseudomonas Aeruginosa*: Subcellular Distribution, Potential Role in Cell Growth and Division and Secretion in Surface Membrane Vesicles. *J Bacteriol* (1996) 178(9):2479–88. doi: 10.1128/jb.178.9.2479-2488.1996
67. Kadurugamuwa JL, Mayer A, Messner P, Sára M, Sleytr UB, Beveridge TJ. S-Layered Aneurinibacillus and Bacillus Spp. Are Susceptible to the Lytic Action Of *Pseudomonas aeruginosa* Membrane Vesicles. *J Bacteriol* (1998) 180(9):2306–11. doi: 10.1128/JB.180.9.2306-2311.1998
68. Schulz E, Goes A, Garcia R, Panter F, Koch M, Muller R, et al. Biocompatible Bacteria-Derived Vesicles Show Inherent Antimicrobial Activity. *J Controll Release* (2018) 290:46–55. doi: 10.1016/j.jconrel.2018.09.030
69. Goes A, Lapuhs P, Kuhn T, Schulz E, Richter R, Panter F, et al. Myxobacteria-Derived Outer Membrane Vesicles: Potential Applicability Against Intracellular Infections. *Cells* (2020) 9(1):194. doi: 10.3390/cells9010194
70. Meers PR, Liu C, Chen R, Bartos W, Davis J, Dziedzic N, et al. Vesicular Delivery of the Antifungal Antibiotics of *Lysobacter Enzymogenes* C3. *Appl Environ Microbiol* (2018) 84(20):e01353–01318. doi: 10.1128/AEM.01353-18
71. Szczepaniak J, Press C, Kleanthous C. The Multifarious Roles of Tol-Pal in Gram-Negative Bacteria. *FEMS Microbiol Rev* (2020) 44(4):490–506. doi: 10.1093/femsre/fuaa018
72. Bernadac A, Gavioli M, Lazzaroni J-C, Raina S, Lloubès R. *Escherichia Coli* Tol-Pal Mutants Form Outer Membrane Vesicles. *J Bacteriol* (1998) 180(18):4872–8. doi: 10.1128/JB.180.18.4872-4878.1998

73. McBroom AJ, Johnson AP, Vemulapalli S, Kuehn MJ. Outer Membrane Vesicle Production by *Escherichia coli* Is Independent of Membrane Instability. *J Bacteriol* (2006) 188:5385–92. doi: 10.1128/JB.00498-06
74. Berlanda Scorza F, Colucci AM, Maggiore L, Sanzone S, Rossi O, Ferlenghi I, et al. High Yield Production Process for Shigella Outer Membrane Particles. *PloS One* (2012) 7(6):e35616. doi: 10.1371/journal.pone.0035616
75. Turner L, Praszkier J, Hutton ML, Steer D, Ramm G, Kaparakis-Liaskos M, et al. Increased Outer Membrane Vesicle Formation in a *Helicobacter Pylori* tolB Mutant. *Helicobacter* (2015) 20(4):269–83. doi: 10.1111/hel.12196
76. Henry T, Pommier S, Journet L, Bernadac A, Gorvel J-P, Lloubès R. Improved Methods for Producing Outer Membrane Vesicles in Gram-Negative Bacteria. *Res Microbiol* (2004) 155(6):437–46. doi: 10.1016/j.resmic.2004.04.007
77. Wang X, Quinn PJ. Lipopolysaccharide: Biosynthetic Pathway and Structure Modification. *Prog Lipid Res* (2010) 49(2):97–107. doi: 10.1016/j.plipres.2009.06.002
78. Lüderitz O, Freudenberg MA, Galanos C, Lehmann V, Rietschel ET, Shaw DH. Lipopolysaccharides of Gram-Negative Bacteria. In: F Bronner, A Kleinteller, editors. *Current Topics in Membranes and Transport*, vol. 17. 111 Fifth Avenue, New York, NY 10003:Academic Press (1982). p. 79–151.
79. Moore RN, Ley PVD, Steeghs L, Hamstra HJ, Hove JT, Zomer B, et al. Modification of Lipid A Biosynthesis in *Neisseria meningitidis lpxL* Mutants: Influence on Lipopolysaccharide Structure, Toxicity, and Adjuvant Activity. *Infect Immun* (2001) 69(10):5981–90. doi: 10.1128/IAI.69.10.5981-5990.2001
80. Kim S-H, Kim K-S, Lee S-R, Kim E, Kim M-S, Lee E-Y, et al. Structural Modifications of Outer Membrane Vesicles to Refine Them as Vaccine Delivery Vehicles. *Biochim Biophys Acta (BBA) - Biomembr* (2009) 1788 (10):2150–9. doi: 10.1016/j.bbamem.2009.08.001
81. Lee DH, Kim S-H, Kang W, Choi YS, Lee S-H, Lee S-R, et al. Adjuvant Effect of Bacterial Outer Membrane Vesicles With Penta-Acylated Lipopolysaccharide on Antigen-Specific T Cell Priming. *Vaccine* (2011) 29 (46):8293–301. doi: 10.1016/j.vaccine.2011.08.102
82. Hase S, Rietschel ET. Isolation and Analysis of the Lipid A Backbone. *Eur J Biochem* (1976) 63(1):101–7. doi: 10.1111/j.1432-1033.1976.tb10212.x
83. Ribi E, Parker R, Strain SM, Mizuno Y, Nowotny A, Von Eschen KB, et al. Peptides as Requirement for Immunotherapy of the Guinea-Pig Line-10 Tumor With Endotoxins. *Cancer Immunol Immunother* (1979) 7(1):43–58. doi: 10.1007/BF00205409
84. Wang Y-Q, Bazin-Lee H, Evans JT, Casella CR, Mitchell TC. MPL Adjuvant Contains Competitive Antagonists of Human TLR4. *Front Immunol* (2020) 11:2716. doi: 10.3389/fimmu.2020.577823
85. Cullen TW, Giles DK, Wolf LN, Ecobichon C, Boneca IG, Trent MS. *Helicobacter Pylori* Versus the Host: Remodeling of the Bacterial Outer Membrane Is Required for Survival in the Gastric Mucosa. *PloS Pathog* (2011) 7(12):e1002454. doi: 10.1371/journal.ppat.1002454
86. Tran AX, Karbarz MJ, Wang X, Raetz CRH, McGrath SC, Cotter RJ, et al. Periplasmic Cleavage and Modification of the 1-Phosphate Group of *Helicobacter Pylori* Lipid A. *J Biol Chem* (2004) 279(53):55780–91. doi: 10.1074/jbc.M406480200
87. Allan ND, Beveridge TJ. Gentamicin Delivery to *Burkholderia cepacia* Group IIIa Strains *via* Membrane Vesicles From *Pseudomonas Aeruginosa* PAO1. *Antimicrob Agents Chemother* (2003) 477(9):2962–5. doi: 10.1128/AAC.47.9.2962-2965.2003
88. Kotnik T, Frey W, Sack M, Haberl Meglič S, Peterka M, Miklavčič D. Electroporation-Based Applications in Biotechnology. *Trends Biotechnol* (2015) 33(8):480–8. doi: 10.1016/j.tibtech.2015.06.002
89. Fuhrmann G, Serio A, Mazo M, Nair R, Stevens MM. Active Loading Into Extracellular Vesicles Significantly Improves the Cellular Uptake and Photodynamic Effect of Porphyrins. *J Controll Release* (2015) 205:35–44. doi: 10.1016/j.jconrel.2014.11.029
90. Lamichhane TN, Raiker RS, Jay SM. Exogenous DNA Loading Into Extracellular Vesicles via Electroporation Is Size-Dependent and Enables Limited Gene Delivery. *Mol Pharm* (2015) 12(10):3650–7. doi: 10.1021/acs.molpharmaceut.5b00364
91. Alvarez-Erviti L, Seow Y, Yin H, Betts C, Lakhal S, Wood MJA. Delivery of siRNA to the Mouse Brain by Systemic Injection of Targeted Exosomes. *Nat Biotechnol* (2011) 29(4):341–5. doi: 10.1038/nbt.1807
92. Wahlgren J, Karlson TDL, Brisslert M, Vaziri Sani F, Telemo E, Sunnerhagen P, et al. Plasma Exosomes Can Deliver Exogenous Short Interfering RNA to Monocytes and Lymphocytes. *Nucleic Acids Res* (2012) 40(17):e130–0. doi: 10.1093/nar/gks463
93. Tian Y, Li S, Song J, Ji T, Zhu M, Anderson GJ, et al. A Doxorubicin Delivery Platform Using Engineered Natural Membrane Vesicle Exosomes for Targeted Tumor Therapy. *Biomaterials* (2014) 35(7):2383–90. doi: 10.1016/j.biomaterials.2013.11.083
94. Gujrati V, Kim S, Kim S-H, Min JJ, Choy HE, Kim SC, et al. Bioengineered Bacterial Outer Membrane Vesicles as Cell-Specific Drug-Delivery Vehicles for Cancer Therapy. *ACS Nano* (2014) 8(2):1525–37. doi: 10.1021/nn405724x
95. Ayed Z, Cuvillier L, Dobhal G, Goreham RV. Electroporation of Outer Membrane Vesicles Derived From *Pseudomonas aeruginosa* With Gold Nanoparticles. *SN Appl Sci* (2019) 1(12):1600. doi: 10.1007/s42452-019-1646-2
96. Kim MS, Haney MJ, Zhao Y, Mahajan V, Deygen I, Klyachko NL, et al. Development of Exosome-Encapsulated Paclitaxel to Overcome MDR in Cancer Cells. *Nanomedicine* (2016) 12(3):655–64. doi: 10.1016/j.nano.2015.10.012
97. Lamichhane TN, Jeyaram A, Patel DB, Parajuli B, Livingston NK, Arumugasaamy N, et al. Oncogene Knockdown via Active Loading of Small RNAs Into Extracellular Vesicles by Sonication. *Cell Mol Bioeng* (2016) 9(3):315–24. doi: 10.1007/s12195-016-0457-4
98. Wang J, Chen D, Ho EA. Challenges in the Development and Establishment of Exosome-Based Drug Delivery Systems. *J Controll Release* (2021) 329:894–906. doi: 10.1016/j.jconrel.2020.10.020
99. Wu S, Huang Y, Yan J, Li Y, Wang J, Yang YY, et al. Bacterial Outer Membrane-Coated Mesoporous Silica Nanoparticles for Targeted Delivery of Antibiotic Rifampicin Against Gram-Negative Bacterial Infection In Vivo. *Adv Funct Mater* (2021) 31:2103442. doi: 10.1002/adfm.202103442
100. Kim J-Y, Doody AM, Chen DJ, Cremona GH, Shuler ML, Putnam D, et al. Engineered Bacterial Outer Membrane Vesicles With Enhanced Functionality. *J Mol Biol* (2008) 380(1):51–66. doi: 10.1016/j.jmb.2008.03.076
101. Daleke-Schermerhorn Maria H, Felix T, Soprova Z, ten Hagen-Jongman Corinne M, Vikström D, Majlessi L, et al. Decoration of Outer Membrane Vesicles With Multiple Antigens by Using an Autotransporter Approach. *Appl Environ Microbiol* (2014) 80(18):5854–65. doi: 10.1128/AEM.01941-14
102. Chen Q, Rozovsky S, Chen W. Engineering Multi-Functional Bacterial Outer Membrane Vesicles as Modular Nanodevices for Biosensing and Bioimaging. *Chem Commun* (2017) 53:7569–72. doi: 10.1039/C7CC04246A
103. van den Berg van Saparoea HB, Houben D, de Jonge Marien I, Jong Wouter SP, Luirink J, Drake Harold L. Display of Recombinant Proteins on Bacterial Outer Membrane Vesicles by Using Protein Ligation. *Appl Environ Microbiol* (2018) 84(8):e02567–02517. doi: 10.1128/AEM.02567-17
104. van den Berg van Saparoea HB, Houben D, Kuijl C, Luirink J, Jong WSP. Combining Protein Ligation Systems to Expand the Functionality of Semi-Synthetic Outer Membrane Vesicle Nanoparticles. *Front Microbiol* (2020) 11:890. doi: 10.3389/fmicb.2020.00890
105. Zakeri B, Fierer JO, Celik E, Chittock EC, Schwarz-Linek U, Moy VT, et al. Peptide Tag Forming a Rapid Covalent Bond to a Protein, Through Engineering a Bacterial Adhesin. *Proc Natl Acad Sci* (2012) 109(12): E690–7. doi: 10.1073/pnas.1115485109
106. Veggiani G, Nakamura T, Brenner MD, Gayet RV, Yan J, Robinson CV, et al. Programmable Polyproteams Built Using Twin Peptide Superglues. *Proc Natl Acad Sci* (2016) 113(5):1202–7. doi: 10.1073/pnas.1519214113
107. Tokuda H, Matsuyama S. Sorting of Lipoproteins to the Outer Membrane in *E. coli*. *Biochim Biophys Acta* (2004) 1693(1):5–13. doi: 10.1016/j.bbamcr.2004.02.005
108. Shimazu M, Nguyen A, Mulchandani A, Chen W. Cell Surface Display of Organophosphorus Hydrolase in *Pseudomonas Putida* Using an Ice-Nucleation Protein Anchor. *Biotechnol Prog* (2003) 19(5):1612–4. doi: 10.1021/bp0340640
109. Turner L, Bitto NJ, Steer DL, Lo C, D'Costa K, Ramm G, et al. *Helicobacter pylori* Outer Membrane Vesicle Size Determines Their Mechanisms of Host Cell Entry and Protein Content. *Front Immunol* (2018) 9:1466 doi: 10.3389/fimmu.2018.01466

110. Zavan L, Bitto NJ, Johnston EL, Greening DW, Kaparakis-Liaskos M. *Helicobacter Pylori* Growth Stage Determines the Size, Protein Composition, and Preferential Cargo Packaging of Outer Membrane Vesicles. *Proteomics* (2019) 19(1-2):1800209. doi: 10.1002/pmic.201970004
111. Maldonado R, Wei R, Kachlany SC, Kazi M, Balashova NV. Cytotoxic Effects of *Kingella Kingae* Outer Membrane Vesicles on Human Cells. *Microb Pathog* (2011) 51(1-2):22–30. doi: 10.1016/j.micpath.2011.03.005
112. Royo F, Théry C, Falcón-Pérez JM, Nieuwland R, Witwer KW. Methods for Separation and Characterization of Extracellular Vesicles: Results of a Worldwide Survey Performed by the ISEV Rigor and Standardization Subcommittee. *Cells* (2020) 9(9):1955. doi: 10.3390/cells9091955
113. Nieuwland R, Falcón-Pérez JM, Théry C, Witwer KW. Rigor and Standardization of Extracellular Vesicle Research: Paving the Road Towards Robustness. *J Extracell Vesicles* (2020) 10(2):e12037–7. doi: 10.1002/jev2.12037
114. Witwer KW, Buzás EI, Bemis LT, Bora A, Lässer C, Lötvall J, et al. Standardization of Sample Collection, Isolation and Analysis Methods in Extracellular Vesicle Research. *J Extracell Vesicles* (2013) 2(1):20360. doi: 10.3402/jev.v2i0.20360

Conflict of Interest: The authors declare that the research was conducted in the absence of any commercial or financial relationships that could be construed as a potential conflict of interest.

Publisher's Note: All claims expressed in this article are solely those of the authors and do not necessarily represent those of their affiliated organizations, or those of the publisher, the editors and the reviewers. Any product that may be evaluated in this article, or claim that may be made by its manufacturer, is not guaranteed or endorsed by the publisher.

frontiers in Microbiology

ORIGINAL RESEARCH
published: 08 October 2021
doi: 10.3389/fmicb.2021.713669

Phage-Mediated Explosive Cell Lysis Induces the Formation of a Different Type of O-IMV in *Shewanella vesiculosa* M7^T

*Nicolás Baeza[1], Lidia Delgado[2], Jaume Comas[3] and Elena Mercade[1]**

[1] *Secció de Microbiologia, Departament de Biologia, Sanitat i Medi Ambient, Universitat de Barcelona, Barcelona, Spain,*
[2] *Crio-Microscòpia Electrònica, Centres Científics i Tecnològics, Universitat de Barcelona (CCiTUB), Barcelona, Spain,*
[3] *Citometria, Centres Científics i Tecnològics, Universitat de Barcelona (CCiTUB), Barcelona, Spain*

OPEN ACCESS

Edited by:
Alejandro J. Yañez, Austral University of Chile, Chile

Reviewed by:
Jun Kawamoto, Kyoto University, Japan
Araceli Contreras-Rodriguez, Instituto Politécnico Nacional (IPN), Mexico

***Correspondence:**
Elena Mercade
mmercade@ub.edu

Specialty section:
This article was submitted to Microbial Physiology and Metabolism, a section of the journal Frontiers in Microbiology

Received: *23 May 2021*
Accepted: *14 September 2021*
Published: *08 October 2021*

Citation:
Baeza N, Delgado L, Comas J and Mercade E (2021) Phage-Mediated Explosive Cell Lysis Induces the Formation of a Different Type of O-IMV in Shewanella vesiculosa M7^T. Front. Microbiol. 12:713669. doi: 10.3389/fmicb.2021.713669

Shewanella vesiculosa M7^T is a cold-adapted Antarctic bacterium that has a great capacity to secrete membrane vesicles (MVs), making it a potentially excellent model for studying the vesiculation process. *S. vesiculosa* M7^T undergoes a blebbing mechanism to produce different types of MVs, including outer membrane vesicles and outer-inner membrane vesicles (O-IMVs). More recently, other mechanisms have been considered that could lead to the formation of O-IMVs derived from prophage-mediated explosive cell lysis in other bacteria, but it is not clear if they are of the same type. The bacterial growth phase could also have a great impact on the type of MVs, although there are few studies on the subject. In this study, we used high-resolution flow cytometry, transmission electron microscopy, and cryo-electron microscopy (Cryo-EM) analysis to determine the amount and types of MVs *S. vesiculosa* M7^T secreted during different growth phases. We show that MV secretion increases during the transition from the late exponential to the stationary phase. Moreover, prophage-mediated explosive cell lysis is activated in *S. vesiculosa* M7^T, increasing the heterogeneity of both single- and double-layer MVs. The sequenced DNA fragments from the MVs covered the entire genome, confirming this explosive cell lysis mechanism. A different structure and biogenesis mechanisms for the explosive cell lysis-derived double-layered MVs was observed, and we propose to name them explosive O-IMVs, distinguishing them from the blebbing O-IMVs; their separation is a first step to elucidate their different functions. In our study, we used for the first time sorting by flow cytometry and Cryo-EM analyses to isolate bacterial MVs based on their nucleic acid content. Further improvements and implementation of bacterial MV separation techniques is essential to develop more in-depth knowledge of MVs.

Keywords: membrane vesicles, gram-negative bacteria, explosive cell lysis, OMV, O-IMV, DNA, flow cytometry, electron microscopy

INTRODUCTION

Membrane vesicles (MVs) are produced by most bacteria and are involved in essential biological functions such as pathogenesis, inter- and intraspecies communication, biofilm formation, nutrient acquisition, and DNA transfer. In addition, they have great potential in immunology and biotechnology applications. For these reasons in recent years, numerous studies have investigated and reviewed all the aspects of bacterial MVs, including their composition, functions, biogenesis mechanisms, immunomodulatory capacity, and potential applications (Mashburn-Warren and Whiteley, 2006; Schooling and Beveridge, 2006; Lee et al., 2008; Kaparakis-Liaskos and Ferrero, 2015; Schwechheimer and Kuehn, 2015; Jan, 2017; Mozaheb and Mingeot-Leclercq, 2020).

Studies on membrane vesicles (MVs) in Gram-negative bacteria established an initial model that demonstrated how MVs formed from outer membrane protrusions solely contained the outer membrane and periplasmic material (Kadurugamuwa and Beveridge, 1996; Beveridge, 1999). These initially discovered MVs were named outer membrane vesicles (OMVs). However, increasing studies have highlighted how, depending on the mechanism of formation, Gram-negative bacteria give rise to different types of MVs having different structures and compositions. The different types of MVs and their origins have recently been discussed in detail (Gill et al., 2019; Toyofuku et al., 2019; Avila-Calderón et al., 2021).

Shewanella vesiculosa M7^T, is a cold-adapted Gram-negative bacteria isolated from marine sediments of Antarctica (Bozal et al., 2009). Specifically, *S. vesiculosa* M7^T was named on the basis of its considerable capacity for producing MVs, which makes it a potentially excellent model for studying the vesiculation process (Frias et al., 2010). In previous studies, we demonstrated that *S. vesiculosa* M7^T produces a type of MV called outer-inner membrane vesicles (O-IMVs) containing two lipid bilayers (Pérez-Cruz et al., 2013). The O-IMVs are formed by the joint protrusion of the outer membrane and the plasma membrane with cytoplasmic content entrapped within the vesicles. These new types of vesicles are also found to be secreted by pathogenic Gram-negative bacteria (Pérez-Cruz et al., 2015). Although the roles played by stress factors such as antibiotics and environmental growth conditions in promoting vesiculation in many bacteria are already known (Mozaheb and Mingeot-Leclercq, 2020), no stress factors have been identified that help to produce blebbing O-IMVs in *S. vesiculosa* M7^T.

More recently, other mechanisms have been considered that could lead to the formation of O-IMVs. Turnbull et al. (2016) demonstrated how explosive cell lysis through cryptic prophage endolysin activity can give rise to MV formation in *Pseudomonas aeruginosa* biofilms. They showed how the endolysin causes cell explosion leading to the fragmentation of the cell membranes that subsequent re-annealing, trapping different cytoplasmic components of the lysed cell. It is interesting to note that this explosive mechanism can give rise to both OMVs and O-IMVs. This model also holds in *Stenotrophomonas maltophilia* treated with ciprofloxacin, which leads to the induction of prophage and explosive cell lysis with the production of a pool of MVs including O-IMVs. These vesicles characteristically contain both outer and inner membranes and are enriched with cytosolic proteins (Devos et al., 2017). Recently, Mandal et al. (2021) demonstrated that bacteriophage infection of *Escherichia coli* generates different types of MVs through explosive cell lysis and membrane blebbing. The activation of prophages and their role in the maintenance of bacterial populations has been extensively studied; however, their importance as a mechanism of biogenesis of MVs is only now being considered (Catalao et al., 2012).

Prophage activation can be due to different stressors such as anoxia, UV radiation, iron depletion and antibiotic treatment among others (Kageyama et al., 1979; Bamford et al., 1987; Beaber et al., 2004; Binnenkade et al., 2014; Fang et al., 2017) and can trigger several morphological and physiological changes in bacteria that are commonly associated to apoptosis-like death (ALD) processes (Peeters and de Jonge, 2018; Mozaheb and Mingeot-Leclercq, 2020). Although prokaryotic ALD is currently a developing field, the morphological changes that have been observed are cell size and shape variation, chromatin condensation, DNA fragmentation and increased MV production (Andryukov et al., 2018). The physiological changes that have been observed are caspases activation, reactive oxygen species formation or metabolites levels alteration (NADH/NAD$^+$, ADP/ATP or pyruvate, among others; Raju et al., 2006; Wadhawan et al., 2010). These stress responses can lead to the release of MVs enriched with stressed response proteins (Devos et al., 2017) or with a significantly higher amount of DNA (Andreoni et al., 2018), hence, prophage activation may play a key role in MV cargo and the functions that they may be involved.

The processes of blebbing or explosive lysis leading to O-IMV generation explain the different cytoplasmic components, such as nucleic acids, proteins, and ATP, found in MVs from various bacteria (Pérez-Cruz et al., 2013; Berleman et al., 2014; Kulkarni and Jagannadham, 2014; Turnbull et al., 2016; Cooke et al., 2019). Numerous studies have described the presence of DNA in MVs, but the mechanism by which it is packaged in the MVs remains largely unexplored (Dorward et al., 1989; Lotvall and Valadi, 2007; Rumbo et al., 2011; Biller et al., 2014, 2017; Bitto et al., 2017). The blebbing model for O-IMV could explain how plasmid and chromosomal DNA are packaged into MVs without cell death, specifically considering the existence of numerous mobile genetic elements capable of moving between plasmids or from a plasmid to the chromosome or vice versa (Partridge et al., 2018). On the contrary, the presence of heterogeneously sized DNA fragments in MVs from different regions of the chromosome points to O-IMV formation by mechanisms that cause cell death. These O-IMV formation mechanisms do not have to be mutually exclusive, although they do give rise to different types of O-IMVs.

Other relevant aspects to be considered are the growth stages in which O-IMVs are formed, and the proportion released to the media. It is unknown if the O-IMVs are produced during all stages of growth or if their formation is induced by stage-specific factors (Kuehn and Kesty, 2005; McBroom and Kuehn, 2007; MacDonald and Kuehn, 2013; Hagemann et al., 2014; Devos et al., 2017). Until now, O-IMV proportion

estimations have mainly been based on Transmission Electron Microscopy (TEM) and Cryo-Electron Microscopy (Cryo-EM) observations. Using these methods, widely varying proportions of O-IMVs have been reported in different bacteria, such as 0.1% in *S. vesiculosa* M7^T, 0.5% for *Pseudomonas* PAO1, 0.23% for *A. baumannii* AB41, or 49% in strains of *Pseudoalteromonas marina* (Pérez-Cruz et al., 2013, 2015; Hagemann et al., 2014; Devos et al., 2017).

In this study, we used flow cytometry with FM4-64 and SYBR™ Gold labeling to show that the various amounts and types of MVs produced by *S. vesiculosa* M7^T change during its growth. TEM after high-pressure freezing and freeze substitution (HPF-FS) of *S. vesiculosa* M7^T cultures revealed changes in the types of MVs during the different growth phases. The high resolution provided by TEM analysis confirmed the activation of a prophage-mediated explosive cell lysis leading to the formation of a different type of O-IMVs, and the production of MVs through re-annealing of ruptured membranes. We also sequenced MV DNA to characterize and map these nucleic acids. The heterogeneity of MVs produced point to the need to separate them for subsequent studies, for this reason, we specifically aimed to separate nucleic acid-containing MVs using flow cytometry-based sorting and Cryo-EM analysis.

MATERIALS AND METHODS

Bacteria Used and the Growth Conditions

All studies were performed with *S. vesiculosa* M7^T (Bozal et al., 2009). For MV isolation and TEM observation, *S. vesiculosa* M7^T was grown in trypticase soy broth (TSB, Oxoid) using 2 L baffled flasks filled with 500 ml medium. Cultures were always inoculated at 1% with a 12 h-incubated pre-inoculum. The flasks were shaken at 180 rpm in an orbital shaker (Innova® 44, New Brunswick Scientific) and incubated at 15°C. For MV analysis directly from supernatants and TEM, cytometry and apoptosis cell analysis, *S. vesiculosa* M7^T was grown in 500 ml baffled flasks filled with 150 ml of TSB (Oxoid) using the same culture conditions described above. When necessary, the growth was monitored by counting colony-forming units (CFU/ml) using the serial dilution method of plating on Trypticase soy agar plates.

MV Isolation

Shewanella vesiculosa M7^T naturally secrete MVs into media. MVs were collected from the 500 ml TSB cultures at different times-points (12, 18, 24, 48, 72 and 96 h) using an adaption of the method described by McBroom et al. (2006). Cells were pelleted by centrifugation at 10,000 × *g* for 30 min at 4°C, and the supernatant was filtered through 0.45-μm pore-size filters to remove the remaining bacterial cells. MVs were obtained by centrifugation at 44,000 × *g* for 1 h at 4°C in an Avanti® J-20 XP centrifuge (Beckman Coulter, Inc). The pelleted MVs were then resuspended in 50 ml of Dulbecco's phosphate-buffered saline (DPBS, Gibco, Life Technologies) and filtered through 0.22-μm pore-size Ultrafree spin filters (Millipore). Finally, the MVs were pelleted again at 44,000 × *g* for 1 h at 4°C and resuspended in a minimal volume of DPBS.

High-Resolution Flow Cytometry for MV Analysis

Flow cytometry analysis of MV was performed as previously described by Wieser et al. (2014) with certain modifications. *S. vesiculosa* M7^T cultures were centrifuged at 10,000 g for 30 min, and 5 ml of the supernatants were filtered through 0.22 μm syringe filters (Puradisc™, Millipore) to analyze and quantify MVs in the supernatants. The supernatants were diluted in sterile DPBS to obtain the desired frequency of events per second (ev/s) between 1,000 and 10,000. The MVs were stained with the lipophilic fluorochrome FM4-64 (Invitrogen, T13320), resuspended in filtered-sterile DPBS at a final concentration of 0.5 μg/ml, and incubated for 5 min in the dark at room temperature (20–22°C). Sterile DPBS and sterile DPBS with FM4-64 were used as background controls. After incubation, controls and samples were analyzed with the BD FACS Aria™ Fusion II cytometer (BD Biosciences). The analyses were carried out for 30 s at a flow rate of 2 with a trigger on FM4-64 fluorescence.

FM4-64 and SYBR™ Gold (Invitrogen, S11494) labeling were carried out to detect MVs with internalized nucleic acids. The SYBR™ Gold labeling was done using a 1/10,000 dilution of the stock solution, and the samples were incubated for 15 min at room temperature in the dark. Samples treated with sterile DPBS, sterile DPBS with FM4-64, and sterile DPBS with FM4-64 and SYBR™ Gold were used as controls, and a fluorescence threshold was established.

A relation between the number of cytometer events and the number of MVs was established using FluoSpheres™ Carboxylate-Modified Microspheres (Life Technologies, F8803), with a size of 100 nm and a concentration of 3.63×10^{13} microspheres/ml, to quantify MVs by flow cytometry. The FluoSpheres™ were diluted in filtered-sterile DPBS to obtain frequencies of events/s between 1,000 and 10,000 to quantify the isolated MVs. The FluoSpheres™ were diluted in filtered-sterile TSB, in the same way to quantify MVs from bacterial culture supernatants.

Sorting of MVs by High-Resolution Cytometry

MVs were isolated and stained with both SYBR™ Gold and FM4-64 to separate MVs from those only stained with FM4-64 to identify the ones with internalized nucleic acids. A 70-μm nozzle was used on the BD FACS Aria™ Fusion II cytometer (BD Bioscience) for separation. First, the controls (sterile and filtered DPBS, sterile and filtered DPBS with FM4-64, and sterile and filtered DPBS with FM4-64 and SYBR™ Gold) and samples to be separated were analyzed to verify the percentage of events detected to have both fluorochrome labels and to identify the range of events/s. Then, two sterile 15 ml collecting tubes (TPP®, Merk) containing 100 μl of sterile water were used to collect each separated sample. PBS FacsFlow™ was used as the dilution buffer used during the sorting process

(Fischer Scientific, United Kingdom). Once the sorting started, the injection flow was monitored and adjusted to keep the separation efficiency above 85%. The collected MVs were transferred to 8 ml polycarbonate centrifuge tubes (Beckman Coulter) and centrifuged in the OPTIMA™ L-90K ultracentrifuge (Beckman Coulter) with Ti/70 rotor at 100.000xg for 90 min at 4°C. Supernatants were discarded, and pellets were resuspended in 20 µl of sterile water and kept at 4°C until fixation for Cryo-EM.

TEM Observation After HPF-FS

TEM observation of *S. vesiculosa* $M7^T$ was performed as described previously (Pérez-Cruz et al., 2015) with some modifications. Briefly, liquid cultures at different incubations times were centrifuged at 40,000 × *g* for 1 h at 4°C and cryo-immobilized using a Leica HPM100 high-pressure freezer (Leica Microsystems, Vienna, Austria) to observe the cells and MVs simultaneously. The cryo-immobilized samples were then freeze-substituted in pure acetone containing 2% (w/v) osmium tetraoxide (EMS, Hatfield, United States) and 0.1% (w/v) uranyl acetate (EMS, Hatfield, United States) at −90°C for 72 h in an EM AFS2 (Leica Microsystems, Vienna, Austria). Then, they were warmed up to 4°C at a 5°C/h slope, kept at 4°C for 2 h, and then kept at room temperature for 2 h in darkness. The samples were washed in acetone at room temperature, infiltrated in increasing concentrations of Epon-812 resin (Epon 812, Ted Pella, Inc., United States) in acetone till pure Epon-812 was obtained. Finally, the samples were embedded and polymerized in Epon-812 at 60°C for 48 h. Ultrathin sections (50–60 nm) were obtained with a UC6 ultramicrotome (Leica Microsystems, Vienna, Austria) and placed on Formvar coated copper grids. The sections were stained with 2% (w/v) uranyl acetate for 30 min and lead citrate for 5 min. The samples were examined in a Tecnai Spirit microscope (FEI, Eindhoven, Netherlands) equipped with a tungsten cathode. Images were captured at 120 kV with a 1,376 × 1,024-pixel CCD camera (FEI, Eindhoven, Netherlands).

Cryo-EM Observation of Isolated MVs

The MVs were cryoimobilized using the Plunge Freezing technique (Delgado et al., 2019) for Cryo-EM visualization. The cryo-immobilization was performed in the Vitrobot Mark III (FEI, Eindhoven, Netherlands). One 3 µl drop of the suspension was applied on the carbon surface of a glow-discharged Lacey Carbon 300 mesh copper grid (Ted Pella, United States) and held for 1–4 min at 100% humidity. The excess liquid was automatically blotted with filter paper, and the sample was immediately plunge-frozen in liquefied ethane. The vitrified sample was then transferred to a Tecnai F20 EM (FEI, Eindhoven, Netherlands) using a cryo-holder (Gatan, Pleasanton, United States). The visualization of samples was carried out at 200 kV, at temperatures between −180 and −170°C and at low-dose image conditions. The images were acquired with a 4,096 × 4,096-pixel CCD Eagle camera (FEI, Eindhoven, Netherlands). The quantification and subsequent analyses of the different MVs were carried out with the ImageJ program (Schindelin et al., 2012).

Analysis of Phosphatidylserine Exposure

The Annexin V-FITC Apoptosis Detection Kit (Sigma) was used to identify the amount of exposed phosphatidylserine of *S. vesiculosa* $M7^T$ cells at different times of growth to investigate apoptosis. Two 1 ml aliquots of each sample were centrifuged at 10,000 g for 10 min at 20°C and washed twice in DPBS. Cells were resuspended and diluted to 10^6 cells/ml in 1 × Binding Buffer (BB). The Annexin V-FITC was added to each sample at a final concentration of 0.5 µg/ml. Propidium iodide (PI) was also added to the samples at a final concentration of 2 µg/ml, and they were incubated for 10 min at room temperature in the dark. Stained cells were analyzed with the BD FACS Aria™ Fusion II cytometer (BD Bioscience). Several negative controls were used to optimize the analyses: 1 × BB, 1 × BB with both the fluorochromes, and 1 × BB with *S. vesiculosa* $M7^T$ cells without fluorochromes. This experiment was carried out with each condition in duplicates in four independent experiments.

DNA Fragmentation Assay

TheAPO-BrdU™ TUNEL Assay (Invitrogen) was performed on the bacteria to analyze their cellular DNA damage at different times of growth. Two 1 ml aliquots of each sample were diluted to 10^7 cells/ml in DPBS in a final volume of 500 µl. The bacterial suspension was added to 4.5 ml of 2% (w/v) paraformaldehyde and incubated for 15 min on ice. The cells were then centrifuged at 10,000 × *g*, at 20°C and the supernatant was discarded. The pellet was resuspended in DPBS and washed twice. The cells resuspended in 100 µl of DPBS were added to 900 µl of 70% (v/v) ethanol and kept at −20°C for 12 h. The alcohol suspension was centrifuged at 10,000 *g* for 5 min to remove the alcohol, and the pellet was resuspended in 50 µl of the labeling solution. The cells were incubated at 37°C in the dark for 4 h and shaken every 15 min. Washing buffer (450 µl) was then added and centrifuged at 10,000 g for 5 min. The pellet was resuspended in 100 µl of the kit antibody solution. The cells were incubated at room temperature in the dark for 30 min. A total of 500 µl of the staining solution containing RNase A and PI was added to the resuspended cells and incubated at room temperature in the dark for 30 min. Cell analysis was performed on the BD FACS Aria™ Fusion II cytometer (BD Bioscience). This experiment was carried out with each condition in duplicates in two independent experiments.

Determination of Intracellular NAD(H) Levels

A colorimetric assay kit for NAD+/NADH Quantification (Sigma-Aldrich) was used to determine the intracellular levels of NADH and NAD+. Two 1 ml aliquots were collected from each bacterial culture and were centrifuged at 10,000 *g* for 10 min and washed twice in DPBS. Extraction of the cytoplasmic material from the *S. vesiculosa* $M7^T$ cells was carried out using the perchloric acid method (Bagnara and Finch, 1972) without

further purification of the NAD+ and NADH molecules. Detection of total NAD (H) and only NADH was carried out according to the manufacturer's instructions. This experiment was carried out with each condition in duplicates in three independent experiments.

Determination of Intracellular ATP Levels

Two 1 ml aliquots of *S. vesiculosa* M7^T liquid cultures were centrifuged at 10,000 *g* for 10 min and washed twice in DPBS. The cytoplasmic material of the cells was extracted using the perchloric acid method (Bagnara and Finch, 1972). Then the intracellular ATP levels were measured using the BacTiter-Glo™ Microbial Cell Viability Assay Reagent kit (Promega). The experiment was carried out with each condition in duplicates in three independent experiments.

Extraction and Sequencing of DNA Coming From the MVs

Isolated MVs were pre-treated with DNase I (2 U/µl, 1 h, 40°C; Thermo Scientific), diluted 1/100 in sterile DPBS, and re-pelleted (44,000 × *g* for 1 h at 4°C) to remove the DNAse I. The amount of MVs was quantified by the Purpald method (Lee and Tsai, 1999). The DNA from the MVs was extracted with the PureLink™ Microbiome DNA Purification kit (Invitrogen). The extraction was performed from 50 µl of MVs resuspended in DPBS with an LPS concentration of 0.5 µg/µl. The extracted DNA was eluted with 50 µl of the elution buffer. Quantification of the DNA extracted from the MVs from *S. vesiculosa* M7^T was carried out with the Quant-iT™ PicoGreen® dsDNA kit (ThermoFisher Scientific). A phage λ DNA standard curve was established with 1:10 serial dilutions from 0.05 ng/ml to 50 ng/ml. TE buffer (10 mm TRIS-HCl, 1 mm EDTA, pH 7.5) was used as the negative control, and a genomic DNA sample of *S. vesiculosa* M7^T of known concentration was used as a positive control. Fluorescence measurement was carried out in the Modulus microplate reader (Turner Biosystems) with an excitation of 485/20 nm and an emission of 528/20 nm. Three independent DNA extraction experiments were performed, and DNA was measured in duplicate for each sample.

Libraries preparation from the DNA samples extracted from the MVs of *S. vesiculosa* M7^T was done using the NEBNext® Ultra DNA Library Prep kit (Illumina). For each sample, the DNA was end-repaired, adenines were added to the 3' end, and the NEB adapters were ligated. The DNA bound to the adapter was cleaned in two steps to select both small and large fragments. A first incubation was carried out with 0.75 × AMPure Beads (Beckman Coulter) to obtain the fraction with the large fragments. Then, the supernatant was purified with 1.1 × AMPure Beads (Beckman Coulter) to obtain the fraction with the small fragments. Both fractions were separated into two aliquots: one (10%) to determine the number of amplification cycles up to the plateau phase using real-time PCR, and the other (remaining 90%) to carry out the PCR with the amplification cycles already optimized. This PCR was done using the NEBNext® Multiplex Oligos for Illumina in both aliquots. Final libraries were analyzed using Agilent Bioanalyzers (Agilent, Germany) to estimate the quantity and size distribution of the quantified PCR products using the KAPA Library Quantification kit (KapaBiosystems) before amplification with Illumina's cBot. This method allowed library preparation from low amounts of DNA and separation of the two fractions according to the size of the DNA fragments. Once the library was prepared, it was sequenced using the HiSeq 2500 System (Illumina), generating paired-end reads of 125 bp in length. The entire sequencing process was monitored using the Sequencer Software HiSeq Control Software 2.2.58.

S. vesiculosa M7^T Genome Sequencing

DNA from *S. vesiculosa* M7^T cells was prepared for subsequent sequencing using the Illumina DNA prep kit (Illumina). Once the library was prepared, it was sequenced using the HiSeq 2500 System (Illumina), generating 125 bp long paired end reads with each fragment generated in the library being sequenced from both ends. The entire sequencing process was monitored using the Sequencer Software HiSeq Control Software 2.2.58. The genome of the strain was also sequenced using the Nanopore system. The library preparation kit used for the DNA extracted from *S. vesiculosa* M7^T cells was SQK-LSK109 (Nanopore Systems) to obtain the assembled and recircularized *S. vesiculosa* M7^T genome by using the Flongle FLO-FLG001 flow cell (Nanopore Systems). The monitoring and capturing of the sequencing results were performed using the main MinKnow software (v3.6.0) and the Bream software (v4.3.12). First, base-calling was performed to obtain the reads resulting from sequencing using the Guppy software (v3.2.8). Minimap2 was used (Li, 2016) to align the nucleotide sequences and correct possible errors. For the assembly of the *S. vesiculosa* M7^T genome, Miniasm software was used (Li, 2016). Finally, Racon (v1.4.13, Vaser et al., 2017) was used to correct raw contigs generated polish the final genome after assembly. Additionally, to further correct assembly errors, the reads from the previous Illumina sequencing studies were mapped to the new assembly using bowtie2 (v 2.3.0, Langmead et al., 2019) and analyzed using Pilon (Walker et al., 2014) to correct the assembly errors. Once the genome was assembled, the genes were predicted using the Quast tool (v5.0.2, Gurevich et al., 2013) and subsequently identified using the Glimmer tool (v3.02, Delcher et al., 2007) that distinguishes coding from non-coding regions in bacterial genomes. The genes identified to code for proteins were translated into amino acid sequence by transeq (v24) and aligned with the Uniref90 database by Diamond (v0.9.24, Buchfink et al., 2015). The closest match to the database was kept as the most likely protein description for each estimated gene. PHASTER tool (PHAge Search Tool Enhancer Release, Arndt et al., 2016) was used to identify potential phage presence in *S. vesiculosa* M7^T genome. The assembled genome was input in the FASTA format.

In silico Analysis of the DNA From MVs of *S. vesiculosa* M7^T

After sequencing the DNA fragments from *S. vesiculosa* M7^T MVs, sequences of the adapters were removed using the

skewer tool (v0.2.2, Jiang et al., 2014), and pairs of overlapping reads were joined using the PEAR tool (v0.9.11, Zhang et al., 2014). Quality control of the resulting sequences was carried out with the FastQC tool (v0.11.8). Before mapping the sequences of the reads from the MVs, an index of the *S. vesiculosa* M7^T genome was constructed with the bowtie2-build tool (v2.3.0, Langmead et al., 2019). Mapping of the MVs DNA fragments with *S. vesiculosa* M7^T genome was carried out using the bowtie2 tool (v2.3.0, Langmead et al., 2019). The above alignment resulted in a sam file for each sample mapped that stores the nucleotide sequence and characteristics of said sequence with a position in a reference genome. The sam files were converted into bam files, containing the same information in binary format using the samtools view tool (v1.11, Danecek et al., 2021). The FASTA file containing the *S. vesiculosa* M7^T genome was transformed into gtf format. The final file was transformed into a bed file by removing certain unnecessary information to reduce the size of the file. The previous bam files were then crossed with the bed file containing the *S. vesiculosa* M7^T genome annotation using the bedtools intersect tool (v2.29.2, Quinlan and Hall, 2010) to determine the genes found in the DNA fragments from MVs. For graphical representations, the bam format of the files of the DNA fragments of the MVs was changed. For that purpose, the bam files were sorted using the samtools sort tool (v1.11, Danecek et al., 2021) and subsequently indexed using the samtools index tool (v1.11, Danecek et al., 2021). Ordered, indexed, and aligned bam files of each sample were stacked using the samtools mpileup tool (v1.11, Danecek et al., 2021) and formatted to the graph coverage extension, to be read by the DNAplotter tool from Artemis (Sanger, United Kingdom; Carver et al., 2012).

Statistics

Statistical analyses of the data were performed using StatGraphics XVII Version 17.2.07 (64-bit; StatGraphics Technologies, Inc., The Plains, Virginia). ANOVA tests were performed to analyze the mean differences between samples. The level of significance was set at $p \leq 0.05$ for all the tests.

RESULTS AND DISCUSSION

It has become evident that the type of bacteria (Gram-positive or Gram-negative) dictates the production of different types of MVs (Nagakubo et al., 2020). However, recent studies have shown that in Gram-negative bacteria, even members of the same species can secrete different types of MVs into the medium (Pérez-Cruz et al., 2013; Hagemann et al., 2014; Devos et al., 2017; Gill et al., 2019; Toyofuku et al., 2019). It is now clear that even careful isolation and purification lead to the recovery of a mixture of different types of MVs. Therefore, it is essential to identify the types of MVs a bacterium produces during its growth and the mechanisms governing MV formation that would influence the results of our subsequent studies.

MV Secretion Depends on the Growth Phase of *S. vesiculosa* M7^T

In this study, we investigated MV secretion during the growth of *S. vesiculosa* M7^T by high-resolution flow cytometry to directly enumerate FM4-64 stained MVs from culture supernatants (Wieser et al., 2014). For this purpose, *S. vesiculosa* M7^T was grown in 500 ml of TSB at 15°C under agitation. At different time points, the number of viable cells and MVs were measured directly from filtered supernatants. Moreover, the number of MVs was normalized to the number of viable cells to measure the vesiculation rate (MV/cell) at each time point. As shown in **Figure 1**, the concentration of MVs increased during growth, but the vesiculation rate did not remain constant over time. During the first hours of incubation (12, 18 h), the exponential growth of the cells and the MV concentration increased with a positive correlation (**Figure 1A**). However, during this time, the MV/cell ratio remained constant, with a value close to 0.05. It is important to note that *S. vesiculosa* M7^T growth halted between 18 and 24 h of incubation, before accelerating again until reaching the stationary phase at approximately 32 h. After 18 h of incubation, there was a significant increase in the ratio of MVs/cell, while the vesiculation rate peaked at 48 h with a stabilized value of 1.59 after that point. The transition from the exponential to the stationary phase, between 24 and 48 h, was accompanied by the export of more MVs to the medium with significant differences in the vesiculation rate (**Figure 1B**), indicating that MV secretion depended on the growth phase.

Consistent with the literature, our results confirm that the concentration of MVs increases exponentially with cell density (Tashiro et al., 2010; Pérez-Cruz et al., 2021). Moreover, we found that the transition from the late exponential to the stationary phase prompted *S. vesiculosa* M7^T to export more MVs to the medium. MV formation depends on multiple factors such as growth phase, nutrient availability or environmental stressors. Transition from exponential to stationary phase is accompanied by changes in protein expression; in this process, misfolded or defective proteins and peptides from protein degradation may accumulate in the periplasmic space increasing the osmotic pressure and, thus, increasing vesiculation. In the same way, peptidoglycan fragments from cell wall turnover can also accumulate in the periplasmic space. MVs formation would release the pressure induced by the accumulation of these macromolecules (McBroom and Kuehn, 2007). In stationary phase, nutrients also begin to lack affecting MVs formation. Vesiculation is also strictly dependant of the outer membrane asymmetry, and this asymmetry is maintained by the VacJ/Yrb ABC system and a phospholipid transferase. The FUR regulator of the former is dependent on iron and in its absence hypervesiculation due to outer membrane asymmetry disruption (Roier et al., 2016). Similarly, sulfur depletion provokes NADPH overproduction, which is necessary for phospholipids production. Thus, the overproduction of phospholipids induces their accumulation in the outer membrane, disrupting its asymmetry and, finally, increasing MVs formation (Gerritzen et al., 2019). Different studies have reported that various stressors (oxidative stress, anoxia, UV radiation, antibiotics) promote prophage

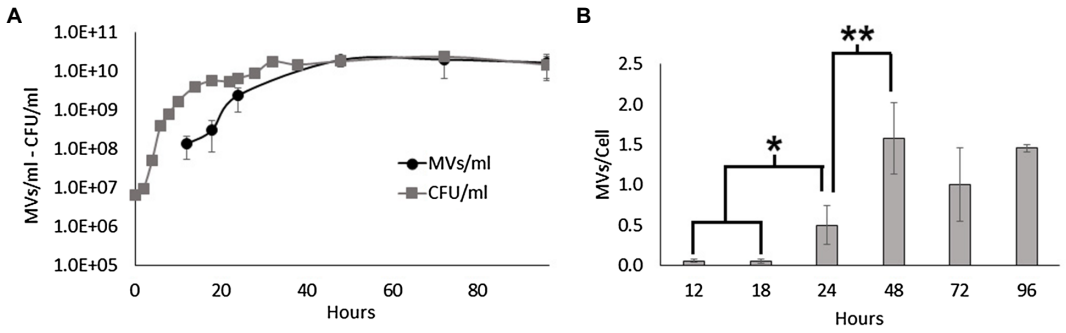

FIGURE 1 | MV production during the growth of *Shewanella vesiculosa* M7^T. **(A)** Growth curve of *S. vesiculosa* M7^T and the MV concentration during growth. Cell concentration was determined by Trypticase soy agar plate counting (CFU/ml). MV concentration was measured by flow cytometry with FM4-64 labeling, and events were extrapolated with the 100 nm FluoSpheres™. **(B)** Graph representing the ratio or number of MVs secreted per cell along the growth curve. $n = 3$, Statistical analysis was done using the ANOVA test, * and ** $p < 0.05$.

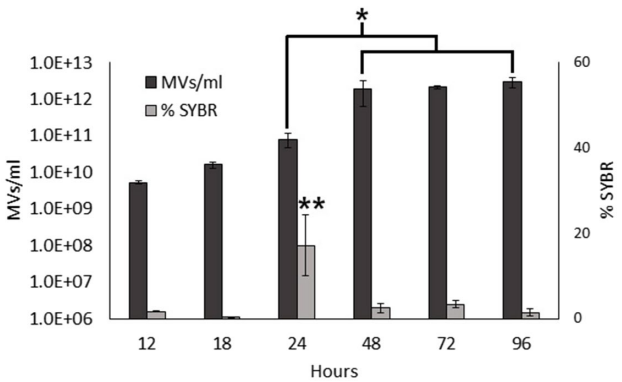

FIGURE 2 | Nucleic acid content in *S. vesiculosa* M7^T MVs. Bar graph representing the total MV concentration (only labeled with FM4-64) and the percentage of nucleic acid-containing MVs (simultaneously labeled with FM4-64 and SYBR™ Gold) during growth. $n = 3$, Statistical analysis was done using ANOVA test, * and ** $p < 0.05$.

activation in prokaryotes which can act as inducers of membrane lysis and, eventually, MVs formation (Kageyama et al., 1979; Bamford et al., 1987; Beaber et al., 2004; Binnenkade et al., 2014; Fang et al., 2017).

Nucleic Acid Content of MVs Varies During the Growth of the Bacteria

Previous studies have shown that MVs from *S. vesiculosa* M7^T contain DNA mainly located inside O-IMVs (Pérez-Cruz et al., 2013). In this study, we aimed to determine if the nucleic acid content of MVs from *S. vesiculosa* M7^T varied during growth. We first isolated MVs at different stages of the growth curve, simultaneously labeled them with FM4-64 and SYBR™ Gold, and analyzed them by flow cytometry. FM4-64 with affinity for lipidic membranes was used to quantify MVs and SYBR™ Gold was used to detect nucleic acids inside them. The analysis of isolated MVs also showed that the concentration of MVs increased exponentially until 48 h of growth and then stabilized up to 96 h. Moreover, it is worth highlighting the marked increase in the concentration of MVs during the transition to the stationary phase between 24 and 48 h (**Figure 2**), as observed before in the analysis in the supernatant. However, the percentage of SYBR™ Gold labeled MVs that contain nucleic acids did not increase similarly. Their percentage remained low for all the assayed times, with values between 0.34 and 3.38%. Moreover, they showed no significant differences between different time points, except at 24 h when the percentage of SYBR™ Gold labeled MVs was very high (17%) and significantly different from all other points of the growth curve (**Figure 2**). These findings confirm that nucleic acid contents in MVs also depend on the growth phase, and suggest a possible induced cell lysis mechanism.

Assuming that nucleic acid-containing MVs are O-IMVs, their rise in concentration at 24 h could be explained by the fact that O-IMVs are actively formed at this time point. This high percentage could imply a mechanism of O-IMV formation different from the blebbing mechanism previously described by us (Pérez-Cruz et al., 2013).

Observation of Explosive Cell Lysis in *S. vesiculosa* M7^T

Next, we aimed to investigate by TEM the appearance of cells and MVs during growth in order to detect events that would confirm an explosive cell lysis mechanism in *S. vesiculosa* M7^T. This will allow us to explain the significant differences in the vesiculation rate during the transition to the stationary phase and the high percentage of SYBR™ Gold labeled MVs at 24 h. For this purpose, TSB cultures of *S. vesiculosa* M7^T were centrifuged at different time points (12, 24, 48 h) at high speed (44,000 × *g*) to sediment cells and MVs simultaneously. Then, the samples were high-pressure fixed, freeze-substituted (FS), sectioned, and observed by TEM.

The appearance of the *S. vesiculosa* M7^T cells and extracellular matter markedly varied according to the time point at which they were observed (**Figure 3**). At 12 h of incubation, most of the cells had regular appearances with well-defined envelopes (**Figures 3A,B**). The cells had a rod or round shape, depending on the section plane, with their cytoplasmic content being

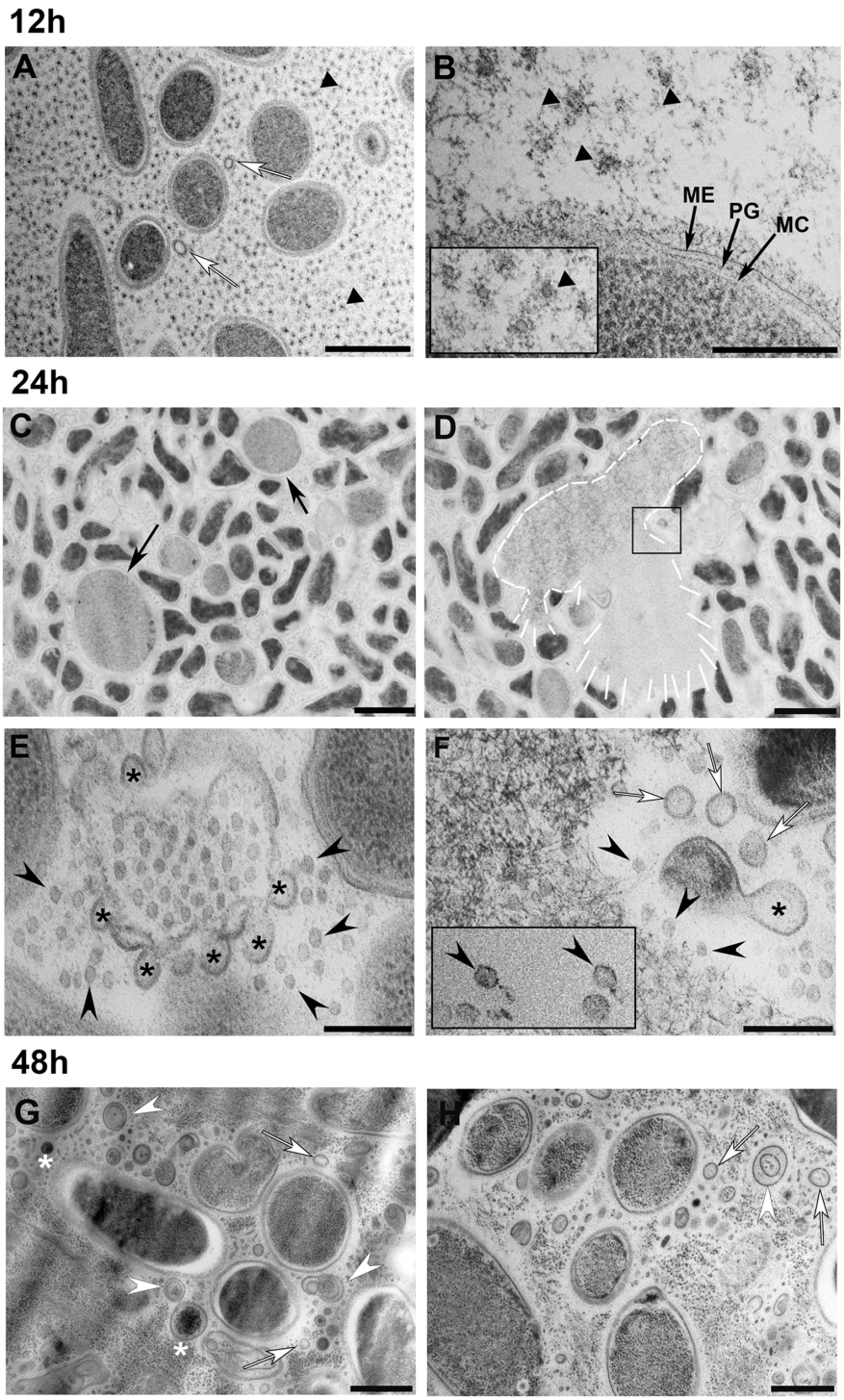

FIGURE 3 | Transmission electron microscopy observation of *S. vesiculosa* M7^T cells and MVs at different times of growth. *S. vesiculosa* M7^T cells were collected from TSB liquid cultures by high-speed centrifugation and processed by high-pressure freezing and freeze substitution. The images are representative of the changes produced in cells and extracellular matter during growth of *S. vesiculosa* M7^T. At 12 h **(A,B)**, the cells appeared normal, and the extracellular space was occupied mainly by small round structures surrounded by fibrillar material (black triangles in **A,B** and inset in **B**). Some outer membrane vesicles (OMVs) were also observed (white arrows in **A**). At 24 h **(C–F)**, being **F** an enlarged view of the inset in **D**, rounded and enlarged cells were visualized (black arrows in **C**). Cells exploding were observed (see white line-drawing in **D**), and reannealing membranes were detected at these points (asterisks in **E–F**) that led to the formation of OMVs (white arrows in **F**). At this time point, bacteriophages were observed (black arrowheads in **E–F**). At 48 h **(G,H)**, the extracellular matter was complex containing the elements previously observed such as OMVs (white arrows in **G**) and complex vesicles with double-layered membranes (white arrowheads in **G,H**) or with electrodense material inside (asterisks in **G**). Scale Bars **A-C,D**, 1 μm; **B-E,F**, 200 nm; **G,H**, 500 nm.

homogeneous, corroborating the characteristic stippling of the ribosomes. Moreover, the cell surfaces were covered by fine perpendicular fibers on the cell walls. The extracellular matter also consisted of vast amounts of round structures (**Figures 3A,B**, black triangles) that resembled small MVs (inset in **Figure 3B**). When viewed at higher magnification (**Figure 3B**), these structures seemed to derive from outer membrane fragments and dragged fibrillar material that surrounded the cells. These small MVs were regular in size with a mean diameter of 26 nm. Larger MVs (around 70–100 nm) having the characteristic appearance of OMVs were also observed, but much less frequently. The same fringe of fine fibers also surrounded the OMVs (**Figure 3A**, white arrows). These smalls MVs appeared to be derived from the outer leaflet of the cell's outer membrane. Similar, uniformly distributed, small MVs (around 26 nm in size) have already been observed by our research group in the extracellular matter of the cold-adapted Antarctic strain *Shewanella livingstonensis* NF22^T, where they were related to cold-adaption (Frias et al., 2010); however, more in-depth analysis is required to determine if they could correspond to a different novel group of MVs with a specific function.

Next, we observed that at 24 h, some of the *S. vesiculosa* M7^T cells lost their bacillary shape and acquired a rounded morphology. Moreover, their sizes became significantly larger than those of the other cells (**Figure 3C**, black arrows). A few cells also appeared exploded, liberating their cytosolic contents to the extracellular space (**Figure 3D**, white profile). TEM analysis corroborated all the morphological traits for explosive cell lysis described by Turnbull et al. (2016) as a biogenesis mechanism of bacterial MVs in *P. aeruginosa* biofilms. On the one hand, a small percentage of giant round cells were observed and exploding cells surrounded by membrane fragments with re-annealing tendencies were detected (**Figure 3E**). The higher resolution provided by TEM and HPF-FS clearly proved that the membrane fragments presented a bilayer structure with the same staining profile as that of the outer membranes of the cells. Interestingly, the regularly sized fragments at 24 h gave rise to MVs with uniform diameters such as OMVs, named explosive-OMVs (EOMVs) by Toyofuku et al. (2019) to distinguish them from blebbing OMVs. In future studies, it would be enlightening to study the elements and mechanisms involved in this uniform membrane lysis and the tendency to re-circulize (**Supplementary Figure S1**).

The enlarged inset of the lysed cell (**Figure 3F**) showed 1,000s of tiny particles that possibly corresponded to the icosahedral heads of a bacteriophage (**Figure 3F**, black arrowheads). Occasionally, particles that possibly corresponded to complete bacteriophages were also observed. These particles had icosahedral heads and tails, which were challenging to visualize when dealing with thin sections (**Figure 3F**, black rectangle). We hypothesized that the explosion mechanism would be similar to that observed by Turnbull et al. (2016) in a *P. aeruginosa* strain using phase contrast, wide-field fluorescence, and f3D-SIM super-resolution microscopy. TEM observation clearly confirmed the explosion of a sub-population of cells in *S. vesiculosa* M7^T and the presence of phages at the point where explosion took place. Although bacteriophages have developed various lysis strategies for most Gram-negative phages, the key players in this process are the holins, endolysins, and spanins (Cahill and Young, 2019). In-depth analysis is required to confirm the presence of these proteins in *S. vesiculosa* M7[7] and how they can affect the outer membrane breakage and, subsequently, the size of the formed MVs.

Explosive cell lysis is an essential mechanism for the generation of MVs of different types (Toyofuku et al., 2019). In our samples, we observed a mixture of shattered fragments of the outer membrane with curling and self-annealing tendencies at the points where the explosive cell lysis took place (**Figures 3E,F**, black asterisks). We observed that they also formed MVs (**Figure 3F**, white arrows; **Supplementary Figure S1**). Most of these re-annealed MVs were homogeneous in size with diameters of around 50 nm with the typical structure of OMVs surrounded by a lipid bilayer and having the same profile as that of the outer membranes of the cells. Moreover, in 24 h samples, the bacteriophages were highly concentrated at the lysis sites (**Figures 3E,F**) and scattered throughout the extracellular space. For our investigations, the samples of cells and MVs were prepared for TEM observation from agitated liquid cultures. Thus, bacteriophages, once liberated, became dispersed in supernatants. The lack of these cellular events in some of the 12 h samples indicated the occurrence of explosive cell lysis between 12 and 24 h.

Next, we observed how samples collected at 48 h were significantly different from the other time points. Numerous MVs were observed scattered between the cells, without any trace of the original lysed cell. This observation could be attributed to the total disintegration of the lysed cell at this time point. Moreover, we observed that some of the MVs corresponded to OMVs (**Figures 3G,H**, white arrows). However, numerous MVs were seen containing electrodense material inside. In some cases, this intracellular material could be ribosomes having a granular appearance in the cell cytoplasm (**Figures 3G,H**, white asterisks). At 48 h, many double-layered MVs were also seen, but most looked different from the O-IMVs previously described by our group. The membrane staining pattern observed in TEM did not allow us to distinguish if the two bilayers corresponded to the outer and inner membranes of the cells or if they arose from the same membrane (**Figures 3G,H**, white arrowheads). Moreover, many of the double-layered MVs observed at 48 h did not show any electron dense material inside the inner layer, unlike the blebbing O-IMVs (**Supplementary Figure S2**). It is highly probable that recircularization of cell fragmented membranes formed the double-layered MVs after explosive lysis and not by extrusion of the outer membrane dragging along the inner membrane with a part of the cytoplasmic content. The name EOMVs was assigned to OMVs generated by explosive cell lysis (Toyofuku et al., 2019); we advocate that the double-layered O-IMVs formed after explosive cell lysis should be named explosive O-IMVs (EOIMV).

Sequencing of Genome and MV DNA Confirmed a Bacteriophage Mediated Explosive Cell Lysis

After confirming nucleic acids in MVs by high-resolution flow cytometry, we further quantified and characterized the DNA by sequencing. For quantification, DNA was extracted from three biological samples of MVs collected from *S. vesiculosa* M7^T treated with DNAse at different time points and quantified. DNA concentrations from the exponentially growing cultures (18 h) were significantly lower than that of the samples collected at the transition from the late exponential to the stationary phase (24 h). However, after this transition, the DNA concentrations remained constant during the stationary phase (**Figure 4A**). This observation corroborated findings from other studies that demonstrate that phage-induced MVs carry a higher amount of DNA and are more effective at horizontal gene transfer (Bearson and Brunelle, 2015; Andreoni et al., 2018; Crispim et al., 2019). Our results contradict the previous reports on *Streptococcus mutans* and *P. aeruginosa* (Liao et al., 2014; Bitto et al., 2017), which found more DNA association with MVs in the exponential phase than in the stationary phase. These last studies did not consider the explosive cell lysis mechanism in which DNA is likely to be entrapped in the recirculating membrane fragments, however more studies are needed to clarify these differences.

Next, to know which type of DNA was exported in MVs, we first sequenced the genome of *S. vesiculosa* M7^T to assemble and recircularize the *S. vesiculosa* M7^T chromosome with Illumina and Nanopore technology (NCBI accession number PRJNA723175). Then, we sequenced MV DNA to map the obtained fragments with *S. vesiculosa* M7^T chromosome., For this purpose the DNA from samples collected at the transition to the stationary phase (24 h) were divided into two aliquots according to the size of the fragments. One of the aliquots contained DNA fragments bigger than 125 bp, while the other contained fragments below 125 bp. The two aliquots were sequenced separately. MVs-DNA sequencing showed that the MV DNA fragments represented the whole genome of *S. vesiculosa* M7^T. **Figure 4B** shows the MV-DNA fragments' representation along the *S. vesiculosa* M7^T genome, with the first half of the chromosome being represented below average (blue) and the second half being represented above average (red), similar to previous studies (Turnbull et al., 2016; Bitto et al., 2017) in different strains of *P. aeruginosa*. Other studies have reported the representation of only half of the genome in DNA isolated from MVs of the cyanobacteria *Prochlorococcus* (Biller et al., 2017). We also found a uniform representation of the fragments, although two over-represented peaks in 1.1 and 3 Mb were detected. These fragments correspond to several coding sequences (CDS), even though most of the resulting proteins remain uncharacterized. Our analysis identified only a tyrosine-type integrase (RefSeq: WP_011637468.1) and a 23S ribosomal RNA that could be mapped to the obtained fragments.

The visualization of bacteriophage-like particles in our TEM analysis prompted us to initiate an *in silico* PHASTER tool-mediated (Arndt et al., 2016) search to identify prophage-like

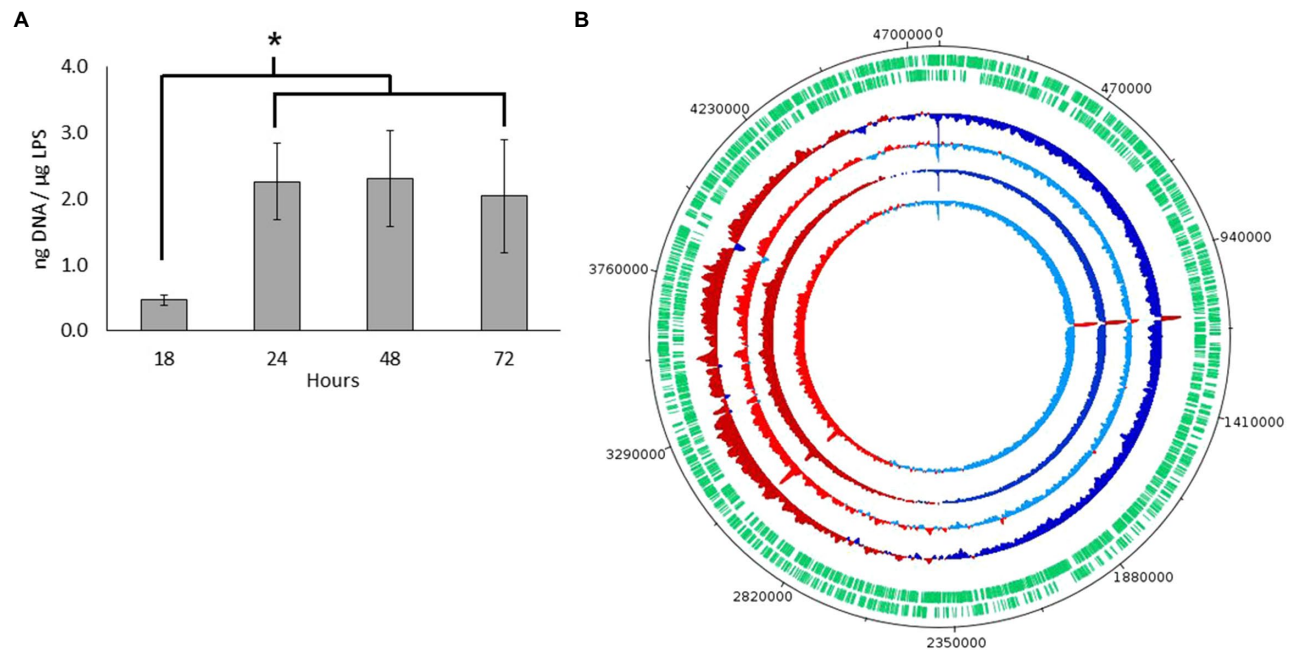

FIGURE 4 | DNA characterization from *S. vesiculosa* M7^T MVs. **(A)** DNA concentration from S. vesiculosa M7^T MVs at different times of growth. $n = 3$, ANOVA test, * $p < 0.05$. **(B)** Circos plot for the MVs-DNA read count across each replicates show read counts at each base pair position. Positions that show greater than average read density are colored in red, and those with less than average density are colored in blue. Darker tones show fractions of fragments larger than 125 bp, and lighter ones show fractions of fragments smaller than 125 bp.

sequences in the *S. vesiculosa* M7^T chromosome. PHASTER showed one region of 37.1 Kb with 52 protein-CDS, placed between 2.15 and 2.19 Mb, that matched a phage-like structure. Moreover, the identified region showed high homology with the phiΦ18P phage previously described in the genus *Aeromonas* (Beilstein and Dreiseikelmann, 2008). The characteristics, localization, and structure of the identified prophage-like region are described in **Supplementary Figure S3**. TEM images and PHASTER tool confirmed that explosive cell lysis in *S. vesiculosa* M7^T was caused by a prophage activation. The morphology of viral particles visualized by TEM was comparable with phage phi18P, although virus isolation is needed to accurately define this new phage's structural characteristics. Similar observations showing explosive cell lysis by prophage induction and secretion of different MVs were also reported in *Stenotrophomonas maltophila* (Devos et al., 2017).

Apoptosis-Like Cell Death Was Observed in *S. vesiculosa* M7^T

Prophage activation leads to DNA damage and activates a series of distinct cell death mechanisms referred to as ALD (Peeters and de Jonge, 2018). As growth arrest was detected in *S. vesiculosa* M7^T cultures at the transition from the late exponential to the stationary phase, we decided to identify the markers of ALD activation, such as the exposure of phosphatidylserine on the external face of the cell membrane or DNA fragmentation patterns.

Exposure of phosphatidylserine was measured by flow cytometry of Annexin V-FITC- and PI-labeled *S. vesiculosa* M7^T cells collected at different time points of their growth. At 24 h, significant differences in the percentage of Annexin V-FITC positive cells were detected compared with the other growth curve time points. Moreover, at the 24 h time point, a non-significant increase in the percentage of PI marked cells indicated the death of a small portion of the population. This increase in PI staining corroborated the data of cell counts between 18 and 24 h, reflecting the growth arrest, probably due to the phage lysis of the cells (**Figures 5A,B**). Next, the extent of DNA fragmentation was estimated by the TUNEL assay with the same samples. At 24 h of incubation, 27% of the cells were positive for Alexa Fluor™ 488 compared with less than 1% at the other incubation times. This significant difference at 24 h confirmed the phage replication-mediated DNA damage (**Figure 5C**). It is known that ALD processes require enzyme activation at the cost of highly energetic molecules like NADH or ATP, with a rise in the concentration of the reduced molecules compared with that of their oxidized counterparts. In our study, the NADH/NAD+ ratio and ATP concentration were significantly higher at 24 h of incubation than for the samples collected from the exponential and stationary phases (**Figure 5D**).

A

Time (h)	% PI	% V-Anx
12	1.07 ± 0.88	3.65 ± 2,84
18	0.25 ± 0.14	2.91 ± 1,52
24	8.57 ± 2.87	5.36 ± 2,98
48	2.89 ± 1.33	1.99 ± 1,52
72	11.51 ± 7.38	0.58 ± 0,25
96	70.23 ± 7.93	2.67 ± 1,65

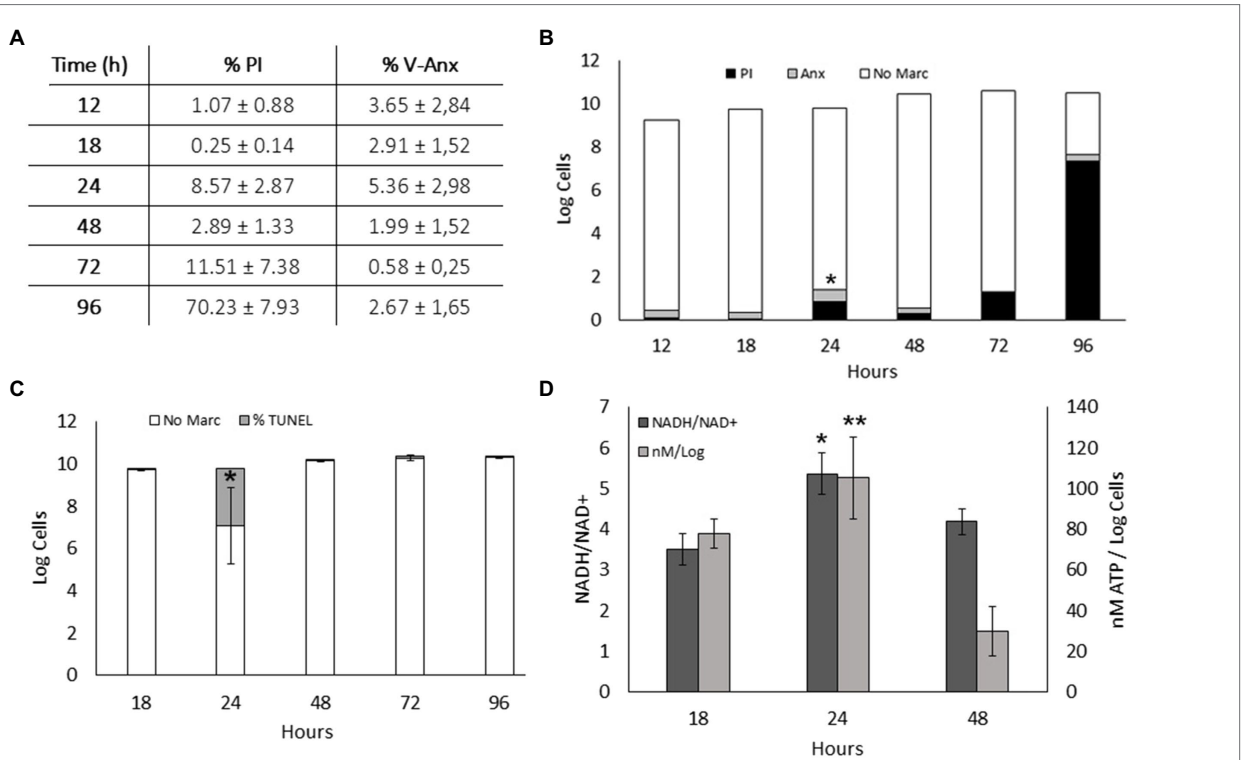

FIGURE 5 | Apoptosis-like death in *S. vesiculosa* M7^T cultures. **(A)** Exposure of phosphatidylserine in *S. vesiculosa* M7^T cells at different time points of the growth curve was analyzed by flow cytometry after PI and Annexin V-FITC staining. **(B)** Bars graph representing percentage of PI (black) and Annexin V-FITC (gray) stained cells and unstained cells (white) at different time points of growth. $n = 3$, ANOVA test, * $p < 0.05$ of Annexin V-FITC stained cells. **(C)** Bars graph representing the percentage of TUNEL (gray) stained and unstained cells (white) at different times of growth. $n = 2$, ANOVA test, * $p < 0.05$. **(D)** Metabolic markers, ATP and NADH, in *S. vesiculosa* M7^T cells at different times of growth. $n = 3$, ANOVA test, * and ** $p < 0.05$.

The lack of apparent stressors (e.g., antibiotics, UV radiation, chemicals, or environmental stress factors) leads to explosive cell lysis, and MV secretion in *S. vesiculosa* M7^T, unlike other strains (Toyofuku et al., 2012; Turnbull et al., 2016; Devos et al., 2017). Spontaneous induction of the lytic cycle can occur despite the stressful condition-mediated transition from the lysogenic to the lytic state of a prophage (Lwoff, 1953; Nanda et al., 2015). Several studies have demonstrated at a single-cell level that spontaneously occurring DNA damage under standard growth conditions induces an SOS pathway that in turn triggers the induction of prophages (Little, 1990; Nanda et al., 2014). Our investigation revealed distinct ALD mechanisms in *S. vesiculosa* M7^T cultures with significant differences in 24-h samples compared with other time points. We hypothesize that spontaneous phage lysis and activation of ALD processes lead to growth arrest at this time point. It is known that activation of a prophage can cause a bacterial community to induce the death of a fraction of their population (Little, 1990). Consequently, the SOS pathway activates the recA protein to induce a series of characteristic mechanisms of ALD (Maslowska et al., 2019).

Separation of Different MVs by Flow Cytometry Sorting

Our previous studies demonstrated that *S. vesiculosa* M7^T produced OMVs and O-IMVs and that the latter contained

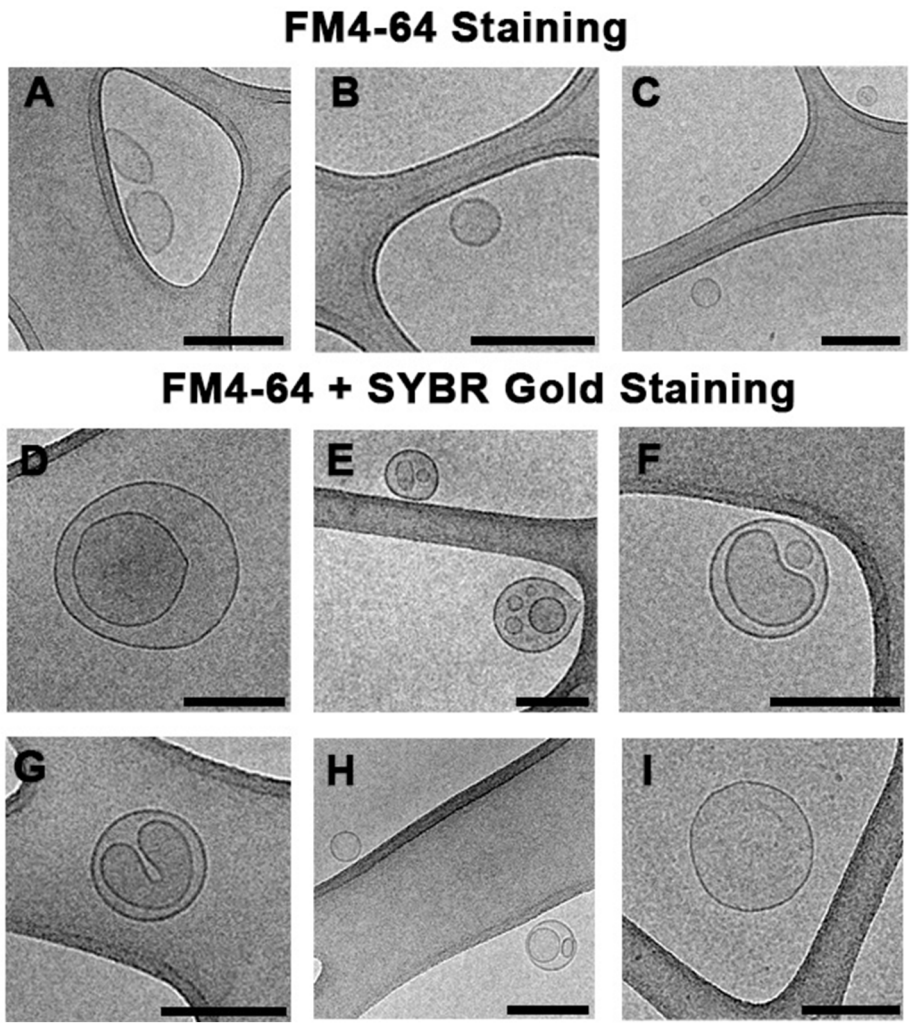

FIGURE 6 | Cryo-electron microscopy images of MVs from *S. vesiculosa* M7^T separated by flow cytometry sorting. MVs were isolated from TSB liquid cultures of *S. vesiculosa* M7^T at 24 h of incubation and were submitted to sorting by flow cytometry. Cytometry events were separated into two channels. Events marked only with FM4-64 were collected in one channel, and events marked with FM4-64 and SYBR™ Gold in another one. Subsequently, they were ultracentrifuged and cryofixed by Plunge Freezing. The images are representative of the different types of MVs observed by Cryo-EM. Images **(A–C)** show that events labeled with only FM4-64 corresponded mostly (90%) to single-layered MVs probably corresponding to OMVs. Images **(D–I)** show events marked with both fluorochromes and corresponded predominantly to double-layered MVs (70%); some of them have the same structure described for outer-inner membrane vesicles **(D)**, while others showed strange shapes with an external layer and more than one vesicle inside **(E–H)**. A lower percentage of MVs (30%) marked with both fluorochromes were visualized as one-layered MVs **(I)**. Bars, 200 nm.

DNA (Pérez-Cruz et al., 2013). The dragging of cytoplasmic components and cytoplasmic membranes and their outer membranes during O-IMV formation facilitated the incorporation of DNA in the O-IMVs. In this study, our TEM analysis confirmed the potential of *S. vesiculosa* M7^T to form various MVs during growth owing to bacteriophage-mediated explosive cell lysis. After cell explosion and lysis, self-annealing of membrane fragments could also explain the presence of double-layer MVs with nucleic acids inside. We aimed to separate the DNA-containing MVs by visually flow cytometry sorting and visualize them via Cryo-EM to determine their types. We isolated MVs from *S. vesiculosa* M7^T cultures at 24 h owing to the significantly high percentage of double-labeled MVs. For flow cytometry-based sorting, we established one channel to collect MVs labeled with FM4-64 and another channel to collect those labeled with FM4-64 and SYBR™ Gold. This experiment was carried out twice, and in each one, between 1–1.5 million events were separated. After sorting, each separated sample was ultracentrifuged at 100,000 *g*, resuspended in a minimal amount of sterile water, and plunge-frozen (PF) for observation by Cryo-EM.

We successfully separated the MVs despite the challenging nature of the experiment (**Figure 6**). We demonstrated that the events labeled with only FM4-64 corresponded mostly to single-layered OMVs (90% of visualized MVs; **Figures 6A–C**). However, events marked with both fluorochromes corresponded predominantly to double-layered MVs (70% of visualized MVs), with several distinguishable types (**Figures 6D–H**). Based on the Cryo-EM structure, we hypothesize that some double-layered MVs in *S. vesiculosa* M7^T could correspond to the previously described O-IMVs (**Figure 6D**). However, many of them have a different appearance, with more than one vesicle inside the external layer and strange shapes of the inside content (**Figures 6E–H**). A percentage of MVs marked with both fluorochromes (30%) were visualized as one-layered MVs, confirming that during the process of membrane re-annealing after cell lysis, OMVs also entrap nucleic acids (**Figures 6H,I**).

CONCLUSION

In summary, our novel findings highlight the growth phase-dependent production of different amounts and types of MVs by *S. vesiculosa* M7^T. Moreover, we demonstrate how a part of the population incurred spontaneous induction of phage-mediated explosive cell lysis in the transition from the late exponential to the stationary phases, and led to the secretion of different types of vesicles. After phage lysis, a different type of O-IMV (EOIMV) was detected with structural differences compared with the blebbing O-IMVs previously identified in *S. vesiculosa* M7^T. High-resolution flow cytometry is a valuable tool to monitor the production of different MVs during growth; here, it facilitated the first separation of MVs based on their nucleic acid content. Even so, there remains a clear need to implement improved bacterial MV separation techniques to advance our knowledge of MVs. This study shows that prophage activation can be a determinant factor in MV formation and should be taken into consideration when studying Gram-negative bacteria MVs.

DATA AVAILABILITY STATEMENT

The data presented in the study are deposited in the NCBI repository, accession number PRJNA723175. Direct link is (www.ncbi.nlm.nih.gov/bioproject/PRJNA723175). The names of the repository/repositories and accession number(s) can be found in the article/**Supplementary Material**.

AUTHOR CONTRIBUTIONS

NB and EM contributed to the conception and design of the study, conducted most experiments, performed the statistical analysis, and wrote the manuscript. JC assisted in the design and performance of the flow cytometry experiments. LD assisted in the performance of TEM and Cryo-EM experiments. All authors contributed to the manuscript, and all have read and approved the submitted version.

FUNDING

This work received funding from grant CTQ2014-59632-R to EM and scholarship BES-2015-074582 to NB, both from the Ministerio de Economia y Competitividad, Spain. Grant 2014SGR1017 was awarded by the Departament d'Innovació, Universitats i Empresa from the Autonomous Government of Catalonia. The funders had no role in the study design, data collection and analysis, decision to publish, or preparation of the manuscript.

ACKNOWLEDGMENTS

We acknowledge the technical support of the cryo-electron microscopy and cytometry services at the Scientific and Technological Centers of the University of Barcelona. We would like to thank Editage (www.editage.com) for English language editing.

SUPPLEMENTARY MATERIAL

The Supplementary Material for this article can be found online at: https://www.frontiersin.org/articles/10.3389/fmicb.2021.713669/full#supplementary-material

Importance of the Study

It is known that bacteria secrete various types of vesicles with different morphological and functional characteristics. Studies to characterize the different types of vesicles are important to harness their multiple potentials in the field of biology and biotechnology. In this study, we used a model vesiculating bacteria to characterize the different kinds of

vesicles secreted. We show that the amount and type of vesicles depends on the growth phase and on the activation of a phage-mediated explosive cell lysis leading to the release of a heterogeneous pool of single- and double-layered vesicles. After phage lysis, a different type of double-layered vesicle was detected with structural differences compared with the blebbing model previously identified in this strain. For the first time, an attempt has been made to separate bacterial vesicles based on their nucleic acid content. However, improvement and implementation of vesicle separation techniques should be a priority to advance knowledge of vesicles and their biological functions.

REFERENCES

Andreoni, F., Toyofuku, M., Menzi, C., Kalawong, R., Mairpady Shambat, S., François, P., et al. (2018). Antibiotics stimulate formation of vesicles in *Staphylococcus aureus* in both phage-dependent and -independent fashions and *via* different routes. *Antimicrob. Agents Chemother.* 63:e01439-18. doi: 10.1128/AAC.01439-18

Andryukov, B. G., Somova, L. M., and Timchenko, N. F. (2018). Molecular and genetic characteristics of cell death in prokaryotes. *Mol. Genet. Microbiol. Virol.* 33, 73–83. doi: 10.3103/S0891416818020039

Arndt, D., Grant, J. R., Marcu, A., Sajed, T., Pon, A., Liang, Y., et al. (2016). PHASTER: a better, faster version of the PHAST phage search tool. *Nucleic Acids Res.* 44, W16–W21. doi: 10.1093/nar/gkw387

Avila-Calderón, E. D., Ruiz-Palma, M. D. S., Aguilera-Arreola, M. G., Velázquez-Guadarrama, N., Ruiz, E. A., Gomez-Lunar, Z., et al. (2021). Outer membrane vesicles of gram-negative bacteria: an outlook on biogenesis. *Front. Microbiol.* 12:557902. doi: 10.3389/fmicb.2021.557902

Bagnara, A. S., and Finch, L. R. (1972). Quantitative extraction and estimation of intracellular nucleoside triphosphates of Escherichia coli. *Anal. Biochem.* 45, 24–34. doi: 10.1016/0003-2697(72)90004-8

Bamford, D. H., Romantschuk, M., and Somerharju, P. J. (1987). Membrane fusion in prokaryotes: bacteriophage phi 6 membrane fuses with the *pseudomonas syringae* outer membrane. *EMBO J.* 6, 1467–1473. doi: 10.1002/j.1460-2075.1987.tb02388.x

Beaber, J. W., Hochhut, B., and Waldor, M. K. (2004). SOS response promotes horizontal dissemination of antibiotic resistance genes. *Nature* 427, 72–74. doi: 10.1038/nature02241

Bearson, B. L., and Brunelle, B. W. (2015). Fluoroquinolone induction of phage-mediated gene transfer in multidrug-resistant *salmonella*. *Int. J. Antimicrob. Agents* 46, 201–204. doi: 10.1016/j.ijantimicag.2015.04.008

Beilstein, F., and Dreiseikelmann, B. (2008). Temperate bacteriophage ΦO18P from an Aeromonas media isolate: characterization and complete genome sequence. *Virology* 373, 25–29. doi: 10.1016/j.virol.2007.11.016

Berleman, J. E., Allen, S., Danielewicz, M. A., Remis, J. P., Gorur, A., Cunha, J., et al. (2014). The lethal cargo of *Myxococcus xanthus* outer membrane vesicles. *Front. Microbiol.* 5:474. doi: 10.3389/fmicb.2014.00474

Beveridge, T. J. (1999). Structures of gram-negative cell walls and their derived membrane vesicles. *J. Bacteriol.* 181, 4725–4733. doi: 10.1128/JB.181.16.4725-4733.1999

Biller, S. J., McDaniel, L. D., Breitbart, M., Rogers, E., Paul, J. H., and Chisholm, S. W. (2017). Membrane vesicles in sea water: heterogeneous DNA content and implications for viral abundance estimates. *ISME J.* 11, 394–404. doi: 10.1038/ismej.2016.134

Biller, S. J., Schubotz, F., Roggensack, S. E., Thompson, A. W., Summons, R. E., and Chisholm, S. W. (2014). Bacterial vesicles in marine ecosystems. *Science* 343, 183–186. doi: 10.1126/science.1243457

Binnenkade, L., Teichmann, L., and Thormann, K. M. (2014). Iron triggers λSo prophage induction and release of extracellular DNA in *Shewanella oneidensis* MR-1 biofilms. *Appl. Environ. Microbiol.* 80, 5304–5316. doi: 10.1128/AEM.01480-14

Bitto, N. J., Chapman, R., Pidot, S., Costin, A., Lo, C., Choi, J., et al. (2017). Bacterial membrane vesicles transport their DNA cargo into host cells. *Sci. Rep.* 7:7072. doi: 10.1038/s41598-017-07288-4

Bozal, N., Montes, M. J., Minana-Galbis, D., Manresa, A., and Mercade, E. (2009). *Shewanella vesiculosa* sp. nov., a psychrotolerant bacterium isolated from an Antarctic coastal area. *Int. J. Syst. Evol. Microbiol.* 59, 336–340. doi: 10.1099/ijs.0.000737-0

Buchfink, B., Xie, C., and Huson, D. H. (2015). Fast and sensitive protein alignment using DIAMOND. *Nat. Methods* 12, 59–60. doi: 10.1038/nmeth.3176

Cahill, J., and Young, R. (2019). Phage lysis: multiple genes for multiple barriers. *Adv. Virus Res.* 103, 33–70. doi: 10.1016/bs.aivir.2018.09.003

Carver, T., Harris, S. R., Berriman, M., Parkhill, J., and McQuillan, J. A. (2012). Artemis: an integrated platform for visualization and analysis of high-throughput sequence-based experimental data. *Bioinformatics* 28, 464–469. doi: 10.1093/bioinformatics/btr703

Catalao, M. J., Moniz-Pereira, F. G., São-José, C., and Pimentel, M. (2012). Divesity in bacterial lysis systems: bacteriophages show the way. *FEMS Microbiol. Rev* 37, 554–571. doi: 10.1111/1574-6976.12006

Cooke, A. C., Nello, A. V., Ernst, R. K., and Schertzer, J. W. (2019). Analysis of *Pseudomonas aeruginosa* biofilm membrane vesicles supports multiple mechanisms of biogenesis. *PLoS One* 14:e0212275. doi: 10.1371/journal.pone.0212275

Crispim, J. S., Dias, R. S., Laguardia, C. N., Araújo, L. C., da Silva, J. D., Vidigal, P. M. P., et al. (2019). *Desulfovibrio alaskensis* prophages and their possible involvement in the horizontal transfer of genes by outer membrane vesicles. *Gene* 703, 50–57. doi: 10.1016/j.gene.2019.04.016

Danecek, P., Bonfield, J. K., Liddle, J., Marshall, J., Ohan, V., Pollard, M. O., et al. (2021). Twelve years of SAMtools and BCFtools. *GigaScience* 10:giab008. doi: 10.1093/gigascience/giab008

Delcher, A. L., Bratke, K. A., Powers, E. C., and Salzberg, S. L. (2007). Identifying bacterial genes and endosymbiont DNA with glimmer. *Bioinformatics* 23, 673–679. doi: 10.1093/bioinformatics/btm009

Delgado, L., Baeza, N., Pérez-Cruz, C., López-Iglesias, C., and Mercadé, E. (2019). Cryo-transmission electron microscopy of outer membrane vesicles naturally secreted by gram-negative pathogenic bacteria. *Bio-protocols.* 9:18. doi: 10.21769/BioProtoc.3367

Devos, S., Van Putte, W., Vitse, J., Van Driessche, G., Stremersch, S., Van Den Broek, W., et al. (2017). Membrane vesicle secretion and prophage induction in multidrug-resistant *Stenotrophomonas maltophilia* in response to ciprofloxacin stress: ciprofloxacin-induced membrane vesicle secretion. *Environ. Microbiol.* 19, 3930–3937. doi: 10.1111/1462-2920.13793

Dorward, D. W., Garon, C. F., and Judd, R. C. (1989). Export and intercellular transfer of DNA *via* membrane blebs of Neisseria gonorrhoeae. *J. Bacteriol.* 171, 2499–2505. doi: 10.1128/jb.171.5.2499-2505.1989

Fang, Y., Mercer, R. G., McMullen, L. M., and Gänzle, M. G. (2017). Induction of Shiga toxin-encoding prophage by abiotic environmental stress in food. *Appl. Environ. Microbiol.* 83:e01378-17. doi: 10.1128/AEM.01378-17

Frias, A., Manresa, A., de Oliveira, E., López-Iglesias, C., and Mercade, E. (2010). Membrane vesicles: a common feature in the extracellular matter of cold-adapted Antarctic bacteria. *Microb. Ecol.* 59, 476–486. doi: 10.1007/s00248-009-9622-9

Gerritzen, M. J. H., Martens, D. E., Uittenbogaard, J. P., Wijffels, R. H., and Stork, M. (2019). Sulfate depletion triggers overproduction of phospholipids and the release of outer membrane vesicles by *Neisseria meningitidis*. *Sci. Rep.* 9:4716. doi: 10.1038/s41598-019-41233-x

Gill, S., Catchpole, R., and Forterre, P. (2019). Extracellular membrane vesicles in the three domains of life and beyond. *FEMS Microbiol. Rev.* 43, 273–303. doi: 10.1093/femsre/fuy042

Gurevich, A., Saveliev, V., Vyahhi, N., and Tesler, G. (2013). QUAST: quality assessment tool for genome assemblies. *Bioinformatics* 29, 1072–1075. doi: 10.1093/bioinformatics/btt086

Hagemann, S., Stöger, L., Kappelmann, M., Hassl, I., Ellinger, A., and Velimirov, B. (2014). DNA-bearing membrane vesicles produced by *Ahrensia kielensis* and

Pseudoalteromonas marina: DNA-bearing membrane vesicles. *J. Basic Microbiol.* 54, 1062–1072. doi: 10.1002/jobm.201300376

Jan, A. T. (2017). Outer membrane vesicles (OMVs) of gram-negative bacteria: a perspective update. *Front. Microbiol.* 8:1053. doi: 10.3389/fmicb.2017.01053

Jiang, H., Lei, R., Ding, S. W., and Zhu, S. (2014). Skewer: a fast and accurate adapter trimmer for next-generation sequencing paired-end reads. *BMC Bioinformatics* 15:182. doi: 10.1186/1471-2105-15-182

Kadurugamuwa, J. L., and Beveridge, T. J. (1996). Bacteriolytic effect of membrane vesicles from *Pseudomonas aeruginosa* on other bacteria including pathogens: conceptually new antibiotics. *J. Bacteriol.* 178, 2767–2774. doi: 10.1128/jb.178.10.2767-2774.1996

Kageyama, M., Shinomiya, T., Aihara, Y., and Kobayashi, M. (1979). Characterization of a bacteriophage related to R-type pyocins. *J. Virol.* 32, 951–957. doi: 10.1128/jvi.32.3.951-957.1979

Kaparakis-Liaskos, M., and Ferrero, R. L. (2015). Immune modulation by bacterial outer membrane vesicles. *Nat. Rev. Immunol.* 15, 375–387. doi: 10.1038/nri3837

Kuehn, M. J., and Kesty, N. C. (2005). Bacterial outer membrane vesicles and the host–pathogen interaction. *Genes Dev.* 19, 2645–2655. doi: 10.1101/gad.1299905

Kulkarni, H. M., and Jagannadham, M. V. (2014). Biogenesis and multifaceted roles of outer membrane vesicles from gram-negative bacteria. *Microbiology* 160, 2109–2121. doi: 10.1099/mic.0.079400-0

Langmead, B., Wilks, C., Antonescu, V., and Charles, R. (2019). Scaling read aligners to hundreds of threads on general-purpose processors. *Bioinformatics* 35, 421–432. doi: 10.1093/bioinformatics/bty648

Lee, E.-Y., Choi, D.-S., Kim, K.-P., and Gho, Y.-S. (2008). Proteomics in gram-negative bacterial outer membrane vesicles. *Mass Spectrom. Rev.* 27, 535–555. doi: 10.1002/mas.20175

Lee, C.-H., and Tsai, C.-M. (1999). Quantification of bacterial lipopolysaccharides by the Purpald assay: measuring formaldehyde generated from 2-keto-3-deoxyoctonate and heptose at the inner core by periodate oxidation. *Anal. Biochem.* 267, 161–168. doi: 10.1006/abio.1998.2961

Li, H. (2016). Minimap and miniasm: fast mapping and de novo assembly for noisy long sequences. *Bioinformatics* 32, 2103–2110. doi: 10.1093/bioinformatics/btw152

Liao, S., Klein, M. I., Heim, K. P., Fan, Y., Bitoun, J. P., Ahn, S.-J., et al. (2014). *Streptococcus mutans* extracellular DNA is upregulated during growth in biofilms, actively released *via* membrane vesicles, and influenced by components of the protein secretion machinery. *J. Bacteriol.* 196, 2355–2366. doi: 10.1128/JB.01493-14

Little, J. W. (1990). Chance phenotypic variation. *Trends Biochem.* 15:138. doi: 10.1016/0968-0004(90)90211-S

Lotvall, J., and Valadi, H. (2007). Cell to cell signalling *via* exosomes through esRNA. *Cell Adhes. Migr.* 1, 156–158. doi: 10.4161/cam.1.3.5114

Lwoff, A. (1953). Lysogeny. *Bacteriol. Rev.* 17, 269–337. doi: 10.1128/br.17.4.269-337.1953

MacDonald, I. A., and Kuehn, M. J. (2013). Stress-induced outer membrane vesicle production by *Pseudomonas aeruginosa*. *J. Bacteriol.* 195, 2971–2981. doi: 10.1128/JB.02267-12

Mandal, P. K., Ballerin, G., Nolan, L. M., Petty, N. K., and Whitchurch, C. B. (2021). Bacteriophage infecion of *Escherichia coli* leads to the formation of membrane vesicles *via* both explosive cell lysis and membrane blebbing. *Microbiology* 167:001021. doi: 10.1099/mic.0.001021

Mashburn-Warren, L. M., and Whiteley, M. (2006). Special delivery: vesicle trafficking in prokaryotes. *Mol. Microbiol.* 61, 839–846. doi: 10.1111/j.1365-2958.2006.05272.x

Maslowska, K. H., Makiela-Dzbenska, K., and Fijalkowska, I. J. (2019). The SOS system: A complex and tightly regulated response to DNA damage. *Environ. Mol. Mutagen.* 60, 368–384. doi: 10.1002/em.22267

McBroom, A. J., Johnson, A. P., Vemulapalli, S., and Kuehn, M. J. (2006). Outer membrane vesicle production by *Escherichia coli* is independent of membrane instability. *J. Bacteriol.* 188, 5385–5392. doi: 10.1128/JB.00498-06

McBroom, A. J., and Kuehn, M. J. (2007). Release of outer membrane vesicles by gram-negative bacteria is a novel envelope stress response. *Mol. Microbiol.* 63, 545–558. doi: 10.1111/j.1365-2958.2006.05522.x

Mozaheb, N., and Mingeot-Leclercq, M.-P. (2020). Membrane vesicle production as a bacterial defense against stress. *Front. Microbiol.* 11:600221. doi: 10.3389/fmicb.2020.600221

Nagakubo, T., Nomura, N., and Toyofuku, M. (2020). Cracking open bacterial membrane vesicles. *Front. Microbiol.* 10:3026. doi: 10.3389/fmicb.2019.03026

Nanda, A. M., Heyer, A., Krämer, C., Grünberger, A., Kohlheyer, D., and Frunzke, J. (2014). Analysis of SOS-induced spontaneous prophage induction in *Corynebacterium glutamicum* at the single-cell level. *J. Bacteriol.* 196, 180–188. doi: 10.1128/JB.01018-13

Nanda, A. M., Thormann, K., and Frunzke, J. (2015). Impact of spontaneous prophage induction on the fitness of bacterial populations and host-microbe interactions. *J. Bacteriol.* 197, 410–419. doi: 10.1128/JB.02230-14

Partridge, S. R., Kwong, S. M., Firth, N., and Jensen, S. O. (2018). Mobile genetic elements associated with antimicrobial resistance. *Clin. Microbiol. Rev.* 31:e00088-17. doi: 10.1128/CMR.00088-17

Peeters, S. H., and de Jonge, M. I. (2018). For the greater good: programmed cell death in bacterial communities. *Microbiol. Res.* 207, 161–169. doi: 10.1016/j.micres.2017.11.016

Pérez-Cruz, C., Briansó, F., Sonnleitner, E., Bläsi, U., and Mercadé, E. (2021). RNA release *via* membrane vesicles in *Pseudomonas aeruginosa* PAO1 is associated with the growth phase. *Environ. Microbiol.* doi: 10.1111/1462-2920.15436 [Epub ahead of print].

Pérez-Cruz, C., Carrión, O., Delgado, L., Martinez, G., López-Iglesias, C., and Mercade, E. (2013). New type of outer membrane vesicle produced by the gram-negative bacterium *Shewanella vesiculosa* M7^T: implications for DNA content. *Appl. Environ. Microbiol.* 79, 1874–1881. doi: 10.1128/AEM.03657-12

Pérez-Cruz, C., Delgado, L., López-Iglesias, C., and Mercade, E. (2015). Outer-inner membrane vesicles naturally secreted by gram-negative pathogenic bacteria. *PLoS One* 10:e0116896. doi: 10.1371/journal.pone.0116896

Quinlan, A. R., and Hall, I. M. (2010). BEDTools: a flexible suite of utilities for comparing genomic features. *Bioinformatics* 26, 841–842. doi: 10.1093/bioinformatics/btq033

Raju, K. K., Gautam, S., and Sharma, A. (2006). Molecules involved in the modulation of rapid cell death in *Xanthomonas*. *J. Bacteriol.* 188, 5408–5416. doi: 10.1128/JB.00056-06

Roier, S., Zingl, F., Cakar, F., and Schild, S. (2016). Bacterial outer membrane vesicle biogenesis: a new mechanism and its implications. *Microb. Cell* 3, 257–259. doi: 10.15698/mic2016.06.508

Rumbo, C., Fernández-Moreira, E., Merino, M., Poza, M., Mendez, J. A., Soares, N. C., et al. (2011). Horizontal transfer of the OXA-24 carbapenemase gene *via* outer membrane vesicles: a new mechanism of dissemination of carbapenem resistance genes in *Acinetobacter baumannii*. *Antimicrob. Agents Chemother.* 55, 3084–3090. doi: 10.1128/AAC.00929-10

Schindelin, J., Arganda-Carreras, I., Frise, E., Kaynig, V., Longair, M., Pietzsch, T., et al. (2012). Fiji: an open-source platform for biological-image analysis. *Nat. Methods* 9, 676–682. doi: 10.1038/nmeth.2019

Schooling, S. R., and Beveridge, T. R. (2006). Membrane vesicles: an overlooked component of the matrices of biofilms. *J. Bacteriol.* 188, 5945–5957. doi: 10.1128/JB.00257-06

Schwechheimer, C., and Kuehn, M. J. (2015). Outer-membrane vesicles from gram-negative bacteria: biogenesis and functions. *Nat. Rev. Microbiol.* 13, 605–619. doi: 10.1038/nrmicro3525

Tashiro, Y., Ichikawa, S., Shimizu, M., Toyofuku, M., Takaya, N., Nakajima-Kambe, T., et al. (2010). Variation of physiochemical properties and cell association activity of membrane vesicles with growth phase in *Pseudomonas aeruginosa*. *Appl. Environ. Microbiol.* 76, 3732–3739. doi: 10.1128/AEM.02794-09

Toyofuku, M., Nomura, N., and Eberl, L. (2019). Types and origins of bacterial membrane vesicles. *Nat. Rev. Microbiol.* 17, 13–24. doi: 10.1038/s41579-018-0112-2

Toyofuku, M., Roschitzki, B., Riedel, K., and Eberl, L. (2012). Identification of proteins associated with the *Pseudomonas aeruginosa* biofilm extracellular matrix. *J. Proteome Res.* 11, 4906–4915. doi: 10.1021/pr300395j

Turnbull, L., Toyofuku, M., Hynen, A. L., Kurosawa, M., Pessi, G., Petty, N. K., et al. (2016). Explosive cell lysis as a mechanism for the biogenesis of bacterial membrane vesicles and biofilms. *Nat. Commun.* 7:11220. doi: 10.1038/ncomms11220

Vaser, R., Sović, I., Nagarajan, N., and Šikić, M. (2017). Fast and accurate de novo genome assembly from long uncorrected reads. *Genome Res.* 27, 737–746. doi: 10.1101/gr.214270.116

Wadhawan, S., Gautam, S., and Sharma, A. (2010). Metabolic stress-induced programmed cell death in *Xanthomonas*. *FEMS Microbiol. Lett.* 312, 176–183. doi: 10.1111/j.1574-6968.2010.02114.x

Walker, B. J., Abeel, T., Shea, T., Priest, M., Abouelliel, A., Sakthikumar, S., et al. (2014). Pilon: an integrated tool for comprehensive microbial variant detection and genome assembly improvement. *PLoS One* 9:e112963. doi: 10.1371/journal.pone.0112963

Wieser, A., Storz, E., Liegl, G., Peter, A., Pritsch, M., Shock, J., et al. (2014). Efficient quantification and characterization of bacterial outer membrane derived nano-particles with flow cytometric analysis. *Int. J. Med. Microbiol.* 304, 1032–1037. doi: 10.1016/j.ijmm.2014.07.012

Zhang, J., Kobert, K., Flouri, T., and Stamatakis, A. (2014). PEAR: a fast and accurate Illumina paired-end reAd mergeR. *Bioinformatics* 30, 614–620. doi: 10.1093/bioinformatics/btt593

Conflict of Interest: The authors declare that the research was conducted in the absence of any commercial or financial relationships that could be construed as a potential conflict of interest.

Publisher's Note: All claims expressed in this article are solely those of the authors and do not necessarily represent those of their affiliated organizations, or those of the publisher, the editors and the reviewers. Any product that may be evaluated in this article, or claim that may be made by its manufacturer, is not guaranteed or endorsed by the publisher.

frontiers in Microbiology

ORIGINAL RESEARCH
published: 15 October 2021
doi: 10.3389/fmicb.2021.748706

Francisella tularensis Outer Membrane Vesicles Participate in the Early Phase of Interaction With Macrophages

Ivona Pavkova[1†], Jana Klimentova[1†], Jan Bavlovic[1], Lenka Horcickova[1], Klara Kubelkova[1], Erik Vlcak[2], Helena Raabova[2], Vlada Filimonenko[2,3], Ondrej Ballek[4] and Jiri Stulik[1]*

[1] Department of Molecular Pathology and Biology, Faculty of Military Health Sciences, University of Defence, Hradec Kralove, Czechia, [2] Electron Microscopy Core Facility, Institute of Molecular Genetics of the Czech Academy of Sciences, Prague, Czechia, [3] Department of Biology of the Cell Nucleus, Institute of Molecular Genetics of the Czech Academy of Sciences, Prague, Czechia, [4] Laboratory of Immunobiology, Institute of Molecular Genetics of the Czech Academy of Sciences, Prague, Czechia

OPEN ACCESS

Edited by:
Alejandro J. Yañez, Austral University of Chile, Chile

Reviewed by:
Lee-Ann H. Allen, University of Missouri, United States
Zhuo Ma, Albany College of Pharmacy and Health Sciences, United States

***Correspondence:**
Jana Klimentova
jana.klimentova@unob.cz

† These authors have contributed equally to this work and share first authorship

Specialty section:
This article was submitted to Microbial Physiology and Metabolism, a section of the journal Frontiers in Microbiology

Received: *28 July 2021*
Accepted: *21 September 2021*
Published: *15 October 2021*

Citation:
Pavkova I, Klimentova J, Bavlovic J, Horcickova L, Kubelkova K, Vlcak E, Raabova H, Filimonenko V, Ballek O and Stulik J (2021) Francisella tularensis Outer Membrane Vesicles Participate in the Early Phase of Interaction With Macrophages. Front. Microbiol. 12:748706. doi: 10.3389/fmicb.2021.748706

Francisella tularensis is known to release unusually shaped tubular outer membrane vesicles (OMV) containing a number of previously identified virulence factors and immunomodulatory proteins. In this study, we present that OMV isolated from the *F. tularensis* subsp. *holarctica* strain FSC200 enter readily into primary bone marrow-derived macrophages (BMDM) and seem to reside in structures resembling late endosomes in the later intervals. The isolated OMV enter BMDM generally *via* macropinocytosis and clathrin-dependent endocytosis, with a minor role played by lipid raft-dependent endocytosis. OMVs proved to be non-toxic and had no negative impact on the viability of BMDM. Unlike the parent bacterium itself, isolated OMV induced massive and dose-dependent proinflammatory responses in BMDM. Using transmission electron microscopy, we also evaluated OMV release from the bacterial surface during several stages of the interaction of *Francisella* with BMDM. During adherence and the early phase of the uptake of bacteria, we observed numerous tubular OMV-like protrusions bulging from the bacteria in close proximity to the macrophage plasma membrane. This suggests a possible role of OMV in the entry of bacteria into host cells. On the contrary, the OMV release from the bacterial surface during its cytosolic phase was negligible. We propose that OMV play some role in the extracellular phase of the interaction of *Francisella* with the host and that they are involved in the entry mechanism of the bacteria into macrophages.

Keywords: *Francisella tularensis*, FSC200, outer membrane vesicles, host–pathogen interaction, macrophage, cell entry

Abbreviations: OMV, outer membrane vesicles; Ft-OMV, *F. tularensis*-derived OMV; LPS, lipopolysaccharide; BHI, brain heart infusion; OD, optical density; DMEM, Dulbecco's modified Eagle's medium; FBS, fetal bovine serum; BMDM, bone marrow-derived macrophages; PFA, paraformaldehyde; PBS, phosphate-buffered saline; MβC, methyl-β-cyclodextrin; MOI, multiplicity of infection; STED, stimulated emission depletion; SB, Sörensen's buffer; PBT, phosphate-buffered saline with 0.01% Tween 20; SEM, standard error of the mean; TEM, transmission electron microscopy.

INTRODUCTION

Release of extracellular vesicles is a highly conserved and natural process known in all kingdoms of life: in Archaea, Bacteria, and Eukarya (Gill et al., 2018). Regarding bacteria, the vesicles are known to be involved in multiple situations during their life cycle. Generally, the vesicle release serves the bacteria for interaction with the environment, for communication with other bacteria in their community, and in the case of pathogenic bacteria, also for interaction with the host (Ellis and Kuehn, 2010; Avila-Calderón et al., 2014; Jan, 2017). Vesicles of Gram-negative bacteria are derived from their outer membrane, thus are termed outer membrane vesicles (OMV), and they are formed by the bulging of the membrane and closing inside a portion of the periplasm (Schwechheimer and Kuehn, 2015). Being derived from the bacterial envelope, OMV are highly enriched in such immunostimulatory materials as the outer membrane proteins, lipids, lipoproteins, glycoproteins, and lipopolysaccharide. The cargo of pathogenic bacteria OMV also often contains virulence factors, toxins, or other biologically active molecules that play important roles in host–pathogen interaction. OMV are known to enhance the invasiveness and survival of bacteria inside the host (Jan, 2017). OMV can increase the bacterial adherence to various surfaces (Ellis and Kuehn, 2010), they are part of the membrane stress response to hostile environments (MacDonald and Kuehn, 2013; Klimentova et al., 2019), and they can modulate the host immune response (Kaparakis-Liaskos and Ferrero, 2015). Great attention is currently focused on the vaccine potential of OMV because of their strong immunomodulatory effect, self-adjuvant characteristic, and the ease of genetic modifications (Acevedo et al., 2014; Bitto and Kaparakis-Liaskos, 2017; Yang et al., 2018; Gerritzen et al., 2019).

The diverse fates of OMV released from extracellular bacteria inside the host encompass interaction with the extracellular matrix or direct effects on the host cells. The latter proceed after binding to one of the host surface structures, either by membrane fusion followed by the release of the vesicle's inner content directly into the host cell cytosol or by the vesicle's internalization. The internalization of OMV may proceed *via* various pathways, and their further intracellular trafficking depends upon the type of vacuole within which they end up. OMV engulfment by immune cells is also the explanation for lipopolysaccharide (LPS) intracellular sensing and the non-canonical inflammasome activation observed in extracellular bacteria (Vanaja et al., 2016). Much less is known about the OMV secretion from intracellularly surviving bacteria during their intracellular phase. The secretion of OMV inside macrophages has been proven by electron microscopy in *Salmonella* (Yoon et al., 2011), *Listeria* (Vdovikova et al., 2017), and *Mycobacteria* (Prados-Rosales et al., 2011; Athman et al., 2015). In *Legionella pneumophila*, OMV have been found to inhibit the phagosome–lysosome fusion and to interrupt phagosome maturation in order to allow the intracellular survival and replication of bacteria (Fernandez-Moreira et al., 2006).

Francisella tularensis, a Gram-negative facultative intracellular bacterium, is one of the most infectious bacteria and is a potential biological warfare agent (Dennis et al., 2001; Oyston, 2008). The extremely high virulence of *Francisella* is caused by its ability to invade and proliferate inside a range of host cell types—macrophages and dendritic cells being its primary target cells (Celli and Zahrt, 2013)—and its ability to successfully overcome innate immune mechanisms (Putzova et al., 2017; Fabrik et al., 2018). After internalization, *Francisella* resides in a phagosomal vacuole, the maturation to phagolysosome of which is arrested by a yet unknown mechanism, it escapes rapidly into the cytosol, and there it proliferates (Clemens and Horwitz, 2007; Celli and Zahrt, 2013; Ozanic et al., 2015). *Francisella* spp. have been described to produce OMV of tubular shape that contain a number of virulence factors and take part in bacterial stress response (McCaig et al., 2013; Sampath et al., 2018; Klimentova et al., 2019, 2021). Similar membrane nanotubes with adhesive and communication functions have been described in *Salmonella typhimurium* (Galkina et al., 2011). In *Francisella novicida*, which is a close relative to *F. tularensis* but displays very low virulence in human, the formation of tubular outer membrane protrusions has been shown to occur in close vicinity to the macrophage cytoplasmic membrane in the early stage of interaction (McCaig et al., 2013).

In the present study, we focused on the effects on the host cells of OMV released by the virulent *F. tularensis* subsp. *holarctica* strain FSC200. We describe here the entry of isolated and purified OMV into the host cells with a view also to their further intracellular fate. The vesicles proved to be non-toxic *in vitro* to primary macrophages, but they triggered a strong proinflammatory response that is in contrast with the ability of the bacterium itself to efficiently inhibit the immune pathways. We also documented OMV release from the parent bacteria in contact with the host cells during the early stage of the bacterial internalization by macrophages. On the contrary, we were not able to prove OMV release from the bacterial surface during its cytosolic phase. Our findings nevertheless point to the engagement of *Francisella* OMV in the pathogenesis of the bacterium and their future potential in the research of protective agents.

MATERIALS AND METHODS

Bacterial Strains and Cultivation

Francisella tularensis subsp. *holarctica* strain FSC200 (Johansson et al., 2000) was kindly provided by Åke Forsberg (Swedish Defence Research Agency, Umeå, Sweden). FSC200 with inactivated production of O-antigen (FSC200/Δ*wbtDEF*) from an earlier study (Balonova et al., 2012) was used here. Stock bacteria were pre-cultivated on McLeod agar supplemented with bovine hemoglobin and IsoVitaleX (Becton Dickinson, Le Pont de Claix, France) at 37°C for 24 h. Brain heart infusion (BHI; Becton Dickinson) was prepared according to the manufacturer's instructions. pH was adjusted with HCl to 6.8, and it was sterile filtered instead of autoclaved.

Outer Membrane Vesicles Isolation and Purification

Outer membrane vesicles were prepared as described earlier (Klimentova et al., 2019). Briefly, bacteria from agar plate were

inoculated to BHI and pre-cultivated for 10–14 h at 37°C and 200 rpm. Starting cultures were pelleted (6,000 × *g*, 15 min at 25°C), diluted with fresh medium to OD_{600} = 0.1, and then cultivated for 14–16 h [final optical density (OD) of approx. 0.6]. Bacteria were removed by low-speed centrifugation and the supernatants sterilized by filtration through a 0.22-μm vacuum-driven filter. Culture filtrates were concentrated using an Amicon® Stirred Ultrafiltration Cell through membrane of regenerated cellulose with 100 kDa cutoff (both Millipore, Billerica, MA, United States) and subsequently pelleted (100,000 × *g*, 90 min at 4°C). The pellet was resuspended in 45% (*w*/*v*) OptiPrep (Sigma-Aldrich, St. Louis, MO, United States) in 10 mM HEPES/0.85% NaCl, pH 7.4 (HEPES buffer), and overlaid with a step OptiPrep gradient of 40%–20%. The gradient was centrifuged at 100,000 × *g* for 16–20 h at 4°C in a swinging-bucket rotor. After centrifugation, the top fractions containing a clearly visible opaque white band were carefully collected, diluted 8× with HEPES buffer, and centrifuged (100,000 × *g*, 2 h at 4°C). The supernatant was removed and the pellet washed again (same conditions) to remove the residual OptiPrep. The final pellet was suspended in physiological saline and the protein concentration determined with Micro BCA™ Protein Assay Kit (Pierce, Rockford, IL, United States). OMV samples were stored at +4°C for up to 2 weeks.

Cell Culture

The human alveolar type II epithelial cell line A549 (ATCC® CCL-185™) and the mouse BALB/c monocyte–macrophage cell line J774.2 (Merck, Darmstadt, Germany) were cultured in Dulbecco's modified Eagle's medium (DMEM) supplemented with 10% (*v*/*v*) fetal bovine serum (FBS; United States origin, Sigma-Aldrich) at 37°C in 5% CO_2.

Bone marrow-derived macrophages (BMDM) were generated from the femurs and tibias of 6- to 10-week-old female BALB/c mice as described previously (Celli, 2008). Briefly, cells flushed from the bone marrow were placed in bacteriological Petri dishes and differentiated in DMEM supplemented with 10% FBS, 20% (*v*/*v*) L929-conditioned medium (as a source of macrophage colony-stimulating factor), and 50 U/ml penicillin/50 μg/ml streptomycin (only for the first 3 days of cultivation). After 6 days of differentiation, the BMDM were seeded on tissue culture-treated multiwell plates at the desired density as further specified in the relevant assay procedure.

Outer Membrane Vesicles Internalization Assays

To detect the ability of OMV to invade host cells, BMDM, J774.2, or A549 cells were seeded onto sterile glass coverslips in 24-well plates (at a concentration of 1 × 10^5 cells/well) and treated with OMV (0.5 μg) for 10 min or for 1, 4, or 24 h. At indicated times, the cells were fixed in 3.7% paraformaldehyde (PFA; pH 7.2) for 10 min at room temperature (RT), washed three times with phosphate-buffered saline (PBS), quenched with 50 mM ammonium chloride for 10 min at RT, and then washed three times with PBS. The cells were next permeabilized with 0.1% Triton X-100 for 5 min at RT and blocked with 3% (*w*/*v*) bovine serum albumin (BSA) in PBS for 60 min at RT. To label the internalized OMV, the cells were first incubated with purified immune rabbit polyclonal anti-*F. tularensis* serum and then, after four washes with PBS, with Alexa Fluor™ 488 anti-rabbit immunoglobulin G (IgG; Life Technologies, Carlsbad, CA, United States). Actin was labeled with phalloidin-TRITC (Sigma-Aldrich) and nuclei with DAPI (Invitrogen, Waltham, MA, United States) according to the manufacturers' instructions. After three washes with PBS and one wash with deionized water, the coverslips were mounted on glass slides with ProLong Diamond Antifade Mountant (Invitrogen) and imaged on a Nikon Eclipse Ti fluorescence microscope equipped with a Plan-Apochromat ×60/1.4 oil immersion objective (Nikon, Tokyo, Japan) and the NIS Elements Image Analyzer (version 4.20, Nikon).

To determine the effects of endocytosis inhibitors on OMV uptake, the BMDM were pretreated with methyl-β-cyclodextrin (MβC, 10 mM), cytochalasin D (10 μM), wortmannin (100 nM), filipin (1 μg/ml), amiloride (10 mM), dansylcadaverine (150 μM), or dynasore (80 μM) (Sigma-Aldrich) for 30 min at 37°C. The cells were then exposed for 1 h to OMV (0.5 μg) isolated from the wild-type FSC200 strain or FSC200/Δ*wbtDEF* and thereafter fixed and further processed for microscopy as described above. Non-treated and DMSO-treated cells were used as negative controls. For cell entry quantification, 200 cells from randomly selected fields were evaluated. Results are reported as percentages of the 200 cells analyzed or as the mean of a given dataset.

Cell Viability, Cytotoxicity Assay, and Apoptotic Assay

To follow the viability and cytotoxic effect of *F. tularensis* FSC200 OMV, the cells were seeded in 96-well tissue culture plates at concentrations of 2 × 10^4 cells/well for BMDM, 0.5 × 10^4 cells/well for J774.2, and 0.5 × 10^3 cells/well for A549 and allowed to adhere overnight. The cell numbers had been optimized by preliminary experiments. The next day, the supernatant was discarded and the cells incubated with OMV (1, 0.5, or 0.05 μg of OMV protein per 1 × 10^4 cells) in 50 μl of DMEM/well. After 30 min, additional DMEM was added to a final volume of 100 μl/well and the cells were incubated in DMEM at 37°C with 5% CO_2. BMDM and J774.2 were infected with *F. tularensis* FSC200 at a multiplicity of infection (MOI) of 50 and 100, respectively, for 30 min. The extracellular bacteria were then washed out and the cells further incubated in DMEM. The cell viability was observed in real time using a non-lytic bioluminescence RealTime-Glo™ MT Cell Viability Assay (Promega, Madison, WI, United States). Cytotoxicity was assayed in parallel using fluorescence CellTox™ Green Cytotoxicity Assay (Promega). The luminescent Caspase-Glo 3/7 Assay (Promega) was used for the measurement of the activity of caspase-3/caspase-7. The samples were processed and the luminescence and fluorescence were measured at indicated time points on a FLUOStar OPTIMA plate reader (BMG Labtech, Ortenberg, Germany) according to the manufacturer's instructions.

Evaluation of Cytokine Release in Outer Membrane Vesicles-Treated Macrophages

For the evaluation of cytokine release by cytokine arrays, the BMDM seeded on 96-well plates at a concentration of 2×10^4 cells/well were treated with 1 or 0.1 μg OMV in 150 μl DMEM or infected with the FSC200 strain at MOI of 50 in the same manner as that for the cell viability assay (see above). The supernatants were collected after 4 and 24 h of co-incubation and stored at −80°C until needed. The cytokine profiles were analyzed in collected undiluted supernatants using a fluorescence-based multiplex Quantibody ELISA microarray chip (RayBiotech, Norcross, GA, United States) with the following set of screened cytokines: granulocyte colony-stimulating factor (G-CSF), granulocyte–macrophage colony-stimulating factor (GM-CSF), interleukin 1α (IL-1α), IL-1β, IL-2, IL-3, IL-4, IL-5, IL-6, IL-7, IL-9, IL-10, IL-12p70, IL-13, IL-15, IL-17, IL-21, IL-23, IFN-γ, tumor necrosis factor alpha (TNF-α), CXCL-1 (keratinocyte-derive chemokine, KC), monocyte chemoattractant protein 1 (MCP-1), macrophage colony-stimulating factor (M-CSF), RANTES (regulated on activation, normal T-cell expressed, and secreted), and vascular endothelial growth factor (VEGF). The evaluation was performed according to the manufacturer's protocol. The cytokine concentrations were calculated against the standards using the software H20 OV Q-Analyzer v8.20.4 (RayBiotech). Three replicates of each sample were evaluated for each cytokine in one experiment. The experiments were repeated two or four times, with comparable results.

For confirmation, cytokines that were significantly changed were also quantified by means of classical enzyme-linked immunosorbent assay (ELISA). BMDM at a concentration of 1×10^5 cells/well were adhered on 24-well plates and treated with 200 μl of DMEM containing 0.5 or 5 μg of OMV or infected with FSC200 at MOI of 50. The plates were centrifuged at 400 × *g* for 5 min at RT. After 1 h of incubation, the infected cells were washed twice with PBS to remove the extracellular bacteria and further cultivated in 500 μl of fresh DMEM. To the OMV-treated cells, 300 μl of fresh DMEM was added at the same time. At 4 and 24 h of co-incubation, the cell supernatants were collected and stored at −80°C until needed. The quantities of secreted cytokines/chemokines were measured using mouse ELISA kits against IL-1α, IL-6, IL-10, IL-12p70, TNF-α, GM-CSF, MCP-1, and CXCL-1 (KC) (Thermo Fisher Scientific, Waltham, MA, United States) according to the manufacturer's instructions. The absorbance was measured at 450 nm on a Paradigm detection platform (Beckman Coulter, Brea, CA, United States). The resulting concentrations were determined from standard calibration curves.

Stimulated Emission Depletion Super-Resolution Microscopy

For immunofluorescence, the staining protocol was adopted from www.cellsignal.com, with some modifications. Briefly, the differentiated BMDM were attached to no. 1.5 CSHP high-precision cover glasses (Paul Marienfeld, Lauda-Königshofen, Germany) at a concentration of 5×10^5 cells/well in 24-well plates and treated with OMV at a dose of 0.5 μg/1×10^5 cells or infected with FSC200 at MOI of 50, followed by centrifugation at 400 × *g* for 5 min at RT for synchronization. The extracellular bacteria were removed by a thorough wash with PBS (three times). At selected time intervals (1, 6, and 12 h post-treatment), the cells were washed with warm PBS (three times), fixed with 4% PFA for 15 min at RT, and then washed again three times with PBS. After PFA fixation, the cells were permeabilized with ice-cold methanol for 10 min at −20°C. The cells were blocked for 1 h in PBS containing 0.1% saponin (Sigma-Aldrich) with the addition of 2.5% fetal calf serum and 2.5% BSA and then incubated with primary antibodies [mouse anti-*F. tularensis* LPS monoclonal antibody FB11 (Abcam, Cambridge, United Kingdom) and rat anti-MHC class II antibody M5/114.15.2 (BioLegend, San Diego, CA, United States)] and secondary antibodies (goat anti-mouse Alexa 555 and goat anti-rat Alexa 488) for 1 h each consecutively. The coverslips were mounted using 4% *n*-propyl gallate in glycerol. Samples were analyzed with stimulated emission depletion (STED) super-resolution microscopy (Leica TCS SP8 STED 3X, 660-nm CW depletion laser). Image reconstruction was performed using Huygens Professional (SVI) software and post-editing was with Fiji imaging software (Schindelin et al., 2012).

Transmission Electron Microscopy

Examination of *F. tularensis* Interaction With Macrophages

For the morphological analysis of the adherence and phagocytic uptake of *F. tularensis*, we proceeded as previously described, albeit with minor modifications (Clemens et al., 2012; McCaig et al., 2013). Briefly, 6×10^6 of BMDM were pelleted (800 × *g*, 10 min at 4°C) and 1 ml of *F. tularensis* FSC200 bacterial suspension (chilled to 4°C) was added to the pelleted cells at an approximate MOI of 2,000. The cells were centrifuged sequentially at 200 × *g* and 800 × *g*, each for 10 min at 4°C. The supernatant was removed and the tube with cells and bacteria pellets was placed in a 37°C water bath for 5 min and then fixed with 2.5% glutaraldehyde in 0.1 M Na/K phosphate buffer, pH 7.2–7.4 (Sörensen's buffer, SB). The cells and bacteria were then resuspended in a very small volume of SB prewarmed to 37°C and added to prewarmed 2% low-melting-point agarose in water in a 1:1 ratio. Hardened agarose with biological material was cut into small pieces and post-fixed with 1% osmium tetroxide in SB for 2 h at RT in darkness. Pieces were dehydrated in an ethanol series, and during this process, additionally stained with 1% uranyl acetate in 50% ethanol overnight at 4°C. Dehydrated pieces were embedded in Epon–Durcupan resin. After polymerization for 72 h at 60°C, resin blocks with samples were cut into 80-nm ultrathin sections and collected on 200-mesh size copper grids. The sections were examined in a JEOL JEM-1400Flash transmission electron microscope operated at 80 kV and equipped with a Matataki Flash sCMOS camera (JEOL Ltd., Tokyo, Japan).

For morphological analysis of the later infection stages, 1×10^6 cells/well adhered to the glass coverslips in 24-well

plates were infected with bacterial suspension at MOI of 100 and centrifuged at 400 × *g*, for 3 min at RT (time 0). After 1 h of incubation at 37°C in 5% CO_2, the cells were washed twice with warm PBS and further incubated in fresh DMEM under the same conditions (for a 6-h interval only). At 5 min and 6 h after infection, BMDM were washed with warm SB and fixed with 2.5% glutaraldehyde in SB for 30 min at RT and subsequently overnight at 4°C. Infected cells on glass coverslips were post-fixed with 1% osmium tetroxide in SB for 2 h at RT in darkness and later dehydrated in an ethanol series. During this process, the cells were additionally stained with 1% uranyl acetate in 50% ethanol overnight at 4°C. Afterward, the cells were embedded in Epon–Durcupan resin. After polymerization for 72 h at 60°C, resin blocks with samples were cut into 80-nm ultrathin sections and collected on 200-mesh size copper grids. Sections were examined with the JEOL JEM-1400Flash transmission electron microscope operated at 80 kV equipped with a Matataki Flash sCMOS camera (JEOL Ltd.).

For statistical analysis of the bacterial infection after 5 min, the Limitless Panorama ultrawide area montage system (JEOL Ltd.) was used, which enables capturing a large area of the sample containing 213 cells. The collected image data were manually processed and every cell was visually evaluated with reference to specific criteria. If a cell was infected, the total number of bacteria in its cytoplasm was counted and an evaluation was made on whether these bacteria were encapsulated in phagosome or had direct contact to the cytoplasm. The number of bacteria in each category was counted. Subsequently, each bacterium was evaluated for the presence of OMV. Those with developed OMV were counted and evaluated for whether they were encapsulated in complete phagosome or had direct contact to the cytoplasm.

Examination of Macrophage Interaction With Isolated Outer Membrane Vesicles

Bone marrow-derived macrophages (1×10^6 cells/well) adhered to the glass coverslips in 24-well plates were treated with approximately 8 μg of OMV in 200 μl/well of DMEM, centrifuged at 800 × *g* for 5 min at RT, and then incubated at 37°C in 5% CO_2. After 1 h, 800 μl of warm DMEM was added to each well. At 1, 6, and 24 h, the cells were briefly rinsed with warm SB and fixed in 3% freshly depolymerized PFA with 0.25% glutaraldehyde in SB (1 h at RT). Chemical fixation continued with incubation in 0.02 M glycine in SB for 10 min and dehydration in an ethanol series, all on ice. The samples were embedded in LR White acrylic resin and polymerized for 72 h at 4°C under UV light. Resin blocks with samples were cut into 80-nm ultrathin sections and collected on 200-mesh size copper grids.

For immunolabeling, 80-nm ultrathin sections on 200-mesh gilded grids were first placed for 20 min on 10% normal serum, 0.2% cold water fish skin gelatin in PBS with 0.01% (*v*/*v*) Tween 20 (PBT) containing 1% (*w*/*v*) BSA, and then incubated with anti-LPS primary antibody in 1% normal serum, 0.2% cold water fish skin gelatin in PBT with 1% BSA for 1 h. After a series of washing with PBT, the sections were incubated with secondary goat anti-mouse 12 nm gold-conjugated antibody in 1% normal serum, 0.2% cold water fish skin gelatin in PBT with 1% BSA for 1 h. The sections were then repeatedly washed in PBT and double-distilled water, air dried, and then examined in the JEOL JEM-1400Flash transmission electron microscope operated at 80 kV equipped with a Matataki Flash sCMOS camera (JEOL Ltd.).

Statistical Analysis

Each experiment was independently repeated at least three times, and the assay was performed in triplicate for each time interval and strain in an experiment. The ELISA experiment was performed in triplicate and repeated twice, with similar results. The Prism 6 program (GraphPad, San Diego, CA, United States) was used for the statistical analysis. The values were expressed as the mean ± standard error of the mean (SEM) and analyzed for significance using ANOVA with a recommended multiple-comparison posttest. Differences were considered statistically significant at $p < 0.05$. Cell viability, cytotoxicity, and caspase-3/caspase-7 activity were expressed as percentages relative to the untreated control.

RESULTS

Interaction of *F. tularensis* Outer Membrane Vesicles With Host Cell

Outer Membrane Vesicles Enter and Accumulate in Macrophages, but Not Epithelial Cell Line A549

The direct interaction or internalization of OMV derived from pathogenic bacteria has been reported in a number of studies. We therefore decided to first verify the ability of *F. tularensis*-derived OMV (Ft-OMV) to interact with macrophages and epithelial cells. Macrophages are generally regarded as the primary mammalian target cells of *F. tularensis* replication, but this pathogen is also able to occupy non-phagocytic epithelial cells (Hall et al., 2007; Craven et al., 2008; Lo et al., 2013). The isolated OMV were co-incubated with primary bone marrow macrophages, the monocyte–macrophage cell line J774.2, or the lung epithelial cell line A549 for 10 min or for 1, 4, and 24 h. OMV were then visualized using the purified immune rabbit polyclonal anti-*F. tularensis* serum and FITC-labeled secondary antibody and evaluated using fluorescence microscopy. Whereas only sporadic amounts of OMV were detected within the A549 epithelial cells in any of the monitored time intervals (**Supplementary Figure 1**), the OMV were observed inside the BMDM after only 10 min of co-incubation. Moreover, the amounts of internalized vesicles increased continuously, and at 24 h, the green fluorescence signal indicating OMV presence was accumulated mostly around the cell nucleus (**Figure 1A**). A similar rate of OMV entry was also observed for the J774.2 cell line. To ensure that OMV really do accumulate inside the host cells and do not stick onto their surfaces, we also confirmed our observation using high-resolution microscopy (STED) (**Figure 1B**).

Outer Membrane Vesicles–Host Cell Interaction Analyzed by Immunoelectron Microscopy

To further analyze the interaction of Ft-OMV with primary macrophages, we utilized immunoelectron microscopy of

ultrathin sections of BMDM exposed to Ft-OMV for 1, 6, and 24 h. The OMV were visualized using immunogold labeling with the anti-LPS antibody (**Figures 2A–C**). Already 1 h after the exposure, multiple clusters of gold particles were observed indicating the position of the anti-LPS antibody binding sites (**Figure 2A**). The labeling was mostly clustered in groups and connected with some underlying medium dark roundish structures, usually with a light spot surrounded by the labels. Because cellular membranes are commonly not well preserved in samples processed for immunolabeling due to mild fixation and the extractive effect of dehydration and monomeric acrylic resin, it is sometimes difficult unambiguously to define by morphology the type of membrane-bounded structures. Due to this uncertainty, the labeled cellular structures were not exactly identified.

The size of these labeled cellular structures was up to 0.6 μm in diameter. Smaller clusters of labeling (5–20 gold particles) were associated with cellular structures of all sizes, while a majority of larger clusters (greater than 20 gold particles) were found at structures with larger sizes (approx. 0.5 μm). These bigger structures with large gold particle clusters were in all samples in the minority compared to the number of structures labeled with small clusters. Labeling clusters surrounding the light spots were mostly rather localized on the periphery of the structure, but wholly covered structures were found as well (**Figure 2D**). The larger structures had either a homogenous appearance or revealed a more complex inner structure with dark spots, morphologically resembling late endosomes. These described types of labeled structures were present in all exposed samples. Nevertheless, the overall labeling characteristic changed with the Ft-OMV exposure time. With prolonged time of exposure of the cells to Ft-OMV, the ratio of the smaller to the larger gold particle clusters, as well as the total number of labeled cellular structures, increased. The smaller clusters were often present in groups within samples that had prolonged exposure times (**Figures 2C,D**). The bigger cellular structures were also labeled at later stages, but the labeling then showed smaller gold particle clusters, while the large clusters still remained in the minority and their numbers did not visibly increase with the exposure time. This overall observation might indicate the accumulation of OMV inside the BMDM over time.

Effect of *F. tularensis*-Derived OMV on Host Cell Viability

As Ft-OMV had previously been shown to contain a number of known virulence factors (McCaig et al., 2013; Klimentova et al., 2019, 2021), we expected that they might have a direct impact on host cells. We therefore examined the effect of isolated Ft-OMV on the viability of host cells by monitoring the cell-reducing potential and changes in the cell membrane integrity. Three various doses of purified Ft-OMV were added to BMDM, J774.2, or A549 cells and the indicated parameters were observed during 48 h of co-incubation. In BMDM and J774.2, we additionally measured the activity of caspase-3 and caspase-7, the primary effector caspases in the apoptosis pathway, 24 h after the co-incubation. In primary BMDM, none of the three applied doses of OMV showed a significant effect on the cell viability and

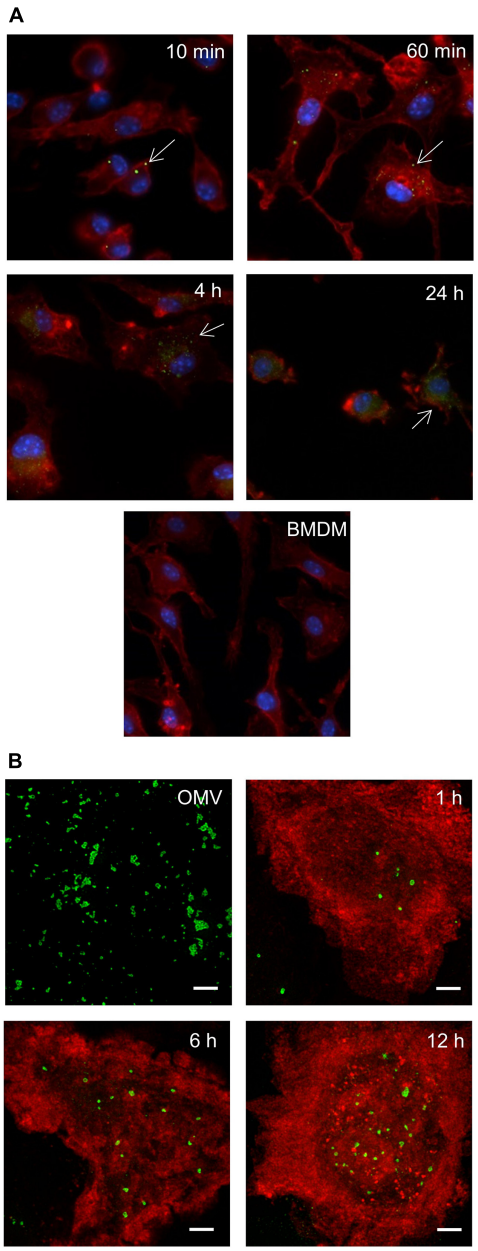

FIGURE 1 | Outer membrane vesicle (OMV) entry into bone marrow-derived macrophages (BMDM) by fluorescence microscopy. BMDM seeded on cover glasses were co-incubated with *Francisella tularensis*-derived OMV (Ft-OMV) for the indicated time, fixed, and immunostained for fluorescence microscopy **(A)** and stimulated emission depletion (STED) microscopy **(B)**. **(A)** Ft-OMV were visualized by immunostaining with purified immune rabbit polyclonal anti-*F. tularensis* serum, followed by Alexa Fluor™ 488 anti-rabbit immunoglobulin G (IgG) (*green* signal). Actin was stained with phalloidin-TRITC (*red* signal) and cell nuclei with DAPI (*blue* signal). Arrows point to the internalized OMV. Untreated BMDM are shown as control. The accumulation of OMV signals around the nucleus is observed in the latest interval. The samples were observed using a ×60 objective. **(B)** Ft-OMV were stained with the anti-*F. tularensis* lipopolysaccharide (LPS) antibody followed by Alexa Fluor™ 555 anti-mouse IgG (*green*) and the BMDM membrane with the anti-MHC class II antibody followed by Alexa Fluor™ 488 anti-rat IgG (*red*). OMV alone are shown on the *upper left*. Shown are the maximal intensity projections of example cells from three independent experiments. Scale bar, 2 μm.

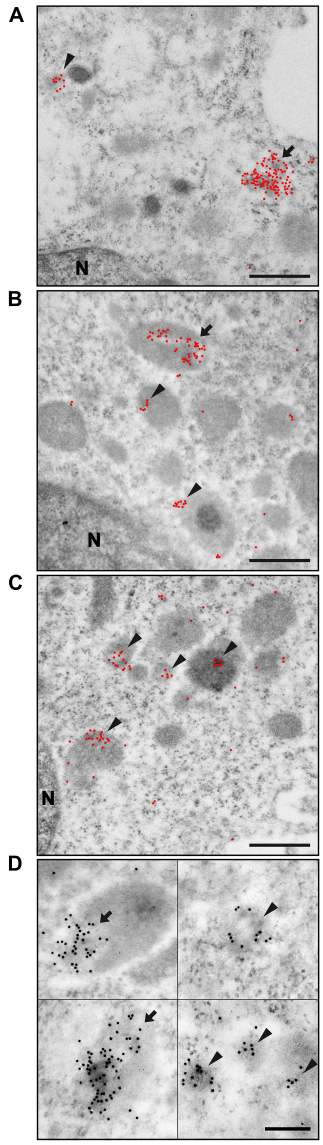

FIGURE 2 | Immunoelectron microscopy of ultrathin sections of bone marrow-derived macrophages (BMDM) exposed to *Francisella tularensis*-derived outer membrane vesicles (Ft-OMV) for 1 h **(A)**, 6 h **(B)**, and 24 h **(C)**. Gold particles are highlighted as *red dots*, small clusters are marked with an *arrowhead*, and large clusters with an *arrow*. **(A)** Immunolabeling after 1 h exposure showed the most significant fraction of large gold particle clusters (more than 20 particles per cluster) associated with darker structures of sizes around 0.5 μm. However, this fraction was still minor when compared with the smaller gold particle clusters. **(B)** After 6 h exposure, the number of large clusters decreased and the number of smaller clusters increased; the total number of clusters increased as well. **(C)** Exposure for 24 h led to a significant increase in the number of small clusters, with the large ones becoming rather rare. The high number of small clusters further increased the total number of clusters. **(D)** Details of the most typical labeled structures irrespective of exposure time. Larger aggregates localized at the periphery of the dark structure (*upper left*) or covering the entire structure (*lower left*). Smaller aggregates found as isolated (*upper right*) or in groups (*lower right*). In the *upper right picture*, typical appearance of the light spot in the darker cellular structure is shown. Scale bar, 500 nm **(A–C)** and 200 nm **(D)**. The original image without highlighted gold particles is in **Supplementary Figure 5**.

membrane integrity (**Figures 3A,B**). Interestingly, the activity rates of caspase-3/caspase-7 were significantly decreased in the OMV-treated primary BMDM compared to those of the non-treated cells or cells infected with the virulent FSC200 strain (**Figure 3C**). On the other hand, the viability of the J774.2 monocyte–macrophage cell line was significantly reduced 24 and 48 h after treatment with Ft-OMV at all dose levels (**Figure 3D**). After 24 h of incubation, higher doses of Ft-OMV caused a significant disruption of membrane integrity and increased the activity of caspase-3/caspase-7 in J774.2 (**Figures 3E,F**). No significant changes were observed in the A549 lung epithelial cell line treated with Ft-OMV (**Supplementary Figure 2**). These results might be related to the reduced ability of Ft-OMV to enter this cell line, as described above.

Taken together, our observations revealed that OMV can have different effects depending on the cell type. While primary macrophages were not significantly affected by the Ft-OMV treatment, significant signs of cytotoxicity were obvious in the macrophage cell line. For subsequent investigations, primary BMDM were selected as the primary host cell model.

F. tularensis FSC200 Outer Membrane Vesicles Enter Macrophages by Several Uptake Routes

The internalization of OMV in BMDM was further evaluated by treatment with various endocytic inhibitors prior to the addition of OMV. About 86% of non-treated or DMSO-treated cells contained an average of 5 OMV per cell after 1 h of co-incubation. Pretreatment with any of the selected inhibitors resulted in a decreased OMV uptake and decreased number of OMV per cell (**Figure 4A**). The smallest statistically non-significant effects on OMV uptake were seen with the cholesterol-binding agent filipin (76% of cells, 3 OMV per cell, a 10% reduction in internalization), the phosphatidylinositol kinase inhibitor wortmannin (77%, 2.5 OMV per cell, a 9% reduction), and dynasore, which blocks the activity of dynamin GTPase (61% of cells, 2.5 OMV per cell, a 25% reduction). On the other hand, a significant inhibition of OMV uptake was caused by the cholesterol sequestering agent MβC (51%, 2 OMV per cell, a 40% reduction), the F-actin depolymerization agent cytochalasin D (48%, 1.6 OMV per cell, a 44% reduction), and dansylcadaverine, which inhibits receptor internalization (41%, 1.8 OMV per cell, a 52% reduction). The most pronounced decrease in OMV uptake was evident with amiloride, the inhibitor of macropinocytosis (28%, 1.9 OMV per cell, a 68% reduction in internalization). These data show that OMV are able to access different uptake routes and that macropinocytosis seems to be the preferred internalization pathway. The observed effect of dansylcadaverine indicates the involvement of clathrin-dependent endocytosis. MβC is known to inhibit the internalization of caveolae and lipid raft through the depletion of cholesterol from the cell membrane. It can also perturb clathrin-mediated endocytosis inasmuch as clathrin uptake requires cholesterol as well (Rodal et al., 1999). As we detected only a minor effect of filipin, the Ft-OMV uptake inhibition induced by MβC might also be associated with its ability to disrupt the clathrin-mediated endocytosis. Neither can the possible involvement of another cholesterol-dependent mechanism be fully ruled out. Our observations are

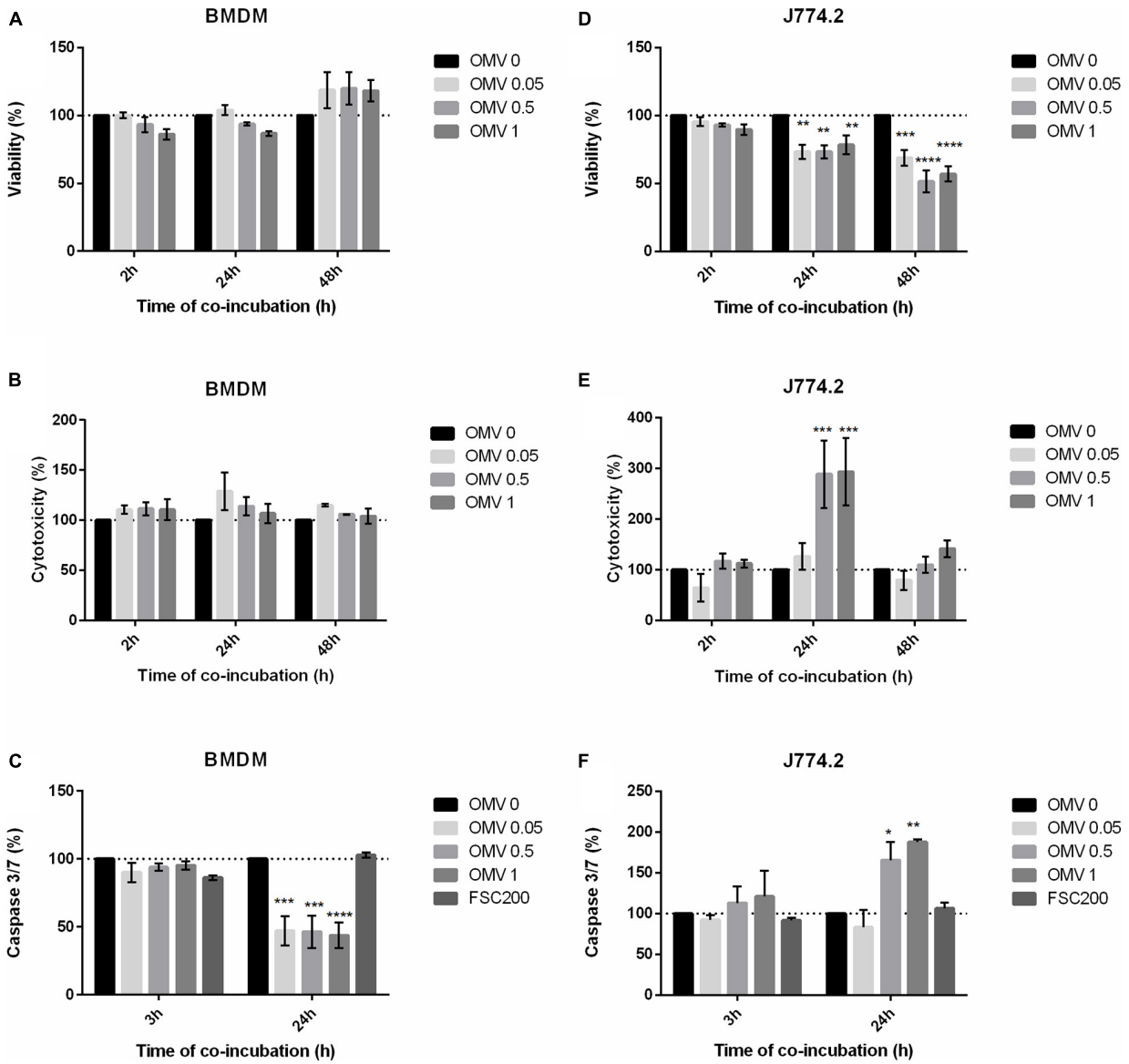

FIGURE 3 | Viability **(A,D)**, induction of cytotoxicity **(B,E)**, and apoptosis **(C,F)** in indicated cells treated with various concentrations of *Francisella tularensis*-derived outer membrane vesicles (Ft-OMV). Control groups: non-treated cells and cells infected with *F. tularensis* FSC200 (for apoptosis only). The values are expressed as percentages relative to the non-treated control (OMV 0) which is highlighted by the dotted line. Experiments were performed in triplicate wells at least three times. Data are the mean ± SEM from three independent experiments. *$p < 0.05$, **$p < 0.01$, ***$p < 0.001$, ****$p < 0.0001$ (*versus* control); two-way ANOVA with Dunnett's multiple comparisons test.

not surprising because the OMV of other bacteria have also been reported to be internalized *via* several routes, and this is widely regarded to be a consequence of their size heterogeneity (O'Donoghue and Krachler, 2016; Turner et al., 2018; Jones et al., 2020). As observed in **Figure 1B**, OMV tend to make clumps, which further contribute to their size heterogeneity. The O-antigen structural region of LPS is known to be critical for OMV entry; therefore, we also tested the uptake of OMV isolated from the *F. tularensis* FSC200 mutant strain with abrogated O-antigen production (FSC200/Δ*wbtDEF*). The only difference, in comparison to the OMV isolated from the O-antigen-positive wild-type strain, was observed in cells pretreated with MβC (**Figure 4B**). This agent had no obvious effect on the uptake of OMV derived from the O-antigen-deficient strain, thereby indicating that the presence of O-antigen is essential for the cholesterol-dependent endocytic route. Because the uptake of O-antigen-depleted OMV was affected by the inhibitor dansylcadaverine to the same extent as was that of the Ft-OMV with intact O-antigen by the cholesterol-dependent endocytic route, the O-antigen seems not to be responsible for the clathrin-dependent endocytosis. The presence of O-antigen thus seems to be crucial for the cholesterol-dependent endocytosis.

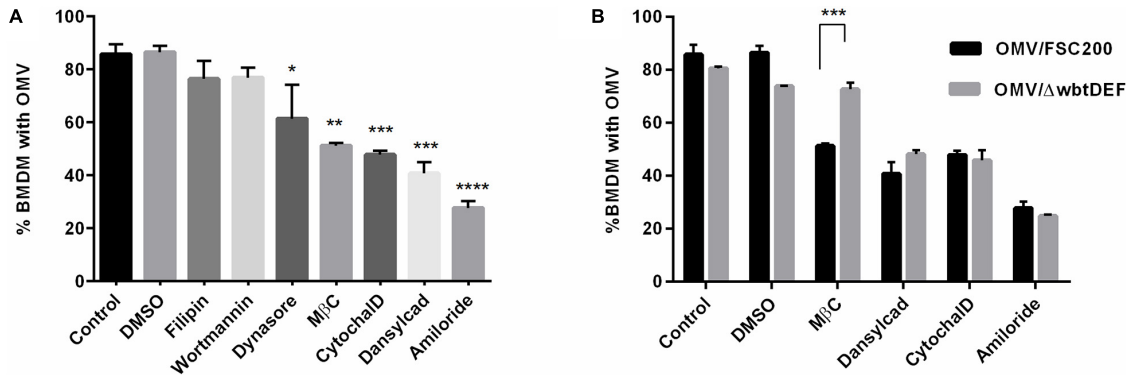

FIGURE 4 | Efficiency of outer membrane vesicle (OMV) uptake by bone marrow-derived macrophages (BMDM) pretreated with the indicated endocytosis inhibitors, DMSO (vehicle control), or untreated (control). **(A)** Pretreated cells were exposed to OMV isolated from the wild-type FSC200 strain for 1 h, and OMV uptake was then expressed as the percentage of cells with at least one internalized OMV from 200 analyzed cells. **(B)** Comparison of the uptake of OMV derived from the Δ*wbtDEF* strain with inactivated O-antigen production. Data are the mean ± SEM from three independent experiments. *$p < 0.05$, **$p < 0.01$, ***$p < 0.001$, ****$p < 0.0001$; one-way ANOVA with Dunnett's multiple comparisons test **(A)** or two-way ANOVA with Sidak's multiple comparisons test **(B)**.

Cytokine and Chemokine Release in Macrophages After Outer Membrane Vesicles Treatment

We next evaluated the immunomodulatory effects of isolated Ft-OMV on BMDM using the fluorescence-based multiplex microarray chip ELISA. As illustrated in **Figure 5**, we detected significantly increased levels of TNF-α, IL-6, IL-12p70, CXCL-1 (KC), MCP-1, IL-1α, and IL-10 and slightly increased levels of GM-CSF in the supernatants of BMDM treated with Ft-OMV. For purposes of confirmation, we also quantified the significantly changed cytokines by means of classical ELISA assay (**Supplementary Figure 3**). The effect of OMV treatment was dose-dependent and increased over time. Inasmuch as the highly induced cytokines are in general regarded as proinflammatory, the Ft-OMV seemed to evoke primarily inflammatory responses in macrophages. In contrast, the infection of BMDM by the whole viable bacterium FSC200 did not induce the release of any of the studied cytokines. This corresponds with the well-described ability of *Francisella* to actively inhibit the innate immune pathways, for which the viability and structural integrity of a bacterium are essential (Telepnev et al., 2003; Singh et al., 2013; Holland et al., 2016; Putzova et al., 2017).

F. tularensis-Derived OMV Production During Infection of Macrophages

The production of OMV in *F. tularensis* has so far been studied in bacteria cultivated extracellularly, and OMV were then isolated from the bacterial culture media (Klimentova et al., 2019, 2021). Here, we also aimed to explore whether this intracellular pathogenic bacterium produces OMV or OMV-like structures when it comes in contact with its primary host cell—the macrophage. For this purpose, we examined *F. tularensis* FSC200 during different stages of infection of BMDM using TEM. The cells were infected with bacteria grown in BHI medium to the early log phase (OD_{600} = 0.3, approx. 4 h of growth), wherein they produced only minimal amounts of vesicles (McCaig et al., 2013). To examine bacterial adherence and uptake, the bacteria at a relatively high MOI (around 2,000 bacteria per cell) were added to BMDM in suspension, fixed after 5 min of co-incubation at 37°C, and then further processed for TEM. This standard procedure should ensure contact with the cell by a sufficient number of bacteria, which is essential for TEM analysis (Clemens et al., 2005). Under these conditions, most of the bacteria were localized outside the host cells, either in contact or in close proximity to the outer side of the cytoplasmic membrane of macrophages. Only rarely were they also seen inside the BMDM (about 5%). The shape of the bacteria was very heterogeneous, but noticeable protrusions from the membrane that might represent the formation of OMV could be distinguished. The main criterion for identifying an OMV-like structure among other membrane protrusions is its distinctively prolonged (100–300 nm long) straight and narrow body with a thin base (20–50 nm wide) and a rounded tip (**Figure 6**). These OMV-like structures were seen in about 62% of the observed outside bacteria (n = 484). Most of these structures (71.4%) faced toward the host cells, and 29% of them were in direct contact with the host cell membrane. The outside bacteria were associated with the macrophages mostly *via* the OMV-like structures (94%). Some of these bacteria (78%) were in contact only *via* these protrusions. In other bacteria (36%), multiple contact points were observed, but at least one of them was *via* these structures. Only 6% of bacteria were associated without the involvement of OMV-like structures. Concerning the bacteria observed inside the BMDM (n = 27), around half of them (56%) had also formed such OMV-like structures. Most of these structures (71%) seemed to mediate the contact of bacteria with the host.

For the TEM analysis of the later infection stages, BMDM monolayers on coverslips were infected with bacteria at MOI of 100. Under these experimental conditions, only the bacteria localized inside the cells could be examined. After a 5-min co-incubation interval, about 29% of all the observed cells (n = 213) were infected with one or

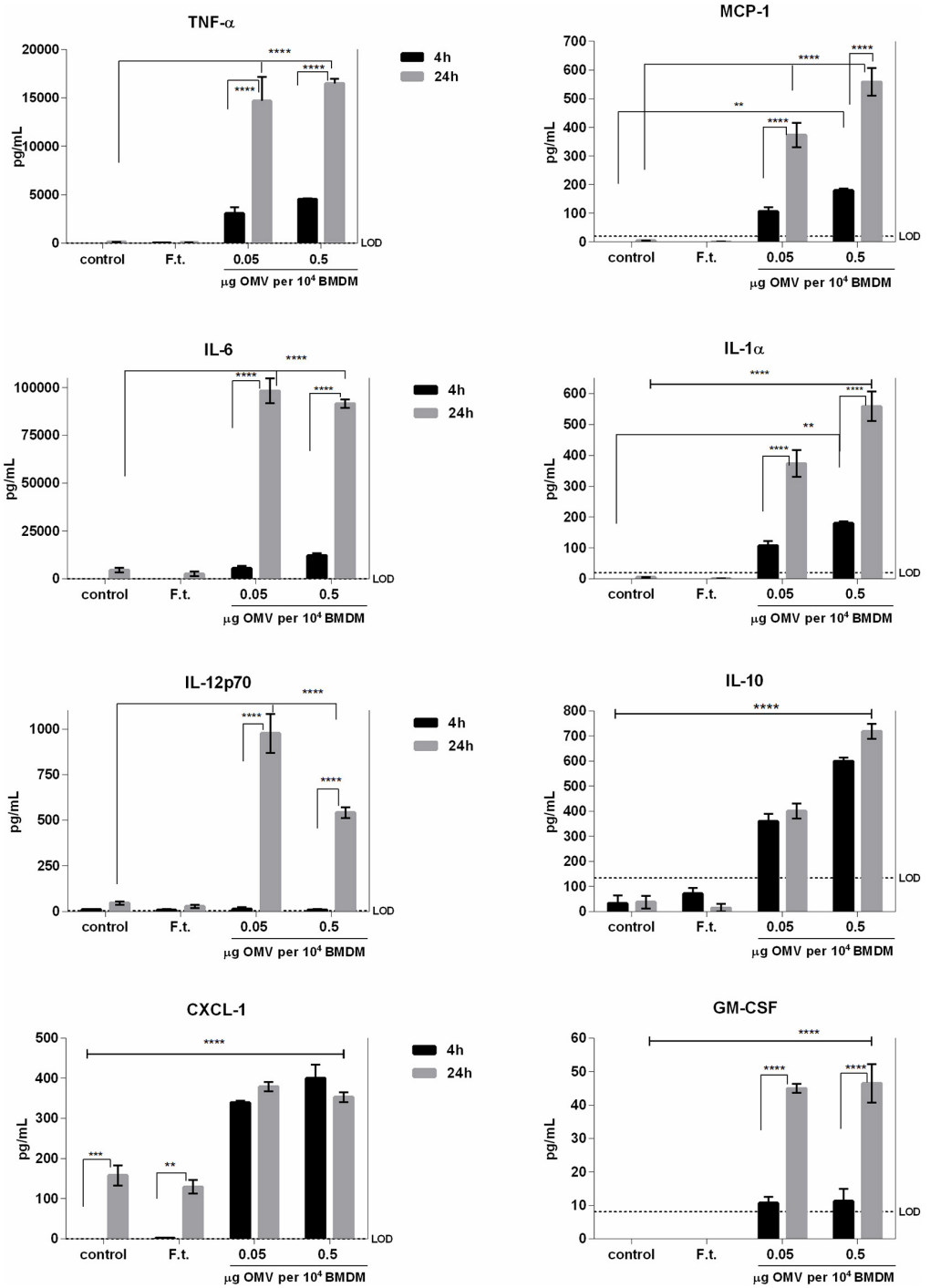

FIGURE 5 | Profiles of cytokine secretion by bone marrow-derived macrophages (BMDM) stimulated with *Francisella tularensis*-derived outer membrane vesicles (Ft-OMV). BMDM were treated with two different doses of Ft-OMV or infected with *F. tularensis* FSC200. Four and 24 h after these stimulations, the cell supernatants were collected and the indicated cytokines were quantified by fluorescence-based multiplex microarray chip ELISA. Data are representative of two to four independent experiments. $^{**}p < 0.01$, $^{***}p < 0.001$, $^{****}p < 0.0001$; two-way ANOVA with Tukey's multiple comparisons test.

two bacteria (the total number of observed bacteria was 98). Most of the bacteria (82.7%) were found in complete phagosome, with the remainder (17.3%) occurring in a phagosome only partially surrounded by the limiting membrane, thus indicating the phase of phagosomal escape. Only 9.2% of these bacteria ($n = 9$) formed an OMV-like structure, with

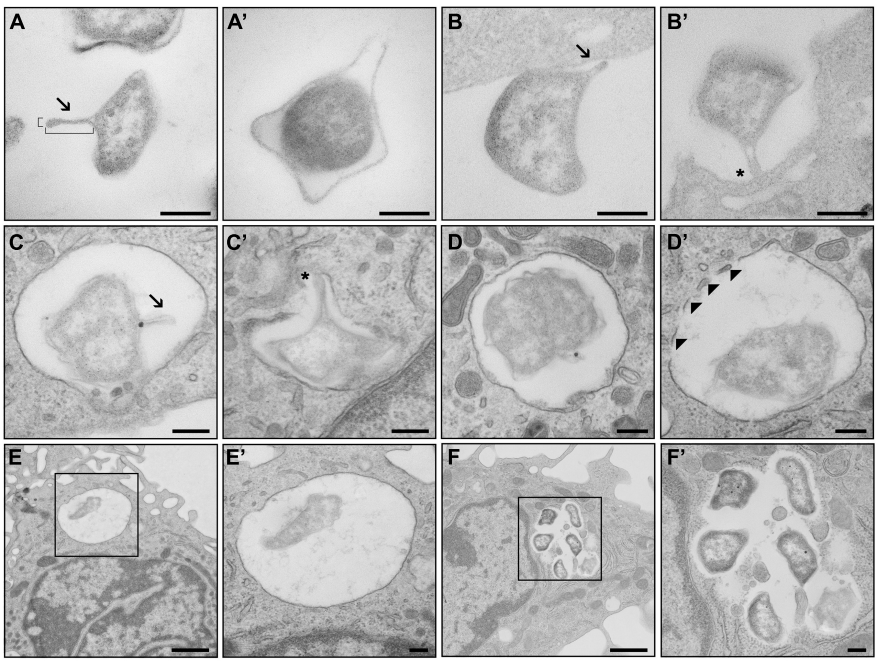

FIGURE 6 | TEM analysis of outer membrane vesicle (OMV) production during infection of macrophages. **(A)** *Francisella tularensis* with developed OMV of standard proportions (180 nm long, 40 nm wide). **(A′)** Protrusions of the outer membrane that are not OMV. **(B)** OMV of *F. tularensis* in direct contact with bone marrow-derived macrophages (BMDM) facing toward the cell. **(B′)** OMV facilitating contact of *F. tularensis* with BMDM. **(C)** *F. tularensis* encapsulated inside a phagosome of BMDM with developed OMV. **(C′)** OMV in connection with the phagosomal membrane. **(D)** *F. tularensis* encapsulated in complete phagosome of BMDM. **(D′)** Decomposition of the phagosomal membrane in the presence of *F. tularensis*. **(E)** Singular *F. tularensis* in complete phagosome 5 min after infection. **(F)** Groups of *F. tularensis* are localized freely to the cytoplasm 6 h after infection. **(E′,F′)** Higher magnification images of black boxes on **(E,F)** respectively. *Arrowheads*, fragments of phagosomal membrane; *arrows*, OMV; *asterisk*, connection of OMV to BMDM. Scale bar, 200 nm and 1 μm **(E,F)**.

nearly all of them being localized in complete phagosome ($n = 8$, 88.9%).

The contrasting data relating to the phagosomal stage most likely reflect the distinct experimental conditions applied for the infection of BMDM in suspension *vs.* BMDM in monolayer. For the BMDM in suspension, we were able to observe and evaluate primarily the adherence and uptake of bacteria and the very early phagosomal stage in only a few infected cells. On the other hand, only the phagosomal stage could be examined in monolayered BMDM infected for the same time interval (5 min). Nevertheless, in both situations, a significantly lower production of OMV-like structures was obvious in bacteria localized within a phagosome.

By 6 h post-infection, almost every cell contained a large number of bacteria. The bacteria were localized free in the cytoplasm, but they gathered in large groups mainly close to the cellular membrane. The outer membrane of the bacteria was wavier, with numerous smaller bulges all around their peripheral membrane, but no typical OMV-like structures could be distinguished.

We also attempted to visualize OMV production from intracellular bacteria 1, 6, and 12 h post-infection using the super-resolution fluorescence microscopy (STED), but no release of OMV-like structures was observed using this approach (**Supplementary Figure 4**).

DISCUSSION

The roles of OMV derived from pathogenic bacteria in relation to host cells have been demonstrated in a number of studies (Cai et al., 2018; Gao and van der Veen, 2020), and it is now widely accepted that they may contribute significantly to bacterial pathogenesis and host–pathogen interaction. Depending on the original bacterial agent and the host cell type, these structures are able to involve themselves in a diverse set of biological functions, and their final roles can be either defensive or offensive (MacDonald and Kuehn, 2012; Avila-Calderón et al., 2014; Jan, 2017). They might reinforce bacterial adhesion and invasion through the host tissues (Elmi et al., 2016; Metruccio et al., 2016). In the host cell, OMV are usually reported to elicit inflammatory responses by the induction of relevant cytokines and chemokines (Kaparakis-Liaskos and Ferrero, 2015). On the other hand, some OMV have been shown to limit inflammation and the viability of immune cells, allowing the bacteria to escape the host defense mechanisms and to proliferate imperceptibly (Chmiela et al., 2018). Many pathogenic bacteria have been reported to use OMV to transfer virulence factors to the host cells, even over a distance within the host. This has been reported not only for extracellular but also for intracellular bacteria. For example, *S. typhimurium* localized inside the *Salmonella*-containing vacuole produces OMV that can deliver genotoxin to the nuclei of bystander cells (Guidi et al., 2013).

Extracellular vesicles released from *Mycobacterium tuberculosis* transfer immunologically active glycolipids to T cells (Athman et al., 2015). On the other hand, *Listeria monocytogenes* release membrane vesicles intracellularly to control the lytic activity of listeriolysin, which promotes the bacteria to survive inside the host cell (Vdovikova et al., 2017). In other intracellular bacteria, the OMV have also been established to modulate cellular processes to favor their internalization and persistence in the host cell. OMV from *Brucella abortus* have been shown to promote bacterial internalization by human monocytes and also to downregulate the innate immune response of these cells to *Brucella* infection (Pollak et al., 2012). The OMV released by *L. pneumophila* into phagosomes are able to inhibit the phagosome–lysosome fusion (Jung et al., 2016).

The production of OMV had also been demonstrated in *Francisella* spp., but data regarding the effect on host cells remain so far very limited and moreover come from studies performed on OMV derived from non-pathogenic *F. novicida* (Pierson et al., 2011; McCaig et al., 2013). Although closely related genetically to *F. tularensis*, *F. novicida* is a separate species with significant differences in its pathogenesis and virulence (Kingry and Petersen, 2014). Pathogenic or non-pathogenic bacterial OMV may, however, show great discrepancies in their biological activity (Behrouzi et al., 2018). Here, we report that, even as OMV derived from the fully virulent *F. tularensis* subsp. *holarctica* strain FSC200 can be internalized into the macrophages, their association with A549 lung epithelial cells was, in our experimental conditions, almost negligible. Consistent with this observation, the viability and membrane integrity of the latter cell type was not affected by the Ft-OMV. Interestingly, Pierson et al. (2011) observed that some OMV from *F. novicida* attached to the A549 cell line, but their internalization also could not be clearly demonstrated. Nevertheless, it should be noted that the *F. novicida* OMV analyzed in their study were prepared from the distinct growth phase of bacteria grown in medium of a different composition. Under these conditions, they obtained small spherical vesicles, in contrast to the large tube-shaped ones characterized by McCaig et al. (2013) in *F. novicida* and by our group in *F. tularensis* (Klimentova et al., 2019). Most of the studies focused on OMV–host cell interaction have demonstrated the internalization of the vesicles into epithelial cells (Kunsmann et al., 2015; Mondal et al., 2016; Bielaszewska et al., 2017; O'Donoghue et al., 2017; Turner et al., 2018). Only a few studies have provided direct evidence for OMV uptake into macrophages (Pollak et al., 2012; Vanaja et al., 2016; Hu et al., 2020). This might mainly be due to the fact that, as professional phagocytes, macrophages are naturally programmed to engulf and eliminate any foreign particles, and therefore the internalization of OMV is highly assumed. *Francisella* proliferates primarily in mononuclear phagocytes (macrophages and dendritic cells), but it is also able to infect non-phagocytic cells (epithelial cells, endothelial cells, and hepatocytes). Such entry is less efficient than that in macrophages (Hall et al., 2007), indicating distinct but so far unknown uptake mechanisms. Whether this may also be related to the observed differences in the association of OMV with macrophages and lung epithelial cells remains a subject for discussion and further research.

Several endocytic uptake routes have been implicated in mediating OMV entry into non-phagocytic cells depending on their origin, size, and cargo (O'Donoghue and Krachler, 2016; Turner et al., 2018). On the other hand, data on the exact mechanism of OMV entry into macrophages are quite sparse. Macrophages are characterized by an exceptionally high endocytic activity. Larger particles (>100 nm) are engulfed by phagocytosis and macropinocytosis and smaller ones by pinocytosis, such as clathrin- and non-clathrin-mediated endocytosis. Our data suggest that the Ft-OMV uptake depends primarily on macropinocytosis, then on clathrin-dependent endocytosis, and, to a lesser extent, probably also on clathrin-independent uptake mechanisms. As the OMV produced by *Francisella* are heterogeneous in shape and size (McCaig et al., 2013; Sampath et al., 2018; Klimentova et al., 2019), the involvement of several distinct uptake routes is not so surprising. Whereas macropinocytosis is a non-specific process, the internalization by clathrin-dependent endocytosis is mediated by cell surface receptors. This means that only receptor-specific substances can utilize this pathway. Macropinocytosis is more probably used by larger particles and the OMV clumps. Several previous studies have demonstrated a role of the LPS O-antigen in OMV entry. In *Escherichia coli*, the presence of the LPS O-antigen increases the entry efficiency of OMV into epithelial host cells. OMV lacking the O-antigen require protein receptors for uptake and use of the clathrin-mediated endocytosis as a main route of entry. In contrast, OMV with intact O-antigen enter host cells by the faster and thus more efficient raft-mediated endocytosis (O'Donoghue et al., 2017). Vanaja et al. (2016) demonstrated the ability of *E. coli* OMV to enter macrophages by clathrin-mediated endocytosis, followed by the release of LPS into the cytosol. Based on the data provided in this study, the *F. tularensis* LPS O-antigen seems not to be responsible for the clathrin-mediated endocytosis, but it did contribute to the uptake of Ft-OMV mediated by the cholesterol-dependent route.

Inside the macrophages, the OMV tend to accumulate in cytoplasmic structures and to reside there for at least 24 h. The OMV thus seem able to evade the classical endosomal degradation mechanisms of macrophages. Unfortunately, we were not able to determine the precise origin of these structures. Some of them seemed to resemble late endosomes, but the electron microscopy approach used in our study did not allow further specification. Hence, the elucidation of the intracellular trafficking of isolated OMV and the mechanisms that allow such long persistence inside a professional phagocyte require further extensive studies.

The OMV produced by pathogenic bacteria are loaded with plenty of biologically active substances, such as toxins, LPS, and other virulence factors. Based on the nature of their content, they can induce distinct host cell responses. In some bacteria, the cytotoxic effect of OMV was shown to be due to the presence of LPS or OmpA (Jin et al., 2011; Vanaja et al., 2016). *Francisella* does not produce any yet known toxin, and its LPS has only low toxicity and immunogenicity. Here, we found that the Ft-OMV had no cytotoxic effect and did not influence the viability of primary murine macrophages. Minor cytotoxicity was reported also for *F. novicida* OMV

(McCaig et al., 2013). In contrast, the viability of the murine macrophage-like cell line J774A.2 was negatively affected by the Ft-OMV. The harmful effect of *F. novicida* OMV on this cell line was also reported by Pierson et al. (2011). It is thus obvious that the use of different cell types and primary cells *vs*. cell lines may lead to significant disparities in the results. Cautious interpretation is therefore highly advised. Despite their zero toxicity, the Ft-OMV elicited a significant dose-dependent release of a number of proinflammatory cytokines in the primary murine macrophages. On the contrary, the whole bacterium revealed an immunosuppressive effect on these cells, and this has also been described by others (Bauler et al., 2014; Gillette et al., 2014; Fabrik et al., 2018). It is a part of the bacterial strategy to invade the very immune system surveillance that would otherwise activate cellular mechanisms directed to bacterial elimination. In this context, however, the diametric difference between the huge amounts of isolated vesicles used for the BMDM treatment in the presented experiments in comparison with the orders of magnitude lower amount that the bacterium releases during host cell entry should be taken into account. For *Francisella*, it is not clear which particular components of the OMV are responsible for their high immunostimulatory effect. McCaig et al. (2013) described in OMV derived from *F. novicida* that the surface-exposed OMV proteins are only partially responsible for this effect because the proinflammatory effect of OMV was not altered after proteinase K treatment, and it was decreased by heat treatment of OMV.

The proinflammatory effect of Ft-OMV—in contrast to the immunosuppressive effect of the whole bacterium—may appear to be irrelevant during the infection. This raises the questions whether and in which phase of its intracellular life cycle *Francisella* produces OMV. Based on the results of the TEM analysis, it seems that the Ft-OMV or the OMV-like protrusions from the outer membrane might play a role in the contact of the bacterium with the host cell and maybe for the bacterial uptake. The number of observed OMV-like protrusions decreased markedly in the bacteria localized inside the phagosome, and no structures that would resemble the OMV were visible in the bacteria within the host cell cytosol. The production of OMV by *F. novicida* during the initial infection phase has also been reported (McCaig et al., 2013). These authors, however, analyzed only the very early phase of bacterial infection, and in contrast to the fully virulent *F. tularensis*, *F. novicida* lacks the ability to induce immunosuppression (Kingry and Petersen, 2014).

To summarize, in the present study, we provide the first deeper insights into the effects of OMV isolated from the fully virulent *F. tularensis* strain on host cells. OMV exert various effects especially on macrophages, whereas their association with non-phagocytic cells appears to be of minor importance. The Ft-OMV enter the macrophages by various uptake routes and accumulate in specific cytosolic structures for at least 24 h. Their negligible cytotoxicity together with their immunostimulatory effect on these cells might point to future research into their potential as a vaccine candidate. Further experimental evaluation of the OMV–host cell interaction is nevertheless still needed. Moreover, we have demonstrated that *F. tularensis* seems to utilize OMV primarily for the initial contact with the host cells, but their exact role in this process warrants further investigations. Furthermore, the processes of OMV isolation and purification suffer from low yields that are far below the requirements for vaccine development; thus, we propose that future research on *Francisella*-derived OMV considered for vaccine development should not focus solely on naturally secreted vesicles.

DATA AVAILABILITY STATEMENT

The original contributions presented in the study are included in the article/**Supplementary Material**, further inquiries can be directed to the corresponding author.

ETHICS STATEMENT

All experiments on mice were conducted under supervision of the Institution's Animal Unit and were approved by the Animal Care and Use Committee of the Faculty of Military Health Sciences, University of Defence, Hradec Kralove under project number 26/16 (50-29/2016-684800).

AUTHOR CONTRIBUTIONS

IP, JK, and JS conceived and designed the study. IP, JK, JB, LH, KK, EV, HR, VF, and OB performed the experiments. IP and JK wrote the manuscript. JS edited the manuscript. All authors contributed to the article and approved the submitted version.

FUNDING

This work was supported by the Czech Science Foundation (project no. 17-04010S); by the Ministry of Education, Youth and Sports of the Czech Republic (specific research project no. SV/FVZ201804); and by the Ministry of Defence of the Czech Republic ("Long Term Development Plan—Medical Aspects of Weapons of Mass Destruction" of the Faculty of Military Health Sciences, University of Defence, Hradec Kralove, Czechia). The Core Facility for Electron Microscopy (Institute of Molecular Genetics, Prague, Czechia) is supported by the Czech-BioImaging large RI project (LM2018129 funded by MEYS CR) and ERDF (CZ.02.1.01/0.0/0.0/16_013/0001775, CZ.02.1.01/0.0/0.0/18_046/0016045 "Modernization and support of research activities of the national infrastructure for biological and medical imaging Czech-BioImaging"). VF was supported by the MEYS CR COST Inter-excellence internship LTC19048 and by an institutional grant (RVO: 68378050).

SUPPLEMENTARY MATERIAL

The Supplementary Material for this article can be found online at: https://www.frontiersin.org/articles/10.3389/fmicb.2021.748706/full#supplementary-material

Supplementary Figure 1 | Fluorescence microscopy of lung epithelial cell line A549 co-incubated with Ft-OMV.

Supplementary Figure 2 | Viability and induction of cytotoxicity in lung epithelial cell line A549 treated with various concentrations of Ft-OMV.

Supplementary Figure 3 | Confirmation of quantification of the cytokines significantly released from BMDM after OMV treatment by classical ELISA assay.

Supplementary Figure 4 | Kinetics of *F. tularensis* internalization into BMDM by STED microscopy.

Supplementary Figure 5 | Immunoelectron microscopy of ultrathin sections of BMDM exposed to Ft-OMV, original TEM image.

REFERENCES

Acevedo, R., Fernández, S., Zayas, C., Acosta, A., Sarmiento, M. E., Ferro, V. A., et al. (2014). Bacterial outer membrane vesicles and vaccine applications. *Front. Immunol.* 5:121. doi: 10.3389/fimmu.2014.00121

Athman, J. J., Wang, Y., McDonald, D. J., Boom, W. H., Harding, C. V., and Wearsch, P. A. (2015). Bacterial membrane vesicles mediate the release of *Mycobacterium tuberculosis* lipoglycans and lipoproteins from infected macrophages. *J. Immunol.* 195, 1044–1053. doi: 10.4049/jimmunol.1402894

Avila-Calderón, E. D., Araiza-Villanueva, M. G., Cancino-Diaz, J. C., López-Villegas, E. O., Sriranganathan, N., Boyle, S. M., et al. (2014). Roles of bacterial membrane vesicles. *Arch. Microbiol.* 197, 1–10. doi: 10.1007/s00203-014-1042-7

Balonova, L., Mann, B. F., Cerveny, L., Alley, W. R., Chovancova, E., Forslund, A.-L., et al. (2012). Characterization of protein glycosylation in *Francisella tularensis* subsp. holarctica. *Mol. Cell. Proteomics* 11:M111.015016. doi: 10.1074/mcp.M111.015016

Bauler, T. J., Chase, J. C., Wehrly, T. D., and Bosio, C. M. (2014). Virulent *Francisella tularensis* destabilize host mRNA to rapidly suppress inflammation. *J. Innate Immun.* 6, 793–805. doi: 10.1159/000363243

Behrouzi, A., Vaziri, F., Riazi Rad, F., Amanzadeh, A., Fateh, A., Moshiri, A., et al. (2018). Comparative study of pathogenic and non-pathogenic *Escherichia coli* outer membrane vesicles and prediction of host-interactions with TLR signaling pathways. *BMC Res. Notes* 11:539. doi: 10.1186/s13104-018-3648-3

Bielaszewska, M., Rüter, C., Bauwens, A., Greune, L., Jarosch, K.-A., Steil, D., et al. (2017). Host cell interactions of outer membrane vesicle-associated virulence factors of enterohemorrhagic *Escherichia coli* O157: intracellular delivery, trafficking and mechanisms of cell injury. *PLoS Pathog.* 13:e1006159. doi: 10.1371/journal.ppat.1006159

Bitto, N. J., and Kaparakis-Liaskos, M. (2017). The therapeutic benefit of bacterial membrane vesicles. *Int. J. Mol. Sci.* 18:1287. doi: 10.3390/ijms18061287

Cai, W., Kesavan, D. K., Wan, J., Abdelaziz, M. H., Su, Z., and Xu, H. (2018). Bacterial outer membrane vesicles, a potential vaccine candidate in interactions with host cells based. *Diagn. Pathol.* 13:95. doi: 10.1186/s13000-018-0768-y

Celli, J. (2008). "Intracellular localization of *Brucella abortus* and *Francisella tularensis* in primary murine macrophages," in *Bacterial Pathogenesis: Methods and Protocols Methods in Molecular Biology*^{TM}, eds F. R. DeLeo and M. Otto (Totowa, NJ: Humana Press), 133–145. doi: 10.1007/978-1-60327-032-8_11

Celli, J., and Zahrt, T. C. (2013). Mechanisms of *Francisella tularensis* intracellular pathogenesis. *Cold Spring Harb. Perspect. Med.* 3:a010314. doi: 10.1101/cshperspect.a010314

Chmiela, M., Walczak, N., and Rudnicka, K. (2018). *Helicobacter pylori* outer membrane vesicles involvement in the infection development and *Helicobacter pylori*-related diseases. *J. Biomed. Sci.* 25:78. doi: 10.1186/s12929-018-0480-y

Clemens, D. L., and Horwitz, M. A. (2007). Uptake and intracellular fate of *Francisella tularensis* in human macrophages. *Ann. N. Y. Acad. Sci.* 1105, 160–186. doi: 10.1196/annals.1409.001

Clemens, D. L., Lee, B.-Y., and Horwitz, M. A. (2005). *Francisella tularensis* enters macrophages via a novel process involving pseudopod loops. *Infect. Immun.* 73, 5892–5902. doi: 10.1128/IAI.73.9.5892-5902.2005

Clemens, D. L., Lee, B.-Y., and Horwitz, M. A. (2012). O-antigen-deficient *Francisella tularensis* live vaccine strain mutants are ingested via an aberrant form of looping phagocytosis and show altered kinetics of intracellular trafficking in human macrophages. *Infect. Immun.* 80, 952–967. doi: 10.1128/IAI.05221-11

Craven, R. R., Hall, J. D., Fuller, J. R., Taft-Benz, S., and Kawula, T. H. (2008). *Francisella tularensis* invasion of lung epithelial cells. *Infect. Immun.* 76, 2833–2842. doi: 10.1128/IAI.00043-08

Dennis, D. T., Inglesby, T. V., Henderson, D. A., Bartlett, J. G., Ascher, M. S., Eitzen, E., et al. (2001). Tularemia as a biological weapon: medical and public health management. *JAMA* 285, 2763–2773. doi: 10.1001/jama.285.21.2763

Ellis, T. N., and Kuehn, M. J. (2010). Virulence and immunomodulatory roles of bacterial outer membrane vesicles. *Microbiol. Mol. Biol. Rev.* 74, 81–94. doi: 10.1128/MMBR.00031-09

Elmi, A., Nasher, F., Jagatia, H., Gundogdu, O., Bajaj-Elliott, M., Wren, B., et al. (2016). *Campylobacter jejuni* outer membrane vesicle-associated proteolytic activity promotes bacterial invasion by mediating cleavage of intestinal epithelial cell E-cadherin and occludin. *Cell. Microbiol.* 18, 561–572. doi: 10.1111/cmi.12534

Fabrik, I., Link, M., Putzova, D., Plzakova, L., Lubovska, Z., Philimonenko, V., et al. (2018). The early dendritic cell signaling induced by virulent *Francisella tularensis* strain occurs in phases and involves the activation of Extracellular Signal-Regulated Kinases (ERKs) and p38 in the later stage. *Mol. Cell. Proteomics* 17, 81–94. doi: 10.1074/mcp.RA117.000160

Fernandez-Moreira, E., Helbig, J. H., and Swanson, M. S. (2006). Membrane vesicles shed by *Legionella pneumophila* inhibit fusion of phagosomes with lysosomes. *Infect. Immun.* 74, 3285–3295. doi: 10.1128/IAI.01382-05

Galkina, S. I., Romanova, J. M., Bragina, E. E., Tiganova, I. G., Stadnichuk, V. I., Alekseeva, N. V., et al. (2011). Membrane tubules attach *Salmonella typhimurium* to eukaryotic cells and bacteria. *FEMS Immunol. Med. Microbiol.* 61, 114–124. doi: 10.1111/j.1574-695X.2010.00754.x

Gao, L., and van der Veen, S. (2020). Role of outer membrane vesicles in bacterial physiology and host cell interactions. *Infect. Microbes Dis.* 2, 3–9. doi: 10.1097/IM9.0000000000000017

Gerritzen, M. J. H., Salverda, M. L. M., Martens, D. E., Wijffels, R. H., and Stork, M. (2019). Spontaneously released *Neisseria meningitidis* outer membrane vesicles as vaccine platform: production and purification. *Vaccine* 37, 6978–6986. doi: 10.1016/j.vaccine.2019.01.076

Gill, S., Catchpole, R., and Forterre, P. (2018). Extracellular membrane vesicles in the three domains of life and beyond. *FEMS Microbiol. Rev.* 43, 273–303. doi: 10.1093/femsre/fuy042

Gillette, D. D., Curry, H. M., Cremer, T., Ravneberg, D., Fatehchand, K., Shah, P. A., et al. (2014). Virulent Type A *Francisella tularensis* actively suppresses cytokine responses in human monocytes. *Front. Cell. Infect. Microbiol.* 4:45. doi: 10.3389/fcimb.2014.00045

Guidi, R., Levi, L., Rouf, S. F., Puiac, S., Rhen, M., and Frisan, T. (2013). *Salmonella enterica* delivers its genotoxin through outer membrane vesicles secreted from infected cells. *Cell. Microbiol.* 15, 2034–2050. doi: 10.1111/cmi.12172

Hall, J. D., Craven, R. R., Fuller, J. R., Pickles, R. J., and Kawula, T. H. (2007). *Francisella tularensis* replicates within alveolar Type II epithelial cells in vitro and in vivo following inhalation. *Infect. Immun.* 75, 1034–1039. doi: 10.1128/IAI.01254-06

Holland, K. M., Rosa, S. J., and Hazlett, K. R. O. (2016). *Francisella tularensis*–immune cell activator, suppressor, or stealthy evader: the evolving view from the petri dish. *J. Bioterror. Biodef.* 7:144. doi: 10.4172/2157-2526.1000144

Hu, R., Lin, H., Li, J., Zhao, Y., Wang, M., Sun, X., et al. (2020). Probiotic *Escherichia coli* Nissle 1917-derived outer membrane vesicles enhance immunomodulation and antimicrobial activity in RAW264.7 macrophages. *BMC Microbiol.* 20:268. doi: 10.1186/s12866-020-01953-x

Jan, A. T. (2017). Outer Membrane Vesicles (OMVs) of gram-negative bacteria: a perspective update. *Front. Microbiol.* 8:1053. doi: 10.3389/fmicb.2017.01053

Jin, J. S., Kwon, S.-O., Moon, D. C., Gurung, M., Lee, J. H., Kim, S. I., et al. (2011). *Acinetobacter baumannii* secretes cytotoxic outer membrane protein a via outer membrane vesicles. *PLoS One* 6:e17027. doi: 10.1371/journal.pone.0017027

Johansson, A., Berglund, L., Eriksson, U., Göransson, I., Wollin, R., Forsman, M., et al. (2000). Comparative analysis of PCR versus culture for diagnosis of ulceroglandular tularemia. *J. Clin. Microbiol.* 38, 22–26.

Jones, E. J., Booth, C., Fonseca, S., Parker, A., Cross, K., Miquel-Clopés, A., et al. (2020). The uptake, trafficking, and biodistribution of bacteroides thetaiotaomicron generated outer membrane vesicles. *Front. Microbiol.* 11:57. doi: 10.3389/fmicb.2020.00057

Jung, A. L., Stoiber, C., Herkt, C. E., Schulz, C., Bertrams, W., and Schmeck, B. (2016). *Legionella pneumophila*-derived outer membrane vesicles promote bacterial replication in macrophages. *PLoS Pathog.* 12:e1005592. doi: 10.1371/journal.ppat.1005592

Kaparakis-Liaskos, M., and Ferrero, R. L. (2015). Immune modulation by bacterial outer membrane vesicles. *Nat. Rev. Immunol.* 15, 375–387. doi: 10.1038/nri3837

Kingry, L. C., and Petersen, J. M. (2014). Comparative review of *Francisella tularensis* and *Francisella novicida*. *Front. Cell. Infect. Microbiol.* 4:35. doi: 10.3389/fcimb.2014.00035

Klimentova, J., Pavkova, I., Horcickova, L., Bavlovic, J., Kofronova, O., Benada, O., et al. (2019). *Francisella tularensis* subsp. holarctica releases differentially loaded outer membrane vesicles under various stress conditions. *Front. Microbiol.* 10:2304. doi: 10.3389/fmicb.2019.02304

Klimentova, J., Rehulka, P., Pavkova, I., Kubelkova, K., Bavlovic, J., and Stulik, J. (2021). Cross-species proteomic comparison of outer membrane vesicles and membranes of *Francisella tularensis* subsp. tularensis versus subsp. holarctica. *J. Proteome Res.* 20, 1716–1732. doi: 10.1021/acs.jproteome.0c00917

Kunsmann, L., Rüter, C., Bauwens, A., Greune, L., Glüder, M., Kemper, B., et al. (2015). Virulence from vesicles: novel mechanisms of host cell injury by *Escherichia coli* O104:H4 outbreak strain. *Sci. Rep.* 5:13252. doi: 10.1038/srep13252

Lo, K. Y.-S., Chua, M. D., Abdulla, S., Law, H. T., and Guttman, J. A. (2013). Examination of in vitro epithelial cell lines as models for *Francisella tularensis* non-phagocytic infections. *J. Microbiol. Methods* 93, 153–160. doi: 10.1016/j.mimet.2013.03.004

MacDonald, I. A., and Kuehn, M. J. (2012). Offense and defense: microbial membrane vesicles play both ways. *Res. Microbiol.* 163, 607–618. doi: 10.1016/j.resmic.2012.10.020

MacDonald, I. A., and Kuehn, M. J. (2013). Stress-induced outer membrane vesicle production by *Pseudomonas aeruginosa*. *J. Bacteriol.* 195, 2971–2981. doi: 10.1128/JB.02267-12

McCaig, W. D., Koller, A., and Thanassi, D. G. (2013). Production of outer membrane vesicles and outer membrane tubes by *Francisella novicida*. *J. Bacteriol.* 195, 1120–1132. doi: 10.1128/JB.02007-12

Metruccio, M. M. E., Evans, D. J., Gabriel, M. M., Kadurugamuwa, J. L., and Fleiszig, S. M. J. (2016). *Pseudomonas aeruginosa* outer membrane vesicles triggered by human mucosal fluid and lysozyme can prime host tissue surfaces for bacterial adhesion. *Front. Microbiol.* 7:871. doi: 10.3389/fmicb.2016.00871

Mondal, A., Tapader, R., Chatterjee, N. S., Ghosh, A., Sinha, R., Koley, H., et al. (2016). Cytotoxic and inflammatory responses induced by outer membrane vesicle-associated biologically active proteases from *Vibrio cholerae*. *Infect. Immun.* 84, 1478–1490. doi: 10.1128/IAI.01365-15

O'Donoghue, E. J., and Krachler, A. M. (2016). Mechanisms of outer membrane vesicle entry into host cells. *Cell. Microbiol.* 18, 1508–1517. doi: 10.1111/cmi.12655

O'Donoghue, E. J., Sirisaengtaksin, N., Browning, D. F., Bielska, E., Hadis, M., Fernandez-Trillo, F., et al. (2017). Lipopolysaccharide structure impacts the entry kinetics of bacterial outer membrane vesicles into host cells. *PLoS Pathog* 13:e1006760. doi: 10.1371/journal.ppat.1006760

Oyston, P. C. F. (2008). *Francisella tularensis*: unravelling the secrets of an intracellular pathogen. *J. Med. Microbiol.* 57, 921–930. doi: 10.1099/jmm.0.2008/000653-0

Ozanic, M., Marecic, V., Abu Kwaik, Y., and Santic, M. (2015). The divergent intracellular lifestyle of *Francisella tularensis* in evolutionarily distinct host cells. *PLoS Pathog.* 11:e1005208. doi: 10.1371/journal.ppat.1005208

Pierson, T., Matrakas, D., Taylor, Y. U., Manyam, G., Morozov, V. N., Zhou, W., et al. (2011). Proteomic characterization and functional analysis of outer membrane vesicles of Francisella novicida suggests possible role in virulence and use as a vaccine. *J. Proteome Res.* 10, 954–967. doi: 10.1021/pr1009756

Pollak, C. N., Delpino, M. V., Fossati, C. A., and Baldi, P. C. (2012). Outer membrane vesicles from *Brucella abortus* promote bacterial internalization by human monocytes and modulate their innate immune response. *PLoS One* 7:e50214. doi: 10.1371/journal.pone.0050214

Prados-Rosales, R., Baena, A., Martinez, L. R., Luque-Garcia, J., Kalscheuer, R., Veeraraghavan, U., et al. (2011). Mycobacteria release active membrane vesicles that modulate immune responses in a TLR2-dependent manner in mice. *J. Clin. Invest.* 121, 1471–1483. doi: 10.1172/JCI44261

Putzova, D., Panda, S., Härtlova, A., Stulík, J., and Gekara, N. O. (2017). Subversion of innate immune responses by *Francisella* involves the disruption of TRAF3 and TRAF6 signalling complexes. *Cell. Microbiol.* 19:e12769. doi: 10.1111/cmi.12769

Rodal, S. K., Skretting, G., Garred, Ø, Vilhardt, F., van Deurs, B., and Sandvig, K. (1999). Extraction of cholesterol with methyl-β-cyclodextrin perturbs formation of clathrin-coated endocytic vesicles. *Mol. Biol. Cell* 10, 961–974.

Sampath, V., McCaig, W. D., and Thanassi, D. G. (2018). Amino acid deprivation and central carbon metabolism regulate the production of outer membrane vesicles and tubes by *Francisella*. *Mol. Microbiol.* 107, 523–541. doi: 10.1111/mmi.13897

Schindelin, J., Arganda-Carreras, I., Frise, E., Kaynig, V., Longair, M., Pietzsch, T., et al. (2012). Fiji–an open source platform for biological image analysis. *Nat. Methods* 9, 676–682. doi: 10.1038/nmeth.2019

Schwechheimer, C., and Kuehn, M. J. (2015). Outer-membrane vesicles from gram-negative bacteria: biogenesis and functions. *Nat. Rev. Microbiol.* 13, 605–619. doi: 10.1038/nrmicro3525

Singh, A., Rahman, T., Malik, M., Hickey, A. J., Leifer, C. A., Hazlett, K. R. O., et al. (2013). Discordant results obtained with *Francisella tularensis* during In vitro and in vivo immunological studies are attributable to compromised bacterial structural integrity. *PLoS One* 8:e58513. doi: 10.1371/journal.pone.0058513

Telepnev, M., Golovliov, I., Grundström, T., Tärnvik, A., and Sjöstedt, A. (2003). *Francisella tularensis* inhibits toll-like receptor-mediated activation of intracellular signalling and secretion of TNF-α and IL-1 from murine macrophages. *Cell. Microbiol.* 5, 41–51. doi: 10.1046/j.1462-5822.2003.00251.x

Turner, L., Bitto, N. J., Steer, D. L., Lo, C., D'Costa, K., Ramm, G., et al. (2018). *Helicobacter pylori* outer membrane vesicle size determines their mechanisms of host cell entry and protein content. *Front. Immunol.* 9:1466. doi: 10.3389/fimmu.2018.01466

Vanaja, S. K., Russo, A. J., Behl, B., Banerjee, I., Yankova, M., Deshmukh, S. D., et al. (2016). Bacterial outer membrane vesicles mediate cytosolic localization of LPS and caspase-11 activation. *Cell* 165, 1106–1119. doi: 10.1016/j.cell.2016.04.015

Vdovikova, S., Luhr, M., Szalai, P., Nygård Skalman, L., Francis, M. K., Lundmark, R., et al. (2017). A novel role of listeria monocytogenes membrane vesicles in inhibition of autophagy and cell death. *Front. Cell. Infect. Microbiol.* 7:154. doi: 10.3389/fcimb.2017.00154

Yang, Y., Hong, Y., Cho, E., Kim, G. B., and Kim, I.-S. (2018). Extracellular vesicles as a platform for membrane-associated therapeutic protein delivery. *J. Extracell. Vesicles* 7:1440131. doi: 10.1080/20013078.2018.1440131

Yoon, H., Ansong, C., Adkins, J. N., and Heffron, F. (2011). Discovery of *Salmonella* virulence factors translocated via outer membrane vesicles to murine macrophages. *Infect. Immun.* 79, 2182–2192. doi: 10.1128/IAI.01277-10

Conflict of Interest: The authors declare that the research was conducted in the absence of any commercial or financial relationships that could be construed as a potential conflict of interest.

Publisher's Note: All claims expressed in this article are solely those of the authors and do not necessarily represent those of their affiliated organizations, or those of the publisher, the editors and the reviewers. Any product that may be evaluated in this article, or claim that may be made by its manufacturer, is not guaranteed or endorsed by the publisher.

frontiers in Microbiology

ORIGINAL RESEARCH
published: 02 November 2021
doi: 10.3389/fmicb.2021.723909

pH Stress Mediated Alteration in Protein Composition and Reduction in Cytotoxic Potential of *Gardnerella vaginalis* Membrane Vesicles

*Parul Shishpal[1], Vainav Patel[2], Dipty Singh[3] and Vikrant M. Bhor[1]**

[1] Department of Molecular Immunology and Microbiology, Indian Council of Medical Research-National Institute for Research in Reproductive Health, Mumbai, India, [2] Department of Biochemistry, Indian Council of Medical Research-National Institute for Research in Reproductive Health, Mumbai, India, [3] Department of Neuroendocrinology and Transmission Electron Microscopy, Indian Council of Medical Research-National Institute for Research in Reproductive Health, Mumbai, India

The vagina of healthy women is predominantly colonized by lactobacilli but it also harbors a limited proportion of certain anaerobes such as *Gardnerella vaginalis*. An increase in *G. vaginalis* along with other anaerobes on account of perturbation in the vaginal microbiota is associated with bacterial vaginosis (BV). Although strategies adopted by *G. vaginalis* for survival and pathogenesis in a conducive environment (i.e., high vaginal pH, characteristic of BV) have been previously studied, the approaches potentially employed for adaptation to the low pH of the healthy vagina are unknown. In the present study, we investigated the effect of acidic stress on the modulation of the production and function of membrane vesicles (MVs) of *G. vaginalis*. pH stress led to a distortion of the bacterial cell morphology as well as an altered biogenesis of MVs, as revealed by transmission electron microscopy (TEM). Both qualitative and quantitative differences in protein content of MVs produced in response to pH stress were observed by flow cytometry. A significant change in the protein composition characterized by presence of chaperones despite a reduction in number of proteins was also noted in the stress induced MVs. Further, these changes were also reflected in the reduced cytotoxic potential toward vaginal epithelial cells. Although, these findings need to be validated in the *in vivo* settings, the modulation of *G. vaginalis* MV biogenesis, composition and function appears to reflect the exposure to acidic conditions prevailing in the host vaginal mileu in the absence of vaginal infection.

Keywords: *Gardnerella vaginalis* membrane vesicles, pH stress, chaperones, flow cytometry, biogenesis, bacterial vaginosis, vaginal epithelial cells

OPEN ACCESS

Edited by:
Araceli Contreras-Rodriguez, Instituto Politécnico Nacional (IPN), Mexico

Reviewed by:
António Machado, Universidad San Francisco de Quito, Ecuador
Juan Alfredo Hernández-García, Instituto Politécnico Nacional (IPN), Mexico

****Correspondence:***
Vikrant M. Bhor
bhorv@nirrh.res.in

Specialty section:
This article was submitted to Microbial Physiology and Metabolism, a section of the journal Frontiers in Microbiology

Received: *11 June 2021*
Accepted: *12 October 2021*
Published: *02 November 2021*

Citation:
Shishpal P, Patel V, Singh D and Bhor VM (2021) pH Stress Mediated Alteration in Protein Composition and Reduction in Cytotoxic Potential of Gardnerella vaginalis Membrane Vesicles. Front. Microbiol. 12:723909. doi: 10.3389/fmicb.2021.723909

INTRODUCTION

The mucosal lining of the vagina and the resident microbiota act as robust barriers against invading pathogens on account of the arsenal of antimicrobial substances such as defensins, mucins, and neutrophil gelatinase-associated lipocalin present in the cervicovaginal fluid (Aldunate et al., 2015).

Besides, the low pH (<4.5) maintained by the healthy vaginal microbiome comprising predominantly of *Lactobacillus* spp. also plays a key role in preventing urogenital infections

including bacterial vaginosis (BV) which can lead to severe reproductive health complications (Reid, 2008; Witkin and Linhares, 2017). BV is characterized by a change in vaginal microbiome composition comprising of reduction in vaginal lactobacilli and a simultaneous increase in the abundance of anaerobic pathogens such as *Atopobium* spp., *Mobilincus* spp., *Streptococcus* spp., *Megasphaera* spp., *Gardnerella* spp., i.e., *G. vaginalis, G. leopoldii, G. piotii,* and *G. swidsinskii,* etc. (Jung et al., 2017; Vaneechoutte et al., 2019). *G. vaginalis* is a virulent, opportunistic microorganism commonly isolated from both symptomatic and asymptomatic women with BV. It has also been reported to be present in healthy women but at a lower abundance (2–7%) compared to women suffering with BV (11–29%; Shipitsyna et al., 2013; Ceccarani et al., 2019). Several studies have discussed the presence of different strains of *G. vaginalis* and their biofilm formation capacity under the conducive environment of high vaginal pH (Patterson et al., 2010; Castro et al., 2015). However, the precise manner in which *G. vaginalis* survives and adapts to the low vaginal pH has not been investigated in detail. This lack of information necessitates an investigation into the adaptive mechanisms employed by the bacterium to sustain under these stress conditions.

All bacteria are known to release membrane vesicles (MVs) which are required for intercellular communication and other vital functions. MVs are lipid-layered, non-replicative, nano-sized particles and have been reported in general to mediate various functions from bacterial defense to host pathogenesis (Avila-Calderón et al., 2014; Yu et al., 2017). Recently, we have reported the characterization of MVs produced by *G. vaginalis.* These MVs act as vehicles for virulence-associated factors and thereby contribute to host cell pathogenesis (Shishpal et al., 2020). However, it is not known whether the MVs produced by *G. vaginalis* play a role in adaptation and survival under stress conditions.

In view of the above, we aimed to study the effect of low pH exposure on the biogenesis, composition and function of *G. vaginalis* MVs. For this we employed, transmission electron microscopy (TEM) and dynamic light scattering (DLS) for determining morphology and size distribution of the MVs, proteomics for studying MV composition and flow cytometry for size based lipid and protein distribution within MVs. Further confocal microscopy and cytotoxicity assays were used for functional assessment of the MVs produced under acidic conditions.

MATERIALS AND METHODS

Bacterial Culture and Growth Conditions

Gardnerella vaginalis ATCC 14019 (American Type Culture Collection, Manassas, VA, United States) was grown on Columbia agar base plates containing 5% human blood (Becton Dickinson) at 37°C for 48 h under anaerobic conditions using Anaerocult® A (Merck Millipore, Germany) system in an anaerobic jar (Patterson et al., 2010). Cells were inoculated in brain heart infusion broth (BHI) supplemented with 2% (w/v) gelatin, 0.5% yeast extract, 0.1% starch, and 1% glucose (HiMedia, India), i.e., sBHI for 48 h at pH 6.5 (Rosca et al., 2020). 2 mL of 9.9M lactic acid (HiMedia, India) was added to sBHI medium (pH 6.5) to lower the pH of the medium to 3.5. Additionally, the cells were also transferred from sBHI medium (pH 6.5) to the same medium with pH 3.5 and allowed to grow for 48 h under conditions similar to that for pH 6.5. The cells cultured as mentioned above were used for all subsequent experiments.

Gardnerella vaginalis Growth Curve

Gardnerella vaginalis was grown overnight in sBHI medium (pH 6.5) and further sub-cultured independently in the same medium, both at pH 6.5 and pH 3.5 under anaerobic conditions using Anaerocult® A system (Merck Millipore, Germany) in an anaerobic jar as mentioned above. An equal volume of the culture was taken to measure the absorbance ($OD_{595\ nm}$) over time. Cells were pelleted at 4,000 × *g* for 10 min and stored at –20°C until preparation of whole cell lysates and determination of protein concentration and protein profile analysis by SDS-PAGE as described later. The growth curve analysis experiment including estimation of protein concentration and subsequent protein profile analysis was performed thrice. Also, cells collected at 48 h time point were plated on sheep blood agar plates (HiMedia, India) and incubated further under anaerobic conditions for 48 h at 37°C to determine the colony forming units (CFU). The CFU analysis was performed twice. The results were analyzed for statistical significance as mentioned in the section on statistical analysis.

Gardnerella vaginalis Membrane Vesicles Isolation

Gardnerella vaginalis was cultured on Columbia agar base plates containing 5% human blood (Becton Dickinson), inoculated in sBHI medium and allowed to grow at pH 6.5 and pH 3.5, respectively, for 48 h. Then, the cell free supernatants (CFS) were filtered through 0.4 μm and 0.2 μm syringe filters (Merck Millipore) to remove cell debris. The filtrates thus obtained were subjected to ultracentrifugation at 100,000 × *g* for 3 h at 4°C to isolate MVs (Shishpal et al., 2020). Additionally, CFS (pH 6.5) was supplemented with 2 mL of 9.9M lactic acid to adjust the pH to 3.5 and was further incubated for 48 h followed by ultracentrifugation at 100,000 × *g* for 3 h at 4°C. The pellets were subsequently resuspended in phosphate buffered saline (PBS) at pH 7.4 (PBS), aliquoted and stored at –20°C till further processing. An aliquot of the MVs was used for determining the protein concentration by the Bradford reagent (Sigma) using BSA (0.1–1.4 mg/mL) as the protein standard as detailed in the subsequent section.

Protein Profile Analysis of *G. vaginalis* Cells and Membrane Vesicles by SDS-PAGE

Stored bacterial pellets of *G. vaginalis* at pH 6.5 and pH 3.5 were subjected to whole cell lysate preparation with BugBuster reagent (BugBuster® HT Protein Extraction Reagent, Novagen) using the manufacturer's protocol. The protein concentration of the whole cell lysates of the bacterial pellets obtained for various

time points during growth curve analysis was estimated by the Bradford assay (Sigma) with BSA (0.1–1.4 mg/mL) as the protein standard using a standard curve. To compare the protein profile of *G. vaginalis* cells at pH 6.5 and pH 3.5 over time, whole cell lysates were resolved using SDS-PAGE (10% resolving gel). Similarly, to compare the protein profile of *G. vaginalis* cells and MVs, an equal amount of protein (16 μg) from the whole cell lysate (collected at 48 h time point) and the *G. vaginalis* MVs were subjected to SDS-PAGE (10% resolving gel) at a constant voltage (100 volts) till the dye front reached the bottom of the gel, followed by staining of the gel with Coomassie brilliant blue R-250 (Sigma). SDS-PAGE analysis was repeated at least 5 times for both the whole cell lysates as well as MVs and qualitative changes in the protein profile were recorded.

Transmission Electron Microscopy

To evaluate the effect of pH variation on bacterial cell morphology, TEM was carried out as previously described by Schooling and Beveridge (2006) with some modifications. 50 μL of bacterial cell suspension (30 mg/mL) was applied on formvar carbon-coated grids and allowed to dry at room temperature (RT) for 10 min. The coated grid containing the bacterial cells was stained with 2% uranyl acetate for 40 s, followed by washing with distilled water to remove excess stain and drying at RT. Micrographs were recorded using a Tecnai 12BT (FEI) transmission electron microscope at an acceleration voltage of 120 KV. TEM analysis was repeated at least three times for each of the conditions, i.e., growth of cells at pH 6.5 and pH 3.5. A total of 7–9 fields were observed per condition and the total number of MVs per field was determined.

Dynamic Light Scattering

Dynamic Light Scattering measurements were performed to study the size distribution of MVs from *G. vaginalis* at the two different pH conditions. Particle size measurement was performed using Zetasizer Nano-ZS (Malvern Instruments, United Kingdom). The autocorrelation functions of the samples were analyzed using the Contin algorithm through the Zetasizer 7.11 software available with the instrument. Samples were run in triplicates.

Flow Cytometry

To quantitate the size, protein and lipid distribution of MVs isolated under normal and acidic stress conditions, two different flow cytometers were used. Firstly, to detect the carboxyfluorescein succinimidyl ester (CFSE) stained MVs, a mixture of non-fluorescent beads of sizes 1, 2, and 4 μm (Invitrogen^{TM}) were acquired with default threshold on FSC-A vs SSC-A scale using BD Accuri^{TM} C6 flow cytometer. The gating strategy included selection of a region corresponding to the region of beads of 1 μm as the MVs are expected to be approximately of a similar size. MVs were acquired at 20K threshold in R5 gate with a slow flow rate. To rule out non-specific staining with CFSE, BHI medium was processed in a manner analogous to the MVs. Further, the pellet of the BHI medium thus obtained as well as the supernatant remaining after isolation of MVs were used as controls.

As the BD Accuri^{TM} C6 flow cytometer was not found to be suitable for sub-micron analysis, it was used only for qualitative analysis. The quantitative analysis of MVs at submicron level was carried out using the BD FACSAria^{TM} Fusion flow cytometer. Prior to acquisition, MVs were stained with 10 μM CFSE (a protein staining dye) for 20 min at 37°C and 10 μg/mL of the lipid staining dye FM 4-64 FX (Invitrogen^{TM}) for 10 min at 37°C (Pospichalova et al., 2015). The dual (i.e., both protein and lipid) stained populations were considered for quantitative analysis. CFSE has an excitation peak at 492 nm and emission at 517 nm and FM 4-64FX has excitation emission peak at 565 nm and 744 nm, being acquired in FITC and PE-Cy7 channels, respectively. A mixture of FITC labeled sub-micron particles (Invitrogen^{TM}) of sizes 100 nm, 200 nm, 500 nm, and 1 μm were acquired on flow cytometry with a threshold of 100 on SSC, at slow flow rates and used to gate the dual stained MVs (Görgens et al., 2019). Similar parameters were used to acquire CFSE and FM 4-64FX stained MVs isolated under both pH conditions. Data analysis was carried out using FlowJo VX (TreeStar, Ashland, OR, United States).

Mass Spectrometry and Data Analysis

To characterize the protein content of the *G. vaginalis* MVs at pH 3.5, nano LC-MS/MS (EASY-nLC 1000 system, Thermo Fisher Scientific) was performed using a methodology identical to that mentioned in our previous publication (Shishpal et al., 2020). Briefly protein sample (100 μg) from *G. vaginalis* MVs at pH 3.5 was treated with 6M guanidine-HCl followed by reduction with 5 mM Tris (2-Carboxyethyl) phosphine (TCEP), alkylation using 50 mM iodoacetamide and trypsin digestion. Trypsin digests were cleaned up using C18 silica cartridge as mentioned by manufacturer (The Nest Group, Southborough, MA, United States) and dried using speed vac. One microgram of the peptide mixture was resolved using 15 cm PicoFrit column (360 μm OD, 75 μm ID, and 10 μm tip) filled with 1.8 μm C18-resin (Dr. Maisch, Germany).

MS/MS scans were acquired at a resolution of 17,500 at m/z 400. The MS/MS spectra of peptides were analyzed using MaxQuant (version 1.5.3.8; with the Andromeda search engine). The peptides thus obtained were analyzed against the total predicted proteome of *G. vaginalis* for identification of proteins associated with the MVs. The protein false discovery rate was set to 1%. Subcellular localization of the proteome of *G. vaginalis* MVs obtained at pH 3.5 was compared with that of MVs obtained at pH 6.5 using UniProt repository[1].

Confocal Microscopy of Vaginal Epithelial Cells Treated With Membrane Vesicles

Confocal microscopy was used to study the effect of *G. vaginalis* MVs (obtained at both pH 6.5 and 3.5) on human vaginal epithelial cells (VK2/E6E7). Vaginal epithelial cells were grown in an eight-chamber slide (SPL Life Sciences, Korea) in keratinocyte serum-free medium supplemented with the bovine pituitary

[1]www.uniprot.org

extract (50 μg/mL) and recombinant epidermal growth factor (0.1 ng/mL; Gibco, Invitrogen™) at 37°C in a humidified atmosphere containing 5% CO_2. Once the confluency reached 70–80%, cells were treated with CFSE stained MVs at a concentration of 300 μg/mL for 24 h, followed by washing with PBS and fixation with pre-chilled 3% formaldehyde for 10 min at RT. To observe changes in the cytoskeleton, cells in each well were stained with 250 μL of Phalloidin conjugated to BODIPY 558/568 dye (Invitrogen™) at a dilution of 1:40 for 45 min at RT. Stained cells were washed twice with Dulbecco's Phosphate Buffered Saline (DPBS) followed by nuclear staining with 250 μL of 1:2000 DAPI for each well and mounted with Vectashield mounting medium (Vector labs, United States). Imaging was done using a confocal laser scanning microscope-CLSM (Olympus Fluoview fv3000, Japan). Internalization of MVs within the vaginal epithelial cells was confirmed by serial Z section at intervals of 1 μm. All the experiments including treatment with MVs and imaging of the treated cells were carried out more than three times and all images thus obtained were studied for qualitative changes compared to untreated cells.

Preparation of BSA Entrapped Liposomes

BSA entrapped liposomes were used as a negative control in experiments related to evaluation of the cytotoxicity of MVs as well as their potential to induce the production of the cytokine, IL-8 in vaginal epithelial cells, VK2. The liposomes were prepared by the thin film hydration method (Zhang, 2017). Briefly, 10 mg/mL phosphatidylcholine, was dissolved in 2:1 mixture of chloroform and methanol. Solvent was evaporated by using rotatory evaporator at 45°C to form a thin layer of lipid and left overnight at RT to evaporate the solvent completely. The dried thin lipid layer was resuspended in 10 mL of DPBS containing 10 mg/mL BSA followed by probe sonication at 30% amplitude for 5 min to obtain unilamellar vesicles.

Cytotoxicity Assay and IL-8 ELISA for Vaginal Epithelial Cells Treated With Membrane Vesicles

VK2 cells were grown in 96 well plates and treated with increasing protein concentrations of MVs obtained at both pH 6.5 and pH 3.5 (9.37–300 μg/mL) and BSA entrapped liposomes (negative control) for 24 h at 37°C with 5% CO_2. After completion of the incubation period, cell supernatants were removed and stored at −80°C for estimation of the levels of the cytokine, IL-8 using a commercially available sandwich ELISA kit (eBioscience, Thermo Fisher Scientific) according to manufacturer's instructions. Cells were processed further by adding 10 μL of methylthiazolyldiphenyltetrazolium bromide (5 mg/mL) to each well, followed by incubation for 2 h in the dark. Following this, 100 μL of dimethyl sulfoxide was added to dissolve the formazan crystals and absorbance at 570 nm was measured. Untreated cells represented the 0% cytotoxicity control. Total lysis of cells following treatment with 1% (w/v) SDS represented the 100% cytotoxicity control.

Statistical Analysis

All the data is representative of independent experiments and has been expressed as mean ± SD. The statistical significance of CFU and TEM analysis of *G. vaginalis* was determined using student's unpaired *t*-test. Bacterial growth curve, protein estimation of the whole cell lysates, determination of percentage of MV sizes, median fluorescence intensity (MFI) of MVs at pH 6.5 and 3.5, cytotoxicity and ELISA were analyzed by two-way ANOVA with Bonferroni *post hoc* test and differences were considered significant at $p < 0.05$.

RESULTS

pH Stress Reduces Growth of *G. vaginalis*

Effect of acidic stress on the growth kinetics of *G. vaginalis* was studied over time (1, 24, 48, and 72 h). The increase in absorbance of the *G. vaginalis* culture at pH 6.5 although not statistically significant, indicates a trend toward gradual increase in growth, over time while the absence of an apparent increase in absorbance suggesting no significant changes in growth was observed for bacteria grown at acidic conditions, i.e., pH 3.5 (**Figure 1A**) indicate pH stress mediated growth restriction. This was also supported by a significant, i.e., 2.7 log reduction ($p < 0.01$) in *G. vaginalis* cells numbers at pH 3.5 for the 48 h time point (**Figure 1B**). Despite a higher baseline protein concentration that was observed in the culture at pH 3.5 no significant change in protein concentration was observed over time. The apparent absence of changes in growth and protein concentration along with the reduction in viability of the *G. vaginalis* culture in response to pH stress was also reflected in the visible changes in the SDS-PAGE protein profile of *G. vaginalis* cells at pH 3.5 such as the reduction in both high and low molecular weight protein bands, reduced sharpness and intensity of the protein bands as well as apparent increase in the intensity of the lowermost protein band, i.e., approximately 10 kDa close to the dye front compared to that observed in cells grown at pH 6.5 (**Figure 1C**).

Modulation in *G. vaginalis* Cells and Membrane Vesicles Under Acidic Stress

Transmission Electron Microscopy of *G. vaginalis* cells exposed to pH stress revealed an increase in budding of MVs ($p = 0.015$, **Supplementary Figure 1**) at the cell surface indicating an increase in MV production compared to those in cells grown at pH 6.5 (**Figures 2A,B**). Additionally, DLS showed a wider distribution as well as larger size of MVs from ∼190 to 615 nm at pH 3.5 compared to those at pH 6.5 (**Figures 2C,D** and **Supplementary Tables 1, 2**). Apart from this, acidic stress also resulted in visible changes in the SDS-PAGE protein profile of MVs compared to MVs from cells grown at pH 6.5. Despite having equal protein concentrations as measured by Bradford assay, MVs produced at pH 3.5 displayed a diffused or smear pattern with absence of distinct protein bands in contrast to distinct and well separated protein bands of MVs obtained at pH 6.5. However, protein profile of MVs (pH 6.5 CFS) exposed to

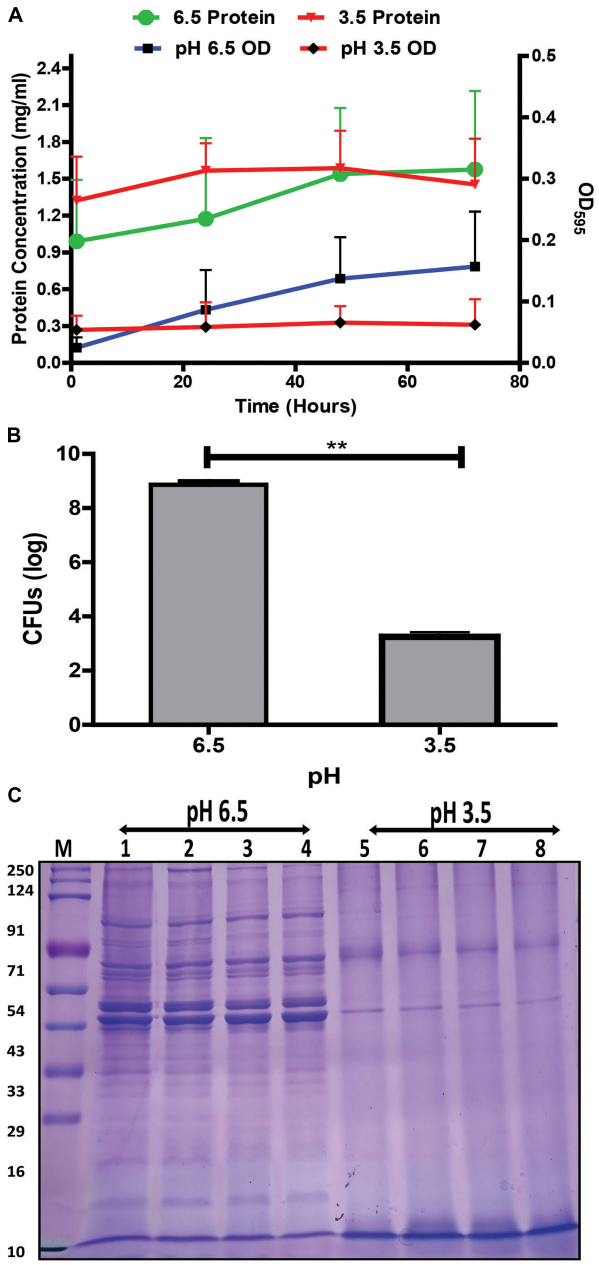

FIGURE 1 | Effect of pH on the growth and protein profile of *G. vaginalis* ATCC 14019. **(A)** Changes in growth and protein concentration of *G. vaginalis* at pH 6.5 and 3.5 over time (1, 24, 48, and 72 h); data are presented as mean ± SD (n = 3). No statistical significance was observed upon analysis by two-way ANOVA with Bonferroni test. **(B)** Reduction in colony forming unit (CFUs) of *G. vaginalis* at pH 3.5 compared to pH 6.5 after 48 h; data are presented as mean ± SD (n = 2). Data was analyzed using student's unpaired t test (**$p < 0.01$). **(C)** Time dependent (1, 24, 48, and 72 h) changes in protein profile of whole cell lysate of *G. vaginalis* at pH 6.5 and 3.5.

acidic conditions (pH 3.5) does not show any smearing pattern similar to that observed in MVs isolated at pH 3.5 (**Figure 2E**). Similar results were obtained in multiple replicates of the SDS-PAGE profiles of the MV proteins.

pH Induced Changes in Morphology and Fluorescence Profiles of *G. vaginalis* Membrane Vesicles

As described previously, micrographs demonstrated the release of MVs at both pH 6.5 and pH 3.5. However, upon observation at a higher magnification, differences in cell morphology and the number of MVs released was apparent in cells exposed to acidic stress. The distortion in cell morphology arising on account of an apparent burst of vesicles at the cell surface observed under the stress condition was not seen at pH 6.5 (**Figures 3A,B**). In addition to this, flow cytometry-based characterization was carried out to determine changes in content of MVs. Non-fluorescent reference beads of 1, 2, and 4 μm were detected and gated based on their forward and side scatter profiles (**Supplementary Figure 2A**) and the region corresponding to beads of 1 μm were gated as R5 (**Supplementary Figure 2B**). Acquisition of CFSE labeled MVs, the supernatant obtained after ultracentrifugation as well as the pellet of the BHI medium obtained after ultracentrifugation was restricted to the R5 gate (**Supplementary Figures 2C,D**). Comparison of the fluorescence signals for all the above revealed a clear shift in the peak for MVs indicating a distinct fluorescence profile (**Supplementary Figure 2E**). Though, the overall fluorescence vs side scatter profiles (acquired in the R5 gate) of MVs obtained at pH 6.5 and 3.5 were similar, a distinct population was observed at pH 3.5 and was further gated as R1 (**Figure 3D**). A similar region was analyzed in case of MVs at pH 6.5 (**Figure 3C**). Doublet discrimination plots of forward scatter height vs area, typically used to identify singlets along the diagonal, were analyzed for the entire population of MVs (acquired in the R5 gate) at both pH 6.5 and pH 3.5. Superimposition of the R1 gated population in the area vs height plots represented in **Figures 3E,F** led to the identification of the portions of the total population which possessed higher fluorescence, i.e., MVs with an appreciable protein content. The P2 subset in MVs of pH 6.5 (**Figure 3E**) possesses higher fluorescence compared to that in MVs of pH 3.5 (**Figure 3G**) while the P1 subset in MVs both pH 6.5 and p H 3.5 possessed approximately equal fluorescence (**Figure 3H**).

Quantitative Analysis of pH Induced Changes in *G. vaginalis* Membrane Vesicles Using Flow Cytometry

Due to the limitations in obtaining a clear separation of sub-micron beads with the BD Accuri flow cytometer, quantification of MVs was carried out using the BD Fusion Aria flow cytometer. Since MVs consist of both lipids and proteins, quantitation of dual protein (CFSE) and lipid (FM 4-64FX) fluorescence was carried out to obtain a better estimate of the changes in *G. vaginalis* MVs brought about due to acidic stress. The distinct regions obtained in the side scatter vs fluorescence profile of the sub-micron beads (0.1, 0.2, 0.5, and 1 μm; **Supplementary Figure 3**) were used to demarcate corresponding regions in the forward vs side scatter profile of the bead mixture (**Figure 4A**). The strategy employed for the flow cytometry analysis is summarized in **Supplementary Figure 4**. In order to characterize

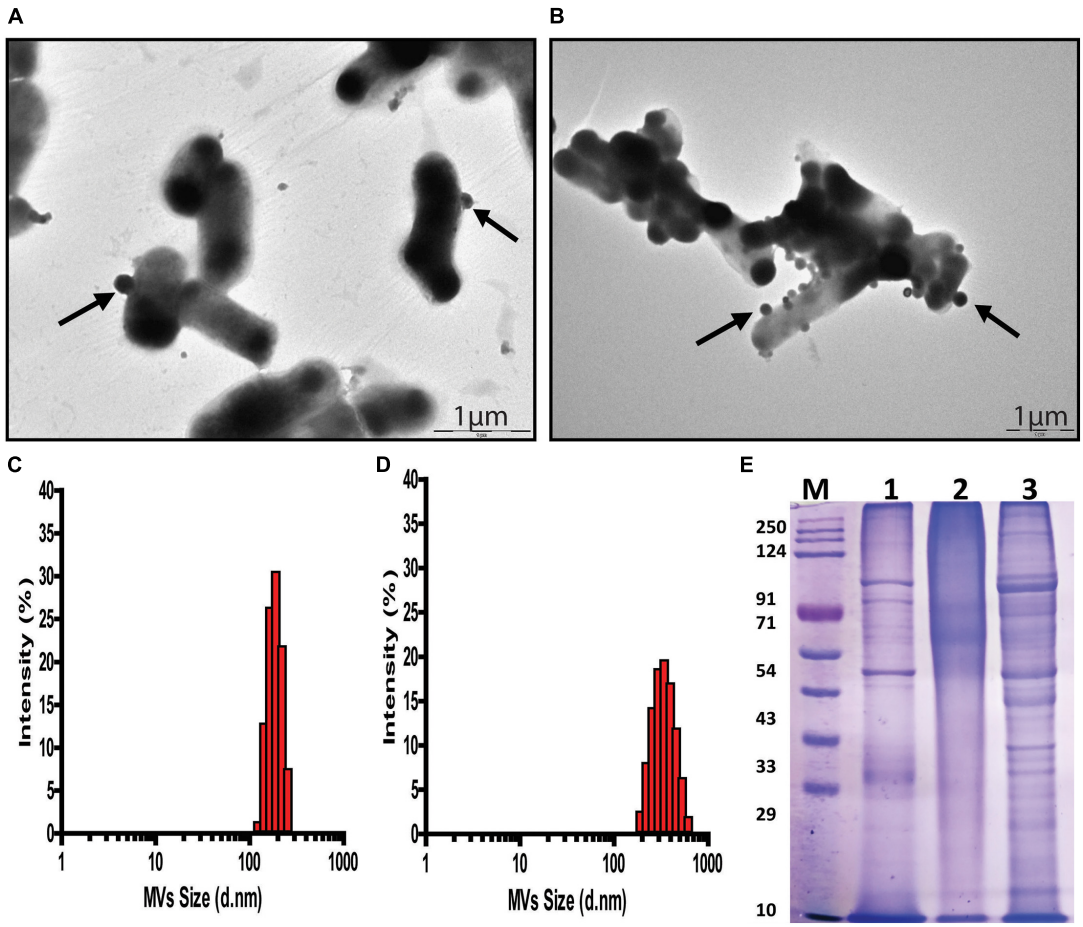

FIGURE 2 | pH dependent changes in *G. vaginalis* ATCC 14019 membrane vesicles (MVs). Transmission Electron Microscopy (TEM) of negatively stained preparation of *G. vaginalis* cells showing released MVs attached to the cell surface (arrow) at pH 6.5 **(A)** and pH 3.5 **(B)**; scale bar-1 μm. Size distribution profile of MVs measured by dynamic light scattering indicates a diameter range of 190–250 nm at pH 6.5 **(C)** and 190–615 nm at pH 3.5 **(D)**. SDS-PAGE profile of *G. vaginalis* MVs isolated from (1) cells grown at pH 6.5, (2) cells grown at pH 3.5, and (3) cell free supernatant (cells grown at pH 6.5) supplemented with lactic acid to produce acidic conditions (pH 3.5) and (M) molecular weight marker **(E)**.

the population of MVs of varying sizes that were obtained at pH 6.5 and pH 3.5, reference gates corresponding to beads of different sizes were applied on the forward vs side scatter profiles (**Figures 4B,C**). A decrease in the percentage of the total dual, i.e., CFSE and FM 4-64FX fluorescent population of MVs in the range of 0.2 μm (**Supplementary Table 3**) was observed at pH 3.5 along with an apparent increase in the percentage of the corresponding population of MVs in the range of 0.5 μm (**Figures 4F,H**). The changes in the percentage of the dual stained MVs observed at pH 3.5 indicate an alteration in the protein and lipid content due to changes in the distribution of protein across the population of lipid membrane bound vesicles, i.e., MVs, on account of the acidic stress (**Figure 4D**). In order to further investigate the apparent changes in protein and lipid distribution, we focused our attention on the MVs in the range of 0.5 μm owing to their higher protein fluorescence compared to those MVs in the range of 0.2 μm. Out of the entire dual fluorescence positive population represented in the Q2 quadrant, the region with maximum overlap of the protein and lipid fluorescence was gated as shown in fluorescence profiles for MVs around 0.5 μm obtained at both pH 6.5 (**Figures 4E,G**) and pH 3.5 (**Figures 4F,H**) from two different experiments. Although an apparent increase in total fluorescence of the dual positive population was observed at pH 3.5 (**Figure 4D**), analysis of the MFIs of the above mentioned regions revealed an overall reduction in protein as well as lipid fluorescence at pH 3.5 compared to that at pH 6.5 (**Figure 4I**). The reason for this apparent discrepancy is not known but the results clearly indicate that acidic stress leads to alteration in the fluorescence profile of the MVs. In case of the fluorescence profile for one experiment, the major dual fluorescence positive population observed at pH 6.5 was significantly diminished at pH 3.5 along with the appearance of two distinct subsets "a" and "b." These subsets were not clearly evident at pH 6.5 (**Figures 4G,H**). Further, the MVs at pH 3.5 corresponding to subset "a" were lipid enriched while those corresponding to subset "b" were found to be protein enriched (**Figure 4J**). These results support the observation of uneven protein and lipid distribution in MVs (**Figure 3**) obtained at pH 3.5.

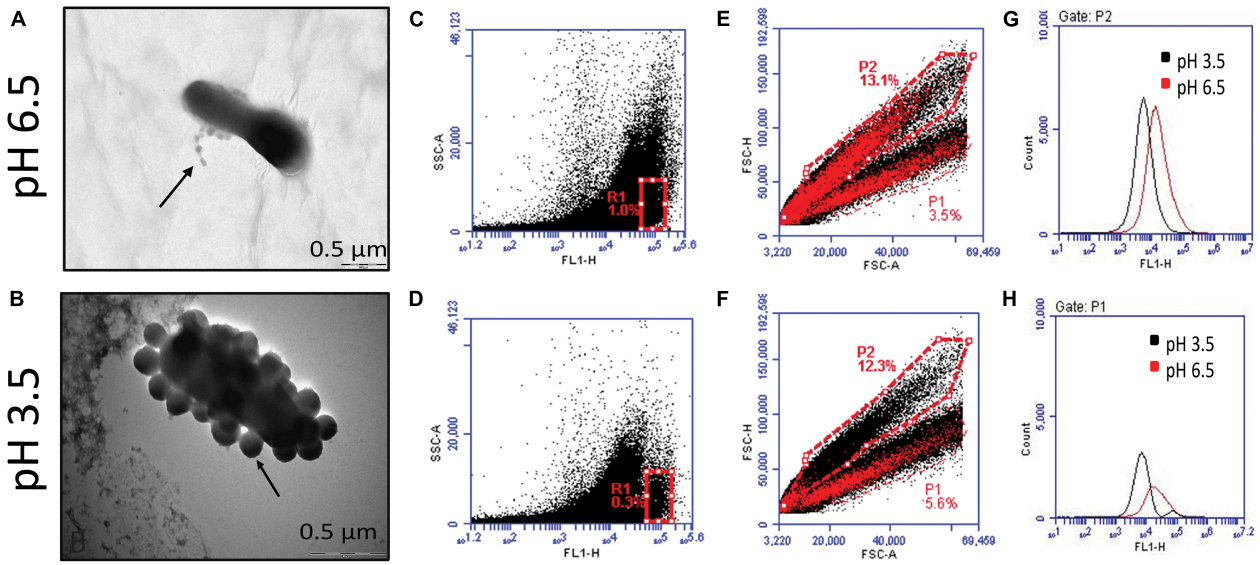

FIGURE 3 | Characterization of *G. vaginalis* ATCC 14019 MVs obtained at pH 6.5 and 3.5 by flow cytometry. Enlarged images of negatively stained bacteria depicting release of MVs at pH 6.5 **(A)** and pH 3.5 **(B)**. Fluorescence based side scatter profile of MVs at pH 6.5 **(C)** and pH 3.5 **(D)** indicating the presence of a distinct subset at pH 3.5 gated as R1. Forward scatter plot of area vs height for total population of MVs at pH 6.5 **(E)** and pH 3.5 **(F)**, superimposed with R1 gated population. Fluorescence profiles of the P2 **(G)** and P1 subsets **(H)** of the total population **(E,F)** at pH 6.5 and pH 3.5.

pH Induced Changes in the Proteome of *G. vaginalis* Membrane Vesicles

Mass spectrometric characterization of the proteome of MVs obtained at pH 3.5 revealed a marked difference in protein composition along with a clear reduction in the total number of proteins compared to MVs obtained at pH 6.5 previously described in Shishpal et al. (2020). Compared to a total of 417 proteins identified in our previous study on MVs obtained from cells grown at pH 6.5, only 26 proteins (**Table 1**) could be identified in MVs at pH 3.5 in the present study. Out of these, 14 were found to have a peptide score more than or equal to 2 and twelve amongst these were also common to those found in MVs at pH 6.5 while one of the remaining two proteins was uncharacterized (**Figure 5A**). These proteins were categorized on the basis of predicted sub-cellular locations. Majority of the proteins (93%) were cytoplasm associated and the remaining (7%) were classified as lipid anchored and extracellular proteins by Locate P and Uniprot databases (**Figure 5B**). Functional annotation of the identified proteins indicated enrichment of cellular and metabolic processes such as carbohydrate metabolism.

Effect of pH Induced Changes in *G. vaginalis* Membrane Vesicles on Uptake by Vaginal Epithelial Cells

The pH induced changes in *G. vaginalis* MVs (CFSE stained; green) appeared to have an effect on their adherence to and uptake by vaginal epithelial cells (VK2 cell line). Compared to pH 6.5 MVs which resulted in both adherence to and uptake by VK2 cells (**Figures 6E,F**), pH 3.5 MVs were found to only adhere to VK2 cells without evidence of any significant uptake (**Figures 6G–I**). Although blebbing and changes in actin cytoskeleton network (phalloidin staining; red) of the VK2 cells were observed upon treatment with MVs compared to untreated controls (**Figures 6A–C**), the extent of changes observed in case of pH 3.5 MVs suggests that the apparent reduction in fluorescence of the actin cytoskeleton (**Figure 6D**) was lesser than that seen with pH 6.5 MVs.

Cytotoxicity and IL-8 Cytokine Induction by *G. vaginalis* Membrane Vesicles

In order to understand the functional relevance of the change in protein composition of MVs in response to acidic stress compared to MVs obtained at pH 6.5, their effect on viability of vaginal epithelial cells, VK2 was investigated. Although the pH 6.5 MVs resulted in a significant reduction in viability of the VK2 cells, pH 3.5 MVs were found to have no significant effect on the viability of VK2 cells with the exception of a reduction in viability at a protein concentration of 9.37 µg (**Figure 7A**). On the contrary, pH 3.5 MVs led to a significant dose-dependent increase in the levels of the pro-inflammatory cytokine IL-8 in the vaginal epithelial cells similar to that observed in case of pH 6.5 MVs (**Figure 7B**).

DISCUSSION

Bacteria are exposed to numerous environmental conditions including an alteration in physiological pH which may induce stress. In order to sustain under stress conditions, bacteria employ different strategies including the modulation of the cell membrane components, changes in macromolecules, synthesis

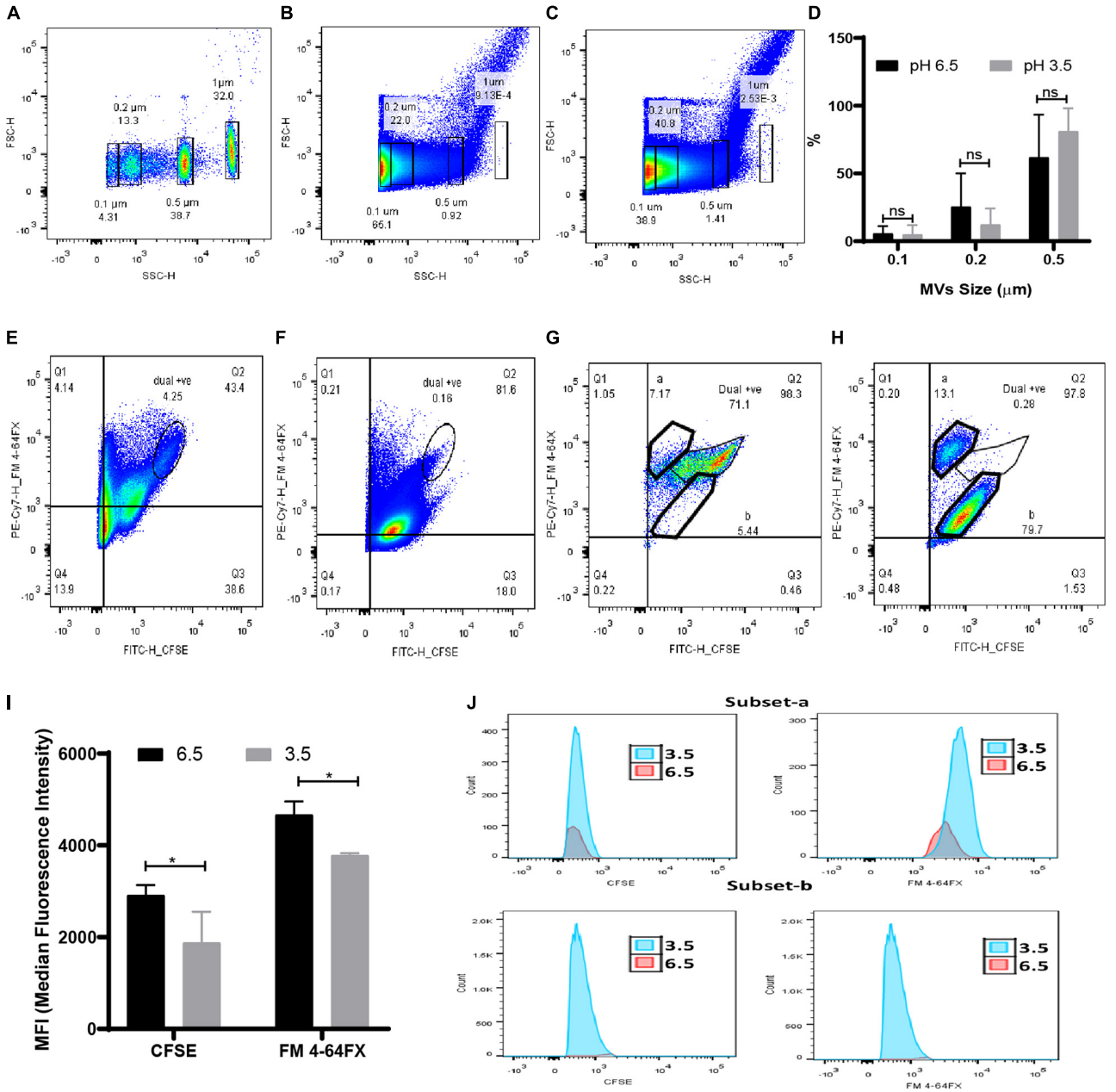

FIGURE 4 | Quantitation of MVs at submicron level under acidic condition by flow cytometry. **(A)** Forward vs side scatter profile of FITC tagged sub-micron beads (0.1, 0.2, 0.5, and 1 µm). Representative scatter profile of protein (CFSE) and lipid stained (FM 4-64FX) MVs of **(B)** pH 6.5 and **(C)** pH 3.5 superimposed with reference beads gate. **(D)** Change in percentage of MVs of varying sizes at pH 6.5 and pH 3.5 corresponds to the superimposed gates on scatter plot of pH 6.5 and pH 3.5 MVs. Data are presented as mean ± SD (n = 3). Quadrant gate, Q2 represents dual positive population of 0.5 µm sized MVs of **(E,G)** pH 6.5 and **(F,H)** pH 3.5 and two sub population at **(G)** pH 6.5 and **(H)** pH 3.5. **(I)** Median Fluorescence intensity of dual positive population of CFSE and FM 4-64FX stained MVs (*p < 0.05). **(J)** Histograms of a and b subsets of pH 6.5 and 3.5 MVs.

of chaperones that are required to prevent protein and DNA damage, etc. (Haruta and Kanno, 2015). The emphasis of studies related to pH stress has been in the context of the microbiota of the gastrointestinal tract (Lund et al., 2014; Sanhueza et al., 2015). Compared to this, fewer studies have focused on stress response of the vaginal microbiota which is also exposed to low pH in case of healthy women. Further, the studies have been restricted only to lactobacilli (Witkin and Linhares, 2017) and there are no studies on mechanisms of adaptation to low pH by anaerobes, which may also inhabit the healthy vagina. In addition to the already mentioned approaches, secretion of MVs has also been proposed as a strategy for adaptation and survival under stress conditions (Volgers et al., 2018). MV formation is a ubiquitous process that occurs in both pathogenic

TABLE 1 | List of proteins identified in *G. vaginalis* MVs at pH 3.5.

Protein names	Accession no	Peptides	Function
Transaldolase	E3D9 × 8	19	Pentose-phosphate pathway
Elongation factor Ts (EF-Ts)	E3D9Z6	12	Translation
Probable phosphoketolase	E3D9B4	8	Unknown
DNA-binding protein HB1*	E3D9I0	4	Stabilization of DNA and preventing its denaturation under extreme environmental conditions
Glyceraldehyde-3-phosphate dehydrogenase, type I	E3D780	5	Glycolysis, moonlighting protein involved in colonization and invasion of host tissues
50S ribosomal protein L17	E3D7W2	2	Translation
Chaperone protein DnaK (HSP70)	E3D8E7	6	Maintains the assembly and disassembly of protein complexes, refolds the misfolded protein
Adenylate kinase (AK; Adenylate monophosphate kinase)	E3D7W7	3	Cellular energy homeostasis and adenine nucleotide metabolism.
30S ribosomal protein S6	E3D771	2	Translation
30S ribosomal protein S16	E3D753	4	Translation
2,3-bisphosphoglycerate-dependent phosphoglycerate mutase (BPG-dependent PGAM)	E3D976	2	Glycolysis, moonlighting protein involved in plasminogen binding
Uncharacterized protein*	E3D7I4	2	Unknown
50S ribosomal protein L11	E3D8P7	2	Translation
50S ribosomal protein L7/L12	E3D8P5	2	Translation
Phosphoglycerate kinase	E3D9V5	1	Glycolysis
50S ribosomal protein L9	E3D768	1	Translation
Ribosome-recycling factor (RRF)	E3D9Z8	1	Translation
Elongation factor P (EF-P)	E3D9U3	1	Translation
50S ribosomal protein L5	E3D7 × 6	1	Translation
Pyruvate kinase	E3DAG4	1	Glycolysis
60 kDa chaperonin (GroEL protein; Protein Cpn60)	E3D9J4	1	Prevents protein misfolding and promotes the refolding
Ribose-5-phosphate isomerase A	E3D8S4	1	Pentose phosphate pathway
ABC transporter, solute-binding protein	E3D881	1	Import of essential nutrients and export of toxic materials
Peptidyl-prolyl *cis*-trans isomerase	E3D8Z5	1	Protein Folding
Alpha-1,4 glucan phosphorylase	E3D7S8	1	Important allosteric enzyme in carbohydrate metabolism
Uncharacterized protein	E3D907	1	Unknown

**Proteins identified only in pH 3.5 MVs.*

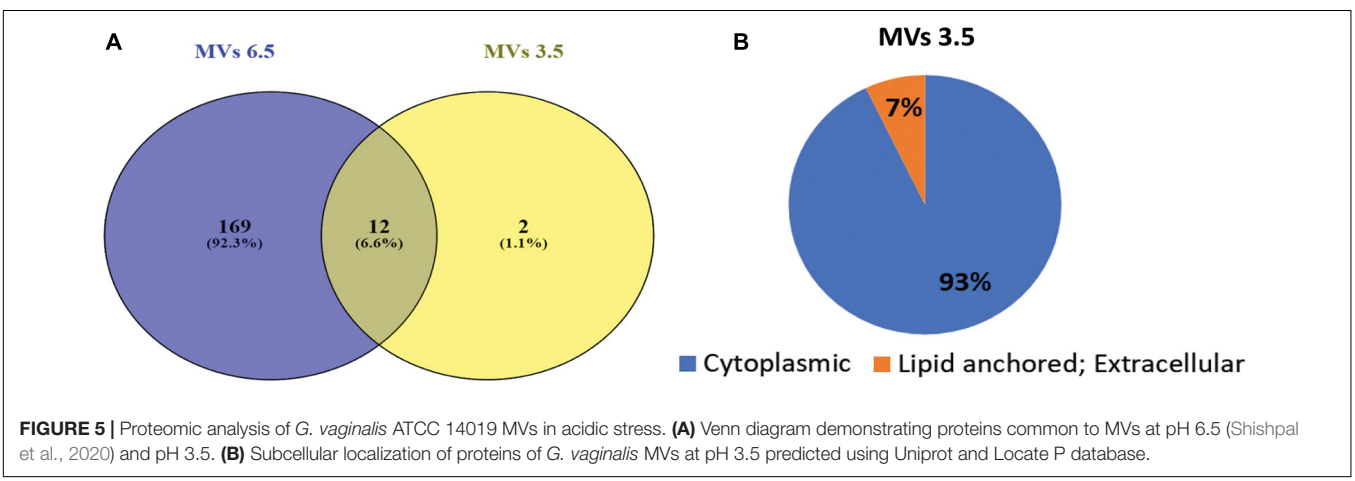

FIGURE 5 | Proteomic analysis of *G. vaginalis* ATCC 14019 MVs in acidic stress. **(A)** Venn diagram demonstrating proteins common to MVs at pH 6.5 (Shishpal et al., 2020) and pH 3.5. **(B)** Subcellular localization of proteins of *G. vaginalis* MVs at pH 3.5 predicted using Uniprot and Locate P database.

and non-pathogenic organisms (Yu et al., 2017). This process has been widely characterized in physiological conditions as a defensive and offensive mechanism. This is on account of the fact that MVs transport virulence factors such as toxins, hydrolytic enzymes and other proteins which facilitate invasion, damage of host cells, down regulation of host immune responses, etc. MVs also carry components which degrade antibiotics, promote biofilm formation, etc. in addition to absorbing cell surface acting antimicrobial agents and protecting the bacterial cells. However, the contribution of MV production as a mechanism

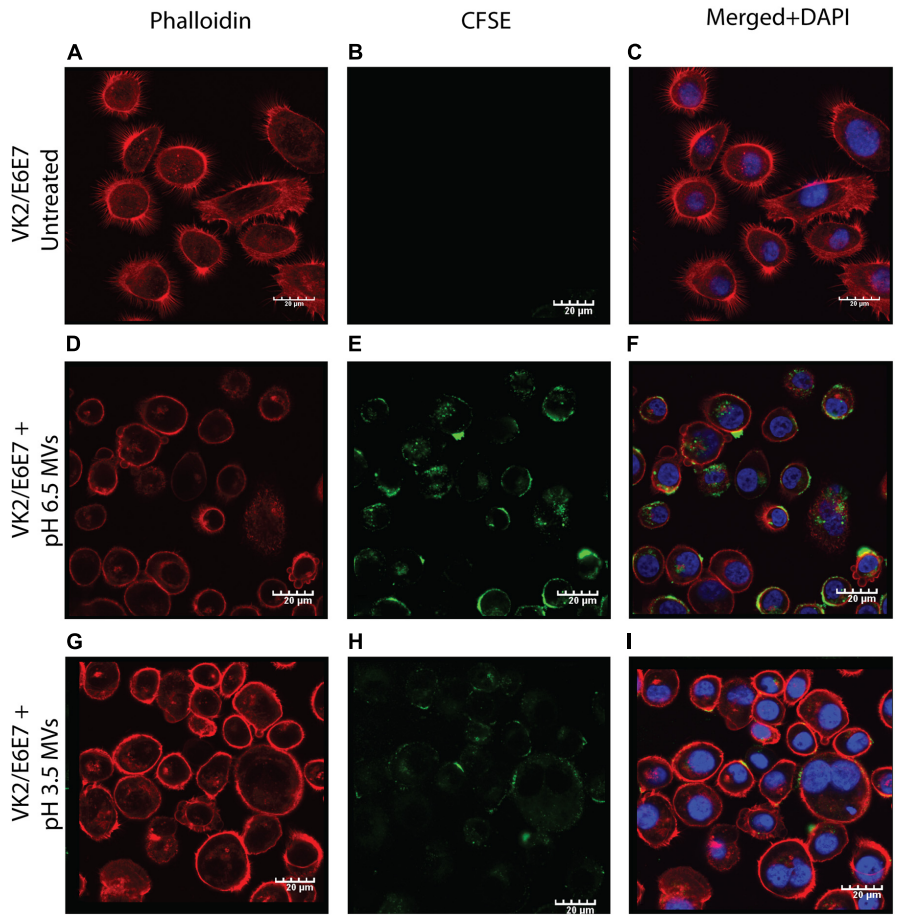

FIGURE 6 | Adherence of *G. vaginalis* ATCC 14019 MVs and uptake by vaginal epithelial cells, VK2. Confocal microscopy sections of phalloidin (red) stained VK2/E6E7 cells treated for 24 h with CFSE (green) stained *G. vaginalis* MVs obtained at pH 6.5 **(D–F)** and pH 3.5 **(G–I)** along with untreated controls **(A–C)**. Nuclei were stained with DAPI (blue). Scale bar 20 μm.

for adaptation to environmental stress has received less attention (MacDonald and Kuehna, 2013; Bonnington and Kuehn, 2015).

Gardnerella vaginalis is an anaerobic bacterium which grows well in less acidic pH (>4.5) of the vaginal milieu during BV, a widely prevalent genital tract infection (Aldunate et al., 2015). However, a healthy vagina characterized by low pH (3.5–4.5) may also harbor *G. vaginalis*, although in reduced numbers (O'Hanlon et al., 2013; Shipitsyna et al., 2013). A significant drop in CFUs of *G. vaginalis* indicates considerable extent of cell death upon exposure to low pH which mimics the physiological environment of a healthy vagina. This has been reported previously (Gottschick et al., 2016) and is also supported by our own results. Further, the reduction in viability of the cells exposed to low pH appears to be accompanied with a reduction in integrity of the proteins or an increase in protein degradation suggested by the qualitative changes in the SDS-PAGE profiles of total cellular proteins from cells grown at pH 3.5 compared to those grown at pH 6.5. Despite the substantial loss of cell viability observed due to acidic stress, there exists a possibility that some of the bacterial cells may survive and adapt to growth in low pH conditions (Aertsen and Michiels, 2004). However, this needs to be still experimentally validated. Nevertheless, the reduction in total protein as well as reduced expression of certain proteins over time could be indicative of both cell death and dormancy. The altered morphology of *G. vaginalis* exposed to pH stress characterized by increased vesiculation therefore reflects altered biogenesis of MVs in cells poised either for lysis or adaptation (Turnbull et al., 2016; Klimentova et al., 2019). The increase in MV production observed in response to pH stress appears to be similar to that reported in case of other stress conditions including stress induced by antibiotic treatment (Devos et al., 2015; Volgers et al., 2018). It is likely that a fraction of the stressed cells may undergo fragmentation followed by "self-annealing" of the fragments leading to generation of larger MVs (Turnbull et al., 2016) while the remaining cells adapt to the stress by actively producing smaller MVs in a regulated manner. This is also supported by the wider size distribution of MVs including both small and large MVs obtained in response to pH stress and demonstrated by DLS measurements which further hint toward altered biogenesis of MVs.

Acidic stress led not only to an increase in the release of MVs but also led to change in the protein integrity, i.e., increased

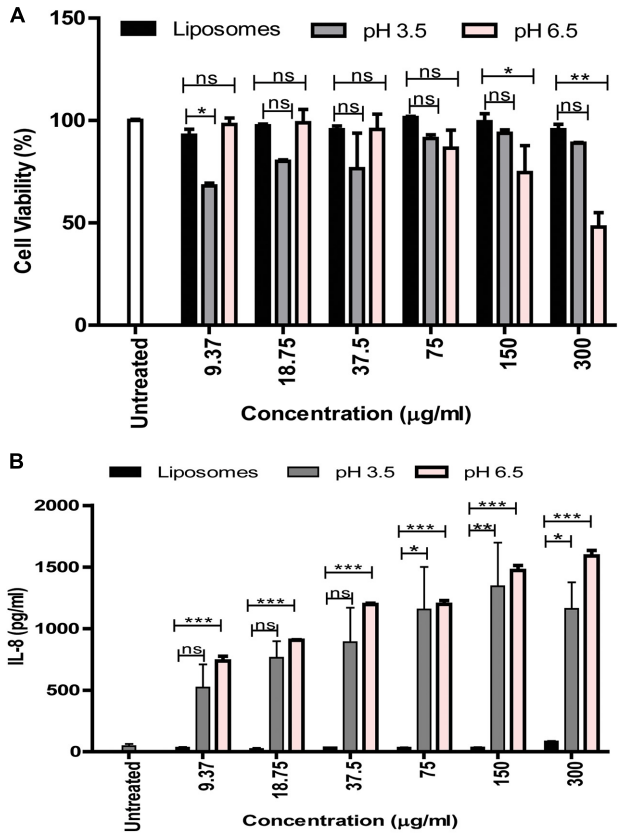

FIGURE 7 | Effect of *G. vaginalis* MVs obtained at pH 6.5 and pH 3.5 on the viability and cytokine induction by vaginal epithelial cells. Cell viability **(A)** and induction of IL-8 **(B)** by VK2 cells in response to treatment with pH 6.5 and pH 3.5 MVs (9.37–300 μg/ml). BSA entrapped liposomes served as control and was used at protein concentrations similar to that of the MVs. Data are presented as mean ± SD. Statistical analysis was done using two-way ANOVA with Bonferroni test $^{*}p < 0.05$; $^{**}p < 0.01$; $^{***}p < 0.001$; and ns, non-significant.

protein degradation, also reflected by the diffused or smear pattern of the SDS-PAGE profile. The fact that MVs isolated from cells grown under non-stressed conditions (pH 6.5) do not exhibit a diffused protein profile upon exposure to acidic conditions post production indicates that the protein degradation observed in MVs isolated from cells grown under acidic stress at pH 3.5 is due to degradation of proteins in the cells from which they have been derived and not due to protein degradation in MVs post production and release from cells. Acidic stress also resulted in reduced protein content of the released MVs, demonstrated by flow cytometry. Qualitative analysis indicated that despite the apparent increase in number of MVs in response to pH stress, there was an overall reduction in protein content of these MVs. Quantitative flow cytometry analysis using dual florescence labeling for proteins and lipids revealed that although pH stress results in an alteration in release of MVs, there is an increase in the percentage of larger MVs (∼0.5 μm) along with a reduction in smaller MVs. It is likely that the increase in release of larger MVs is contributed by both cell death as well as cellular adaptation to stress. Further, there appeared to exist two distinct sub populations of these larger MVs arising most likely due to non-uniform protein distribution as a response to stress compared to a population of MVs without stress (pH 6.5). It is not clear whether pH stress results in either dysregulation of protein packaging to MVs or in selective protein packaging to a distinct subset of MVs.

It is known that stress conditions (such as pH stress) lead to a change in bacterial cell physiology (Baatout et al., 2007). This is reflected by an altered protein composition and may help the cell to survive in an environment characterized by reduced macromolecular stability and increased cellular damage. The protein composition of MVs is altered in response to pH stress with a drastic reduction in the number of proteins compared to non-stressed conditions. The presence of chaperones like Dnak and GroEL as well as the DNA binding protein-HB1 despite the overall reduction in protein diversity suggests that they could play an important role in acid tolerance by prevention of protein and nucleic acid denaturation (Susin et al., 2006; Henderson and Martin, 2011). It is evident that the presence of some of the proteins required for translation and carbohydrate metabolism, i.e., glycolysis and pentose phosphate pathway in the MVs is on account of their essential role in the survival of the bacterial cell. It is likely that some of the bacterial cells which have adapted to the pH stress may transfer these proteins via the MVs to rescue surrounding bacterial cells (Schwechheimer et al., 2014). It is notable that some of the protein constituents of the MVs produced under non-stressed conditions, e.g., proteins suggested to be involved in host cell invasion and virulence (Shishpal et al., 2020) including the pore forming toxin, vaginolysin are missing in MVs produced in response to pH stress.

Additionally, the absence of these proteins in the stress induced MVs could explain the apparent reduction of their ability to be internalized by the host cells as well as their diminished cytotoxic potential. Despite the reduced internalization and cytotoxicity of the vaginal epithelial cells, acidic stress induced MVs resulted in induction of the pro-inflammatory cytokine, IL-8. A likely explanation for this effect could be the presence of cell membrane and cell wall constituents such as lipopolysaccharide and peptidoglycan which may also be associated with these MVs (Pivarcsi et al., 2005).

This study for the first time provides an insight into the probable mechanisms for adaptation to acidic stress employed by *G. vaginalis*, an anaerobe usually associated with BV but also found in the vaginal tract of healthy women. The results of the study demonstrate that acidic stress encountered by *G. vaginalis* on account of exposure to low pH leads to modulation of the biogenesis of MVs. This is also reflected in the altered morphology of the bacterial cells as well as altered size distribution and protein content and composition as well as reduced cytotoxic potential of the stress induced MVs. Apart from being required for survival of *G. vaginalis* in the vaginal lactobacilli dominated, lactic acid induced, low pH environment of a healthy vagina, the modulation of MV composition and function is also in concordance with host physiology in absence of vaginal infection. The relevance of these findings could be further validated by comparing the compositional and functional

profile of MVs obtained from vaginal tract of healthy women and women with BV. Though the present study focused on potential mechanisms of stress adaptation by *G. vaginalis* ATCC 14019, similar approaches could be used to investigate the phenomenon of adaptation to low pH by other anaerobes found, in the healthy vagina.

DATA AVAILABILITY STATEMENT

The original contributions presented in the study are included in the article/**Supplementary Material**; further inquiries can be directed to the corresponding author/s.

AUTHOR CONTRIBUTIONS

PS designed and performed the experiments, analyzed the results, and prepared the figures. VP provided vital support for design and interpretation of the flow cytometry experiments. DS provided support for performing electron microscopy experiments and also captured electron microscopy images. VB conceived the study, designed the experiments, interpreted the data, and critically reviewed the manuscript for intellectual content. VB and PS wrote the manuscript. All authors have read and approved the final manuscript.

FUNDING

This work was supported by intramural funds received from ICMR-NIRRH.

ACKNOWLEDGMENTS

The authors thank the former Director Smita Mahale and current Director Geetanjali Sachdeva, ICMR-NIRRH for financial support in the form of intramural funds for conducting this study. The technical support provided by Shilpa Velhal and Shilpa Bhowmick for sample acquisition for the flow cytometry experiments is acknowledged. The authors also thank Vandana Patravale, Institute of Chemical Technology (ICT), Matunga, Mumbai, India for providing access to the Zetasizer Nano-ZS for DLS experiments. The award of senior research fellowship to PS by the University Grants Commission (UGC) New Delhi is also acknowledged.

SUPPLEMENTARY MATERIAL

The Supplementary Material for this article can be found online at: https://www.frontiersin.org/articles/10.3389/fmicb.2021.723909/full#supplementary-material

REFERENCES

Aertsen, A., and Michiels, C. W. (2004). Stress and how bacteria cope with death and survival. *Crit. Rev. Microbiol.* 4, 263–273. doi: 10.1080/10408410490884757

Aldunate, M., Srbinovski, D., Hearps, A. C., Latham, C. F., Ramsland, P. A., Gugasyan, R., et al. (2015). Antimicrobial and immune modulatory effects of lactic acid and short chain fatty acids produced by vaginal microbiota associated with eubiosis and bacterial vaginosis. *Front. Physiol.* 6, 1–23. doi: 10.3389/fphys.2015.00164

Avila-Calderón, E. D., Araiza-Villanueva, M. G., Cancino-Diaz, J. C., López-Villegas, E. O., Sriranganathan, N., Boyle, S. M., et al. (2014). Roles of bacterial membrane vesicles. *Arch. Microbiol.* 197:1. doi: 10.1007/s00203-014-1042-7

Baatout, S., Leys, N., Hendrickx, L., Dams, A., and Mergeay, M. (2007). Physiological changes induced in bacteria following pH stress as a model for space research. *Acta Astronaut.* 60, 451–459. doi: 10.1016/j.actaastro.2006.09.012

Bonnington, K. E., and Kuehn, M. J. (2015). Protein selection and export via outer membrane vesicles. *Biochim. Biophys. Acta* 8, 1612–1619. doi: 10.1016/j.bbamcr.2013.12.011

Castro, J., Alves, P., Sousa, C., Cereija, T., Franca, A., Jefferson, K. K., et al. (2015). Using an in-vitro biofilm model to assess the virulence potential of Bacterial Vaginosis or non-Bacterial Vaginosis Gardnerella vaginalis isolates. *Sci. Rep.* 5, 1–10. doi: 10.1038/srep11640

Ceccarani, C., Foschi, C., Parolin, C., D'Antuono, A., Gaspari, V., Consolandi, C., et al. (2019). Diversity of vaginal microbiome and metabolome during genital infections. *Sci. Rep.* 9:14095. doi: 10.1038/s41598-019-50410-x

Devos, S., Van Oudenhove, L., Stremersch, S., Van Putte, W., De Rycke, R., Van Driessche, G., et al. (2015). The effect of imipenem and diffusible signaling factors on the secretion of outer membrane vesicles and associated Ax21 proteins in *Stenotrophomonas* maltophilia. *Front. Microb.* 6:298. doi: 10.3389/fmicb.2015.00298

Görgens, A., Bremer, M., Ferrer-Tur, R., Murke, F., Tertel, T., Horn, P. A., et al. (2019). Optimisation of imaging flow cytometry for the analysis of single extracellular vesicles by using fluorescence-tagged vesicles as biological reference material. *J. Extracell. Vesicles* 8:1. doi: 10.1080/20013078.2019.1587567

Gottschick, C., Szafranski, S. P., Kunze, B., Sztajer, H., Masur, C., Abels, C., et al. (2016). Screening of compounds against gardnerella vaginalis biofilms. *PLoS One* 4, 1–16. doi: 10.1371/journal.pone.0154086

Haruta, S., and Kanno, N. (2015). Survivability of microbes in natural environments and their ecological impacts. *Microbes Environ.* 2, 123–125. doi: 10.1264/jsme2.ME3002rh

Henderson, B., and Martin, A. (2011). MINIREVIEW Bacterial Virulence in the Moonlight: Multitasking Bacterial Moonlighting Proteins Are Virulence Determinants in Infectious Disease. *Infect. Immun.* 9, 3476–3491. doi: 10.1128/IAI.00179-11

Jung, H. S., Ehlers, M. M., Lombaard, H., Redelinghuys, M. J., and Kock, M. M. (2017). Etiology of bacterial vaginosis and polymicrobial biofilm formation. *Crit. Rev. Microbiol.* 6, 651–667. doi: 10.1080/1040841X.2017.1291579

Klimentova, J., Pavkova, I., Horcickova, L., Bavlovic, J., Kofronova, O., Benada, O., et al. (2019). Francisella tularensis subsp. holarctica Releases Differentially Loaded Outer Membrane Vesicles Under Various Stress Conditions. *Front. Microbiol.* 10, 1–16. doi: 10.3389/fmicb.2019.02304

Lund, P., Tramonti, A., and De Biase, D. (2014). Coping with low pH: Molecular strategies in neutralophilic bacteria. *FEMS Microbiol. Rev.* 6, 1091–1125. doi: 10.1111/1574-6976.12076

MacDonald, I. A., and Kuehna, M. J. (2013). Stress-induced outer membrane vesicle production by *Pseudomonas aeruginosa*. *J. Bacteriol.* 13, 2971–2981. doi: 10.1128/JB.02267-12

O'Hanlon, D. E., Moench, T. R., and Cone, R. A. (2013). Vaginal pH and microbicidal lactic acid when lactobacilli dominate the microbiota. *PLoS One* 11, 1–8. doi: 10.1371/journal.pone.0080074

Patterson, J. L., Stull-lane, A., Girerd, P. H., Jefferson, K. K., and Jefferson, K. K. (2010). Analysis of adherence, biofilm formation and cytotoxicity suggests a greater virulence potential of Gardnerella vaginalis relative to other bacterial-vaginosis-associated anaerobes. *Microbiology* 156, 392–399. doi: 10.1099/mic.0.034280-0

Pivarcsi, A., Nagy, I., Koreck, A., Kis, K., Kenderessy-Szabo, A., Szell, M., et al. (2005). Microbial compounds induce the expression of pro-inflammatory

cytokines, chemokines and human β-defensin-2 in vaginal epithelial cells. *Microbes Infect.* 9–10, 1117–1127. doi: 10.1016/j.micinf.2005.03.016

Pospichalova, V., Svoboda, J., Dave, Z., Kotrbova, A., Kaiser, K., Klemova, D., et al. (2015). Simplified protocol for flow cytometry analysis of fluorescently labeled exosomes and microvesicles using dedicated flow cytometer. *J. Extracell. Vesicles* 2015, 1–15. doi: 10.3402/jev.v4.25530

Reid, G. (2008). Probiotic Lactobacilli for urogenital health in women. *J. Clin. Gastroenterol.* 42, 234–236. doi: 10.1097/MCG.0b013e31817f1298

Rosca, A. S., Castro, J., Cerca, N., and Rosca, A. S. (2020). Evaluation of different culture media to support in vitro growth and biofilm formation of bacterial vaginosis-associated anaerobes. *PeerJ* 8:e9917. doi: 10.7717/peerj.9917

Sanhueza, E., Paredes-Osses, E., González, C. L., and García, A. (2015). Effect of pH in the survival of Lactobacillus salivarius strain UCO_979C wild type and the ph acid acclimated variant. *Electron. J. Biotechnol.* 5, 343–346. doi: 10.1016/j.ejbt.2015.06.005

Schooling, S. R., and Beveridge, T. J. (2006). Membrane vesicles: An overlooked component of the matrices of biofilms. *J. Bacteriol.* 16, 5945–5957. doi: 10.1128/JB.00257-06

Schwechheimer, C., Kulp, A., and Kuehn, M. J. (2014). Modulation of bacterial outer membrane vesicle production by envelope structure and content Modulation of bacterial outer membrane vesicle production by envelope structure and content. *BMC Microbiol.* 14:324. doi: 10.1186/s12866-014-0324-1

Shipitsyna, E., Roos, A., Datcu, R., Hallén, A., Fredlund, H., Jensen, J. S., et al. (2013). Composition of the vaginal microbiota in women of reproductive age–sensitive and specific molecular diagnosis of bacterial vaginosis is possible? *PLoS One* 8:e60670. doi: 10.1371/journal.pone.0060670

Shishpal, P., Kasarpalkar, N., Singh, D., and Bhor, V. M. (2020). Characterization of Gardnerella vaginalis membrane vesicles reveals a role in inducing cytotoxicity in vaginal epithelial cells. *Anaerobe* 61:102090. doi: 10.1016/j.anaerobe.2019.102090

Susin, M. F., Baldini, R. L., Gueiros-Filho, F., and Gomes, S. L. (2006). GroES/GroEL and DnaK/DnaJ have distinct roles in stress responses and during cell cycle progression in Caulobacter crescentus. *J. Bacteriol.* 23, 8044–8053. doi: 10.1128/JB.00824-06

Turnbull, L., Hynen, A. L., Kurosawa, M., Pessi, G., Petty, N. K., Osvath, S. R., et al. (2016). Explosive cell lysis as a mechanism for the biogenesis of bacterial membrane vesicles and biofilms. *Nat. Commun.* 2016:7. doi: 10.1038/ncomms11220

Vaneechoutte, M., Guschin, A., Van Simaey, L., Gansemans, Y., Van Nieuwerburgh, F., Cools, P., et al. (2019). Emended description of Gardnerella vaginalis and description of Gardnerella leopoldii sp. nov., Gardnerella piotii sp. nov. and Gardnerella swidsinskii sp. nov., with delineation of 13 genomic species within the genus Gardnerella. *Internat. J. Syst. Evol. Microb.* 69, 679–687. doi: 10.1099/ijsem.0.003200

Volgers, C., Savelkoul, P. H. M., and Stassen, F. R. M. (2018). Gram-negative bacterial membrane vesicle release in response to the host-environment: different threats, same trick? *Crit. Rev. Microbiol.* 3, 258–273. doi: 10.1080/1040841X.2017.1353949

Witkin, S. S., and Linhares, I. M. (2017). Why do lactobacilli dominate the human vaginal microbiota? *BJOG Int. J. Obstet. Gynaecol.* 4, 606–611. doi: 10.1111/1471-0528.14390

Yu, Y., Wang, X., and Fan, G. (2017). Versatile effects of bacterium-released membrane vesicles on mammalian cells and infectious / inflammatory diseases. *Nat. Publ. Gr.* 4, 514–533. doi: 10.1038/aps.2017.82

Zhang, H. (2017). Thin-Film Hydration Followed by Extrusion Method for Liposome Preparation. *Methods Mol Biol.* 1522, 17–22. doi: 10.1007/978-1-4939-6591-5_2

Conflict of Interest: The authors declare that the research was conducted in the absence of any commercial or financial relationships that could be construed as a potential conflict of interest.

Publisher's Note: All claims expressed in this article are solely those of the authors and do not necessarily represent those of their affiliated organizations, or those of the publisher, the editors and the reviewers. Any product that may be evaluated in this article, or claim that may be made by its manufacturer, is not guaranteed or endorsed by the publisher.

frontiers in Microbiology

ORIGINAL RESEARCH
published: 29 November 2021
doi: 10.3389/fmicb.2021.747606

Incorporation of Plasmid DNA Into Bacterial Membrane Vesicles by Peptidoglycan Defects in *Escherichia coli*

Sharmin Aktar[1†], Yuhi Okamoto[2†], So Ueno[1], Yuhei O. Tahara[3,4], Masayoshi Imaizumi[2], Masaki Shintani[1,2,5,6], Makoto Miyata[3,4], Hiroyuki Futamata[1,2,5,6], Hideaki Nojiri[7] and Yosuke Tashiro[1,2,5,8]*

[1] Department of Engineering, Graduate School of Integrated Science and Technology, Shizuoka University, Hamamatsu, Japan, [2] Faculty of Engineering, Shizuoka University, Hamamatsu, Japan, [3] Graduate School of Science, Osaka City University, Osaka, Japan, [4] The OCU Advanced Research Institute for Natural Science and Technology (OCARINA), Osaka City University, Osaka, Japan, [5] Graduate School of Science and Technology, Shizuoka University, Hamamatsu, Japan, [6] Research Institute of Green Science and Technology, Shizuoka University, Shizuoka, Japan, [7] Agro-Biotechnology Research Center, Graduate School of Agricultural and Life Sciences, The University of Tokyo, Tokyo, Japan, [8] JST PRESTO, Kawaguchi, Japan

OPEN ACCESS

Edited by:
Rafael A. Garduno, Retired, Fredericton, NB, Canada

Reviewed by:
Jun-Seob Kim, Incheon National University, South Korea
Sara Domingues, University of Coimbra, Portugal

***Correspondence:**
Yosuke Tashiro
tashiro.yosuke@shizuoka.ac.jp

[†] These authors have contributed equally to this work and share first authorship

Specialty section:
This article was submitted to Microbial Physiology and Metabolism, a section of the journal Frontiers in Microbiology

Received: *26 July 2021*
Accepted: *29 October 2021*
Published: *29 November 2021*

Citation:
Aktar S, Okamoto Y, Ueno S, Tahara YO, Imaizumi M, Shintani M, Miyata M, Futamata H, Nojiri H and Tashiro Y (2021) Incorporation of Plasmid DNA Into Bacterial Membrane Vesicles by Peptidoglycan Defects in Escherichia coli. Front. Microbiol. 12:747606. doi: 10.3389/fmicb.2021.747606

Membrane vesicles (MVs) are released by various prokaryotes and play a role in the delivery of various cell-cell interaction factors. Recent studies have determined that these vesicles are capable of functioning as mediators of horizontal gene transfer. Outer membrane vesicles (OMVs) are a type of MV that is released by Gram-negative bacteria and primarily composed of outer membrane and periplasm components; however, it remains largely unknown why DNA is contained within OMVs. Our study aimed to understand the mechanism by which DNA that is localized in the cytoplasm is incorporated into OMVs in Gram-negative bacteria. We compared DNA associated with OMVs using *Escherichia coli* BW25113 cells harboring the non-conjugative, non-mobilized, and high-copy plasmid pUC19 and its hypervesiculating mutants that included Δ*nlpI*, Δ*rseA,* and Δ*tolA*. Plasmid copy per vesicle was increased in OMVs derived from Δ*nlpI*, in which peptidoglycan (PG) breakdown and synthesis are altered. When supplemented with 1% glycine to inhibit PG synthesis, both OMV formation and plasmid copy per vesicle were increased in the wild type. The bacterial membrane condition test indicated that membrane permeability was increased in the presence of glycine at the late exponential phase, in which cell lysis did not occur. Additionally, quick-freeze deep-etch and replica electron microscopy observations revealed that outer-inner membrane vesicles (O-IMVs) are formed in the presence of glycine. Thus, two proposed routes for DNA incorporation into OMVs under PG-damaged conditions are suggested. These routes include DNA leakage due to increased membrane permeation and O-IMV formation. Additionally, our findings contribute to a greater understanding of the vesicle-mediated horizontal gene transfer that occurs in nature and the utilization of MVs for DNA cargo.

Keywords: membrane vesicles, plasmid, peptidoglycan, glycine, quick-freeze deep-etch and replica electron microscopy, outer membrane vesicles

INTRODUCTION

The release of membrane vesicles (MVs) is a widespread phenomenon in prokaryotic cells. These spherical particles are 20–400 nm in a diameter and have been reported to facilitate a number of biological functions, including the delivery of proteins, signals, and toxins to target cells and the release unnecessary substances in the context of the envelope stress response (Tashiro et al., 2012). In particular, MVs derived from Gram-negative bacteria that are also known as outer membrane vesicles (OMVs) are composed of outer membrane (OM) and periplasmic components (Toyofuku et al., 2015).

In bacteria and archaea, genome revolution via recombination with foreign DNA requires horizontal gene transfer (HGT). Vesicle-mediated gene transfer has been identified as a novel mechanism of HGT that functions in addition to the three traditional mechanisms, including conjugation, transformation and transduction (Hasegawa et al., 2015; Tashiro et al., 2019; Soler and Forterre, 2020). Gene exchange via MVs has been observed across a broad range of bacterial species that include Gram-negative bacteria (Dorward et al., 1989; Kolling and Matthews, 1999; Yaron et al., 2000; Rumbo et al., 2011; Fulsundar et al., 2014), Gram-positive bacteria (Klieve et al., 2005) and archaea (Gaudin et al., 2013) that are derived from various environments such as seawater, rumen, gut, and periodontitis (Domingues and Nielsen, 2017). Additionally, bacterial MVs can transfer DNA into the nucleus of eukaryotic cells (Bitto et al., 2017). MV-mediated gene transfer possesses several advantages over other HGT mechanisms. This process protects packaged DNA from degradative enzymes and permits DNA transfer over long distances and time frames. In contrast to transduction with bacteriophages, recipients are not strictly limited in MV-mediated HGT (Tran and Boedicker, 2017). Although plasmid characteristics such as plasmid copy number and origin of replication can affect the efficiency of MV-mediated HGT, this process does not require a donor to possess a specialized set of gene products like conjugation (Tran and Boedicker, 2019).

A variety of Gram-negative bacteria release OMVs, but it remains unclear how DNA localized in the cytoplasm is packaged into OMVs. Proteomic analyses have indicated that cytoplasmic and inner membrane proteins and also periplasmic and outer membrane proteins (OMPs) are all present in OMVs derived from various Gram-negative bacteria (Lee et al., 2007; Choi et al., 2011; Aguilera et al., 2014). A proposed mechanism for the incorporation of DNA into MVs in Gram-negative bacteria is the formation of outer-inner membrane vesicles (O-IMVs) that exist as double membrane structures of OM and inner membrane (IM). These unique MVs were first identified in the ocean bacterium *Shewanella vesiculosa* $M7^T$ (Pérez-Cruz et al., 2013). It was subsequently confirmed that O-IMVs are naturally secreted by several Gram-negative bacteria such as *Neisseria gonorrhoeae*, *Pseudomonas aeruginosa*, and *Acinetobacter baumannii,* and DNA and ATP were both detected in the O-IMVs (Pérez-Cruz et al., 2015). Another possible route for the formation of MVs containing cytoplasmic components in Gram-negative bacteria is explosive cell lysis that is triggered by phage-derived endolysin (Turnbull et al., 2016; Toyofuku et al., 2018). Endolysin degrades the peptidoglycan (PG) cell wall to facilitate the formation of MVs that are likely composed of OM or IM. Cell lysis is considered as an underlying reason for the existence of cytoplasmic components such as DNA in MVs. However, it remains unknown how DNA is sorted into OMVs through processes other than the formation of O-IMVs and explosive cell lysis. Additionally, little is known regarding the timing and contributing factors of O-IMV formation.

Currently, several mechanisms have been suggested to be responsible for the blebbing observed in OMV biogenesis based on studies examining mutants that are lacking genes related to bacterial surfaces in Gram-negative bacteria. One of the best-characterized factors is encoded by a gene cluster known as *tol-pal* that is conserved across most Gram-negative bacteria. The Tol-Pal system is comprised of five proteins (TolA, TolB, TolQ, TolR, and Pal), and these components are linked to the inner membrane, PG, and OM (Sturgis, 2001). The deletion of one of these components results in increased vesicle formation due to dissociation of the OM from the underlying PG in various Gram-negative bacteria (Sonntag et al., 1978; Bouveret et al., 1995; Bernadac et al., 1998; Turner et al., 2015; Takaki et al., 2020). The deletion of *nlpI* also induces OMV formation in *E. coli* (McBroom et al., 2006). It has been postulated that the balance between PG breakdown and synthesis is altered in the *nlpI* mutant, and covalent crosslinks are not properly formed between PG and Lpp, which is a major lipoprotein in *E. coli* (Schwechheimer et al., 2015; Schwechheimer and Kuehn, 2015). Additionally, the deletion of σ^E-related genes, including *rseA*, *degP*, and *degS*, is also known to enhance OMV formation (McBroom et al., 2006). These mutations cause accumulation of misfolded proteins within the periplasm and increase OMV formation in Gram-negative bacteria (McBroom and Kuehn, 2007; Tashiro et al., 2009; Schwechheimer et al., 2014).

In this study, we explored which blebbing mechanism affects the incorporation of DNA into OMVs. We analyzed the DNA content of OMVs derived from an *E. coli* wild type (WT) strain and from several hypervesiculating mutants, including Δ*nlpI*, Δ*rseA*, and Δ*tolA*, using plasmid pUC19. We demonstrated that PG defects increase plasmid sorting into OMVs and that glycine-induced vesicles includes higher concentration of plasmid. Our findings contribute to a greater understanding of how plasmids are contained in OMVs.

MATERIALS AND METHODS

Bacterial Strains, Plasmids, and Growth Conditions

All bacterial strains and plasmids used in this study were listed in **Supplementary Table 1**. *E. coli* K12 BW25113 (used as WT) and its derivatives (KEIO collection) were obtained from National BioResource Project (National Institute of Genetics) (Baba et al., 2006). Plasmid pCP20 was introduced into each mutant harboring FRT-Km-FRT cassette and the kanamycin (Km) cassette was eliminated using flippase/flippase recognition target (Flp/FRT) recombination. Plasmid pUC19 was introduced into non-marker mutants and the transformants were used for

further experiments. *E. coli* cells were grown in lysogeny broth (LB) Miller (1% w/v tryptone, 0.5% w/v yeast extract and 1% w/v NaCl) at 37°C with shaking at 200 rpm or on solid LB agar plates. When required, antibiotics were added to the medium at 100 μg/mL ampicillin or 50 μg/mL kanamycin. 10% glycine was added to be a final concentration of 1%, when necessary.

Extraction and Quantification of Vesicles

Vesicle extraction from *E. coli* was performed as previously described with some modifications (Ojima et al., 2015). Precultures were inoculated into 100 mL of LB broth with or without 1% glycine at an initial OD_{600} of 0.01, and they were grown with shaking for 16 h at 37°C. Bacterial cells were removed by centrifugation, and the supernatants were filtered through 0.45 μm and 0.2 μm-pore-size filters. Ammonium sulfate was added to the filtrates (final concentration of 400 g/L), and the samples were incubated at room temperature for 1 h. Vesicles were recovered from the suspensions by centrifugation at 9,500 × *g* for 30 min at 20°C. Pellets were resuspended in 15% (v/v) glycerol and concentrated by ultracentrifugation at 150,000 × *g* for 1 h at 4°C using an Himac CP80WX and a P50A3 rotor (Eppendorf Himac Technologies, Hitachinaka, Japan), and they were then resuspended in 50 mM HEPES (pH 6.8)-0.85% (w/v) NaCl (HEPES-NaCl buffer). The vesicles were stored at −80°C until further use.

For quantification of vesicles, extracted vesicles were incubated with 5 μg/mL of FM4-64 for 30 min on a 96-well black plate at 37°C in the dark. The fluorescence intensities of the fluorescently labeled samples were measured using a microplate reader (PerkinElmer, Waltham, MA, United States) at 506/750 nm (excitation/emission wavelength). Water-soluble linoleic acid was used as a standard. Vesicle formation is presented as the amount of vesicles normalized to the cell density.

Quantification of DNA Concentration

Extracellular and vesicle-associated DNA was quantified using a Quant-iT PicoGreen assay (Thermo Fisher Scientific, Waltham, MA, United States). For quantification of extracellular DNA, cell cultures were centrifugated and the supernatants were filtered through 0.45 μm and 0.2 μm-pore-size filters to remove bacterial cells. If necessary, vesicle-free supernatants were prepared by the ultracentrifugation at 150,000 × *g* for 1 h at 4°C. DNA concentration of the supernatant was measured using the PicoGreen. A Tris-EDTA (TE) buffer (pH 8.0) was used to dilute the PicoGreen and lambda-DNA. A standard curve was constructed by serial dilution of DNA based on quantitation by the commercial provider and then incubated for 5 min at room temperature while protected from light. After incubation, the sample fluorescence was measured using a microplate reader (PerkinElmer) at 480 nm for excitation and 520 nm for emission.

For quantification of vesicle-associated DNA, extracted vesicles were treated with GES lysis reagent (5M guanidinum thiocyanate, 100 mM EDTA, 0.5% w/v sodium *N*-lauroylsarcosinate) for prior to labeling. DNA concentrations were measured by PicoGreen, and the values were normalized to the vesicle protein concentration. Vesicles were lysed with 1% (w/v) SDS and protein concentration of vesicles were determined using a Micro BCA Protein Assay Reagent Kit (Thermo Fisher Scientific).

Internal vesicle-associated DNA was obtained by the treatment of vesicles (20 μg protein) with 2 U DNase I (Fujifilm Wako Pure Chemical Co., Osaka, Japan) at 37°C for 30 min according to the manufacturer's directions, followed by release of the internal DNA by lysis of vesicles with GES reagent. External and internal DNA associated with vesicles derived from *E. coli* grown with and without 1% glycine was quantified using PicoGreen.

Particle Analyses

Hydrodynamic diameters of vesicles were measured by a Zetasizer Nano ZS particle analyzer (Malvern Panalytical Ltd., Malvern, United Kingdom) in HEPES-NaCl buffer at 30°C. The hydrodynamic zeta average diameter was calculated using the dynamic light scattering (DLS) method. The concentration of vesicles was measured by nanoparticle tracking analysis (NTA) using a NanoSight LM10 instrument (Malvern) equipped with an sCMOS camera (Andor, Belfast, United Kingdom) as described previously (Tashiro et al., 2017). Briefly, the samples were diluted in HEPES-NaCl buffer, five replicate videos were collected from each sample, and particle movement was analyzed using NTA software (Version 3.1, Malvern). The velocity of particle movement was used to calculate the particle size according to the two-dimensional Stokes-Einstein equation.

Quantitative PCR Analyses

The plasmid copy number was determined by real-time PCR analysis. For quantification of internal vesicle-associated plasmid, extracted vesicles were treated with DNase I at 37°C for 30 min to remove external DNA, DNase I was inactivated at 75°C for 15 min, and internal DNA was released from vesicles at 100°C for 10 min. DNA fragments were amplified and quantified using LightCycler FastStart DNA Master SYBR Green I (Roche, Basel, Switzerland) with specific primer pairs (M13-F/M13-R for pUC19 and dxs-F/dxs-R for chromosome listed in **Supplementary Table 1**) on a LightCycler 2.0 (Roche) according to the manufacturer's instructions.

Membrane Permeability Assays

The permeability of bacterial membrane was analyzed by using *Bac*Light Live/Dead bacterial viability staining kit (Thermo Fisher Scientific). Bacterial cells grown at the late exponential phase was centrifuged and washed twice with 0.85% NaCl. Cell suspension was treated with SYTO9 and propidium iodide (PI) following the manufacturer's instruction. Cells were observed using the Olympus IX73 (Olympus, Tokyo, Japan) microscope, and images were captured with the charge-coupled-device (CCD) camera DP73 and processed by the imaging software cellSens.

The permeability of the outer membrane was analyzed by using fluorescent probe 1-*N*-phenylnaphthylamine (NPN) as previously described (Soh et al., 2020). Briefly, bacterial cells were centrifuged and washed twice with 5 mM HEPES buffer (pH 7.2) containing 1 mM sodium azide. Cell suspension was adjusted to OD_{600} = 0.5 and kept at room temperature for 30 min. 200 μL of samples were applied to black microtiter

plate and 4 μL of 500 mM NPN was mixed to achieve a final concentration of 10 μM. The NPN fluorescence was measured using a microplate reader (PerkinElmer) at 350 nm for excitation and 420 nm for emission.

Transmission Electron Microscopic Observation

For observation of negatively stained vesicles, samples were placed on Cu400 mesh grids (JEOL, Tokyo, Japan) that were pretreated with 0.01% α-poly-L-lysine. Bacterial cells and vesicles were stained with 2% $(NH_4)_6Mo_7O_{24}$ and observed using a JEM-1010 (JEOL) at 80 kV that was equipped with a FastScan-F214 (T) CCD camera (TVIPS, Gauting, Germany).

For quick freeze and replica electron microscopic (QFDE-EM) observations, the protocol was as described previously (Takaki et al., 2020). Briefly, bacterial cells were centrifuged, washed, mixed with a rabbit lung slab and mica flakes, and then placed on a paper disk attached to an aluminum disc. The samples were quickly frozen in liquid helium using a CryoPress (Valiant Instruments, St. Louis, MO, United States). The specimens were placed in a chamber maintained at −180°C using a JFDV freeze-etching device (JEOL). The samples were freeze-fractured with a knife and freeze-etched. Subsequently, the samples were coated with platinum and then coated with carbon. The replicas were floated in full-strength hydrofluoric acid, rinsed in water, cleaned with a commercial bleach containing sodium hypochlorite, and rinsed in water. Replica specimens were placed onto grids and observed using a JEM-1010 (JEOL).

RESULTS

Incorporation of Plasmid Into Vesicles Is Increased in *nlpI* Mutant

The incorporation of plasmid DNA into OMVs has previously been reported in *E. coli* (Tran and Boedicker, 2017, 2019); however, the mechanism by which plasmid DNA moves from the cytoplasm to OMVs has not been fully elucidated. To gain further insight regarding this process, we focused our studies on examining the relationship between OMV biogenesis and the incorporation of plasmids into MVs. We used *E. coli* BW25113 WT and three high OMV-producing strains (Δ*nlpI*, Δ*rseA*, or Δ*tolA*) that possessed differing hypervesiculating mechanisms. The non-conjugative, non-mobilized and high copy number plasmid pUC19 was used in this experiment, as the copy number per vesicle was the highest among plasmids as previously tested by Tran and Boedicker (2017). These mutants harboring pUC19 exhibited higher OMV formation compared to that of the control strain WT/pUC19 (**Figure 1**). The average hydrodynamic diameter of OMVs derived from Δ*nlpI* was slightly less than that from WT, and those from Δ*rseA* and Δ*tolA* did not differ from that of WT (**Supplementary Figure 1**).

To investigate the association of DNA with OMVs, DNA concentration was investigated using the PicoGreen assay that detects double-stranded DNA. First, we measured the DNA concentration of the supernatant before and after ultracentrifugation to examine the extent of DNA associated with OMVs. Concentrations of extracellular DNA (eDNA) in Δ*nlpI* and Δ*rseA* were higher than those in WT, while the eDNA concentration was significantly decreased in the OMV-free supernatant (**Figure 2A**), suggesting that most of eDNA is associated with OMVs. Next, we investigated the DNA concentration associated with the extracted OMVs. As PicoGreen reagent is not permeable through the cellular membrane in the absence of additional treatments, OMVs were lysed with guanidium thiocyanide prior to labeling with PicoGreen. The DNA associated with OMVs derived from Δ*nlpI* was slightly increased compared to levels derived from WT (**Figure 2B**), thus indicating that the total of external and internal DNA associated with OMVs was highest in OMVs from Δ*nlpI*.

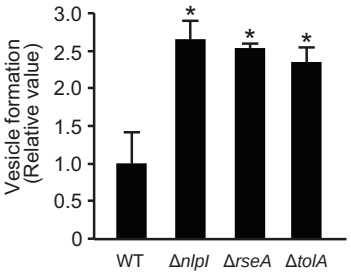

FIGURE 1 | Vesicle formation from *E. coli* BW25113 and mutants. WT, Δ*nlpI*, Δ*rseA*, and Δ*tolA*, all harboring plasmid pUC19, were grown in LB medium containing ampicillin overnight. The amount of vesicles extracted from the supernatants was normalized to cell density, and each value shown is relative to that of WT. The data are presented as the mean ± standard deviation from three replicates. *$P < 0.05$ compared to WT.

To analyze the plasmid DNA concentration in OMVs, extracted OMVs were treated with DNase I to remove externally associated DNA from OMVs, and the ratio of plasmid to vesicle was evaluated using real-time PCR and nano-tracking analysis. The amount of plasmid DNA in vesicles was increased threefold in Δ*nlpI*/pUC19 and was significantly decreased in Δ*rseA*/pUC19 and Δ*tolA*/pUC19 compared to that in WT/pUC19. By contrast, the relative plasmid copy number in bacterial cells was not significantly different among the samples (**Supplementary Figure 2**). These results suggest that defects in peptide crosslinks in PG can increase the incorporation of plasmids into OMVs in Δ*nlpI* even though the average size of these OMVs was smaller than that of the OMVs from the other strains.

Glycine Enhances the Vesicle Release in *E. coli* BW25113

To understand the relationship between defects in peptide crosslinks in PG and the association of DNA with OMVs, we investigated the impact of glycine on OMV formation. Glycine inhibits PG synthesis by substituting glycine for the D- or L-alanine of PG during growth in *E. coli* (Hammes et al., 1973), and the addition of glycine significantly enhances OMV formation in *E. coli* Nissle 1917 (Hirayama and Nakao, 2020). As described in a previous report, the addition of a final

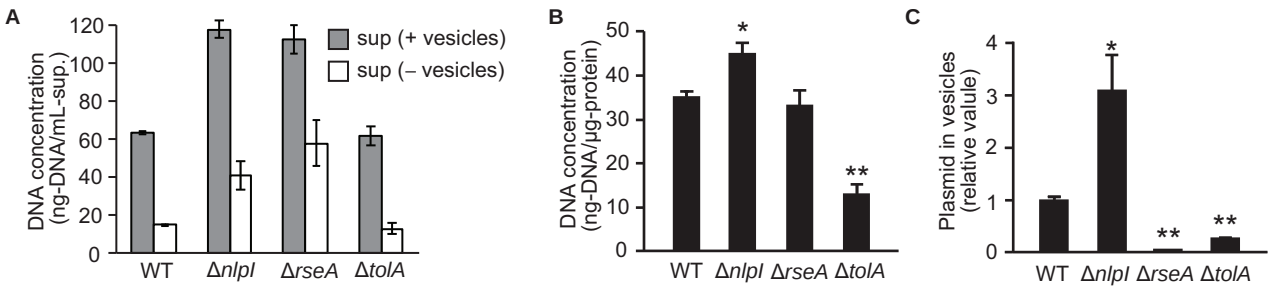

FIGURE 2 | DNA associated with vesicles. *E. coli* BW25113 WT, Δ*nlpI*, Δ*rseA*, and Δ*tolA*, all harboring pUC19, were grown overnight in LB medium containing ampicillin. **(A)** The extracellular DNA (eDNA) concentration of the supernatant (sup.) with and without vesicles was measured by PicoGreen. **(B)** DNA associated with vesicles derived from *E. coli*. Vesicles were lysed with guanidium thiocyanide prior to labeling. DNA concentrations were measured by PicoGreen, and the values were normalized to the vesicle protein concentration. **(C)** The ratio of plasmid to DNase I-treated vesicles. The amount of plasmid and vesicles were measured by real-time PCR and nano-tracking analysis, respectively, and the values (plasmid/vesicle) relative to control (WT/pUC19) are provided. In all figures, the data are presented as the mean ± standard deviation from three replicates. *$P < 0.05$; **$P < 0.005$ compared to WT.

concentration of 1% (w/v) glycine enhanced OMV formation in *E. coli* BW25113 harboring pUC19 (**Figure 3A**). The presence of OMVs surrounding bacterial cells with 1% glycine was confirmed by TEM (**Figure 3B**), which are thought to be vesicles that did not leave the cell surface due to increased formation. The size distribution of OMVs was not significantly different between OMVs in the presence and absence of 1% glycine, although OMVs derived from Δ*nlpI*/pUC19 did exhibit smaller diameters (**Figure 3C**).

Glycine Promotes the Incorporation of DNA Into Vesicles

To investigate the association between glycine-induced PG deficiency and DNA secretion, we examined the DNA content within the supernatant and in OMVs. The amount of eDNA released per cell was quantified using the PicoGreen assay and according to cellular density, and the results revealed that eDNA release in the presence of 1% glycine was fourfold higher than that in the control (**Figure 4A**). To compare DNA content inside and outside of OMVs, DNA concentrations were measured in OMVs treated with or without DNase. The percentage of internal DNA relative to total DNA associated with OMVs was 13% in OMVs derived from *E. coli* in LB medium and 70% in OMVs with glycine (**Figure 4B**), thus suggesting that the addition of glycine enhances the amount of internal DNA in OMVs. Furthermore, real-time PCR analysis indicated that the ratio of plasmid to OMVs induced by glycine were higher than were those in the control (**Figure 4C**). These results support the idea that PG defects increase the incorporation of plasmid DNA into OMVs.

Peptidoglycan Defects Increases Membrane Permeability

As glycine inhibits the proper alignment of PGs in *E. coli* (Hammes et al., 1973; Jonge et al., 1996), we evaluated the growth and membrane integrity of *E. coli* in the absence and presence of glycine. We analyzed membrane permeability using SYOT9 and PI, both of which are frequently used to test bacterial viability. The growth curve revealed that the presence of 1% glycine slightly repressed *E. coli* growth in LB medium (**Supplementary Figure 3**). At the late exponential phase (3 h culture), the percentage of PI-labeled cells was increased (**Figures 5A,B**); however, the colony forming unit (CFU) did not change significantly in the presence or absence of glycine (**Figure 5C**), suggesting that glycine increases the membrane permeability.

To further analyze the effect of glycine on membrane permeability, we used the fluorescent probe 1-*N*-phenylnaphthylamine (NPN) that is a small hydrophobic molecule (219 Da) and cannot cross the OM. When the membrane is damaged, the hydrophobic molecule NPN can enter into the phospholipid layer, resulting in prominent fluorescence (Muheim et al., 2017). At the late exponential phase, the membrane permeability of OM showed a high level (approximately threefold) in the presence of 1% glycine (**Figure 5D**). Thus, membrane remodeling already occurred at the late exponential phase, although the bacterial viability was not altered at that point.

Visualization of Released Vesicles and Cellular Surface Exposure to Glycine

O-IMVs have been suggested as a route for MV-mediated gene transfer in several bacterial species (Pérez-Cruz et al., 2013, 2015). To evaluate the relationship between DNA incorporation and the appearance of OMVs, OMVs derived from WT (with and without 1% glycine), and Δ*nlpI* were analyzed by negative staining using transmission electron microscopy (TEM). Most OMVs were single spherical vesicles in all samples; however, double lamellar vesicles were observed in OMVs of WT grown with glycine or from Δ*nlpI* (**Figure 6** and **Supplementary Figure 4**). This suggested that these double lamellar vesicles are O-IMVs and may contain cytoplasmic components, including DNA.

To investigate the spatial structure of the bacterial envelope after exposure to glycine, we used quick-freeze deep-etch and replica electron microscopy (QFDE-EM) to observe bacterial cellular surface with high spatial and sub-millisecond time resolutions (Tulum et al., 2019; Takaki et al., 2020). When *E. coli* cells were grown without glycine, abnormally altered cellular

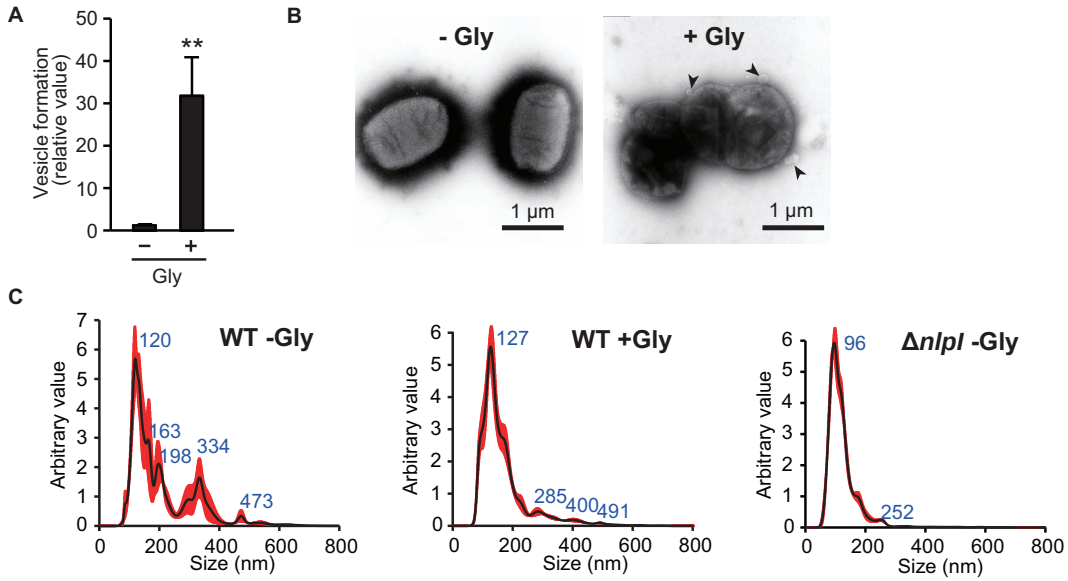

FIGURE 3 | Vesicle formation was increased by glycine. **(A)** Vesicle formation of *E. coli* BW25113/pUC19 in the absence (-Gly) and presence (+ Gly) of 1% glycine. The amount of vesicles extracted from the supernatants was normalized to the cell density, and each value presented is relative to that of control. $^{**}P < 0.005$ compared to WT. **(B)** *E. coli* BW25113 grown with and without 1% glycine was negative-stained and observed by transmission electron microscopy. Black arrows indicate vesicles. Scale bars are 1 μm. **(C)** Nano-tracking analysis of vesicles from *E. coli* BW25113 WT (with and without glycine) and Δ*nlpI*. Blue numbers indicate the size (nm) of peaks. Each sample was measured three times.

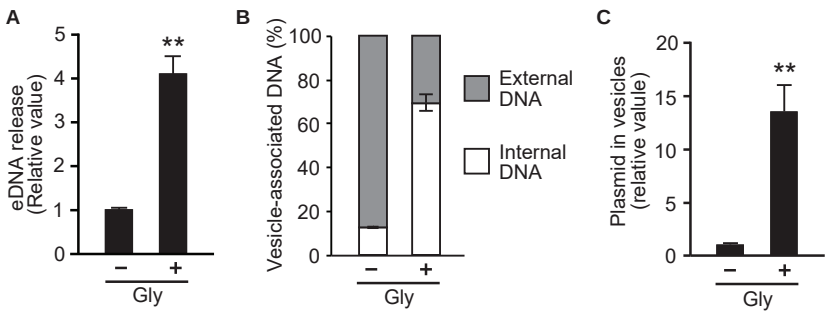

FIGURE 4 | Glycine induces the incorporation of plasmid into vesicles. **(A)** The production of extracellular DNA (eDNA) in *E. coli* BW25113 in the absence (-Gly) and presence (+ Gly) of 1% glycine. DNA concentration in the supernatant was normalized to cell densities, and values relative to that of control are presented. **(B)** Percentage of external and internal DNA of vesicles from *E. coli* BW25113. Vesicles were treated with or without DNase I, and the DNA concentration was measured using PicoGreen. **(C)** The ratio of plasmid to DNase I-treated vesicles. The amount of plasmid and vesicles were measured by real-time PCR and nano-tracking analysis, respectively, and the values (plasmid/vesicle) relative to control (-Gly) are provided. In all figures, the data are presented as the mean ± standard deviation from three replicates. $^{**}P < 0.005$ compared to the control.

surfaces were not observed in the freeze-fractured sections (**Figures 7A,B**). The QFDE-EM method enables visualization of the intracellular compartments such as the presumptive OM, IM, and cytoplasm (CP) (**Figures 7B,C**). The addition of glycine caused the separation of OM and IM and resulted in curvature of the OM (**Figure 7D**). Furthermore, a large amount of OMVs were observed on the cellular surface in the presence of glycine (**Figure 7E**). Interestingly, vesicles composed of double membranes were observed in the sample containing glycine (**Figure 7F**). The freeze-fractured section of the blebbing cells revealed that the multilamellar vesicles were O-IMVs and contained cytoplasmic components (**Figures 7G,H**), thus suggesting that O-IMVs are a possible route for incorporation of DNA into OMVs in the presence of glycine.

DISCUSSION

A number of previous studies have reported the presence of DNA in OMVs in several Gram-negative bacteria (Dorward et al., 1989; Dorward and Garon, 1990; Kadurugamuwa and Beveridge, 1995), and OMV-mediated gene exchange has been extensively investigated (Domingues and Nielsen, 2017; Soler and Forterre, 2020).

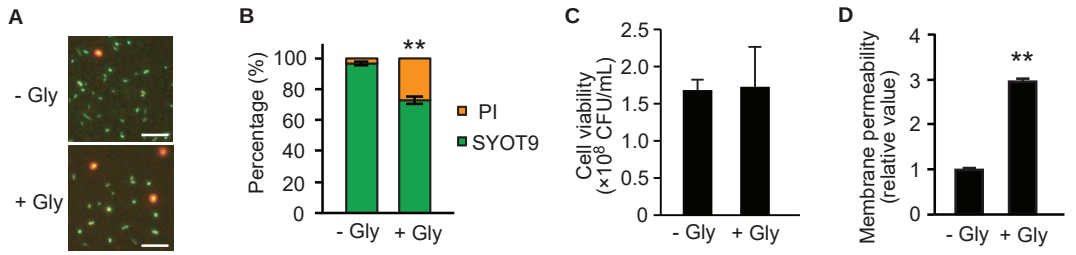

FIGURE 5 | Effect of glycine on membrane permeability. *E. coli* BW25113 was grown to the late exponential phase in the presence and absence of 1% glycine. **(A)** Membrane permeability analyses using SYTO9 and propidium iodide (PI). Bacterial cells exhibiting membrane integrity and deficiency were labeled green and red, respectively. Representative images are presented. Bar = 100 μm. **(B)** The percentages of SYTO9- and PI-labeled cells. The data are presented as the mean ± standard deviation from more than three representative images. $^{**}P < 0.005$ compared to the control (-Gly). **(C)** Cell viability in the presence and absence of glycine. Bacterial cells were adjusted to equal optical densities (OD_{600} = 1.0), diluted samples were plated onto LB agar, and colony forming units (CFUs) were calculated. The data are presented as the mean ± standard deviation from three replicates. **(D)** The permeability of the outer membrane was assessed by measuring the fluorescence of 1-*N*-phenylnaphthylamine (NPN), and the values relative to that of control are presented. The data are presented as the mean ± standard deviation from three replicates. $^{**}P < 0.005$ compared to the control (-Gly).

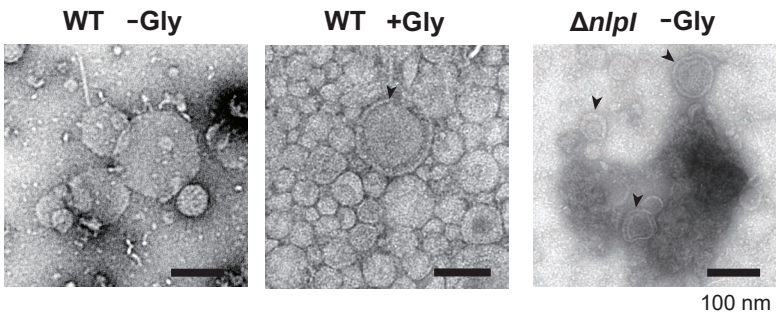

FIGURE 6 | Transmission electron microscopy observation of vesicles. *E. coli* BW25113 WT and Δ*nlpI* harboring pUC19 were grown in LB containing ampicillin with or without 1% glycine, and vesicles extracted from the supernatant were observed after negative staining. Bar = 100 nm.

Although vesicle-mediated gene transfer is estimated to occur at a low rate compared to that of the other three HGT mechanisms (transformation, transduction, and conjugation) according to mathematical models (Nazarian et al., 2018), this process possesses unique characteristics compared to those of the others; where specific genes such as *dprA* and *com* operon for natural transformation, phage genes for transduction, and type IV secretion system genes (relaxase, type IV coupling protein, and type IV secretion system) for conjugation are not required. To use vesicles as DNA cargo among bacterial species, the general mechanism of gene exchange has recently been studied using OMVs from *E. coli* (Tran and Boedicker, 2017, 2019). In contrast, much less is known regarding the mechanism by which DNA passes through the inner membrane and is sorted into OMVs in Gram-negative bacteria. In the present study, we explored factors that influence DNA packing into vesicles using OMV-overproducing *E. coli* mutants, and showed that PG defects increase the incorporation of plasmid DNA into OMVs. Furthermore, glycine was identified as a stimulator for OMV production and incorporation of plasmid DNA into OMVs.

In this study, the presence of plasmid DNA in OMVs was examined using hypervesiculating *E. coli* mutants harboring high-copy plasmids. Tran and Boedicker (2017) reported that an average of 3.62 pUC19 plasmids were loaded per *E. coli* vesicle. However, both their and our experiments evaluated the relative ratio of the specific region of the plasmid to that of chromosome, and we cannot debate the absolute copy number of plasmid per vesicle from those results. Further quantitative analyses are required to estimate the copy number present inside the vesicles. As the radius of gyration of pUC19 was estimated to be 65.6 nm (Störkle et al., 2007), several copies at a maximum are presumed to be contained per vesicle. In our results, the loading of pUC19 into vesicles was increased by approximately threefold in the Δ*nlpI* in which peptide crosslinks were defective in PGs (**Figure 2C**). Interestingly, OMVs from Δ*nlpI* possessed small diameters according to both hydrodynamic (**Supplementary Figure 1**) and nano-tracking (**Figure 3C**) analyses despite harboring higher plasmid copies. The PG defects disturb OM-PG links, and OMVs derived from the cellular surface through such mechanisms tend to exhibit smaller diameters compared to those of OMVs derived from cell-binding sites (Deatherage et al., 2009). Thus, we speculated that the incorporation of DNA into OMVs is driven by PG defects.

To further corroborate if PG defect-based OMV production enhances the encapsulation of plasmid DNA into OMVs, the influence of 1.0% glycine supplementation on plasmid copy numbers within OMVs was investigated. Glycine substitutes for D- and L-alanine of PGs during growth (Hammes et al., 1973; Jonge et al., 1996), and it also induces OMV production (Hirayama and Nakao, 2020). The mechanism for OMV induction by glycine is considered to be a similar phenomenon to that observed in the depletion of *nlpI*, where the loss of the OM-PG bridge (i.e., Braun's lipoprotein Lpp) increases OM looseness and the accumulation of PG fragments increases OM protrusion, thus resulting in OMV production (**Figures 8A,B**). Our data demonstrated that supplementation with 1% glycine enhanced both OMV and eDNA release (**Figures 3A**, **4A**).

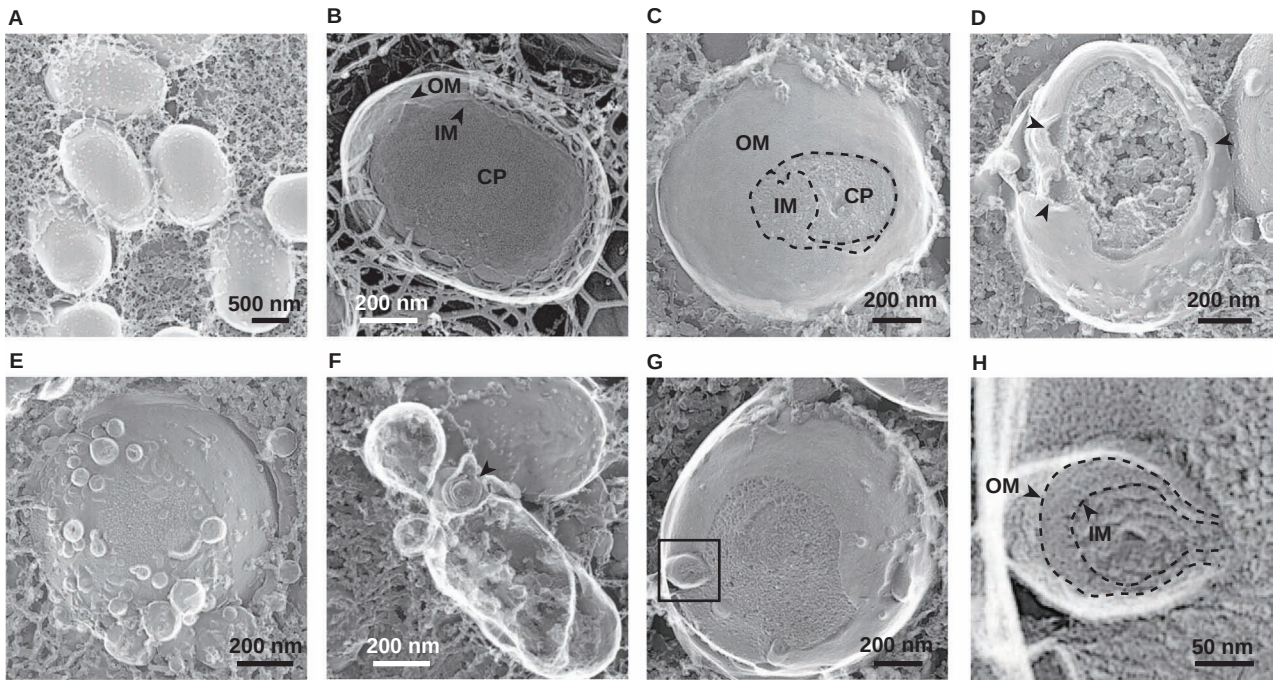

FIGURE 7 | Visualization of bacterial surfaces by quick freeze deep-etch and replica electron micrograph (QFDE-EM) analyses. *E. coli* BW25113 was grown in LB in the absence **(A,B)** and presence **(C–H)** of 1% glycine. The outer membrane (OM), inner membrane (IM), and cytoplasm (CP) are shown **(B,C)**. The black arrows indicate loose and curved OM portions **(D)** and double lamellar vesicles **(F)**, respectively. Enlarged image of the black box in image **(G)** are shown in image **(H)**.

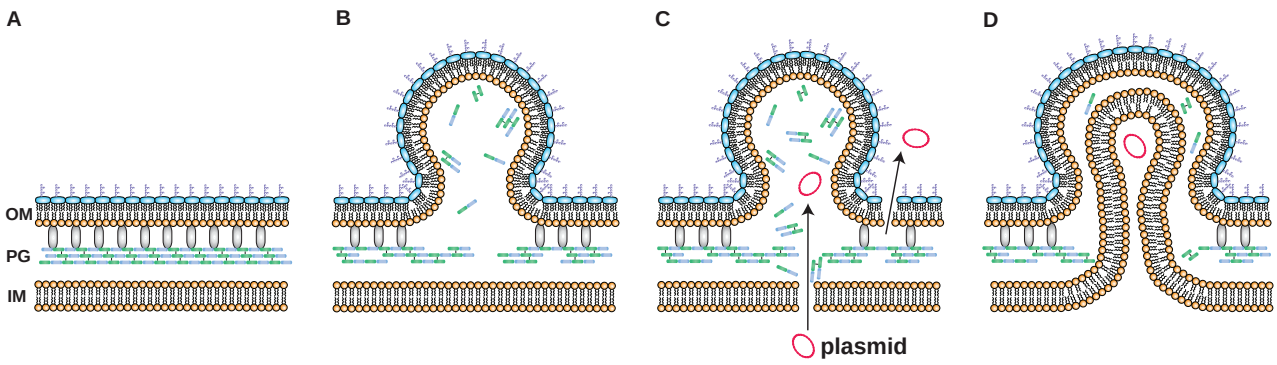

FIGURE 8 | A possible model for DNA incorporation into vesicles. **(A)** The spatial image of the surface of *Escherichia coli*. Peptidoglycan (PG) is localized between the outer membrane (OM) and the inner membrane (IM). Braun's lipoprotein Lpp (gray) forms crosslinks between OM and PG. **(B)** Defects in PG increase outer membrane vesicle (OMV) formation. The depletion of NlpI or the addition of glycine causes defects in peptide crosslinks in PG. The loss of bridges between OM and PG and the accumulation of PG fragments increase OM curvature, ultimately resulting in OMV formation. **(C,D)** Mechanisms for the incorporation of plasmids into OMVs in *E. coli* cells after exposure to glycine are explained by two proposal models. One is the leakage of plasmids **(C)**. The membrane permeabilities of both OM and IM are increased when PG is not synthesized normally. The other mechanism is the formation of outer-inner membrane vesicles (O-IMVs) **(D)**. IM and cytoplasmic components such as plasmids are included in the vesicle that is leaving the cell. The encapsulation of IM is considered to occur at the site where peptidoglycan is not normally synthesized.

Additionally, approximately 70% of the DNA associated with OMVs from *E. coli* treated with glycine was the internal DNA in OMVs (**Figure 4B**). Notably, glycine-induced OMVs contained 13-fold higher pUC19 copies per vesicle compared to those without glycine (**Figure 4C**). Therefore, glycine can function as an effective additive for producing plasmid-containing OMVs.

Two mechanisms for the incorporation of plasmid DNA into OMVs under PG-defective conditions were proposed in this study. One mechanism is the leakage of DNA from the cytoplasm. Our data revealed that glycine increased the percentage of PI-labeled cells despite no differences in CFUs at the late exponential phase (**Figures 4A**, **5D**), thus indicating that glycine enhances membrane permeability prior to the occurrence of cell lysis. Moreover, eDNA release and OM permeability were increased by glycine (**Figures 5A,D**). Taken together, our results indicated that cytoplasmic plasmid DNA is leaked into the periplasmic space and the extracellular milieu, ultimately leading to the incorporation of DNA into OMVs and eDNA release (**Figure 8C**). While PI is permeable to pores that are approximately 1.5 nm in diameter (Nesin et al., 2011), much larger pores could contribute to plasmid DNA penetration. The effect of glycine on PG weakness has been used for effective transformation in several previous studies (Holo and Nes, 1989; Thompson and Collins, 1996; Buckley et al., 1999; Ito and Nagane, 2001), and our results are consistent with those from previous reports indicating that PG defects contribute to DNA permeation through cellular membranes. The internal existence of double-stranded DNA in a single OM bilayer vesicle has also been reported in *Acinetobacter baylyi* (Fulsundar et al., 2014) and *P. aeruginosa* (Bitto et al., 2017), and increased membrane permeability may be one of the proposed mechanisms underlying these observations. It is not yet clear to what extent the existence of vesicles containing interior DNA is due to elevated IM permeability, and quantitative analyses will allow for improved understanding of vesicle-mediated gene transfer in future studies.

The other proposed mechanism for DNA incorporation into OMVs is the production of O-IMVs. The O-IMV production is a natural event for the growth of pathogenic bacteria, including *N. gonorrhoeae*, *P. aeruginosa* and *A. baumannii* (Pérez-Cruz et al., 2015). In our results, O-IMVs were observed in OMVs from Δ*nlpI* and WT supplemented with glycine, but not in those from WT without glycine (**Figure 6** and **Supplementary Figure 4**). When PG is not synthesized accurately, IM can become protruded and encapsulated into OMVs (**Figure 8D**). The presumption is also supported by a recent report; double lamellar vesicle formation is promoted in a hypervesiculating *E. coli* mutant Δ*mlaE*Δ*nlpI* (Ojima et al., 2021), in which phospholipids are accumulated at the OM in the Δ*nlpI* background (Ojima et al., 2020). Intracellular vesicles, considered to be derived from IM, are accumulated in the periplasmic spaces and finally multilamellar vesicles are formed in the Δ*nlpI* and Δ*mlaE*Δ*nlpI* mutants. We have recently observed excessive intracellular vesicle accumulation in the periplasm and multilamellar/multivesicular outer membrane vesicle (M-OMV) formation in *Buttiauxella agrestis* Δ*tolB* mutant (Takaki et al., 2020), but it is still unclear whether common factors are related to in M-OMV and O-IMV formations. MV formation beyond the PG also occurs in Gram-positive bacteria, where MVs are pinched off from the sites where PG is damaged by the expression of a prophage-encoded endolysin in *Bacillus subtilis* (Toyofuku et al., 2017). As IM exists within the PG in Gram-negative bacteria, an analogous principle may exist in Gram-negative bacterial O-IMV formation and Gram-positive MV formation.

Damage to PG frequently occurs in nature due to incomplete PG synthesis or PG degradation. PG-hydrolyzing enzymes are widespread and classified as endolysins, exolysins, and autolysins based on their origin and role (Vermassen et al., 2019). These PG hydrolyzing enzymes are used for cell division, lytic bacteriophage, and several types (type II, IV, and VI) of secretion systems. Indeed, the existence of autolysins has been confirmed in MVs from *P. aeruginosa*, and endolysin is an endopeptidase that cleaves a critical amide bond between the glycan moiety and the peptide moiety of the PG (Kadurugamuwa and Beveridge, 1995; Li et al., 1996). Therefore, PG damage-based incorporation of plasmid DNA into OMVs has potentially occurred during normal growth.

CONCLUSION

We demonstrated that PG defects contribute to the incorporation of DNA into OMVs in addition to OMV formation in *E. coli*. Glycine may provide a useful tool for the development of DNA-containing vesicles for genetic manipulation. Encapsulation of DNA in OMVs under PG defects is considered to occur by two proposed mechanisms that include increased membrane permeability and O-IMV formation. The results of this study are important for providing a better understanding of vesicle-mediated HGT in the nature and the utilization of vesicles for DNA cargo.

DATA AVAILABILITY STATEMENT

The authors acknowledge that the data presented in this study must be deposited and made publicly available in an acceptable repository, prior to publication. Frontiers cannot accept a manuscript that does not adhere to our open data policies.

AUTHOR CONTRIBUTIONS

MS, HN, and YT planned and designed the experiments. SA, YO, and MI extracted vesicles, quantified DNA, and analyzed the vesicles. SU, YOT, and MM contributed to the electron microscopic analyses. HF and YT supervised. SA, YO, and YT wrote the manuscript. All authors critically reviewed the manuscript, analyzed, and discussed the data.

FUNDING

This work was supported by the JSPS KAKENHI (JP19H02920 to YT, JP18K19168 to HN and YT, JP19H05686 to HN and MS, JP19K22927 to

HF, and JP25117501 to MM), JST PRESTO (JPMJPR19H8 to YT), JST CREST (JPMJCR19S5 to MM) and the Osaka City University Strategic Research Grant 2017 for top priority researches (to MM).

ACKNOWLEDGMENTS

We gratefully acknowledge the helpful discussions with Satoru Hirayama (Niigata University), Ryoma Nakao (National Institute of Infectious Diseases) and Yoshihiro Ojima (Osaka City University). We thank Nobuyuki Mase and Kohei Sato (Shizuoka University) for assistance with the nanoparticle tracking analysis and Junko Shiomi (Osaka City University) for help with the QFDE-EM analysis. We also thank the Instrumental Research Support Office of the Research Institute of Green Science and Technology in Shizuoka University for the use of the Zetasizer and the Genome Analysis Project in Japan for providing the KEIO collection.

SUPPLEMENTARY MATERIAL

The Supplementary Material for this article can be found online at: https://www.frontiersin.org/articles/10.3389/fmicb.2021.747606/full#supplementary-material

REFERENCES

Aguilera, L., Toloza, L., Giménez, R., Odena, A., Oliveira, E., Aguilar, J., et al. (2014). Proteomic analysis of outer membrane vesicles from the probiotic strain *Escherichia coli* Nissle 1917. *Proteomics* 14, 222–229. doi: 10.1002/pmic.201300328

Baba, T., Ara, T., Hasegawa, M., Takai, Y., Okumura, Y., Baba, M., et al. (2006). Construction of *Escherichia coli* K-12 in-frame, single-gene knockout mutants: the Keio collection. *Mol. Syst. Biol.* 2:2006.0008. doi: 10.1038/msb4100050

Bernadac, A., Gavioli, M., Lazzaroni, J., Raina, S., and Lloubès, R. (1998). *Escherichia coli tol-pal* mutants form outer membrane vesicles. *J. Bacteriol.* 180, 4872–4878. doi: 10.1128/JB.180.18.4872-4878.1998

Bitto, N. J., Chapman, R., Pidot, S., Costin, A., Lo, C., Choi, J., et al. (2017). Bacterial membrane vesicles transport their DNA cargo into host cells. *Sci. Rep.* 7:7072. doi: 10.1038/s41598-017-07288-4

Bouveret, E., Derouiche, R., Rigal, A., Lloubes, R., Lazdunski, C., and Benedetti, H. (1995). Peptidoglycan-associated lipoprotein-TolB interaction. A possible key to explaining the formation of contact sites between the inner and outer membranes of *Escherichia coli*. *J. Biol. Chem.* 270, 11071–11077. doi: 10.1074/jbc.270.19.11071

Buckley, N. D., Vadeboncoeur, C., Leblanc, D. J., Lee, L. N., and Frenette, M. (1999). An effective strategy, applicable to *Streptococcus salivarius* and related bacteria, to enhance or confer electroporation competence. *Appl. Environ. Microbiol.* 65, 3800–3804.

Choi, D.-S., Kim, D.-K., Choi, S. J., Lee, J., Choi, J.-P., Rho, S., et al. (2011). Proteomic analysis of outer membrane vesicles derived from *Pseudomonas aeruginosa*. *Proteomics* 11, 3424–3429. doi: 10.1002/pmic.201000212

Deatherage, B. L., Lara, J. C., Bergsbaken, T., Barrett, S. L. R., Lara, S., and Cookson, B. T. (2009). Biogenesis of bacterial membrane vesicles. *Mol. Microbiol.* 72, 1395–1407. doi: 10.1111/j.1365-2958.2009.06731.x

Domingues, S., and Nielsen, K. M. (2017). Membrane vesicles and horizontal gene transfer in prokaryotes. *Curr. Opin. Microbiol.* 38, 16–21. doi: 10.1016/j.mib.2017.03.012

Dorward, D. W., and Garon, C. F. (1990). DNA is packaged within membrane-derived vesicles of Gram-negative but not Gram-positive bacteria. *Appl. Environ. Microbiol.* 56, 1960–1962. doi: 10.1128/aem.56.6.1960-1962.1990

Dorward, D. W., Garon, C. F., and Judd, R. C. (1989). Export and intercellular transfer of DNA via membrane blebs of *Neisseria gonorrhoeae*. *J. Bacteriol.* 171, 2499–2505. doi: 10.1128/jb.171.5.2499-2505.1989

Fulsundar, S., Harms, K., Flaten, G. E., Johnsen, P. J., Chopade, B. A., and Nielsen, K. M. (2014). Gene transfer potential of outer membrane vesicles of *Acinetobacter baylyi* and effects of stress on vesiculation. *Appl. Environ. Microbiol.* 80, 3469–3483. doi: 10.1128/AEM.04248-13

Gaudin, M., Gauliard, E., Schouten, S., Houel-Renault, L., Lenormand, P., Marguet, E., et al. (2013). Hyperthermophilic archaea produce membrane vesicles that can transfer DNA. *Environ. Microbiol. Rep.* 5, 109–116. doi: 10.1111/j.1758-2229.2012.00348.x

Hammes, W., Schleifer, K. H., and Kandler, O. (1973). Mode of action of glycine on the biosynthesis of peptidoglycan. *J. Bacteriol.* 116, 1029–1053. doi: 10.1128/jb.116.2.1029-1053.1973

Hasegawa, Y., Futamata, H., and Tashiro, Y. (2015). Complexities of cell-to-cell communication through membrane vesicles: implications for selective interaction of membrane vesicles with microbial cells. *Front. Microbiol.* 6:633. doi: 10.3389/fmicb.2015.00633

Hirayama, S., and Nakao, R. (2020). Glycine significantly enhances bacterial membrane vesicle production: a powerful approach for isolation of LPS-reduced membrane vesicles of probiotic *Escherichia coli*. *Microbial. Biotechnol.* 13, 1162–1178. doi: 10.1111/1751-7915.13572

Holo, H., and Nes, I. F. (1989). High-frequency transformation, by electroporation, of *Lactococcus lactis* subsp. cremoris grown with glycine in osmotically stabilized media. *Appl. Environ. Microbiol.* 55, 3119–3123. doi: 10.1128/aem.55.12.3119-3123.1989

Ito, M., and Nagane, M. (2001). Improvement of the electro-transformation efficiency of facultatively alkaliphilic *Bacillus pseudofirmus* OF4 by high osmolarity and glycine treatment. *Biosci. Biotechnol. Biochem.* 65, 2773–2775. doi: 10.1271/bbb.65.2773

Jonge, B. L. D., Chang, Y. S., Xu, N., and Gage, D. (1996). Effect of exogenous glycine on peptidoglycan composition and resistance in a methicillin-resistant *Staphylococcus aureus* strain. *Antimicrob. Agents Chemother.* 40, 1498–1503. doi: 10.1128/AAC.40.6.1498

Kadurugamuwa, J. L., and Beveridge, T. J. (1995). Virulence factors are released from *Pseudomonas aeruginosa* in association with membrane vesicles during normal growth and exposure to gentamicin: a novel mechanism of enzyme secretion. *J. Bacteriol.* 177, 3998–4008. doi: 10.1128/jb.177.14.3998-4008.1995

Klieve, A. V., Yokoyama, M. T., Forster, R. J., Ouwerkerk, D., Bain, P. A., and Mawhinney, E. L. (2005). Naturally occurring DNA transfer system associated with membrane vesicles in cellulolytic *Ruminococcus* spp. of ruminal origin. *Appl. Environ. Microbiol.* 71, 4248–4253. doi: 10.1128/AEM.71.8.4248-4253.2005

Kolling, G. L., and Matthews, K. R. (1999). Export of virulence genes and Shiga toxin by membrane vesicles of *Escherichia coli* O157:H7. *Appl. Environ. Microbiol.* 65, 1843–1848. doi: 10.1128/AEM.65.5.1843-1848.1999

Lee, E., Bang, J., Park, G., Choi, D., Kang, J., Kim, H., et al. (2007). Global proteomic profiling of native outer membrane vesicles derived from *Escherichia coli*. *Proteomics* 7, 3143–3153. doi: 10.1002/pmic.200700196

Li, Z., Clarke, A. J., and Beveridge, T. J. (1996). A major autolysin of *Pseudomonas aeruginosa*: subcellular distribution, potential role in cell growth and division and secretion in surface membrane vesicles. *J. Bacteriol.* 178, 2479–2488. doi: 10.1128/jb.178.9.2479-2488.1996

McBroom, A. J., and Kuehn, M. J. (2007). Release of outer membrane vesicles by Gram-negative bacteria is a novel envelope stress response. *Mol. Microbiol.* 63, 545–558. doi: 10.1111/j.1365-2958.2006.05522.x

McBroom, A., Johnson, A., Vemulapalli, S., and Kuehn, M. (2006). Outer membrane vesicle production by *Escherichia coli* is independent of membrane instability. *J. Bacteriol.* 188, 5385–5392. doi: 10.1128/JB.00498-06

Muheim, C., Götzke, H., Eriksson, A. U., Lindberg, S., Lauritsen, I., Nørholm, M. H. H., et al. (2017). Increasing the permeability of *Escherichia coli* using MAC13243. *Sci. Rep.* 7:17629. doi: 10.1038/s41598-017-17772-6

Nazarian, P., Tran, F., and Boedicker, J. Q. (2018). Modeling multispecies gene flow dynamics reveals the unique roles of different horizontal gene transfer mechanisms. *Front. Microbiol.* 9:2978. doi: 10.3389/fmicb.2018.02978

Nesin, O. M., Pakhomova, O. N., Xiao, S., and Pakhomov, A. G. (2011). Manipulation of cell volume and membrane pore comparison following single cell permeabilization with 60- and 600-ns electric pulses. *Biochim. Biophys. Acta Biomembr.* 1808, 792–801. doi: 10.1016/j.bbamem.2010.12.012

Ojima, Y., Nguyen, M. H., Yajima, R., and Taya, M. (2015). Flocculation of *Escherichia coli* cells in association with enhanced production of outer membrane vesicles. *Appl. Environ. Microbiol.* 81, 5900–5906. doi: 10.1128/AEM.01011-15

Ojima, Y., Sawabe, T., Konami, K., and Azuma, M. (2020). Construction of hypervesiculation *Escherichia coli* strains and application for secretory protein production. *Biotechnol. Bioeng.* 117, 701–709. doi: 10.1002/bit.27239

Ojima, Y., Sawabe, T., Nakagawa, M., Tahara, Y. O., Miyata, M., and Azuma, M. (2021). Aberrant membrane structures in hypervesiculating *Escherichia coli* strain Δ*mlaE* Δ*nlpI* visualized by electron microscopy. *Front. Microbiol.* 12:706525. doi: 10.3389/fmicb.2021.706525

Pérez-Cruz, C., Carrión, O., Delgado, L., Martinez, G., López-Iglesias, C., and Mercade, E. (2013). New type of outer membrane vesicle produced by the Gram-negative bacterium *Shewanella vesiculosa* M7T: implications for DNA content. *Appl. Environ. Microbiol.* 79, 1874–1881. doi: 10.1128/AEM.03657-12

Pérez-Cruz, C., Delgado, L., López-Iglesias, C., and Mercade, E. (2015). Outer-inner membrane vesicles naturally secreted by Gram-negative pathogenic bacteria. *PLoS One* 10:e0116896. doi: 10.1371/journal.pone.0116896

Rumbo, C., Fernández-Moreira, E., Merino, M., Poza, M., Mendez, J. A., Soares, N. C., et al. (2011). Horizontal transfer of the OXA-24 carbapenemase gene via outer membrane vesicles: a new mechanism of dissemination of carbapenem resistance genes in *Acinetobacter baumannii*. *Antimicrob. Agents Chemother.* 55, 3084–3090. doi: 10.1128/AAC.00929-10

Schwechheimer, C., and Kuehn, M. J. (2015). Outer-membrane vesicles from Gram-negative bacteria: biogenesis and functions. *Nat. Rev. Microbiol.* 13, 605–619. doi: 10.1038/nrmicro3525

Schwechheimer, C., Kulp, A., and Kuehn, M. (2014). Modulation of bacterial outer membrane vesicle production by envelope structure and content. *BMC Microbiol.* 14:324. doi: 10.1186/s12866-014-0324-1

Schwechheimer, C., Rodriguez, D. L., and Kuehn, M. J. (2015). NlpI-mediated modulation of outer membrane vesicle production through peptidoglycan dynamics in *Escherichia coli*. *Microbiologyopen* 4, 375–389. doi: 10.1002/mbo3.244

Soh, S. M., Jang, H., and Mitchell, R. J. (2020). Loss of the lipopolysaccharide (LPS) inner core increases the electrocompetence of *Escherichia coli*. *Appl. Microbiol. Biotechnol.* 104, 7427–7435. doi: 10.1007/s00253-020-10779-6

Soler, N., and Forterre, P. (2020). Vesiduction: the fourth way of HGT. *Environ. Microbiol.* 22, 2457–2460. doi: 10.1111/1462-2920.15056

Sonntag, I., Schwarz, H., Hirota, Y., and Henning, U. (1978). Cell envelope and shape of *Escherichia coli*: multiple mutants missing the outer membrane lipoprotein and other major outer membrane proteins. *J. Bacteriol.* 136, 280–285. doi: 10.1128/jb.136.1.280-285.1978

Störkle, D., Duschner, S., Heimann, N., Maskos, M., and Schmidt, M. (2007). Complex formation of DNA with oppositely charged polyelectrolytes of different chain topology:? cylindrical brushes and dendrimers. *Macromolecules* 40, 7998–8006. doi: 10.1021/ma0711689

Sturgis, J. N. (2001). Organisation and evolution of the *tol-pal* gene cluster. *J. Mol. Microbiol. Biotechnol.* 3, 113–122.

Takaki, K., Tahara, Y. O., Nakamichi, N., Hasegawa, Y., Shintani, M., Ohkuma, M., et al. (2020). Multilamellar and multivesicular outer membrane vesicles produced by a *Buttiauxella agrestis tolB* mutant. *Appl. Environ. Microbiol.* 86, e1131–e1220. doi: 10.1128/AEM.01131-20

Tashiro, Y., Hasegawa, Y., Shintani, M., Takaki, K., Ohkuma, M., Kimbara, K., et al. (2017). Interaction of bacterial membrane vesicles with specific species and their potential for delivery to target cells. *Front. Microbiol.* 8:571. doi: 10.3389/fmicb.2017.00571

Tashiro, Y., Sakai, R., Toyofuku, M., Sawada, I., Nakajima-Kambe, T., Uchiyama, H., et al. (2009). Outer membrane machinery and alginate synthesis regulators control membrane vesicle production in *Pseudomonas aeruginosa*. *J. Bacteriol.* 191, 7509–7519. doi: 10.1128/JB.00722-09

Tashiro, Y., Takaki, K., and Futamata, H. (2019). Targeted delivery using membrane vesicles in prokaryotes. *Biophys. Physicobiol.* 16, 114–120. doi: 10.2142/biophysico.16.0_114

Tashiro, Y., Uchiyama, H., and Nomura, N. (2012). Multifunctional membrane vesicles in *Pseudomonas aeruginosa*. *Environ. Microbiol.* 14, 1349–1362. doi: 10.1111/j.1462-2920.2011.02632.x

Thompson, K., and Collins, M. A. (1996). Improvement in electroporation efficiency for *Lactobacillus plantarum* by the inclusion of high concentrations of glycine in the growth medium. *J. Microbiol. Methods* 26, 73–79. doi: 10.1016/0167-7012(96)00845-7

Toyofuku, M., Cárcamo-Oyarce, G., Yamamoto, T., Eisenstein, F., Hsiao, C.-C., Kurosawa, M., et al. (2017). Prophage-triggered membrane vesicle formation through peptidoglycan damage in *Bacillus subtilis*. *Nat. Commun.* 8:481. doi: 10.1038/s41467-017-00492-w

Toyofuku, M., Nomura, N., and Eberl, L. (2018). Types and origins of bacterial membrane vesicles. *Nat. Rev. Microbiol.* 17, 13–24. doi: 10.1038/s41579-018-0112-2

Toyofuku, M., Tashiro, Y., Hasegawa, Y., Kurosawa, M., and Nomura, N. (2015). Bacterial membrane vesicles, an overlooked environmental colloid: biology, environmental perspectives and applications. *Adv. Colloid Interface Sci.* 226, 65–77. doi: 10.1016/j.cis.2015.08.013

Tran, F., and Boedicker, J. Q. (2017). Genetic cargo and bacterial species set the rate of vesicle-mediated horizontal gene transfer. *Sci. Rep.* 7:8813. doi: 10.1038/s41598-017-07447-7

Tran, F., and Boedicker, J. Q. (2019). Plasmid characteristics modulate the propensity of gene exchange in bacterial vesicles. *J. Bacteriol.* 201, e430–e518. doi: 10.1128/JB.00430-18

Tulum, I., Tahara, Y. O., and Miyata, M. (2019). Peptidoglycan layer and disruption processes in *Bacillus subtilis* cells visualized using quick-freeze, deep-etch electron microscopy. *Microscopy* 68, 441–449. doi: 10.1093/jmicro/dfz033

Turnbull, L., Toyofuku, M., Hynen, A. L., Kurosawa, M., Pessi, G., Petty, N. K., et al. (2016). Explosive cell lysis as a mechanism for the biogenesis of bacterial membrane vesicles and biofilms. *Nat. Commun.* 7:11220. doi: 10.1038/ncomms11220

Turner, L., Praszkier, J., Hutton, M. L., Steer, D., Ramm, G., Kaparakis-Liaskos, M., et al. (2015). Increased outer membrane vesicle formation in a *Helicobacter pylori tolB* mutant. *Helicobacter* 20, 269–283. doi: 10.1111/hel.12196

Vermassen, A., Leroy, S., Talon, R., Provot, C., Popowska, M., and Desvaux, M. (2019). Cell wall hydrolases in bacteria: insight on the diversity of cell wall amidases, glycosidases and peptidases toward peptidoglycan. *Front. Microbiol.* 10:331. doi: 10.3389/fmicb.2019.00331

Yaron, S., Kolling, G., Simon, L., and Matthews, K. (2000). Vesicle-mediated transfer of virulence genes from *Escherichia coli* O157:H7 to other enteric bacteria. *Appl. Environ. Microbiol.* 66, 4414–4420. doi: 10.1128/AEM.66.10.4414-4420.2000

Conflict of Interest: The authors declare that the research was conducted in the absence of any commercial or financial relationships that could be construed as a potential conflict of interest.

Publisher's Note: All claims expressed in this article are solely those of the authors and do not necessarily represent those of their affiliated organizations, or those of the publisher, the editors and the reviewers. Any product that may be evaluated in this article, or claim that may be made by its manufacturer, is not guaranteed or endorsed by the publisher.

Advantages of publishing in Frontiers

OPEN ACCESS
Articles are free to read for greatest visibility and readership

FAST PUBLICATION
Around 90 days from submission to decision

HIGH QUALITY PEER-REVIEW
Rigorous, collaborative, and constructive peer-review

TRANSPARENT PEER-REVIEW
Editors and reviewers acknowledged by name on published articles

Frontiers
Avenue du Tribunal-Fédéral 34
1005 Lausanne | Switzerland

Visit us: www.frontiersin.org
Contact us: frontiersin.org/about/contact

REPRODUCIBILITY OF RESEARCH
Support open data and methods to enhance research reproducibility

DIGITAL PUBLISHING
Articles designed for optimal readership across devices

FOLLOW US
@frontiersin

IMPACT METRICS
Advanced article metrics track visibility across digital media

EXTENSIVE PROMOTION
Marketing and promotion of impactful research

LOOP RESEARCH NETWORK
Our network increases your article's readership